

# Search for $VH \rightarrow VWW$ SM Higgs Production in the Trilepton Signature

Jason Nett<sup>1</sup>

---

<sup>1</sup>Contact: Jason Nett jnett@wisc.edu

## Abstract

We present here the first search for Standard Model  $VH \rightarrow VWW \rightarrow l\nu l\nu l\nu$  production, where  $V$  is the  $W$  and  $Z$  weak vector bosons, using  $4.8 \text{ fb}^{-1}$  of integrated luminosity. This analysis adds to the existing CDF  $HWW$  group's dilepton analysis two new regions characterized by a **tri**-lepton signature, which are chosen to isolate the  $WH \rightarrow WWW$  and  $ZH \rightarrow ZWW$  associated production signals in the three-lepton bin. As such, we define two new regions denoted *trilepton-NoZPeak* (for the  $WH$ -centered analysis) and *trilepton-InZPeak* (for the  $ZH$ -centered analysis) with which we expect to contribute an additional  $\sim 5.8\%$  (for  $m_H = 160 \text{ GeV}$ ) acceptance to the current  $H \rightarrow WW$  dilepton analysis. The *trilepton-InZPeak* region is defined by events having at least one lepton pairing (among three possible pairings) with opposite-sign, same flavor, and a dilepton invariant mass within  $[91.0, 101.0] \text{ GeV}$ —a  $10 \text{ GeV}$  window around the  $Z$ -boson mass. The *trilepton-NoZPeak* region is then defined by those trilepton events which do not match the *InZPeak* definition. In this note, we shall refer to the study of the *trilepton-NoZPeak* region as the  $WH$  analysis and the study of the *trilepton-InZPeak* region as the  $ZH$  analysis, though note that both regions do contain at least some of both signals.

These two new regions are poised to make a substantial contribution to the  $H \rightarrow WW$  group result. At  $m_H = 165 \text{ GeV}$ , the  $WH$  analysis expected limits reach 8.9 times the standard model cross section; the  $ZH$  analysis is set at 12.6 times the expected standard model cross section; and the combined trilepton analysis is set at 6.3 times the expected standard model cross section. Finally, for the combined  $H \rightarrow WW$  analysis result, in the  $165 \text{ GeV}$  bin the expected limit drops from 1.21 for the dilepton analyses alone to 1.15 while the observed limit drops from 1.23 to 1.08.[4] As such, we are poised to begin excluding the standard model Higgs boson at 95% confidence level with CDF-only analyses in short order.[3]

# Contents

<b>1</b>	<b>Introduction</b>	<b>6</b>
<b>2</b>	<b>The Higgs Mechanism and the Standard Model of Particle Physics</b>	<b>9</b>
2.1	Intro. to the Standard Model of Particle Physics . . . . .	9
2.2	Elementary Particles in the Standard Model . . . . .	9
2.2.1	Fermions . . . . .	10
2.2.2	Bosons . . . . .	10
2.3	Electroweak Interactions in the Standard Model: Spontaneously Broken Local $SU(2)_L \times U(1)_Y$ Symmetry . . . . .	11
2.3.1	Global $U(1)$ Symmetry . . . . .	12
2.3.2	Local $U(1)$ Symmetry . . . . .	13
2.3.3	Global $SU(2)$ Symmetry . . . . .	14
2.3.4	Local $SU(2)$ Symmetry . . . . .	15
2.3.5	Isospin, Weak Hypercharge, and $SU(2) \times U(1)$ Symmetry . . . . .	17
2.4	The Higgs Mechanism and Fermion Masses . . . . .	20
2.4.1	$SU(2) \times U(1)$ Symmetry For Massless Fermions . . . . .	20
2.4.2	The Higgs Mechanism in Fermion Mass Generation . . . . .	22
2.5	The Higgs Field, Quark Mixing, and the $CKM$ Matrix . . . . .	24
2.6	Higgs Boson Associated Production with a Vector Boson . . . . .	25
2.7	Higgs Boson Decay ( $H \rightarrow WW$ ) . . . . .	28
<b>3</b>	<b>The Tevatron</b>	<b>30</b>
3.1	Beginning of the Beam: Cockcroft-Walton . . . . .	30
3.2	LINAC: The Linear Accelerator . . . . .	31
3.3	Booster . . . . .	31
3.4	Main Injector . . . . .	31
3.5	Anti-protons . . . . .	31
3.6	The Tevatron . . . . .	32
3.7	The Performance of the Tevatron in Run II . . . . .	34
<b>4</b>	<b>The CDF II Detector</b>	<b>35</b>
4.1	CDF Coordinates . . . . .	36
4.2	Trackers . . . . .	37
4.2.1	The Silicon Detectors . . . . .	37
4.2.2	Central Outer Tracker . . . . .	39
4.3	Calorimeters . . . . .	39
4.3.1	CDF Central Electromagnetic Calorimeter (CEM) . . . . .	40
4.3.2	CDF Hadronic Calorimeters (CHA, WHA) . . . . .	40
4.3.3	CDF Forward Calorimeters (PEM, PHA) . . . . .	40
4.4	Muon Detectors . . . . .	41

4.5	CDF Detector Summary for $VH \rightarrow VWW \rightarrow$ Trileptons . . . . .	41
<b>5</b>	<b>Triggers, Datasets, and Event Selection</b>	<b>43</b>
5.1	Level 1 . . . . .	43
5.2	Level 2 . . . . .	43
5.3	Level 3 . . . . .	43
5.4	Trigger Paths (“Datasets”) of the $H \rightarrow WW$ Group . . . . .	44
5.4.1	ELECTRON_CENTRAL18 . . . . .	44
5.4.2	MUON_CMUP18 . . . . .	44
5.4.3	MUON_CMX18 . . . . .	45
5.4.4	MET_PEM . . . . .	45
5.4.5	MUON_CMP18_PHI_GAP . . . . .	46
<b>6</b>	<b>High <math>p_T</math> Object Identification in the High Mass Higgs Boson Search</b>	<b>47</b>
6.1	Lepton Identification . . . . .	47
6.1.1	Electron ID . . . . .	47
6.1.2	Muon ID . . . . .	47
6.1.3	Unspecified Track ID . . . . .	47
6.2	Missing Transverse Energy ( $\cancel{E}_T$ ) . . . . .	47
6.3	Fake Leptons . . . . .	47
6.4	Lepton Efficiencies . . . . .	47
6.5	Lepton ID Scale Factors . . . . .	47
<b>7</b>	<b>Computations with Artificial Neural Networks</b>	<b>48</b>
<b>8</b>	<b>Statistics of Confidence Level Limits In the Search for New Physics</b>	<b>49</b>
<b>9</b>	<b>The High Mass Higgs Boson Analysis in the Trilepton Signature</b>	<b>50</b>
9.1	Motivation for Trileptons . . . . .	50
9.2	Event Summary and Signatures of the $WH$ and $ZH$ Trilepton Analyses . .	52
9.2.1	Lepton Selection . . . . .	52
9.2.2	Trilepton Signal Regions Defined . . . . .	54
9.2.3	Backgrounds . . . . .	55
9.2.4	Signal Yields in the <i>NoZPeak</i> and <i>InZPeak</i> Regions . . . . .	57
9.3	Neural Net . . . . .	58
9.4	Control Regions . . . . .	67
9.5	Systematic Errors . . . . .	70
9.6	Results . . . . .	74
<b>10</b>	<b>Conclusions</b>	<b>79</b>

<b>A Appendix</b>	<b>82</b>
A.1 Neural Net Input Variables . . . . .	82
A.2 Input Variables in Control Regions . . . . .	98
A.3 $U(1)$ Global Symmetry Breaking . . . . .	108
A.4 $U(1)$ Local Symmetry Breaking . . . . .	112
A.5 $SU(2)$ Global Symmetry Breaking . . . . .	115
A.6 $SU(2)$ Local Symmetry Breaking . . . . .	117
A.7 The Higgs Mechanism in the $SU(2) \times U(1)$ Local Spontaneous Symmetry Breaking . . . . .	121
A.8 The $SU(2)_L \times U(1)_Y$ Local Gauge Invariant Lagrangian and the [massless] Fermions . . . . .	125
A.8.1 The $\mathcal{L}_R$ terms . . . . .	126
A.8.2 The $\mathcal{L}_L$ terms . . . . .	126
A.8.3 Find the $Z$ -boson and Photon Interactions . . . . .	129
A.9 The Higgs Mechanism and Fermion Mass Generation . . . . .	134
A.10 The Higgs Sector in Standard Model Electroweak Physics . . . . .	138
A.11 $WH$ Production Amplitude . . . . .	142
A.12 $H \rightarrow WW$ Lagrangian Density To Invariant Amplitude . . . . .	149
A.13 $H \rightarrow WW$ Invariant Amplitude to Decay Rate ( $\Gamma$ ) . . . . .	151

# Forward

The field of particle physics studies the most fundamental constituents of nature and the forces by which they interact. It is the study of the deepest realities of the universe from which all else manifests. In a physical universe, everything from the human brain to the sun and beyond are composed of matter that is reducible to those fundamental constituents that compose them; hence, the mechanism by which the human brain generates consciousness to the mechanism by which the sun generates light and energy are manifestations of the interactions between the particles that compose them. One small piece of the universe composed of such fundamental particles and functioning via the natural forces governing their interactions presents here an equivalently modest attempt by the universe to understand itself.

## 1 Introduction

The Standard Model of particle physics describes the known fundamental constituents of matter (categorized as “quarks” and “leptons”) and the particles that carry the forces by which they interact. That is, the electromagnetic force arises from the exchange of a “photon” ( $\gamma$ ); the weak force arises from the exchange of a “weak vector boson” ( $W^+, W^-, Z$ ); and the strong force arises from the exchange of a “gluon” ( $g$ ). The final piece of the Standard Model is the Higgs boson, which remains the sole particle whose existence or non-existence has yet to be confirmed experimentally. If the Higgs boson does exist as postulated in the Standard Model, it is a key consequence of our understanding of the origin of mass in the universe.

The Higgs boson was postulated in 1964 by Peter Higgs as a consequence of a mathematical mechanism that rectified an apparent contradiction in the fledgling quantum field theories being formulated at that time. With Schrodinger equation-based quantum mechanics describing the physics of very small particles and special relativity describing the physics of high energy motion, physicists were naturally attempting to formulate a theory consistent with both realms—effectively, the physics of high energy fundamental particles. Before the Higgs mechanism was postulated, there was an inherent contradiction. Particles are known to have nonzero mass from experience and experiment, but introducing mass terms directly into the Lagrangian breaks certain symmetry requirements. The Higgs mechanism resolved the problem and lead to the formulation of a coherent quantum field theory that allows for massive fundamental particles.

The first serious experimental search for the Higgs boson was conducted by the Large Electron-Positron Collider (LEP) at the European Organization for Nuclear Research (CERN “*Organisation Europenne pour la Recherche Nucléaire*”) which operated from 1989 to 2000. The Higgs sector of the Standard Model does not directly postulate or predict the mass of the Higgs boson, so a wide range of possible masses must be explored. LEP experimentally ruled out the existence of a Standard Model Higgs boson for masses

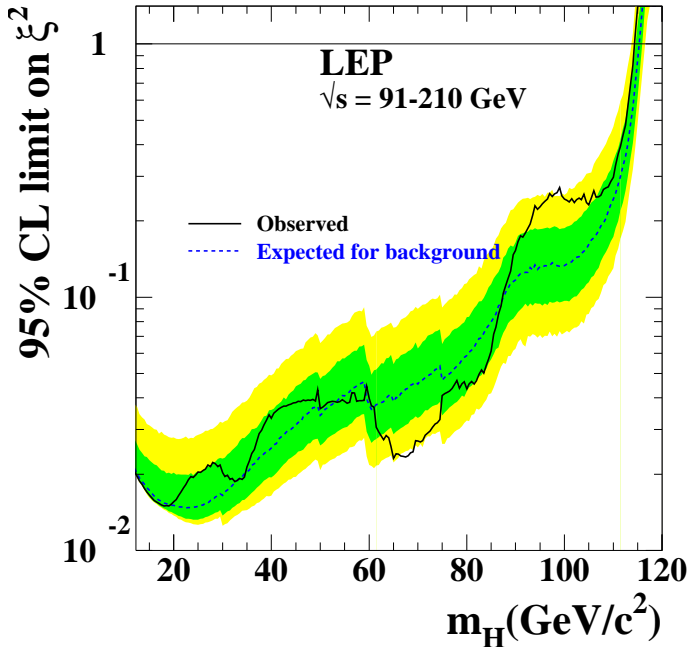


Figure 1: Experimental exclusion limits at 95% confidence level from the LEP collider at CERN.

$m_H < 114 \text{ GeV}/c^2$ . The LEP exclusion limits are shown in figure 1.

The Tevatron, a proton-antiproton ( $p\bar{p}$ ) collider at the Fermi National Accelerator Laboratory, has carried the torch since LEP was dismantled in 2000 to construct the Large Hadron Collider (LHC) in its place. In  $p\bar{p}$  interactions, the search for the Higgs boson is divided between a “high mass” region ( $114 < m_H < 135 \text{ GeV}/c^2$ ) and a “low mass” region ( $135 < m_H < 200 \text{ GeV}/c^2$ ). Observe in figure 2 that this low mass region corresponds to masses of the Higgs boson where it decays primarily to  $b$ -quark pairs and the high mass region corresponds to masses where it decays primarily to vector boson ( $W^+, W^-, Z$ ) pairs. This thesis contributes a new search for the Standard Model Higgs boson in the high mass region ( $H \rightarrow WW$ ), orthogonal to and augmenting the search that preceded it.

Until recently, the high mass Higgs search exclusively studied  $H \rightarrow WW$  interactions that result in a two-lepton signature [3]. The reason is that the dominant production of a high mass Higgs boson is via gluon fusion, which is then best studied in the case where both Higgs- $W$ -bosons decay leptonically. The cases of having one or both Higgs- $W$ -bosons decay hadronically is severely limited by large backgrounds. This thesis presents for the first time a search for a high mass Higgs boson in the three-lepton signature, shifting focus to the associated production channels  $WH \rightarrow WWW \rightarrow l\nu, l\nu, l\nu$  and  $ZH \rightarrow ZWW \rightarrow ll, l\nu, \text{jet}$ , where the jet is the result of a  $W$ -boson decaying hadronically.

This dissertation focuses on two new regions chosen specifically to isolate the  $WH \rightarrow WWW$  and  $ZH \rightarrow ZWW$  associated production processes because of their unique char-

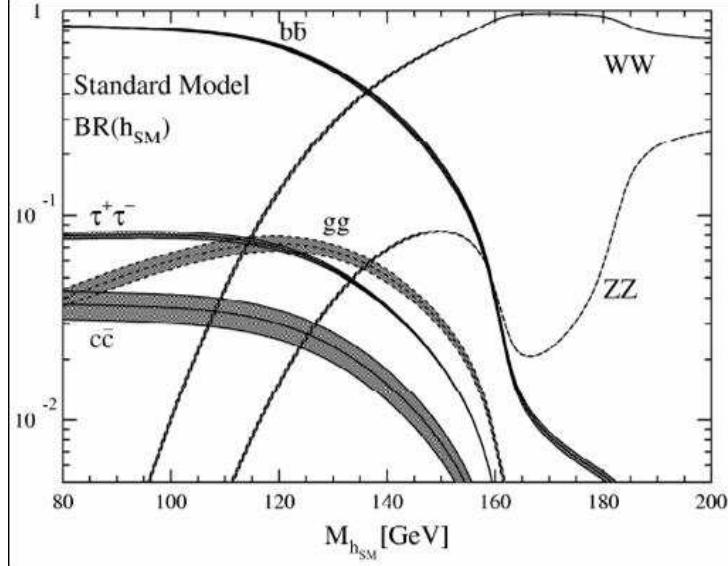


Figure 2: Standard Model branching ratios for the Higgs boson at the Tevatron.

acteristics. The signal of  $WH$  associated production in the three lepton bin requires the  $W$ -boson to radiate a standard model Higgs boson that decays to two more  $W$ -bosons. Subsequently, all three  $W$ -bosons decay leptonically to produce a trilepton signature. Similarly, the  $ZH$  associated production signal requires a  $Z$ -boson to radiate a standard model Higgs boson that decays to two  $W$ -bosons. The  $Z$ -boson then decays to two leptons and we need one of the Higgs- $W$ -bosons to decay leptonically and the other hadronically to produce an exact three-lepton signature (four-lepton events are rejected from this analysis). Correspondingly, the two new regions we introduce for trileptons in  $H \rightarrow WW$  are denoted trilepton-*NoZPeak* (for the  $WH$ -centered analysis) and trilepton-*InZPeak* (for the  $ZH$ -centered analysis) to be defined in section 9.2.

The three lepton +  $\cancel{E}_T$  signature with an unspecified number of jets is a relatively complex event topology that introduces a correspondingly large number of variables that describe the event. This is a fortuitous circumstance as it allows the formulation of many complex variables that powerfully discriminate the signals from backgrounds in both of these new trilepton-*NoZPeak* ( $WH$  analysis) and trilepton-*InZPeak* ( $ZH$  analysis) regions. Together, they represent a strong addition to the search for the standard model Higgs boson.

We will see in the Results section (section 9.6) that, at  $m_H = 160$  GeV, the  $WH$  analysis expected limits reach 8.9 times the standard model cross section; the  $ZH$  analysis is set at 12.6 times the expected standard model cross section; and the combined trilepton analysis is set at 6.3 times the expected standard model cross section. Finally, for the combined  $H \rightarrow WW$  analysis result, in the 165 GeV bin the expected limit drops from 1.21[4] to 1.15 while the observed limit drops from 1.23 to 1.08. As such, we are poised to begin excluding the standard model Higgs boson at 95% confidence level with CDF-only analyses in short order.

## 2 The Higgs Mechanism and the Standard Model of Particle Physics

### 2.1 Intro. to the Standard Model of Particle Physics

The “Standard Model” of particle physics is a collection of gauge “quantum field theories,” reformulations of Schrödinger-based quantum mechanics that are consistent with Einstein’s special theory of relativity. Of the four known forces in nature (gravity, electromagnetism, weak force, and strong force), the Standard Model incorporates and establishes a quantum theory for all but gravity. Although hypothesized models exist, there is not yet a quantum theory of gravity, which is instead described macroscopically by Einstein’s general theory of relativity.

The standard model is based on the gauge group formed from the product space of three special unitary gauge groups:  $SU(3)_C \times SU(2)_L \times U(1)_Y$ . The  $SU(3)_C$  component represents the symmetry group describing the strong force interaction, with the  $C$  subscript referring to “color charge” of quantum chromodynamics. The rest of the gauge group is the “electroweak” portion of the Standard Model, represented by the  $SU(2)_L \times U(1)_Y$  group. The “ $L$ ” refers to the  $SU(2)$  group’s containing particularly *left-handed* weak doublets and the “ $Y$ ” (a conserved quantum number) refers to the  $U(1)$  group’s *right-handed* weak hypercharge singlets.

The Standard Model also contains known particles that interact via these forces. The known particles are categorized as “fermions” (see section 2.2.1) and “bosons” (see section 2.2.2). The fermions of the Standard Model are then divided among “quarks” and “leptons,” which are the known fundamental constituents of matter. The forces by which they interact manifest from the exchange of gauge bosons that exist as a consequence of various symmetries in the Standard Model’s  $SU(3)_C \times SU(2)_L \times U(1)_Y$  gauge group. The existence of all the quarks, leptons, and gauge bosons described so far have been verified experimentally.

There does remain one last constituent of the Standard Model has not yet been experimentally verified: the Higgs boson. Unlike the other bosons that are related to the forces of nature, the Higgs boson is postulated as a consequence of a spontaneously broken symmetry in the electroweak sector ( $SU(2)_L \times U(1)_Y$ ) which is hypothesized to be the property of the universe that results in fundamental particles and weak gauge bosons with non-zero mass. The rest of this chapter will describe the function of the Higgs boson in the Standard Model and the focus of this thesis is on a new contribution to the experimental search for the Higgs boson at the CDFII experiment.

### 2.2 Elementary Particles in the Standard Model

Particle physics is the study of the most fundamental known constituents of matter in the universe and the forces by which they interact. The “Standard Model” of particle physics

is composed of all known fundamental particles, plus the postulated Higgs boson and the forces by which they interact.

We separate the known fundamental particles of the Standard Model into two categories: fermions and bosons.

### 2.2.1 Fermions

$u^{\pm\frac{2}{3}}$ “up”	$c^{\pm\frac{2}{3}}$ “charm”	$t^{\pm\frac{2}{3}}$ “top”
$d^{\mp\frac{1}{3}}$ “down”	$s^{\mp\frac{1}{3}}$ “strange”	$b^{\mp\frac{1}{3}}$ “bottom”

Table 1: Quarks of the Standard Model. The superscript indicates the particles’ electric charges (the top charge refers to the “particles” while the bottom charge refers to the “anti-particles”). As fermions, all quarks have spin of 1/2.

$e^{\mp 1}$ “electron”	$\mu^{\mp 1}$ “muon”	$\tau^{\mp 1}$ “tau”
$\nu_e$ “electron neutrino”	$\nu_\mu$ “muon neutrino”	$\nu_\tau$ “tau neutrino”

Table 2: Leptons of the Standard Model. The particles in the top row exist as both “matter” (electric charge of  $-1$ ) and “anti-matter” (electric charge of  $+1$ ). The bottom row consists of the associated “neutrinos” which have no electric charge. As fermions, all particles listed here have spin 1/2.

Fundamental particles are known from experiment to have intrinsic angular momentum denoted colloquially as “spin.” In quantum mechanical systems, particles are capable of assuming only discrete spin states, just as they are also capable of only discrete energy states. Fermions are defined as particles with half-integer spin magnitudes:  $1/2, 3/2, 5/2, \dots$ , where the spin is given in units of the Plank constant  $\hbar = 6.582 \times 10^{-16}(\text{eV} \cdot \text{s})$ [12]. Physically,  $\hbar$  relates cycles (in radians because  $\hbar = h/2\pi$ ) to energy as  $E = \hbar\omega$ . All the fundamental particles listed in tables 1 and 2 have spin magnitude 1/2.

### 2.2.2 Bosons

Bosons are defined as particles with integer spin magnitudes:  $0, 1, 2, \dots$ . The three forces of nature described by the Standard Model manifest from an exchange of a boson among the quarks and leptons. These force-carrying bosons arise from symmetries in the Standard Model’s  $SU(3)_C \times SU(2)_L \times U(1)_Y$  gauge group. They are:

- *photons ( $\gamma$ )*: The gauge boson of the  $SU(2)_L \times U(1)_Y$  group which manifests as the electromagnetic force.

- $W^+, W^-, Z^0$ : The gauge bosons of the  $SU(2)_L \times U(1)_Y$  group which manifest as the weak force.
- *gluons (g)*: The gauge bosons of the  $SU(3)_C$  group which manifest as the strong force.

The Standard Model Higgs boson is unique in that it is not associated with a force of nature and that it arises as a consequence of a broken symmetry referred to as “electroweak symmetry breaking.” We will look at this electroweak symmetry breaking in section 2.3. Then in section 2.4, we will see how the fermion masses are consequences of the Higgs field. Section 2.5 will briefly discuss the role the Higgs boson plays in quark mixing and the CKM matrix. Finally, sections 2.6 and 2.7 will discuss phenomenological calculations of Higgs production and decay, respectively, involved in the experimental search covered by this thesis.

### 2.3 Electroweak Interactions in the Standard Model: Spontaneously Broken Local $SU(2)_L \times U(1)_Y$ Symmetry

The forces of nature appear to manifest from inherent symmetries. The logical foundation of a physical system is a postulated “lagrangian,” from which the interactions of nature can then be derived. When the fields in a lagrangian can be transformed by an arbitrary element of a particular algebraic “group” and the lagrangian (and therefore the consequential physics) is left unchanged, then we say the lagrangian is “symmetric” to transformations under that particular group.

**Definition 1** *A group is a set  $G$  along with any binary operation  $\star$  on  $G$  that satisfies the following three axioms[15]:*

- *Associativity*:  $(a \star b) \star c = a \star (b \star c)$ ,  $\forall a, b, c \in G$
- *Identity*:  $\exists e \in G$ , denoted the identity, such that  $\forall a \in G$  we have  $a \star e = e \star a = e$ .
- *Inverse*:  $\forall a \in G$ ,  $\exists a^{-1} \in G$ , denoted the inverse of  $a$ , such that  $a \star a^{-1} = a^{-1} \star a = e$ .

For electroweak physics, we will be concerned with just two groups:  $U(1)$  and  $SU(2)$ . Both of these groups are “unitary,” which is critical to establishing such symmetries in the lagrangian.

**Definition 2** *A unitary matrix is an  $n \times n$  complex matrix  $M$  that satisfies  $M^\dagger M = M M^\dagger = I_n$ , where  $I_n$  is the  $n$ -dimensional identity matrix and  $\dagger$  denotes the Hermitian conjugate (complex conjugate and transpose).*

### 2.3.1 Global $U(1)$ Symmetry

**Definition 3** *The unitary group  $U(n)$  is a group of unitary  $n \times n$  matrices with the binary operation of matrix multiplication. The  $U(1)$  unitary group is then the group of complex numbers that equal 1 when multiplied by their complex conjugate, effectively becoming the group of rotations in the complex plane via Euler's relation:  $\cos x + i \sin x = e^{ix}$ .*

Let's begin by assuming a scalar, complex particle  $\phi = \frac{1}{\sqrt{2}}(\phi_1 + i\phi_2)$  and the corresponding Klein-Gordon lagrangian:

$$\mathcal{L} = (\partial_\mu \phi)^\dagger (\partial^\mu \phi) - m_0^2 \phi^\dagger \phi - \frac{1}{4} \lambda (\phi^\dagger \phi)^2 \quad (1)$$

This lagrangian is invariant to a  $U(1)$  "global" (not dependent on spacetime coordinate) transformation  $\phi \rightarrow \phi' = e^{i\alpha} \phi$  because of the unitary nature of  $U(1)$ [14]. Lagrangians have the structure of kinetic energy minus potential energy, so the potential described here is  $V(\phi) = m_0^2 \phi^\dagger \phi + \frac{1}{4} \lambda (\phi^\dagger \phi)^2$ . This potential is symmetric in the complex plane and has an extremum at the origin. If  $m_0^2 > 0$ , then the extremum is a minimum and we determine the particle spectrum by calculating perturbative oscillations about the minimum. The system describes a complex scalar particle of mass  $m_0$ .

However, Higgs physics in the Standard Model is based on *broken* symmetry, so assume  $m_0^2 < 0$ . Now the extremum at the origin is unstable and we instead have a minima circle of radius  $v$ . To find the particle spectrum in this case, express the field  $\phi$  in polar coordinates

$$\phi(x) = \underbrace{\frac{\rho(x)}{\sqrt{2}}}_{\text{Radial Perturbation}} \cdot \underbrace{e^{i\theta(x)}}_{\text{Angular Perturbation}} \quad (2)$$

$$\rho(x) \equiv v + h(x) \quad (3)$$

and expand about any arbitrary point in the minima manifold. Substituting this form back into the lagrangian yields

$$\mathcal{L} = \frac{1}{2}(\partial_\mu h)^2 + v(\partial_\mu h) + \frac{1}{2}v^2 + \left( \frac{1}{2v^2}h^2 + \frac{1}{v^2}hv + \frac{1}{2v^2}v^2 \right) (\partial_\mu \theta)^2 \quad (4)$$

$$- \frac{1}{2}m_0^2 h^2 - m_0^2 vh - \frac{1}{2}m_0^2 v^2 - \frac{1}{16}\lambda(h+v)^4 \quad (5)$$

$$= \frac{1}{2}(\partial_\mu h)^2 + \frac{1}{2}(\partial_\mu \theta)^2 - \frac{1}{2}m_0^2 h^2 + \dots \quad (6)$$

$$(7)$$

Hence, we find that the field perturbation in the radial direction  $h$  acquires a mass (note: the direction that climbs the potential) while the angular field perturbation  $\theta$  (note:

directed within the minima manifold) does not acquire a mass. So field perturbations that climb the potential represent particle states that acquire mass, while not climbing away from the minima manifold of the potential keeps the particle massless. Also, given this parametrization of  $\phi(x)$ , the vacuum expectation value is

$$\langle 0 | \phi | 0 \rangle = \frac{v}{\sqrt{2}} \quad (8)$$

See appendix A.3 for a detailed calculation of these results.

This is a situation where a symmetric field potential is spontaneously broken in nature and this breaking manifests in a physical system different from the situation of the origin being a stable extremum, in which case the symmetry would not spontaneously break in nature.

### 2.3.2 Local $U(1)$ Symmetry

The global  $U(1)$  symmetry of section 2.3.1 is a special case of “local” (the transformation *does* depend on spacetime coordinate)  $U(1)$  symmetry. Now, let the angle of rotation in the complex plane  $\alpha$  depend on coordinate:  $\phi \rightarrow \phi' = e^{i\alpha(x)}\phi$ . The lagrangian (eqn. 1) of the previous section is not invariant to local  $U(1)$  transformations.

To have a lagrangian that is invariant to  $U(1)$  local transformations, we must replace the derivative with a “covariant derivative”

$$\partial_\mu \rightarrow D_\mu = \partial_\mu + iqA_\mu \quad (9)$$

Thus, to keep the lagrangian invariant, we are postulating the existence of a “gauge field”  $A_\mu$  and must introduce kinetic terms  $F^{\mu\nu} = \partial^\mu A^\nu - \partial^\nu A^\mu$  for it. So the new postulated  $U(1)$  locally invariant lagrangian is

$$\mathcal{L} = [(\partial^\mu + iqA^\mu)\phi]^\dagger [(\partial_\mu + iqA_\mu)\phi] - \frac{1}{4}F_{\mu\nu}F^{\mu\nu} - \frac{1}{4}\lambda(\phi^\dagger\phi)^2 - m_0^2(\phi^\dagger\phi) \quad (10)$$

$$(11)$$

where the gauge field itself transforms as

$$A^\mu(x) \rightarrow A'^\mu(x) = A^\mu(x) + \frac{1}{q}\partial^\mu\alpha(x) \quad (12)$$

(see appendix A.4). If we then use the field parametrization as in the  $U(1)$  global case (eqn. 2) we find that the field equation is

$$\square A^\nu - \partial^\nu(\partial_\mu A^\mu) = -v^2q^2 \left( A^\nu - \frac{\partial^\nu\theta}{vq} \right) \quad (13)$$

where on the right hand side we see the angular field perturbation  $\theta$  in a term that looks just like the form of the gauge field transformation. As such, define

$$A'^\nu = A^\nu - \frac{\partial^\nu \theta}{vq} \quad (14)$$

Then the field equation becomes

$$(\square + v^2 q^2) A'^\nu - \partial^\nu \partial_\mu A'^\mu = 0 \quad (15)$$

Thus, because of  $U(1)$  local gauge symmetry, we have two physical consequences: first, we must postulate the existence of a gauge field  $A_\mu$ ; second, the symmetry allows us to choose a particular  $U(1)$  transformation that causes the gauge field  $A_\mu$  to absorb the  $\theta$  term and become massive. This technique will be critical for computing the weak vector bosons and the photon. See appendix A.4 for a detailed calculation of these results.

### 2.3.3 Global $SU(2)$ Symmetry

**Definition 4** *The special unitary groups  $SU(n)$  are groups of  $n \times n$  matrices with determinant 1 that have the binary operation matrix multiplication. The particular case of  $n = 2$  is critical to electroweak physics.*

Consider a doublet of complex scalar particles

$$\phi = \begin{bmatrix} \phi^+ \\ \phi^0 \end{bmatrix} = \begin{bmatrix} \frac{1}{\sqrt{2}}(\phi_1 + i\phi_2) \\ \frac{1}{\sqrt{2}}(\phi_3 + i\phi_4) \end{bmatrix} \quad (16)$$

where  $\phi^+$  destroys positively charged particles and creates negatively charged particles, and  $\phi^0$  destroys neutral particles and creates neutral antiparticles.

Postulate the form of the lagrangian as a direct generalization of section 2.3.1.

$$\mathcal{L} = (\partial_\mu \phi)^\dagger (\partial^\mu \phi) - m_0^2 \phi^\dagger \phi - \frac{\lambda}{4} (\phi^\dagger \phi)^2 \quad (17)$$

where  $m_0^2 < 0$ . This lagrangian is not only invariant to global  $SU(2)$  transformations, but also to the global  $U(1)$  transformations of section 2.3.1 (and appendix A.3). We treat the global  $SU(2)$  case here, so  $\alpha$  is not dependent on spacetime coordinate. The  $SU(2)$  transformation takes a form similar to the  $U(1)$  case:

$$\phi \rightarrow \phi' = e^{-\frac{i}{2} \vec{\alpha} \cdot \vec{\tau}} \phi \quad (18)$$

where the  $\vec{\tau}$  are the Pauli spin matrices.

To determine the particle spectrum, we again want to find the minima manifold of the potential and compute oscillations from a point in it. The minimum is found at

$$\frac{\partial \mathcal{L}}{\partial(\phi^\dagger\phi)} = -m_0^2 - \frac{\lambda}{2}(\phi^\dagger\phi)_{\min} = 0 \quad (19)$$

$$(\phi^\dagger\phi)_{\min} = \frac{-2m_0^2}{\lambda} \equiv \frac{v^2}{2} \quad (20)$$

As before, we take the minimum to be the vacuum.

$$\langle 0 | \phi^\dagger\phi | 0 \rangle = \frac{v^2}{2} = \langle 0 | \phi_1^2 + \phi_2^2 + \phi_3^2 + \phi_4^2 | 0 \rangle \quad (21)$$

To obtain the particle spectrum we expand the fields  $\phi$  about the choice of vacuum. Again, rather than a single point, we have a whole space of minima to choose from. Let,

$$\langle 0 | \phi | 0 \rangle = \begin{bmatrix} 0 \\ \frac{v}{\sqrt{2}} \end{bmatrix} \quad (22)$$

Oscillations about this vacuum choice are parametrized by

$$\phi = e^{-\frac{i}{2}(\vec{\theta}(x)\cdot\vec{\tau})v} \begin{bmatrix} 0 \\ \frac{1}{\sqrt{2}}(v + H(x)) \end{bmatrix} \quad (23)$$

We now have three “angular” field oscillations  $\vec{\theta}$  and one radial  $H(x)$ . Just as in the  $U(1)$  case, the angular oscillations are massless particles while  $H(x)$  is massive. The lagrangian becomes:

$$\mathcal{L} = \frac{1}{8v^2}(\partial^\mu\vec{\theta}\cdot\vec{\tau})(\partial_\mu\vec{\theta}\cdot\vec{\tau})(v + H)^2 + \frac{1}{2}(\partial^\mu H)(\partial_\mu H) - \frac{m_0^2}{2}v^2 - \frac{m_0^2}{2}vH - \frac{m_0^2}{2}H^2 - \frac{\lambda}{4}(v + H)^4 \quad (24)$$

where we see mass terms for  $H(x)$  and no mass terms for the  $\vec{\theta}$  fields. We will again exploit the symmetry to gauge the  $\vec{\theta}$  fields away. See appendix A.5 for a detailed calculation of these results.

### 2.3.4 Local $SU(2)$ Symmetry

To generalize to local  $SU(2)$  symmetry, we again must assume  $\vec{\alpha}$  to be spacetime coordinate dependent.

$$\phi(x) \rightarrow \phi'(x) = e^{\frac{ig}{2}\vec{\tau}\cdot\vec{\alpha}(x)}\phi(x) \quad (25)$$

where the factor  $g$  is inserted to represent the coupling strength.

Just as in the local  $U(1)$  case, our particles are not covariant under this transformation unless we replace the derivatives with suitable covariant derivatives.[13] Our  $SU(2)$  covariant derivative is

$$D^\mu \equiv \partial^\mu + \frac{ig}{2} \vec{\tau} \cdot \vec{W}^\mu \quad (26)$$

where  $\vec{W}^\mu \equiv (W_1^\mu, W_2^\mu, W_3^\mu)$ , a slight precursor to the weak vector bosons. These three gauge fields transform as (see appendix A.6 for this derivation)

$$\vec{W}'^\mu = \vec{W}^\mu - \partial^\mu \vec{\epsilon}(x) - g \left[ \vec{\epsilon}(x) \times \vec{W}^\mu \right] \quad (27)$$

Now that we know how the gauge field and the covariant derivative transform with an  $SU(2)$  gauge transformation, we can compute the consequences from our basic postulated lagrangian, which can now be repostulated in  $SU(2)$  invariant form

$$\mathcal{L} = (D_\mu \phi)^\dagger (D^\mu \phi) - m_0^2 \phi^\dagger \phi - \frac{\lambda}{4} (\phi^\dagger \phi)^2 - \frac{1}{4} \vec{W}_{\mu\nu} \cdot \vec{W}^{\mu\nu} \quad (28)$$

where  $\vec{W}_{\mu\nu} \equiv \partial_\mu \vec{W}_\nu - \partial_\nu \vec{W}_\mu - g \vec{W}_\mu \times \vec{W}_\nu$ , where the last term is necessary because of the non-Abelian nature of the  $SU(2)$  group.

Note that if  $m_0^2 > 0$ , then we just have a system of four scalar particles of mass  $m_0$ . However, we are interested in the  $m_0^2 < 0$  symmetry breaking case. Just as for the  $U(1)$  case, we want to find the minima manifold.

$$\frac{\partial \mathcal{L}}{\partial (\phi^\dagger \phi)} = 0 \quad (29)$$

$$(\phi^\dagger \phi)_{\min} = -\frac{2m_0^2}{\lambda} = \frac{1}{2} (\phi_1^2 + \phi_2^2 + \phi_3^2 + \phi_4^2) \quad (30)$$

We must choose some particular point on the minima manifold upon which to expand and calculate the particle spectrum, so choose  $\phi_1 = \phi_2 = \phi_4 = 0$  and then we are left with

$$\frac{1}{2} \phi_3^2 = \frac{-2m_0^2}{\lambda} \quad (31)$$

$$\phi_3 = 2 \sqrt{\frac{-m_0^2}{\lambda}} \equiv v \quad (32)$$

Then our complex field doublet at this minimum becomes

$$\phi_{\min} = \frac{1}{\sqrt{2}} \begin{bmatrix} \phi_1 + i\phi_2 \\ \phi_3 + i\phi_4 \end{bmatrix} = \frac{1}{\sqrt{2}} \begin{bmatrix} 0 \\ v \end{bmatrix} \quad (33)$$

Again, completely analogous to the  $U(1)$  case, we can parametrize perturbations about this minimum as

$$\phi(x) = \frac{\rho(x)}{\sqrt{2}} e^{\frac{i}{v} \vec{\tau} \cdot \vec{\theta}(x)} \quad , \text{ where} \quad (34)$$

$$\rho(x) = \begin{bmatrix} 0 \\ v + h(x) \end{bmatrix} \quad (35)$$

and analogous to the  $U(1)$  case again, we can choose particular  $SU(2)$  transformations to gauge away the  $\vec{\theta}$  fields to be left with massive gauge bosons  $\vec{W}$  and  $H(x)$ . This is another example of the Higgs mechanism.

See appendix A.6 for a detailed calculation of these results.

### 2.3.5 Isospin, Weak Hypercharge, and $SU(2) \times U(1)$ Symmetry

We have now discussed the two basic symmetries, invariance to  $U(1)$  and  $SU(2)$  transformations that are fundamental to understanding electroweak physics. Just as translational symmetry implied conservation of momentum and temporal symmetry implies conservation of energy in classical physics, for example, these symmetries also imply conserved quantities or “quantum numbers.” From  $U(1)$  symmetry, we have conserved quantum number  $Y$  (“weak hypercharge”); and from  $SU(2)$  symmetry, we have conserved quantum number  $t_3$  (“weak isospin”). In this section, we explore the physics implied by symmetries under the product group  $SU(2) \times U(1)$  and see that our choice of location on the minima manifold to expand on will leave the vacuum invariant to a transformation of the form ‘ $U(1) + 3^{\text{rd}}$  component of  $SU(2)$ .’  $Y$  and  $t_3$  will together define the electric charge of the fundamental particles according to

$$Q = t_3 + \frac{Y}{2} \quad (36)$$

Examples of values for the first generation of quarks and leptons are given in tables 3 and 4.

Leptons	$Q$	$t_3$	$Y$
$\nu_e$	0	$\frac{1}{2}$	-1
$e_L^-$	-1	$-\frac{1}{2}$	-1
$e_R^-$	-1	0	-2

Table 3: Weak isospin and hypercharge quantum numbers for the first generation of leptons. Left and right handed electrons are listed separately.[14]

For a theory that is invariant to local transformations, we must introduce three  $SU(2)$  gauge fields (see appendix A.6) and one  $U(1)$  gauge field (see appendix A.4). Denote

Quarks	$Q$	$t_3$	$Y$
$u_L$	$\frac{2}{3}$	$\frac{1}{2}$	$\frac{1}{3}$
$d_L$	$-\frac{1}{3}$	$-\frac{1}{2}$	$\frac{1}{3}$
$u_R$	$\frac{2}{3}$	0	$\frac{1}{3}$
$d_R$	$-\frac{1}{3}$	0	$-\frac{2}{3}$

Table 4: Weak isospin and hypercharge quantum numbers for the first generation of quarks. Left and right handed quarks are listed separately.[14]

them here as  $W_i^\mu(x)$  for  $i = 1, 2, 3$  and  $B^\mu(x)$ , respectively. Also, the derivatives must be replaced with a covariant derivative for both  $U(1)$  and  $SU(2)$ .

$$D^\mu \phi = \left( \partial^\mu + \underbrace{\frac{ig}{2} \vec{\tau} \cdot \vec{W}^\mu}_{SU(2)\text{piece}} + \underbrace{\frac{ig'Y}{2} B^\mu}_{U(1)\text{piece}} \right) \phi \quad (37)$$

Kinetic terms for the new gauge fields must also be included.

$$\vec{F}^{\mu\nu} = \partial^\mu \vec{W}^\nu - \partial^\nu \vec{W}^\mu - g \vec{W}^\mu \times \vec{W}^\nu \quad (38)$$

$$G^{\mu\nu} = \partial^\mu B^\nu - \partial^\nu B^\mu \quad (39)$$

So the new full lagrangian is

$$\mathcal{L} = (D_\mu \phi)^\dagger (D^\mu \phi) + m_0^2 \phi^\dagger \phi - \frac{\lambda}{4} (\phi^\dagger \phi)^2 - \frac{1}{4} \vec{F}_{\mu\nu} \cdot \vec{F}^{\mu\nu} - \frac{1}{4} G_{\mu\nu} G^{\mu\nu} \quad (40)$$

(41)

For electroweak theory, we should be left with three massive gauge bosons ( $W^\pm, Z$ ) and one massless gauge boson (photon). Being massless, the photon corresponds to some symmetry that is left unbroken. Weinberg suggested [13]

$$\langle 0 | \phi | 0 \rangle = \begin{bmatrix} 0 \\ \frac{\sqrt{2}m_0}{\sqrt{\lambda}} \end{bmatrix} \equiv \begin{bmatrix} 0 \\ \frac{v}{\sqrt{2}} \end{bmatrix} \quad (42)$$

This choice leaves the vacuum invariant to a transformation of  $U(1)$ + third component of  $SU(2)$ . That is,

$$(1 + \tau_3) \langle 0 | \phi | 0 \rangle = (1 + \tau_3) \begin{bmatrix} 0 \\ \frac{v}{\sqrt{2}} \end{bmatrix} = \begin{bmatrix} 2 & 0 \\ 0 & 0 \end{bmatrix} \begin{bmatrix} 0 \\ \frac{v}{\sqrt{2}} \end{bmatrix} = \begin{bmatrix} 0 \\ 0 \end{bmatrix} \quad (43)$$

where the  $\vec{\tau}$  are the Pauli matrices. This is also why we eventually find the electric charge to be expressed in terms of weak hypercharge  $Y$  and third component of isospin  $t_3$  [14].

We are about to see that this interplay between the  $U(1)$  symmetry (corresponding to  $Y$ ) and the third component of  $SU(2)$  symmetry (corresponding to  $t_3$ ) manifests as a mixing of the  $W_3^\mu$  and  $B^\mu$  gauge fields to yield the photon field  $A^\mu$  and the neutral weak vector boson  $Z$ .

To consider oscillations about the vacuum, parametrize the degrees of freedom by

$$\phi = e^{-\frac{i}{2v}\vec{\theta}(x)\cdot\vec{r}} \begin{bmatrix} 0 \\ \frac{1}{\sqrt{2}}(v + H(x)) \end{bmatrix} \quad (44)$$

However, recall that the three  $\vec{\theta}$  field perturbations, which would become Goldstone bosons, disappear if we make the appropriate gauge transformation. So we effectively use

$$\phi = \begin{bmatrix} 0 \\ \frac{1}{\sqrt{2}}(v + H(x)) \end{bmatrix} \quad (45)$$

The consequences for the lagrangian are (details of how the following form of the lagrangian are calculated are in appendix A.10)

$$\mathcal{L} = \frac{1}{2}(\partial_\mu H)(\partial^\mu H) + \frac{m_0^2}{2}(v + H)^2 - \frac{\lambda}{16}(v + H)^4 - \frac{1}{4}\vec{F}_{\mu\nu} \cdot \vec{F}^{\mu\nu} - \frac{1}{4}G_{\mu\nu}G^{\mu\nu} \quad (46)$$

$$\mathcal{L} = \frac{1}{2}(\partial_\mu H)(\partial^\mu H) + \frac{m_0^2}{2}(v + H)^2 - \frac{\lambda}{16}(v + H)^4 \quad (47)$$

$$- \frac{1}{4}(\partial_\mu W_{1\nu} - \partial_\nu W_{1\mu})(\partial^\mu W_1^\nu - \partial^\nu W_1^\mu) + \frac{1}{8}g^2v^2W_{1\nu}W_1^\nu \quad (48)$$

$$- \frac{1}{4}(\partial_\mu W_{2\nu} - \partial_\nu W_{2\mu})(\partial^\mu W_2^\nu - \partial^\nu W_2^\mu) + \frac{1}{8}g^2v^2W_{2\nu}W_2^\nu \quad (49)$$

$$- \frac{1}{4}(\partial_\mu W_{3\nu} - \partial_\nu W_{3\mu})(\partial^\mu W_3^\nu - \partial^\nu W_3^\mu) - \frac{1}{4}G_{\mu\nu}G^{\mu\nu} \quad (50)$$

$$+ \frac{1}{8}v^2(gW_{3\mu} - g'YB_\mu)(gW_3^\mu - g'YB^\mu) + \text{Higgs interactions} \quad (51)$$

The second and third lines show that the  $W_1$  and  $W_2$  gauge fields are massive and have the same mass  $m_W = \frac{gv}{2}$ . These are the  $W^+, W^-$  vector gauge bosons in electroweak theory. The Higgs interaction terms are being ignored here because we are focusing on the generation of the Standard Model gauge bosons in this section. In appendix A.10, I go through the details of deriving the full version of this and discuss the interactions between the Higgs and gauge bosons that are produced. The Higgs boson decaying to gauge bosons is precisely the kind of interaction that this dissertation explores experimentally.

The last two lines show that the gauge fields  $W_3$  and  $B$  are mixed. The key clue is to notice in the last line it is the combination  $(gW_3^\mu - g'YB^\mu)$  that has a mass. Introduce

the linear combinations

$$Z^\mu \equiv W_3^\mu \cos \theta_W - B^\mu \sin \theta_W \quad (52)$$

$$A^\mu \equiv W_3^\mu \sin \theta_W + B^\mu \cos \theta_W \quad (53)$$

where

$$\cos \theta_W = \frac{g}{\sqrt{g^2 + g'Y^2}} \quad (54)$$

$$\sin \theta_W = \frac{g'Y}{\sqrt{g^2 + g'Y^2}} \quad (55)$$

Using this, we can write the last two lines of the lagrangian in terms of  $A^\mu$  and  $Z^\mu$ , instead of  $B^\mu$  and  $W_3^\mu$ . They become:

$$-\frac{1}{4}(Z_{\mu\nu}Z^{\mu\nu} + \mathcal{F}_{\mu\nu}\mathcal{F}^{\mu\nu}) + \frac{1}{8}v^2Z_\mu Z^\mu(g^2 + g'Y^2) \quad (56)$$

for  $\mathcal{F}_{\mu\nu} \equiv \partial_\mu A_\nu - \partial_\nu A_\mu$  and  $Z_{\mu\nu} \equiv \partial_\mu Z_\nu - \partial_\nu Z_\mu$ .

Hence, we have unmixed the two fields. They become the  $Z$  boson and the photon.

$$m_Z = \frac{1}{2}v^2\sqrt{g^2 + g'Y^2} = \frac{m_W}{\cos \theta_W} \quad (57)$$

$$m_A = 0 \quad (58)$$

where  $Y = 1$  and  $t_3 = -1/2$  breaks both  $SU(2)$  and  $U(1)_Y$  symmetries, but leaves the  $U(1)_{em}$  symmetry unbroken ( $Q = t_3 + Y/2 = -1/2 + 1/2 = 0$ ).[14]

See appendix A.7 for a detailed calculation of these results.

## 2.4 The Higgs Mechanism and Fermion Masses

Section 2.3 explored  $SU(2) \times U(1)$  spontaneous symmetry breaking and the Higgs mechanism for scalar particles, with Klein-Gordon lagrangians. However, leptons and quarks are fermions. We will first explore spontaneous  $SU(2)_L \times U(1)_Y$  symmetry breaking for a massless fermion doublet, then focus on how the Higgs mechanism generates the fermion masses. We will also see that the same covariant derivatives used for scalar particles will be applicable here and produce the gauge bosons.

For more extensive computational details pertinent to this section, please refer to the appendices A.8 and A.9.

### 2.4.1 $SU(2) \times U(1)$ Symmetry For Massless Fermions

We know now from section 2.3 what our postulated lagrangian should look like in order to be both  $U(1)$  and  $SU(2)$  invariant, which necessarily involved the weak vector bosons

and the photon. Let's look at  $SU(2) \times U(1)$  gauge invariance for the first generation of quarks; the calculation is identical for the higher generations. The calculation for the lepton generations is also very similar and so not repeated in this dissertation.

The Higgs mechanism is *not* included here so the quarks will still be massless; that will be dealt with in section 2.4.2. Instead, we will deal with fermions that appear as a left-handed doublet and right-handed singlets for both particles.

Suppose we have the (fermion) quark doublet

$$q = \begin{bmatrix} u \\ d \end{bmatrix} \quad (59)$$

and recall that

$$\psi_L = \left( \frac{1 - \gamma_5}{2} \right) \psi \quad (60)$$

$$\psi_R = \left( \frac{1 + \gamma_5}{2} \right) \psi \quad (61)$$

are relations distinguishing the left and right handed components.

As always, we must postulate a lagrangian. In the sections exploring  $U(1)$  and  $SU(2)$  symmetries, we used generalizations of the Klein-Gordon equation's lagrangian for scalar particles. Now we want to look at spin-1/2 fermions, so we must use the Dirac lagrangian in our gauge invariant form.

Recall the Dirac lagrangian

$$\mathcal{L} = i\bar{\psi}\gamma_\mu\partial^\mu\psi - m\bar{\psi}\psi \quad (62)$$

Now we want a massless version for a fermion doublet:

$$\mathcal{L} = \bar{q}i\mathcal{D}q \quad (63)$$

$$\mathcal{L} = \bar{q}_L i\mathcal{D}_L q_L + \bar{u}_R i\mathcal{D}_R u_R + \bar{d}_R i\mathcal{D}_R d_R \quad (64)$$

where the covariant derivative for the doublet  $\mathcal{D}_L$  is  $SU(2) \times U(1)$  invariant, and  $\mathcal{D}_R$  is only  $U(1)$  invariant for the singlet:

$$D_L^\rho = \partial^\rho + \frac{ig}{2}\vec{\tau} \cdot \vec{W}^\rho + \frac{ig'Y}{2}B^\rho \quad (65)$$

$$D_R^\rho = \partial^\rho + \frac{ig'Y}{2}B^\rho \quad (66)$$

After exhaustive computation reminiscent of previous sections (and found in appendix

A.8) we arrive at

$$\mathcal{L} = i\bar{u}\gamma_\rho \left( \frac{1 + \gamma_5}{2} \right) (\partial^\rho u) + i\bar{d}\gamma_\rho \left( \frac{1 + \gamma_5}{2} \right) (\partial^\rho d) + i\bar{u}\gamma_\rho \left( \frac{1 - \gamma_5}{2} \right) (\partial^\rho u) + i\bar{d}\gamma_\rho \left( \frac{1 - \gamma_5}{2} \right) (\partial^\rho d) \quad (67)$$

$$+ \frac{1}{\sqrt{2}} g \bar{u}\gamma_\rho W^\rho \left( \frac{1 - \gamma_5}{2} \right) d + \frac{1}{\sqrt{2}} g \bar{d}\gamma_\rho W^{\rho\dagger} \left( \frac{1 - \gamma_5}{2} \right) u \quad (68)$$

$$+ \frac{g}{2 \cos \theta_W} Z^\rho \left[ \bar{u}\gamma_\rho \left( \frac{1 + \gamma_5}{2} \right) u \left( \frac{4}{3} \sin^2 \theta_W \right) - \bar{d}\gamma_\rho \left( \frac{1 + \gamma_5}{2} \right) d \left( \frac{2}{3} \sin^2 \theta_W \right) \right] \quad (69)$$

$$+ \bar{u}\gamma_\rho \left( \frac{1 - \gamma_5}{2} \right) u \left( -1 + \frac{4}{3} \sin^2 \theta_W \right) - \bar{d}\gamma_\rho \left( \frac{1 - \gamma_5}{2} \right) d \left( -1 + \frac{2}{3} \sin^2 \theta_W \right) \quad (70)$$

$$- \frac{2e_0}{3} \bar{u}\gamma_\rho u A^\rho + \frac{e_0}{3} \bar{d}\gamma_\rho d A^\rho \quad (71)$$

where the electric charge is defined as  $e_0 = g \sin \theta_W$ . This form illustrates the interactions among the quarks in the fermion doublet and the gauge bosons.

#### 2.4.2 The Higgs Mechanism in Fermion Mass Generation

The kinetic part of a free Dirac fermion does not mix the left and right components of the field:

$$\bar{\psi} \gamma_\mu \partial^\mu \psi = \bar{\psi}_R \gamma_\mu \partial^\mu \psi_R + \bar{\psi}_L \gamma_\mu \partial^\mu \psi_L \quad (72)$$

Because of this, we can gauge the left and right handed components differently. Weak interactions are parity violating in the Standard Model and the  $SU(2)_L$  covariant derivative acts only on the left-handed term. However, a Dirac mass term has the form

$$-m (\bar{\psi}_L \psi_R + \bar{\psi}_R \psi_L) \quad (73)$$

when we write the left and right handed components separately. So the components are coupled, meaning any such mass term breaks  $SU(2)_L$  gauge invariance.

In a theory with spontaneous symmetry breaking, there is a way of giving mass to fermions without explicitly introducing gauge invariance breaking mass terms in the lagrangian. Consider the electron  $SU(2)_L$  doublet

$$l = \begin{bmatrix} \nu \\ e \end{bmatrix}_L \quad (74)$$

the Higgs doublet

$$\phi = \begin{bmatrix} \phi^+ \\ \phi^0 \end{bmatrix} \quad (75)$$

$$\phi^+ = \frac{1}{\sqrt{2}}(\phi_1 - i\phi_2) \quad (76)$$

$$\phi^0 = \frac{1}{\sqrt{2}}(\phi_3 - i\phi_4) \quad (77)$$

and the right handed electron singlet in a Yukawa model.

$$\mathcal{L}_e = -g_e \bar{l}_L \phi e_R - g_e \bar{e}_R \phi^\dagger l_L \quad (78)$$

Recall from section 2.3.5 that the vacuum expectation value of the Higgs doublet assumes the value

$$\langle 0 | \phi | 0 \rangle = \begin{bmatrix} 0 \\ \frac{v}{\sqrt{2}} \end{bmatrix} \quad (79)$$

The consequence for a fermion doublet in this lagrangian is

$$\mathcal{L}_e = -g_e \bar{l}_L \phi e_R - g_e \bar{e}_R \phi^\dagger l_L \quad (80)$$

$$= -\frac{g_e v}{\sqrt{2}} [\bar{e}_L e_R + \bar{e}_R e_L] \quad (81)$$

This is exactly a Dirac mass with  $m_e = \frac{g_e v}{\sqrt{2}}$ . That was precisely the vacuum. Now let's see that if we consider also oscillations about the vacuum we generate a coupling between the electron and the Higgs field. In the last line, use  $v + H$  instead of just  $v$ .

$$\langle 0 | \mathcal{L}_e | 0 \rangle = -\frac{g_e v}{\sqrt{2}} [\bar{e}_L (v + H) e_R + \bar{e}_R (v + H) e_L] \quad (82)$$

$$= -\frac{g_e v}{\sqrt{2}} \left[ \underbrace{\bar{e}_L e_R}_{\text{Dirac electron mass}} + \underbrace{\bar{e}_R e_L}_{\text{electron-Higgs coupling}} \right] \quad (83)$$

Notice for the coupling term

$$\left( \frac{-g_e}{\sqrt{2}} \right) \bar{e}_R e_L = \left( -\frac{m_e}{v} \right) \bar{e}_R e_L = \left( -\frac{g m_e}{2 m_W} \right) \bar{e}_R e_L \quad (84)$$

So in addition to interactions of the form  $f\bar{f} \rightarrow (\gamma \text{ or } Z^0) \rightarrow W^+W^-$  we also have the possibility  $f\bar{f} \rightarrow H \rightarrow W^+W^-$ —precisely the interaction this dissertation conducts an experimental search for. The presence of the fermion mass in the coupling to the Higgs is significant.

Summarily, to give the electron-neutrino  $SU(2)$  doublet mass (as well as the other lepton and quark doublets), we are adding more terms to the lagrangian derived at the end of section A.8 of the form:

$$\mathcal{L}_{f,\text{Higgs}} = \sum_{l=e,\mu,\tau} \left[ -\frac{g_l}{\sqrt{2}} \left[ v \bar{l} l + \bar{l} H l \right] - \frac{g_{\nu_l}}{\sqrt{2}} \left[ v \bar{\nu}_l \nu_l + \bar{\nu}_l H \nu_l \right] \right] \quad (85)$$

for the three lepton generations and similar terms for the three quark doublets. Because of the Higgs mechanism, we now have sensible masses for Standard Model particles; however, it should be noted that this does not quite give the final form of the quark mass terms. A similar treatment for all three generations of quarks yields a results that includes “quark mixing,” the ability of quarks to change flavor via charged weak interations in which the Higgs boson plays a central role. This treatment is outlined in section 2.5. (See appendix A.9 for more details).

## 2.5 The Higgs Field, Quark Mixing, and the CKM Matrix

Generating the masses of quarks and leptons is not the only function the Higgs boson serves in the Standard Model. It also plays a central role in “quark mixing,” the ability of quarks to change flavor via weak charge changing interactions.

Consider three doublets of left-handed quark fields:

$$q_{L1} = \begin{bmatrix} u_{L1} \\ d_{L1} \end{bmatrix}; \quad q_{L2} = \begin{bmatrix} u_{L2} \\ d_{L2} \end{bmatrix}; \quad q_{L3} = \begin{bmatrix} u_{L3} \\ d_{L3} \end{bmatrix} \quad (86)$$

and the six corresponding right-handed singlets:  $u_{R1}, d_{R1}, u_{R2}, d_{R2}, u_{R3}, d_{R3}$ . The lagrangian is then similar to the case for leptons already considered. The difference is that there are three quark families and each  $SU(2)_L$  scalar (such as  $\bar{q}_{Li} \phi_c$ ) can be paired with any of the three  $u_{Rj}$ , for  $i, j \in \{1, 2, 3\}$ . So allowing “mixing” of the families results in nine pairings. The nine couplings form the  $3 \times 3$  CKM matrix.

We begin with the lagrangian

$$\mathcal{L} = \sum_{\{i,j\}=1,2,3} \left[ a_{ij} \bar{q}_{Li} \phi_c u_{Rj} + a_{ij}^\dagger \bar{u}_{Rj} \phi_c^\dagger q_{Li} + b_{ij} \bar{q}_{Li} \phi_d d_{Rj} + b_{ij}^\dagger \bar{d}_{Rj} \phi_d^\dagger q_{Li} \right] \quad (87)$$

So far,  $a_{ij}$  and  $b_{ij}$  may be any complex value and are included as values to gauge the coupling strength. After much working over, the lagrangian becomes[13]

$$\mathcal{L} = \sum_k \left[ m_{a,k} \left( \bar{u}_{Lk} u_{Rk} \left( 1 + \frac{H}{v} \right) + \bar{u}_{Rk} u_{Lk} \left( 1 + \frac{H}{v} \right) \right) \right. \quad (88)$$

$$\left. + m_{b,k} \left( \bar{d}_{Lk} d_{Rk} \left( 1 + \frac{H}{v} \right) + \bar{d}_{Rk} d_{Lk} \left( 1 + \frac{H}{v} \right) \right) \right] \quad (89)$$

where  $v$  appears again from the parametrization of the potential minimum in the Higgs mechanism, and  $m_{a,k} = a_{kk}v/\sqrt{2}$ ,  $m_{b,k} = b_{kk}v/\sqrt{2}$  are the quark masses. Notice also that quark couplings to the Higgs boson are another consequence.

It is important to note that the mass and Higgs interaction terms are not the only places that quark field appear in the Standard Model lagrangian. There were certain variable transformations performed to get this result—whose details are not pertinent to this dissertation—that must be propagated in the terms of line 68, above. Beginning with that line for all three generations of quarks:

$$\sum_{k=1,2,3} \frac{1}{\sqrt{2}} g \bar{u}_k \gamma_\rho W^\rho \left( \frac{1 - \gamma_5}{2} \right) d_k + \frac{1}{\sqrt{2}} g \bar{d}_k \gamma_\rho W^{\rho\dagger} \left( \frac{1 - \gamma_5}{2} \right) u_k \quad (90)$$

We now perform a change of variables on the  $u$  and  $d$  quarks with unitary matrices  $S$  and  $T$ :

$$u_k = U_{ki} u_i \quad (91)$$

$$d_k = S_{kj} d_j \quad (92)$$

to get the following:

$$= \frac{g}{\sqrt{2}} \sum_{i,j,k} \left[ (U_{ki} u_i)^\dagger \gamma_0 W (S_{kj} d_j) \left( \frac{1 - \gamma_5}{2} \right) + (S_{kj} d_j)^\dagger \gamma_0 W^\dagger (U_{ki} u_i) \left( \frac{1 - \gamma_5}{2} \right) \right] \quad (93)$$

$$= \frac{g}{\sqrt{2}} \sum_{i,j,k} \left[ u_i^\dagger U_{ik}^* \gamma_0 W S_{kj} d_j \left( \frac{1 - \gamma_5}{2} \right) + d_j^\dagger S_{jk}^* \gamma_0 W^\dagger U_{ki} u_i \left( \frac{1 - \gamma_5}{2} \right) \right] \quad (94)$$

$$= \frac{g}{\sqrt{2}} \sum_{i,j,k} \left[ \bar{u}_i W d_j (U_{ik}^* S_{kj}) \left( \frac{1 - \gamma_5}{2} \right) + \bar{d}_j W^\dagger u_i (S_{jk}^* U_{ki}) \left( \frac{1 - \gamma_5}{2} \right) \right] \quad (95)$$

$$(96)$$

That is, the charge changing weak interactions link the three  $u_i$  quarks with a unitary rotation of the triplet of  $d_i$  quarks, with this rotation given by the unitary matrix  $V \equiv U^\dagger S$ ,

$$V = \begin{bmatrix} V_{ud} & V_{us} & V_{ub} \\ V_{cd} & V_{cs} & V_{cb} \\ V_{td} & V_{ts} & V_{tb} \end{bmatrix} \quad (97)$$

## 2.6 Higgs Boson Associated Production with a Vector Boson

There are four major way to produce a Standard Model Higgs boson in the mass range relevant to the high mass search: gluon fusion, vector boson fusion, associated production with a  $W$ -boson, and associated production with a  $Z$ -boson. In the  $H \rightarrow WW$  trilepton

channel, only the two associated production processes contribute a non-negligible amount of signal.

The Tevatron consists of a proton beam and an anti-proton beam that collide within the heart of the CDF detector. Protons are composite particles of two up quarks and one down quark while anti-protons are composed of one up quark and two down quarks, so the specific interactions involved are:

- $u^{+\frac{2}{3}} + \bar{d}^{+\frac{1}{3}} \rightarrow W^+ \rightarrow HW^+$
- $\bar{u}^{-\frac{2}{3}} + d^{-\frac{1}{3}} \rightarrow W^- \rightarrow HW^-$
- $\bar{q} + q \rightarrow Z \rightarrow HZ$

To calculate the cross section for one of these interactions, we begin with the fundamental postulate of experimentally verified physics (except, of course, for the Higgs boson itself): the Standard Model Lagrangian. The relevant terms for the first interaction listed above, for example, are:

$$\mathcal{L} = \underbrace{\frac{1}{2}(\partial_\mu H)(\partial^\mu H) + \frac{1}{2}\mu^2 H^2 + \frac{g^2 v^2}{4} W_\mu^\dagger W^\mu + \frac{g^2 v}{2} W_\mu^\dagger W^\mu H}_{\text{Higgs Sector}} \quad (98)$$

$$\underbrace{-\frac{1}{4} \sum_{i=1,2} (\partial_\mu W_{i\nu} - \partial_\nu W_{i\mu})(\partial^\mu W_i^\nu - \partial^\nu W_i^\mu)}_{\text{W boson kinetic terms}} \quad (99)$$

$$\underbrace{+i\bar{u}\gamma_\rho \left(\frac{1-\gamma_5}{2}\right) \partial^\rho u + i\bar{d}\gamma_\rho \left(\frac{1-\gamma_5}{2}\right) \partial^\rho d + \frac{gV_{ud}}{\sqrt{2}} \bar{d}\gamma_\rho W^{\dagger\rho} \left(\frac{1-\gamma_5}{2}\right) u}_{\text{Quark Doublet}} \quad (100)$$

We see in the first line the “Higgs Sector” which contains the kinetic term for the Higgs boson, the self-energy of the Higgs boson and  $W$  boson, and the term allowing interactions between the  $W$ -boson and the Higgs boson. The second line contains the  $W$ -boson kinetic terms and the third line yields the left-handed quark doublet (the  $(\frac{1-\gamma_5}{2})$  factor ensures left-handedness) and their interaction with the  $W$ -boson. Following the computations of appendix A.11, we arrive at the invariant amplitude.

$$i\mathcal{M} = \left[ -i \frac{\alpha m_W V_{ud}}{\sqrt{2} \sin^2 \theta_W} \right] \epsilon_\mu^{s*}(k') \left[ \frac{-g^{\mu\rho} + \frac{q^\mu q^\rho}{m_W^2}}{q^2 - m_W^2 + i\varepsilon} \right] \bar{d}^{r_1}(p') \gamma_\rho \left(\frac{1-\gamma_5}{2}\right) u^{r_2}(p) \quad (101)$$

The next step in finding the differential cross section is to compute  $|\mathcal{M}|^2$ , for which

we first need  $\mathcal{M}^*$ .

$$\mathcal{M}^* = -\frac{\alpha m_W V_{ud}}{\sqrt{2} \sin^2 \theta_W} \left[ \epsilon_\mu^{s*}(k') \left[ \frac{-g^{\mu\rho} + \frac{q^\mu q^\rho}{m_W^2}}{q^2 - m_W^2 + i\varepsilon} \right] \bar{d}^{r_1}(p') \gamma_\rho \left( \frac{1 - \gamma_5}{2} \right) u^{r_2}(p) \right]^* \quad (102)$$

$$= -\frac{\alpha m_W V_{ud}}{\sqrt{2} \sin^2 \theta_W} \bar{u} \gamma_\rho \left( \frac{1 - \gamma_5}{2} \right) d \left[ \frac{-g^{\mu\rho} + \frac{q^\mu q^\rho}{m_W^2}}{q^2 - m_W^2 + i\varepsilon} \right] \epsilon_\mu^s(k') \quad (103)$$

The beam at the Tevatron is unpolarized, so average over spins  $r_1, r_2$  of the quarks. The polarization of the end states is not measured, so the cross section is a sum of the possible polarization states of the  $W$ . As such, we want to compute

$$\frac{1}{2} \sum_{r_1} \frac{1}{2} \sum_{r_2} \sum_s |\mathcal{M}|^2 \quad (104)$$

To do this, we use the spin sums (see eqns. (3.66), (3.67) of Peskin and Schroeder [11])

$$\sum_s u^s(p) \bar{u}^s(p) = \gamma \cdot p + m \quad (105)$$

$$\sum_s v^s(p) \bar{v}^s(p) = \gamma \cdot p - m \quad (106)$$

$$\sum_s \epsilon_\sigma^s(k') \epsilon_\mu^{s*}(k') = -g_{\sigma\mu} + \frac{k'_\sigma k'_\mu}{m_W^2} \quad (107)$$

to get

$$\frac{1}{4} \sum_{r_1, r_2, s} |\mathcal{M}|^2 = \frac{1}{4} \left( \frac{\alpha m_W V_{ud}}{\sqrt{2} \sin^2 \theta_W} \right)^2 \sum_{r_1, r_2, s} \left[ \epsilon_\mu^{s*}(k') \left[ \frac{-g^{\mu\rho} + \frac{q^\mu q^\rho}{m_W^2}}{q^2 - m_W^2 + i\varepsilon} \right] \bar{d}^{r_1}(p') \gamma_\rho \left( \frac{1 - \gamma_5}{2} \right) u^{r_2}(p) \bar{u}^{r_2}(p) \gamma_\nu \left( \frac{1 - \gamma_5}{2} \right) d^{r_1}(p') \left[ \frac{-g^{\sigma\nu} + \frac{q^\sigma q^\nu}{m_W^2}}{q^2 - m_W^2 + i\varepsilon} \right] \epsilon_\mu^s(k') \right] \quad (108)$$

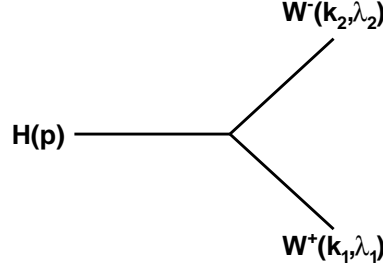
$$= \frac{1}{4} \left( \frac{\alpha m_W V_{ud}}{\sqrt{2} \sin^2 \theta_W} \right)^2 \left[ \left( -g_{\sigma\mu} + \frac{k'_\sigma k'_\mu}{m_W^2} \right) \left( \frac{-g^{\mu\rho} + \frac{q^\mu q^\rho}{m_W^2}}{q^2 - m_W^2 + i\varepsilon} \right) \left( \frac{-g^{\sigma\nu} + \frac{q^\sigma q^\nu}{m_W^2}}{q^2 - m_W^2 + i\varepsilon} \right) \right] \quad (109)$$

$$= \frac{1}{4} \left( \frac{\alpha m_W V_{ud}}{\sqrt{2} \sin^2 \theta_W} \right)^2 \left[ \left( -g_{\sigma\mu} + \frac{k'_\sigma k'_\mu}{m_W^2} \right) \left( \frac{-g^{\mu\rho} + \frac{q^\mu q^\rho}{m_W^2}}{q^2 - m_W^2 + i\varepsilon} \right) \left( \frac{-g^{\sigma\nu} + \frac{q^\sigma q^\nu}{m_W^2}}{q^2 - m_W^2 + i\varepsilon} \right) \right] \quad (110)$$

$$\text{Tr} \left[ \gamma_\rho \left( \frac{1 - \gamma_5}{2} \right) (\not{p} + m_u) \gamma_\nu \left( \frac{1 - \gamma_5}{2} \right) (\not{p}' - m_d) \right] \quad (111)$$

It remains to evaluate the trace and simplify the terms, then use the invariant amplitude squared to compute the cross section with general form [11]

$$d\sigma = \frac{1}{2E_A \cdot 2E_B |v_A - v_B|} \left[ \frac{d^3 k}{2E_k (2\pi)^3} \frac{d^3 k'}{2E'_k (2\pi)^3} \right] \frac{1}{4} \sum_{r_1, r_2, s} |\mathcal{M}|^2 (2\pi)^4 \delta^4(k + k' - p - p') \quad (112)$$



where  $|v_A - v_B| \cong 2c$  is the relative velocity difference in the lab frame.

Finally, the cross section for Higgs boson associated production with a  $W$  boson is (in terms of the Mandelstam variables) [16]

$$\boxed{\sigma(u\bar{d} \rightarrow WH) = \frac{\pi\alpha^2|V_{ud}|^2}{36\sin^4\theta_W} \frac{2k}{\sqrt{s}} \frac{k^2 + 3m_W^3}{(s - m_W^2)^2}} \quad (113)$$

Similarly, the cross section for associated production with a  $Z$  boson is[16]

$$\boxed{\sigma(q\bar{q} \rightarrow ZH) = \frac{2\pi\alpha^2(l^2 + r^2)}{144\sin^4\theta_W \cos^4\theta_W} \frac{2k}{\sqrt{s}} \frac{k^2 + 3m_Z^3}{(s - m_Z^2)^2}} \quad (114)$$

where  $l \equiv 2(t_3 - Q \sin^2\theta_W)$ ,  $r \equiv -2Q \sin^2\theta_W$ ,  $Q$  is the electric charge, and  $t_3$  is the weak isospin quantum number.

## 2.7 Higgs Boson Decay ( $H \rightarrow WW$ )

Now that we have a physical model with a Higgs boson and have computed the cross sections of its production channels pertinent to our experimental search, let's see how it decays.

Consider the decay in figure 2.7. The lagrangian density for a Standard Model Higgs boson decaying to two  $W$ -bosons comes from the Higgs sector of the Standard Model lagrangian.

$$\mathcal{L} = \underbrace{\frac{1}{2}(\partial_\mu H)(\partial^\mu H) + \frac{1}{2}\mu^2 H^2 + \frac{g^2 v^2}{4} W_\mu^\dagger W^\mu + \frac{g^2 v}{2} W_\mu^\dagger W^\mu H}_{\text{Higgs Sector}} \quad (115)$$

$$\underbrace{-\frac{1}{4} \sum_{i=1,2} (\partial_\mu W_{i\nu} - \partial_\nu W_{i\mu}) (\partial^\mu W_i^\nu - \partial^\nu W_i^\mu)}_{\text{W boson kinetic terms}} \quad (116)$$

$$(117)$$

The decay rate derived from this lagrangian is (see appendix A.12 for details):

$$\Gamma = \frac{G_F m_H^3}{8\sqrt{2}\pi} \left( 1 - \frac{4m_W^2}{m_H^2} + \frac{12m_W^4}{m_H^4} \right) \sqrt{1 - \frac{4m_W^2}{m_H^2}} \quad (118)$$

(119)

## FERMILAB'S ACCELERATOR CHAIN

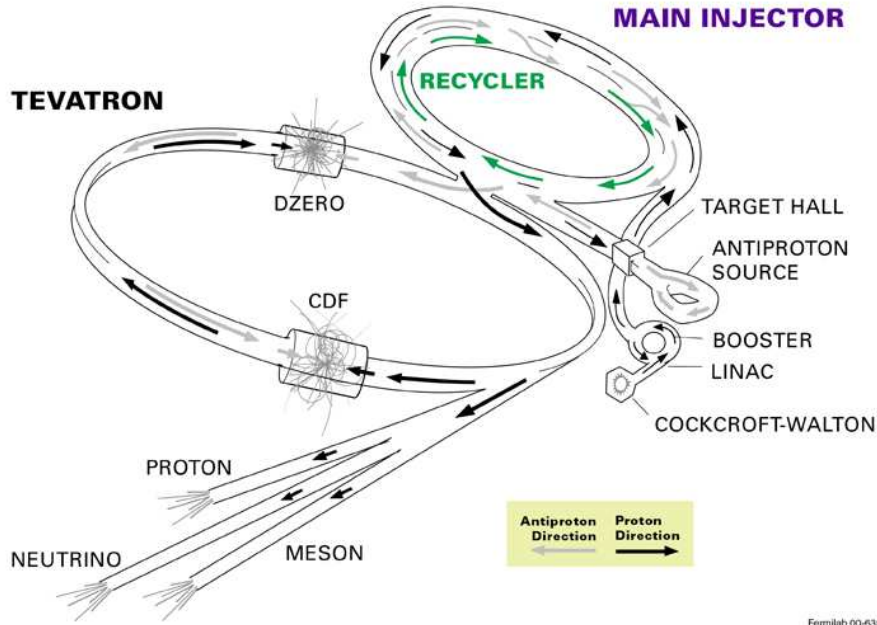


Figure 3: The Tevatron Accelerator Chain [18]

### 3 The Tevatron

This contribution to the search for the Standard Model Higgs boson is conducted at the Fermi National Accelerator Laboratory with the “Tevatron,” a roughly four mile circular track around which protons and antiprotons are accelerated and collided with a center of mass energy of 1.96 TeV. These collisions occur at the “Collider Detector at Fermilab” experiment (CDF) where the data is recorded for future analysis. The collection, manipulation, and collision of protons and antiprotons is a formidable task. This chapter outlines process that leads to the colliding beams of the Tevatron while the CDF collider experiment is detailed in chapter 4

Figure 3 illustrates the stages of producing the colliding beams, beginning with the Cockcroft-Walton site and ending with the Tevatron collisions in the CDF and D0 experiments.

#### 3.1 Beginning of the Beam: Cockcroft-Walton

The beams begin simply as hydrogen gas. The gas is injected into an electric field that is strong enough to strip the electrons from the hydrogen nuclei, leaving positively charged hydrogen ions ( $H^+$ ). In the electric field, these ions are then directed towards a ce-

sium anode where they acquire two electrons, become *negatively* charged  $H^-$  ions now. With a newly acquired negative net charge, these  $H^-$  ions are repelled from the anode and accelerated to 750 KeV by a Cockcroft-Walton accelerator—a type of Van de Graaf accelerator—towards a linear accelerator.

### 3.2 LINAC: The Linear Accelerator

The 750 KeV hydrogen ions enter a linear accelerator that operates with a succession of drift tubes generating an electric field oscillating with a radio frequency.  $H^-$  ions arriving at the linac in phase with the field oscillation are accelerated to 400 MeV over a distance of 130 meters, while those arriving out of phase with the linac’s field are lost. This creates a beam of discrete bunches of ions rather than a steady stream. At the end of the linac, the bunched beam of ions impigns on a carbon barrier that strips the electrons from the hydrogen nuclei which are now just protons that pass.

### 3.3 Booster

Observe in figure 3 that the linac tangentially intersects the circular “booster.” Sequentially, this is the first synchrotron—a circular accelerator with carefully synchronized electric and magnetic field to direct the beam of ions—that the protons encounter on their path to the colliders. The booster accelerates the protons from 400 MeV to 8 GeV.

### 3.4 Main Injector

After being ramped to an energy of 8 GeV in the Booster, the protons are redirected towards the “main injector”—another larger synchrotron that accelerates the proton bunches to 150 GeV for injection into the Tevatron. The main injector also plays a central role in the production of the antiprotons. Some protons from the main injector are used to produce antiprotons, which are accumulated separately. They are then also directed into the main injector which will inject the antiprotons into the tevatron. [23]

### 3.5 Anti-protons

Protons in the main injector are accelerated to 150 GeV if they are to be injected into the Tevatron, but are accelerated to 120 GeV if they are to be used for antiproton production. These 120 GeV protons are directed to impact a nickel-based target every 1.5 seconds causing a variety of interactions. For every one million protons that hit the nickel target, only  $\sim 20$  antiprotons are produced with enough energy to enter the “accumulator.”

After passing the nickel target, the products pass through a “lithium lens” that focuses them into a beam that passes through a magnet. This magnet then filters the antiprotons by redirecting them on a unique path that leads them to the “debuncher.” Because of

the radio-frequency used to accelerate the 120 GeV protons in the main injector, the antiprotons are still in a beam of discrete bunches. These antiprotons also have a large spread in energy, so the debuncher is tuned in a way that decelerates higher energy antiprotons and accelerates lower energy antiprotons.

After the debuncher is finished with the antiprotons, they are successively stored in the “accumulator” at 8 GeV over many hours (or even up to a few days) while waiting to be transferred to the Tevatron for a fresh beam. When the Tevatron is ready for new colliding beams, the antiprotons are transferred from the accumulator to the “recycler” (also an 8 GeV ring) before moving on to the main injector and the Tevatron. [20]

### 3.6 The Tevatron

The first version of the tevatron became operational in 1983. It was the world’s first superconducting synchrotron, containing about 1000 superconducting magnets. Because superconducting wires provide no resistance to the flow of charge, stronger magnetic fields are achievable and operational costs are reduced because electricity is not lost to dissipation.

The collider physics program at the Tevatron is separated between a *Run I* (1992-1996, 1.8 TeV) and *Run II* (2001-present, 1.96 TeV). As the Tevatron approaches the last years of *Run II* operation, the CDF and D0 experiments are quickly closing in on achieving Standard Model sensitivity for the Higgs boson search. [22]

The Tevatron receives the proton and antiproton beams from the main injector, both at 150 GeV. Both beams are injected in 36 discrete bunches, though not in equal densities since antiprotons are far more difficult to collect than protons. Each bunch contains on the order of  $10^{11}$  protons or  $10^{10}$  antiprotons.

Once all 36 bunches of each beam have been injected into the Tevatron, the beam is ramped from the 150 GeV to its colliding energy of 980 GeV. They are then focused, or “squeezed,” and collimators are used to absorb extraneous particles orbiting the beam. This is sometimes denoted the “beam halo.”

The instantaneous luminosity for the collisions is given by:

$$L_{\text{inst.}} = \frac{36fN_pN_{\bar{p}}}{4\sigma_x\sigma_y} \quad (120)$$

where the 36 denotes the number of bunches in each beam,  $f$  is the frequency of the revolutions,  $N_p$  is the number of protons in the bunch,  $N_{\bar{p}}$  is the number of antiprotons in a bunch, and  $\sigma_x$ ,  $\sigma_y$  are Gaussian profiles of a transverse cross section of the beams. Integrated (over time) luminosities are typically given in units of inverse barns, which can then be easily multiplied by the cross section for a particular process (units in barns) to obtain the expected number of occurrences for that physical interaction. [21]

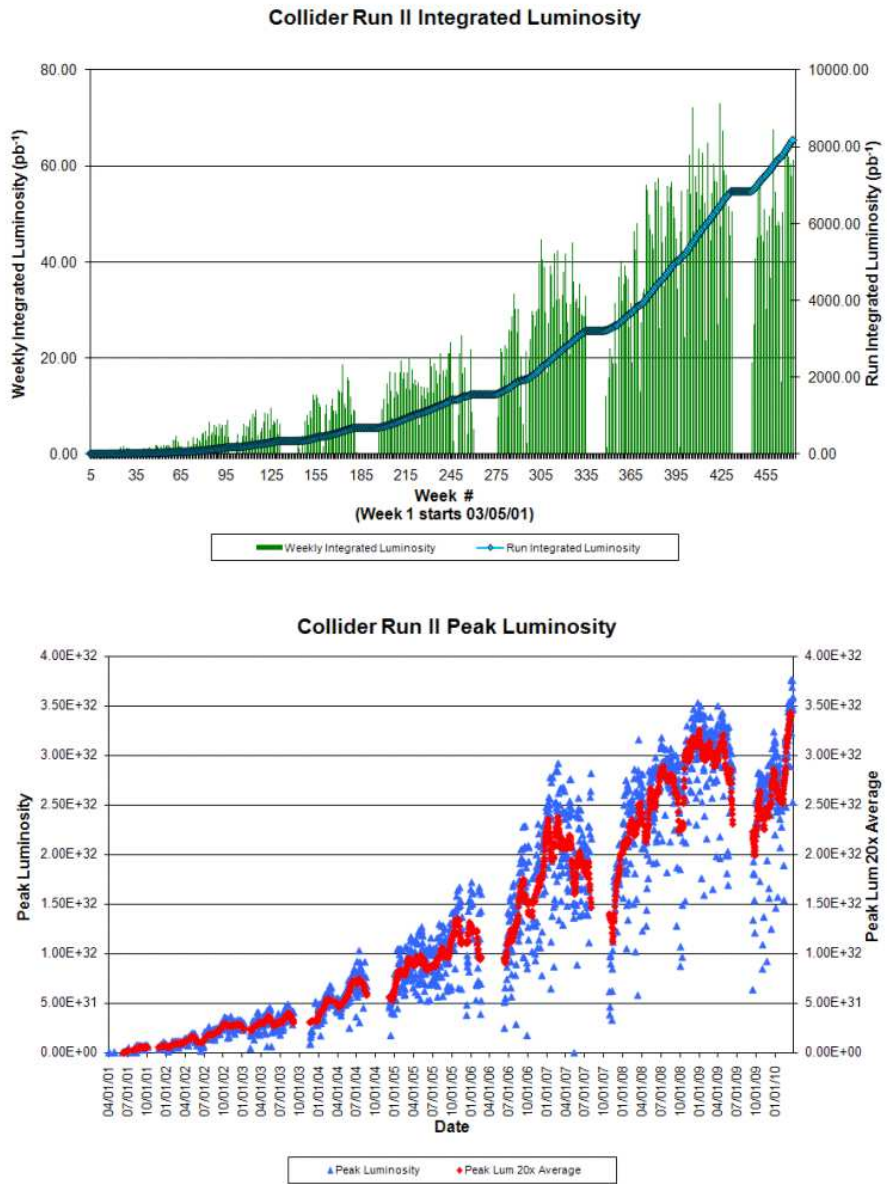


Figure 4: The Tevatron Run II luminosity performance [19]

### 3.7 The Performance of the Tevatron in Run II

As of March 30, 2010, the Tevatron is no longer the world's most powerful particle collider. The LHC produced collisions at 7 TeV. However, the Tevatron continues to produce impressive results. During the same calendar month, the Tevatron broke two of its own records: it delivered  $272.7\text{pb}^{-1}$  of integrated luminosity and saw an initial instantaneous luminosity record of  $371 \times 10^{30}\text{cm}^{-2}\text{s}^{-1}$ . It has also been consistently seeing initial instantaneous luminosities of  $\sim 350 \times 10^{30}\text{cm}^{-2}\text{s}^{-1}$ . Further, figure 3 illustrates consistent and accelerating progress in data delivery.

As such, the Tevatron will still retain a leading role in particle physics research for at least the next few years as of this writing (spring 2010).

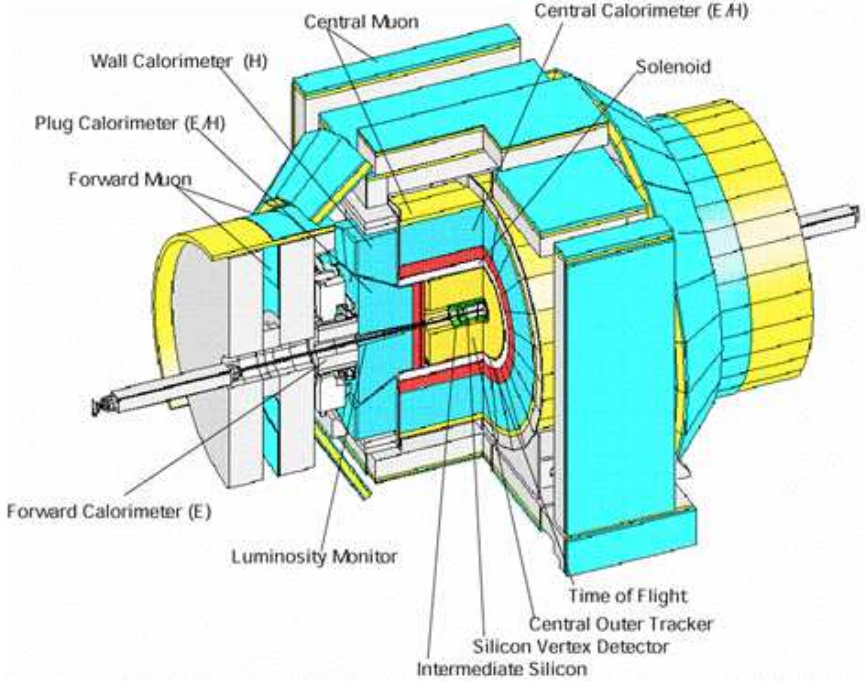


Figure 5: The CDF II Detector

## 4 The CDF II Detector

The CDF experiment resides at the B0 site of the Tevatron and is one of two experimental detectors that collide the proton-antiproton beams to record the consequences of the collisions. The present incarnation of the CDF detector (“Run II”) has been operational since 2001. It was originally designed with several specific purposes in mind: [10]

- Study the properties of the top quark
- Obtain more precise measurements of important quantities in electroweak physics
- Test perturbative Quantum Chromodynamics
- Constrain the CKM matrix with measurements of  $B$  decays
- Directly search for new physics

Since the Higgs boson has not been experimentally verified, the study presented in this dissertation falls into the “search for new physics” category, though is certainly related to electroweak measurements as well.

An overview of the experimental apparatus can be seen in figure 5. It contains a variety of different detection systems designed to collectively distinguish a variety of objects

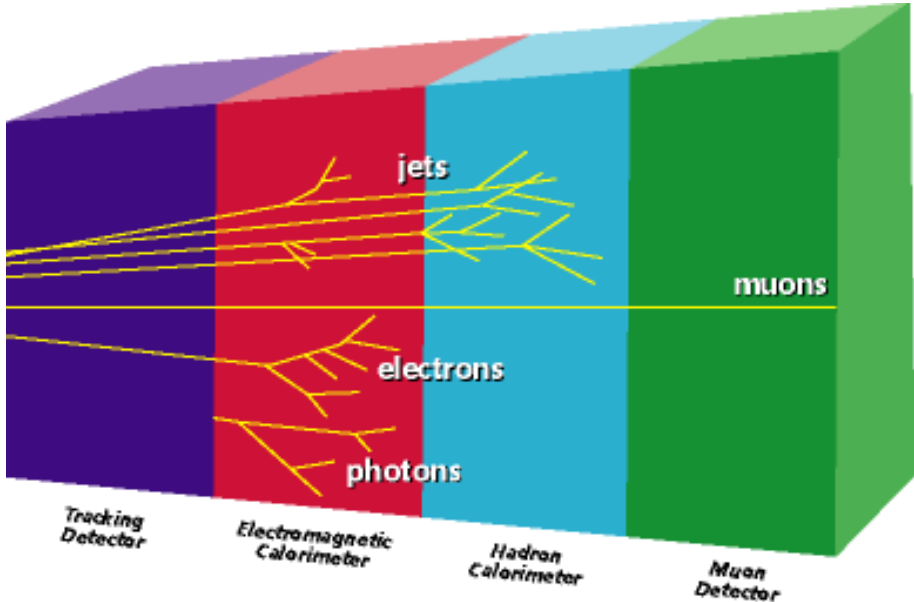


Figure 6: Diagram showing the types of objects various layers are constructed to detect.

that may result from the  $p\bar{p}$  collisions. Closest to the beamline is the silicon detector, which records the tracks of charged particles like leptons and charged hadrons. The silicon is encased in the “Central Outer Tracker” (COT), which also provides tracking information (see section 4.2). The next layer outward is the electromagnetic calorimeter, which is designed to absorb and measure the energy of photons and electrons as indicated by figure 6. Hadrons tend to be more massive and are measured in the subsequent “hadronic calorimeter” (see section 4.3). Though charged, muons tend to punch through the calorimeter system and are then detected by one of several muon detection systems (see section 4.4).

The various systems are used interactively to detect any particular kind of object. Electrons are tracked through the silicon and COT, then these tracks are matched to energy deposits in the electromagnetic calorimeter, for example. Muons are also tracked through the silicon and COT, then matched to signals left in the muon system. Jets are collections of particles that deposit energy in both the electromagnetic and hadronic calorimeter systems. All together, the CDF detector is designed to record the presence of any kind of electron, muon, photon, or jet produced in  $p\bar{p}$  collisions.

## 4.1 CDF Coordinates

Tracking the paths of various detector quantities requires a common coordinate system and CDF places the origin at the center of the experiment, on the beamline, where collisions are most likely to occur. The positive  $x$  coordinate points radially away from

the center of the Tevatron,  $y$  points vertically upward, and  $z$  is directed tangent to the path of the proton beam.

The azimuthal angle is denoted  $\phi$  and given by

$$\phi = \arctan\left(\frac{y}{x}\right) \quad (121)$$

The polar angle is denoted  $\theta$  and given by

$$\theta = \arctan\left(\frac{y}{z}\right) \quad (122)$$

The angle  $\theta$ , however, is not often used. Instead, we use “pseudorapidity,” where “rapidity” is defined as

$$\text{rapidity} = \frac{1}{2} \ln \frac{E + p_z}{E - p_z} \quad (123)$$

and in its massless approximation ( $p \gg m$ ) becomes pseudorapidity:

$$\eta = -\ln \tan\left(\frac{\theta}{2}\right) \quad (124)$$

## 4.2 Trackers

The CDF II tracking system is composed of three major components: a silicon microstrip system that provides precise tracking of charged particles close to the beamline; the “Central Outer Tracker” (COT) that envelops the silicon system; and finally a solenoid magnet generating a 1.4 T field along the  $\hat{z}$  direction. The two tracking systems trace the paths of charged particles while the solenoid’s field causes those paths to follow a helical pattern. Positive and negative charges can then be distinguished by the direction the helical path curves, while the particle’s momentum can be calculated by the magnitude of the curvature.

### 4.2.1 The Silicon Detectors

The CDF II silicon detector is composed of three components: L00, SVXII, and ISL. Layer zero-zero (L00) is a single sided, radiation tolerant silicon strip detector, which is closest to the beamline. It is 87 cm long, centered on  $z = 0$ , and has a radius of just 1.1 cm (see figure 8). L00 is constructed in six segments in both  $z$  and  $\phi$ . Each  $\phi$  segment contains 128 channel of narrow, inner sensors and 256 channels of wider, outer sensors. Each  $z$  segment is composed of two long sensors. In total, L00 contains 13,824 channels. [24]

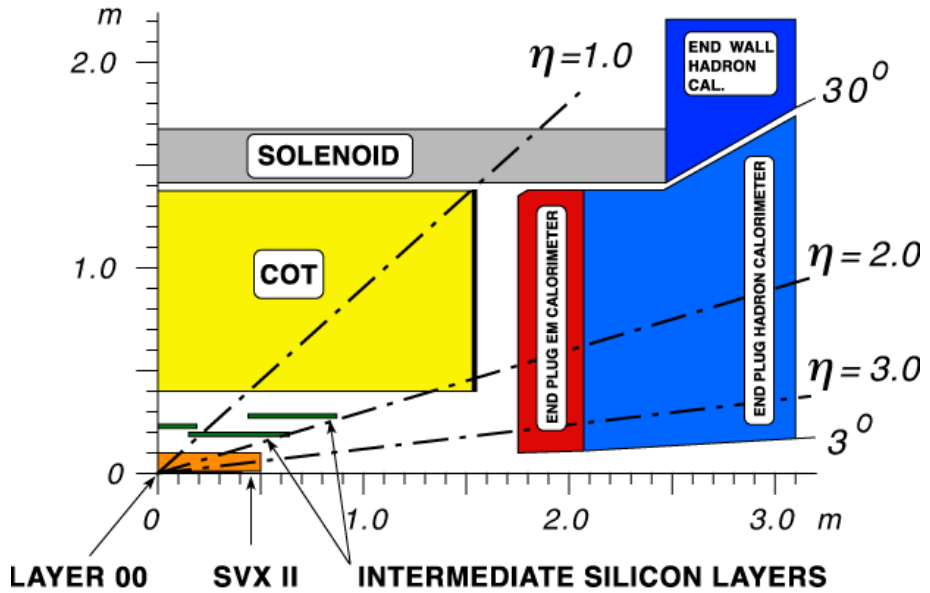


Figure 7: Diagram showing a side view of the tracking, solenoid, and forward calorimeter systems. The horizontal axis is the  $\hat{z}$ -direction from the interaction vertex and the vertical axis is the radial direction from the beamline.

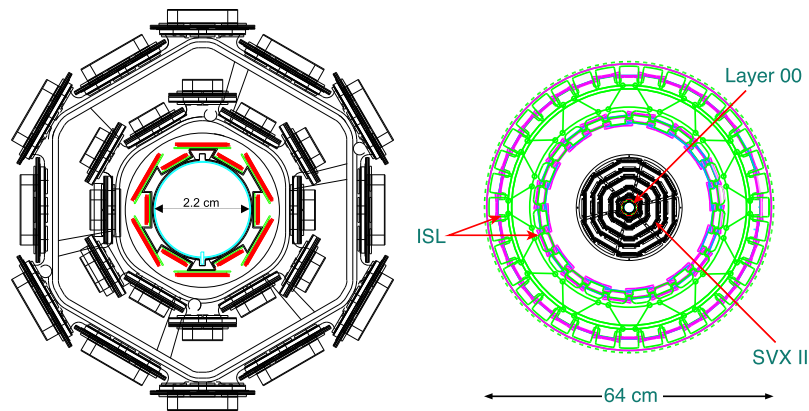


Figure 8: End view of L00 (left) and the full silicon system (right)[24],[25]

The SVX II silicon detector encapsulates L00. It is composed of three barrels, positioned end-to-end to achieve a length of 81 cm and full coverage in  $\phi$ . Each barrel contains five layers of silicon microstrip detectors ranging from 2.4 cm to 10.6 cm from the beamline. In all, the SVX contains 405,504 detection channels and covers  $|\eta| < 2.0$ .[25],[10]

The “intermediate silicon layers” (ISL) are the outermost section of the silicon detector system, between the SVX and the COT (see figure 7). The ISL are an important compliment to the SVX and COT (see section 4.2.2) in that they provide extra tracking information in  $1.0 < |\eta| < 2.0$ , where COT coverage is partial. In this forward region, there are two silicon layers placed at 20 cm and 28 cm from the beamline. There is also an additional ISL layer in the central region at 22 cm from the beamline. [26],[10]

#### 4.2.2 Central Outer Tracker

The CDF Central Outer Tracker (COT) compliments the silicon tracking system to provide additional tracking information. It covers the comparatively larger range of 40 cm to 130 cm from the beamline and is approximately three meters long. Instead of the wafers of silicon, the COT operates as a 96-layered drift chamber. The 96 layers are partitioned into 8 “superlayers” alternating between axial and stereo. “Axial” layers provide hit coordinates in the transverse plane (radial and azimuthal angle) while “stereo” layers supply the  $z$  coordinate, together yielding hit information in three dimensions.

The COT is filled with an equal mixture of argon and ethane in an electric field. When a charged particle enters the COT apparatus, it ionizes the gas by creating  $e^+e^-$  pairs. Electrons then drift under the influence of the electric field toward anode wires and signals are induced from the flow of charge.[27],[9]

Use of these tracking systems—in conjunction with the calorimeters and muon systems—is critical to the detection of leptons emanating from the  $p\bar{p}$  collisions. This dissertation is devoted to the rare events that contain three recognized leptons, so a clear understanding of how physical leptons produced in  $p\bar{p}$  interactions translate into detected leptons used for analysis is critical. This dissertation devotes chapter 6 to a detailed understanding of how the CDF subsystems are collectively used to identify leptons from charged tracks and other detector information.

### 4.3 Calorimeters

The calorimeter systems are located outside the solenoid and record the energies of particles resulting from  $p\bar{p}$  interactions. They are composed of scintillators with layers of heavy metal to induce electromagnetic or hadronic showers.

Electromagnetic showers are induced for high energy photons and electrons via a combination of bremsstrahlung and pair production. When impinging on the heavy metal layer, a high energy electron will radiate high energy photons, which then converts to  $e\bar{e}$  pairs, which go on to emit more photons, etc. This cycle continues until the individual

photons and electrons no longer have enough energy to pair-produce and the ionization loss prevents further radiation. The physical depth achieved by this “shower” is then an indicator of how much energy the original electron or photon possessed. [17]

Hadronic showers occur when a high energy hadron experiences an inelastic nuclear collision with the heavy metal layer, producing secondary hadrons that go onto have their own collisions. This cycle continues until the individual hadrons no longer have enough energy to break up nuclei. Hadrons tend to be much more massive than electrons and a relatively large amount of energy is released from nuclear interactions, so the depth that a hadronic shower penetrates is larger and such calorimeters must be physically larger than the electromagnetic calorimeters.[17]

#### 4.3.1 CDF Central Electromagnetic Calorimeter (CEM)

CDF’s central electromagnetic calorimeter (CEM) is composed of 48 wedges that each cover  $15^\circ$  in azimuth and 0.11 in pseudorapidity ( $\eta$ ). Each  $15^\circ$  wedge has alternating lead and scintillator layers. The energy resolution (in GeV) of the EM calorimeter is

$$\frac{\delta E}{E} = 13.5\%/\sqrt{E_T} + 1.7\% \quad (125)$$

[10]

#### 4.3.2 CDF Hadronic Calorimeters (CHA,WHA)

The central hadronic calorimeter (CHA) and the endwall hadronic calorimeter (WHA) wedges are composed of alternating layers of iron and scintillator. Both the CHA and WHA are an array of 48 wedges, with the CHA covering  $|\eta| < 0.9$  and the WHA covering  $0.7 < |\eta| < 1.3$ . The energy resolution of the CHA and WHA detectors are

$$\frac{\delta E}{E_T} = \frac{50\%}{\sqrt{E_T}} \quad (126)$$

and

$$\frac{\delta E}{E_T} = \frac{75\%}{\sqrt{E_T}} \quad (127)$$

respectively.

#### 4.3.3 CDF Forward Calorimeters (PEM, PHA)

The forward calorimeters are also divided between a “plug electromagnetic calorimeter” (PEM) and a “plug hadronic calorimeter” (PHA), covering  $1.1 < |\eta| < 3.6$  and  $1.2 <$

$|\eta| < 3.6$ , respectively. The design and function is similar to the central calorimeters. The energy resolution of the PEM is

$$\frac{\delta E}{E} = 16\%/\sqrt{E_T} + 1\% \quad (128)$$

and the energy resolution of the PHA is

$$\frac{\delta E}{E} = 80\%/\sqrt{E_T} + 5\% \quad (129)$$

[10]

#### 4.4 Muon Detectors

The first thing to know about muon detectors is that there is no such thing as a muon detector, just a charged particle detector located behind so much material that only muons tend to reach it. Given that, the CDF muon detectors are located outside the calorimeter system from the beamline. This way, any high energy photons will have already been absorbed by the EM calorimeter and any high energy hadrons will have already been absorbed by the hadronic calorimeter—aside from the occasional “punch through” hadron. The three muon detectors used for this analysis are the “Central MUon chambers” (CMU), “Central Muon uPgrade” (CMP), and the “Central Muon eXtension” (CMX). Not used is the “Intermediate MUon” (IMU) system in the forward region of the detector ( $|\eta| > 1.0$ ), which contains the “Barrel MUon” chamber (BMU) and BSU/TSU scintillators (see table 5 for a summary).

The CMP and CMX muon detectors contain two systems: a stack of four single-cell drift chambers that provide a short track called a “stub” and a scintillation counter. The CMU has only a drift chamber. These muons detectors are used in tandem with the silicon and COT trackers to establish muon tracks from which the transverse momentum  $p_T$  is gauged by the track curvature. Since this analysis focuses on a signal with a leptonic signature, the detection of muon (along with electrons) is critical to finding, excluding, or setting limits on a signal. Also, we shall see in chapter 9 that distinguishing muons from electrons will be a useful tool in using a neural net (see chapter 9.3) to distinguish signal from particular backgrounds.

#### 4.5 CDF Detector Summary for $VH \rightarrow VWW \rightarrow \text{Trileptons}$

This chapter explored the basic structure and design of the CDF II detector. At the broadest level, the CDF detector is composed of trackers, calorimeters, and the muon detectors (very similar to the trackers). The trackers trace the paths of the charged particles while the calorimeters absorb and record their energies.

Chambers/Counters	$\Delta\eta$	$\Delta\phi$	$T_{\max}$ drift	# channels
CMU	[0.0, 0.6]	360°	800 ns	2304
CMP/CSP	[0.0, 0.6]	360°	1500 ns	1076/274
CMX/CSX	[0.6, 1.0]	360°	1600 ns	2208/324
BMU/BSU,TSU	[1.0/(1.0,1.3),1.5/(1.5,1.5)]	270°/270°, 360°	800 ns	1728/432,144

Table 5: Basic Summary of CDF Muon Detectors [28]

This analysis searches for a  $VH \rightarrow VWW \rightarrow$  Trilepton +  $\cancel{E}_T$  signature, so understanding how physical leptons (electrons and muons) translate into detector quantities is critical for matching the Standard Model physics of chapter 2 to experimental observation.

The Tevatron generates collisions very quickly and most will produce interactions that are not of interest to the experimentalist. Therefore, collider detectors have “trigger systems” that can quickly use tracker and calorimeter information to make decisions in real time about whether or not a particular event ( $p\bar{p}$  interaction) has generated products that are interesting for some reason. Because the  $VH \rightarrow VWW$  signature of interest to this analysis contains leptons and  $\cancel{E}_T$ , triggers that are programmed to record specifically these events are of particular interest. We shall subsequently explore the idea of triggers and the particular triggers used in this analysis in chapter 5. Once the triggers have recorded datasets that *may* have the signature of interest, offline algorithms perform more computationally intensive calculations to more accurately decide if a collection of detector quantities does constitute a reconstructed lepton. Such reconstructed lepton identification will be explored in more detail in chapter 6. Although jet identification will be useful for distinguishing signal from backgrounds ( $ZH$  tends to have  $\sim 2$  jets while it’s background tend to have 0 jets, for example), jet-based triggers will not be an item of interest to this analysis.

## 5 Triggers, Datasets, and Event Selection

The Tevatron  $p\bar{p}$  collisions happens every 396 ns; or equivalently, with a frequency of 2.5 MHz. The CDF detector cannot—and would not want to—record the products of every single collision that occurs. Instead, it has a three level “trigger” system that can decide whether or not to record an event using basic detector information. Ultimately, CDF is capable of recording at a rate only up to 100 Hz, so the trigger system is designed to filter the events to those of interest for current analyses. This is done with hardware systems at level 1 and 2, then a computer farm at level 3. Each particular “trigger” refers to a collection of decisions at all three levels.

### 5.1 Level 1

The level 1 trigger has  $\sim 5.5 \mu\text{s}$  to make a decision and a maximum accept rate of  $\sim 20$  kHz. This hardware system is composed of three parallel processing streams. One stream finds calorimeter based objects (L1CAL), one looks for primitive muon signals (MUON PRIM-L1MUON), and the last finds tracks in the COT with the “eXtremely Fast Tracker” (XFT). Up to 64 level 1 triggers can be formed from the objects in these streams using simple boolean logic (AND & OR operators). [10]

### 5.2 Level 2

After a level 1 acceptance, the information of an event proceeds to level 2 for a more detailed decision. The level 2 trigger has  $\sim 20 \mu\text{s}$  to make a decision and a maximum accept rate of  $\sim 300$  kHz. There are four buffers for processing an event coming from level 1, when a particular one of these buffers is busy processing an event it is not available for further use. When all four buffers are in use, further events coming from level 1 are lost. The time that level 2 is busy processing and incapable of accepting more events from level 1 is denoted as “deadtime.”

Level 2 is capable of using silicon, shower max, and calorimeter information in addition to the level 1 information to perform further reconstruction of an event. Once the event data is loaded into the level 2 processors, a decision can be made about whether the event satisfies any of the level 2 triggers. [10]

### 5.3 Level 3

The level 3 trigger has a maximum accept rate of  $\sim 20$  kHz. It is divided between an event builder that stores raw detector data and a linux PC farm that makes a decision on whether to store an event using higher level event objects. Level 3 is designed to make a decision on an event using data that approximates full reconstruction.

## 5.4 Trigger Paths (“Datasets”) of the $H \rightarrow WW$ Group

“Trigger” tends to be a bit of an overloaded term; it may refer colloquially to a variety of objects. Any particular criteria within any of the three levels are often denoted as triggers, collections of criteria within one of the three levels are denoted as “LX triggers” (X= 1, 2, 3), as well as sets of criteria from all three levels. For the purposes of this dissertation, “trigger bits” will refer to particular criteria that exist within any one of the three “trigger levels” just discussed. There will be “LX triggers” (X= 1, 2, 3) for collective decision at a particular level. “Trigger paths” will be the broadest categories of collections of trigger bits that are chosen by analyses interested in data with particular features. For instance, the  $H \rightarrow WW$  group is interested in leptonic decays from the weak vector bosons, so it chooses to use data from “trigger paths” that record high  $p_T$  lepton events during online operations.

The following are the triggers paths, or “datasets,” used for the CDF high mass Higgs boson group and this analysis. Trigger design may evolve over time, so note that these trigger paths refer to their incarnations in trigger table PHYSICS\_5\_04\_v-3. This trigger table can be referenced for a more detailed breakdown of the trigger bits within each trigger level. [29]

### 5.4.1 ELECTRON\_CENTRAL\_18

The ELECTRON\_CENTRAL\_18 trigger path is designed to select data with high  $p_T$  electrons absorbed by the central calorimeter.

- Level 1 (L1\_CEM8\_PT8\_v-5): This trigger requires a cluster of energy in the central EM calorimeter with at least 8 GeV, the ratio of  $E_{\text{Had}}/E_{\text{EM}} < 0.125$  to distinguish the EM energy deposit from charged hadrons that may deposit some of its energy in the EM calorimeter, and an XFT track with  $p_T > 8.34$ .
- Level 2 (L2\_CEM18\_PT8\_v-1): Additional requirements of an EM cluster with at least 18 GeV and  $|\eta| < 1.317$  are imposed here.
- Level 3 (L3\_ELECTRON\_CENTRAL\_18\_v-6):
  - $L_{\text{shr}} < 0.4$ , a variable that compares lateral shower profile in towers next to the seed tower to some expected profile.
  - $\Delta z$  between the COT track and the central EM calorimeter shower to match within 8 cm.
  - a COT track with  $p_T$  at least 9 GeV

### 5.4.2 MUON\_CMUP18

The MUON\_CMUP18 trigger path is designed to identify high  $p_T$  muons with tracks in both the CMU and CMP muon detectors.

- Level 1 (L1\_CMUP6\_PT4\_v-2): This trigger requires an XFT track with  $p_T > 4.09$  GeV and fiducial to a CMU stub with  $pt > 6$  GeV, and a CMP stub.
- Level 2 (L2\_CMUP6\_PT15\_3DMATCH\_v-1): This trigger tightens the XFT criteria by requiring a four layer track with  $p_T > 14.77$  GeV.
- Level 3 (L3\_MUON\_CMUP\_18\_v-3 ): This trigger raises the  $p_T$  cut to 18 GeV and continues the requirement of matching the track to stubs in the CMU and CMP.

#### 5.4.3 MUON\_CMX18

The MUON\_CMX18 trigger path is designed to identify high  $p_T$  muons with tracks that lead to the CMX muon detector.

- Level 1 (L1\_CMX6\_PT8\_CSX\_v-2): This trigger requires an XFT track with  $p_T > 8.34$  GeV and fiducial to a CMX stub with  $p_T > 6$  GeV, as well as a hit in the CSX scintillator.
- Level 2 (L2\_CMX6\_PT15\_3DMATCH\_HTDC\_v-1): This trigger tightens the XFT criteria by requiring a four layer track with  $p_T > 14.77$  GeV.
- Level 3 (L3\_MUON\_CMX18\_v-2): This trigger raises the  $p_T$  cut to 18 GeV and continues the requirement of matching the track to a CMX stub.

#### 5.4.4 MET\_PEM

The leptonic decays studied by the  $H \rightarrow WW$  group, and especially the associated production leptonic decay of  $WH \rightarrow WWW \rightarrow l\nu l\nu l\nu$ , also tend to exhibit high values of missing transverse energy ( $\cancel{E}_T$ ). So we are also interested in the dataset pertaining to the MET\_PEM trigger path that is designed to accept events with energy clusters in the plug electromagnetic calorimeter in association with  $\cancel{E}_T$ . Note that this online version of  $\cancel{E}_T$  – denoted here as  $\cancel{E}_T^{\text{raw}}$  – simply uses the sum of transverse energies over the calorimeter towers and does not employ the muon or jet corrections described later in chapter 6.

- Level 1 (L1\_EM8\_&\_MET15\_v-11): At this level, the trigger requires either a central or plug EM cluster with  $E_T > 8$  GeV, with  $E_{\text{Had}}/E_{\text{EM}} < 0.125$  for a central cluster and  $E_{\text{Had}}/E_{\text{EM}} < 0.0625$  for a plug cluster. The L1\_MET15 trigger bit is also employed for a  $\cancel{E}_T^{\text{raw}} > 15$  GeV cut.
- Level 2 (L2\_PEM20\_MET15\_v-1): This trigger continues to require a  $\cancel{E}_T^{\text{raw}} > 15$  GeV cut, requires a plug EM object with  $E_T > 20$  GeV, and  $1.1 < |\eta| < 3.6$ .
- Level 3 (L3\_PEM20\_MET15\_v-8): This level imposes a plug calorimeter requirement of 3 towers with  $E_T > 20$  GeV,  $E_{\text{Had}}/E_{\text{EM}} < 0.125$  for the plug cluster, and a  $\cancel{E}_T^{\text{raw}} > 15$  GeV cut again.

### 5.4.5 MUON\_CMP18\_PHI\_GAP

This trigger path has been working properly only since period 21 data-taking [2]. The MUON\_CMP18\_PHI\_GAP trigger path is designed to account for gaps in  $\phi$  coverage between the calorimeter wedges. This puts a 2.25 degree gap in the CMU  $\phi$  coverage every 15 degrees. The basic idea of this trigger is to require tracks that point towards a gap to be coincidence with a CMP stub and a CSP hit. Previous incarnations of this trigger had problems keeping the rate under reasonable levels at high instantaneous luminosities, so it does employ a dynamic prescale up to a factor of 60. [8]

- Level 1 (L1\_CMP3\_PT15\_3D\_PHIGAP\_DPS\_v-2): This trigger requires an XFT track with  $p_T > 14.77$  GeV.
- Level 2 (L2\_CMP3\_PT15\_3D\_PHIGAP\_CSP\_v-1): This level goes on to require a CSP hit.
- Level 3 (L3\_MUON\_CMP18\_v-1): At level 3, this trigger requires
  - cmpDx=20
  - $p_T > 18$  GeV
  - CMP stub

## 6 High $p_T$ Object Identification in the High Mass Higgs Boson Search

### 6.1 Lepton Identification

#### 6.1.1 Electron ID

#### 6.1.2 Muon ID

#### 6.1.3 Unspecified Track ID

### 6.2 Missing Transverse Energy ( $\cancel{E}_T$ )

### 6.3 Fake Leptons

### 6.4 Lepton Efficiencies

### 6.5 Lepton ID Scale Factors

## 7 Computations with Artificial Neural Networks

## 8 Statistics of Confidence Level Limits In the Search for New Physics

## 9 The High Mass Higgs Boson Analysis in the Trilepton Signature

### 9.1 Motivation for Trileptons

The production cross sections for  $WH$  and  $ZH$  may be small relative to the gluon fusion cross section of the current  $H \rightarrow WW$  analysis, but until now the trilepton signature has been completely unexplored, the uniqueness of the trilepton signature keeps background low, and every little bit counts as we push observed limits toward the standard model cross section.

Leptons decaying from a  $W$ -boson are physically detectable from an experimental point of view if the  $W$  decays to an electron, a muon, or a tau provided that the tau goes on to decay to an electron or muon. Given a generic  $W$ -boson, the probability of getting a lepton via any of these decays is : <sup>2</sup>[1]

$$\begin{aligned} P(W \rightarrow l) &= P(W \rightarrow e) + P(W \rightarrow \mu) + P(W \rightarrow \tau) [P(\tau \rightarrow e) + P(\tau \rightarrow \mu)] \\ &= 0.2528 \end{aligned}$$

The relevant cross sections are (from tables 7, 8, and see [3])

- $\sigma_{ggH160} = 0.4607 \text{ pb}$
- $\sigma_{WH160} = 0.0510 \text{ pb}$
- $\sigma_{ZH160} = 0.0331 \text{ pb}$

The dominant mode for the current  $H \rightarrow WW$  group analysis is gluon fusion in the two-lepton bin, which has an expected yield of:

$$\sigma_{ggH160} \cdot \mathcal{BR}(H \rightarrow WW) \cdot P(W \rightarrow l)^2 = 0.02653 \text{ pb}$$

By comparision, the expected yield for  $WH$  associated production in the three-lepton bin is:

$$\sigma_{WH160} \cdot \mathcal{BR}(H \rightarrow WW) \cdot P(W \rightarrow l)^3 = 7.425 \times 10^{-4} \text{ pb}$$

or 2.8% the yield of the dilepton analysis (for  $m_H = 160 \text{ GeV}$ ).

$ZH$  associated production may have a smaller cross section than  $WH$ , but given one such event there is a higher probability of producing three leptons. In this case, the  $Z$

---

<sup>2</sup>Basic decay values are from PDG Particle Physics Booklet (July 2006), Institute of Physics

decays to two leptons so we need only one of the two Higgs- $W$ -bosons to decay leptonically and there are two ways for this to happen:

$$\begin{aligned} P(W \rightarrow l, W \rightarrow l) &= P(W \rightarrow l)^2 = 0.06391 \\ P(W \rightarrow l, W \rightarrow \text{had.}) &= P(W \rightarrow l) [1 - P(W \rightarrow l)] = 0.1889 \\ P(W \rightarrow \text{had.}, W \rightarrow l) &= P(W \rightarrow l) [1 - P(W \rightarrow l)] = 0.1889 \\ P(W \rightarrow \text{had.}, W \rightarrow \text{had.}) &= [1 - P(W \rightarrow l)]^2 = 0.5583 \end{aligned}$$

<sup>3</sup> So the expected  $ZH$  yield is

$$\sigma_{ZH160} \cdot \mathcal{BR}(H \rightarrow WW) \cdot P(Z \rightarrow ll) \cdot 2 \cdot P(W \rightarrow l, W \rightarrow \text{had.}) = 7.582 \times 10^{-4} \text{ pb}$$

or 3.0% of the current  $H \rightarrow WW$  dilepton analysis (for  $m_H = 160$  GeV). Thus, based on cross sections and branching ratios alone we pursued this trilepton analysis expecting to contribute another  $\sim 5.7\%$  compared to the gluon fusion process in the current  $H \rightarrow WW$  dilepton analysis.

Incidentally, one of the future improvements to this analysis is to accept  $\tau$  leptons directly. Noting that the above prediction assumes that vector boson decays to  $\tau$ 's result in a detectable lepton only if that  $\tau$  decays to an electron or muon, if we repeat the prediction assuming we may accept one hadronically decaying tau into the trilepton analysis, then the 5.7% becomes 6.9% (for  $m_H = 160$  GeV).

---

<sup>3</sup>Observe that  $0.06391+0.1889+0.1889+0.5583=1.0$

mode	Period	Stntuple	$\sigma \times \mathcal{B}$ (pb)	K-factor <sup>a</sup>	Filter Eff
$WZ$	0-23	we0s6d,we0scd,we0shd we0sld,we0sod,we0sbf we0shf	$3.46 \times 0.101$	1.0	0.754
$ZZ$	0-23	we0s7d,we0sdd,we0sid we0smd, we0spd,we0scf we0sif	1.511	1.0	0.233
$t\bar{t}$	0-11	te0s2z	$7.9 \times 0.1027$	1.0	1.0
$Z\gamma$	0-11	re0s33, re0s34, re0s37	14.05	1.36 <sup>b</sup>	1.0

<sup>a</sup> If cross section is NLO, then K-factor is one.

<sup>b</sup> [http://www-cdf.fnal.gov/tiki/tiki-index.php?page=EwkDatasets#\\_Drell\\_Yan\\_Z\\_gamma\\_Sample](http://www-cdf.fnal.gov/tiki/tiki-index.php?page=EwkDatasets#_Drell_Yan_Z_gamma_Sample)

Table 6: Monte Carlo samples used in this analysis

## 9.2 Event Summary and Signatures of the $WH$ and $ZH$ Trilepton Analyses

### 9.2.1 Lepton Selection

This trilepton analysis is a high mass ( $m_H > 135$  GeV) standard model higgs boson search conducted by the  $H \rightarrow WW$  group, so the lepton selection criteria of the  $H \rightarrow WW$  group follow implicitly as well. The lepton categories used are [3]:

- Electrons: LBE, PHX (TCE has been replaced with the likelihood-based electron selection)
- Muons: CMUP, CMP, CMU, CMX, CMXMsKs, BMU, CMIOCES, CMIOPES, CrkTrk

The  $H \rightarrow WW$  group also recently replaced the standard selection method of hard cuts with a likelihood-based selection for electrons. This new selection method is therefore also assumed in this trilepton analysis and detailed further in [3].

The datasets used are bhel0d/0h/0i/0j/0k/0m for electrons, bmu0d/0h/0i/0j/0k/0m for muons, and bpel0d/0h/0i/0j/0k/0m for MET+PEM; with the following corresponding trigger paths:

- ELECTRON\_CENTRAL\_18
- MUON\_CMUP18
- MUON\_CMX18
- MUON\_PEM

$M_H(GeV^2)$	Period	Stntuple	$\sigma$ (pb)	BR ( $H \rightarrow WW$ )	Filter Efficiency
110	0-23	fhgs4a,fhgs6a	0.2075	0.0441	0.6880
120	0-23	fhgs4b,fhgs6b	0.1529	0.1320	0.6978
130	0-23	fhgs4c,fhgs6c	0.1141	0.2869	0.7032
140	0-23	fhgs4d,fhgs6d	0.0860	0.4833	0.7065
150	0-23	fhgs4e,fhgs6e	0.0654	0.6817	0.7085
160	0-23	fhgs4f,fhgs6f	0.0510	0.9011	0.7108
170	0-23	fhgs4g,fhgs6g	0.0389	0.9653	0.7125
180	0-23	fhgs4h,fhgs6h	0.0306	0.9345	0.7141
190	0-23	fhgs4i,fhgs6i	0.0243	0.7761	0.7151
200	0-23	fhgs4j,fhgs6j	0.0193	0.7347	0.7165
145	0-23	fhgs4o,fhgs6o	0.0749	0.5731	0.7075
155	0-23	fhgs4p,fhgs6p	0.0572	0.8007	0.7098
165	0-23	fhgs4q,fhgs6q	0.0441	0.9566	0.7114
175	0-23	fhgs4r,fhgs6r	0.0344	0.9505	0.7130

Table 7: Associated Higgs production with a  $W$  boson (from CDF Note 9863).

$M_H(GeV^2)$	Period	Stntuple	$\sigma$ (pb)	BR ( $H \rightarrow WW$ )	Filter Efficiency
110	0-23	uhgs4a,uhgs6a	0.1236	0.0441	0.6930
120	0-23	uhgs4b,uhgs6b	0.0927	0.1320	0.7031
130	0-23	uhgs4c,uhgs6c	0.0705	0.2869	0.7087
140	0-23	uhgs4d,uhgs6d	0.0542	0.4833	0.7122
150	0-23	uhgs4e,uhgs6e	0.0421	0.6817	0.7151
160	0-23	uhgs4f,uhgs6f	0.0331	0.9011	0.7172
170	0-23	uhgs4g,uhgs6g	0.0261	0.9653	0.7184
180	0-23	uhgs4h,uhgs6h	0.0208	0.9345	0.7204
190	0-23	uhgs4i,uhgs6i	0.0166	0.7761	0.7220
200	0-23	uhgs4j,uhgs6j	0.0135	0.7347	0.7239
145	0-23	uhgs4o,uhgs6o	0.0477	0.5731	0.7135
155	0-23	uhgs4p,uhgs6p	0.0373	0.8007	0.7155
165	0-23	uhgs4q,uhgs6q	0.0294	0.9566	0.7183
175	0-23	uhgs4r,uhgs6r	0.0233	0.9505	0.7196

Table 8: Associated Higgs production with a  $Z$  boson (from CDF Note 9863).

- MUON\_CMP18\_PHI\_GAP

### 9.2.2 Trilepton Signal Regions Defined

The current  $H \rightarrow WW$  group analysis is constrained only to the study of events with exactly two leptons, which focuses primarily on the gluon fusion Higgs boson signal because of its large cross section relative to associated production. The trilepton analysis, however, focuses virtually entirely on the two associated production channels because there are three vector bosons that allow for decays to more than two leptons, whereas the gluon fusion and vector boson fusion signals do not contribute a real third lepton. Monte Carlo signal simulation does indicate that gluon fusion and vector-boson fusion have negligible contribution to the three-lepton bin. Thus, we are left with two signals to study: a  $WH \rightarrow WWW \rightarrow l\nu, l\nu, l\nu$  signal and a  $ZH \rightarrow ZWW \rightarrow ll, l\nu, \text{jet}$  signal. With two signals we naturally define two new trilepton signal regions attempting to isolate each, ameliorating the effort to discriminate each from background based on their unique characteristics.

Consider the three leptons as ordered by their transverse momentum  $p_T$  (or transverse energy  $E_T$  for electrons) such that the highest  $p_T$  lepton is the 1<sup>st</sup> and the lowest  $p_T$  lepton is the 3<sup>rd</sup>. First, we filter trilepton events into an *InZPeak* category if any of the three possible dilepton pairings (that is, pairing the 1<sup>st</sup> lepton with the 2<sup>nd</sup> lepton; the 1<sup>st</sup> lepton with the 3<sup>rd</sup> lepton; or the 2<sup>nd</sup> lepton with the 3<sup>rd</sup> lepton) has an invariant mass value that falls within a 10 GeV window of the  $Z$ -boson mass at 91 GeV, have opposite signs, and have same flavor. This *InZPeak* region is chosen to isolate the  $ZH$  signal process. The rest of the trileptons events are directed toward the *NoZPeak* region, which focuses on the  $WH$  signal process. These regions are new to the  $H \rightarrow WW$  analysis group.

Additionally, the  $WH$  analysis has a missing energy cut of  $\cancel{E}_T > 20$  GeV. This cut drastically reduces the  $Z\gamma$  background contribution and also provides a  $WH$  control region in  $10.0\text{GeV} < \cancel{E}_T < 20.0$ . Because the  $WH \rightarrow WWW \rightarrow l\nu l\nu l\nu$  event topology has three  $W \rightarrow l\nu$  decays, the missing energy is relatively large and a negligible amount of signal is lost from moving the  $\cancel{E}_T$  cut up to 20.0 GeV from 10.0 GeV.

The  $\cancel{E}_T$  distribution for the  $ZH \rightarrow ZWW$  trilepton events is somewhat lower than that of the  $WH$  analysis because it produces fewer neutrinos ( $WWW \rightarrow l\nu, l\nu, l\nu$  has three neutrinos while  $ZWW \rightarrow ll, l\nu, \text{jet}$  has only one), so defining a control region by a higher  $\cancel{E}_T$  cut is less appropriate. The  $ZH$  analysis also has somewhat larger backgrounds than the  $WH$  region and is topologically similar to the most significant background,  $WZ$ . However, for a  $ZH \rightarrow ZWW$  event to produce a three-lepton signature we either have one of the  $W$ -leptons decaying hadronically or-less frequently—we have a  $ZH \rightarrow ZWW \rightarrow llll$  physics event that loses one of its leptons to an area of the detector that is incapable of reconstructing a track (detector holes or too far forward in pseudorapidity, for example) but is still recorded by the calorimeter system. Therefore,  $ZH$  trilepton events inherently have a higher number of jets than the backgrounds and very little signal in the  $\text{NJet} = 0$

bin. This characteristic of the  $ZH$  trilepton signal allows us to create a control region for the  $ZH$  analysis in the  $\text{NJet}=0$  bin with very little signal loss, and so  $\text{NJet}=0$  events are not included in the  $ZH$  analysis.

Observe in table 9.2.3 that  $\sim 77\%$  of the signal in the *NoZPeak* region is  $WH$ , while  $\sim 96\%$  of the signal in the *InZPeak* region is  $ZH$ . We will see in section 9.6 how this division allows us to focus on the unique characteristic of each signal for discrimination from the background in the NeuroBayes neural net treatment.

### 9.2.3 Backgrounds

Both regions of this trilepton analysis have five background categories considered:  $WZ$ ,  $ZZ$ ,  $Z\gamma$  (replacing Drell-Yan), Fakes (data-based  $WW$  and  $Z$ +jets), and  $t\bar{t}$ . Each is summarized in table 9.2.3 along with the predicted signal for a  $m_H = 160$  GeV standard model Higgs boson and the data.

CDF Run II Prebless			$\int \mathcal{L} = 5.3 \text{ fb}^{-1}$	
$(m_H = 165 \text{ GeV}/c^2)$	WH Signal Region	ZH Signal Region		
$WZ$	7.01 $\pm$ 0.96 <sub>syst</sub>	9.01 $\pm$ 1.74 <sub>syst</sub>		
$ZZ$	1.49 $\pm$ 0.20 <sub>syst</sub>	4.41 $\pm$ 0.68 <sub>syst</sub>		
$Z\gamma$	2.47 $\pm$ 0.42 <sub>syst</sub>	3.00 $\pm$ 0.63 <sub>syst</sub>		
Fakes ( $WW, Z$ +Jets)	3.22 $\pm$ 0.97 <sub>syst</sub>	7.74 $\pm$ 2.32 <sub>syst</sub>		
$t\bar{t}$	0.18 $\pm$ 0.07 <sub>syst</sub>	0.03 $\pm$ 0.01 <sub>syst</sub>		
<b>Total Background</b>	14.5 $\pm$ 1.58 <sub>syst</sub>	24.3 $\pm$ 3.57 <sub>syst</sub>		
$WH$	0.58 $\pm$ 0.08 <sub>syst</sub>	0.02 $\pm$ 0.004 <sub>syst</sub>		
$ZH$	0.18 $\pm$ 0.02 <sub>syst</sub>	0.58 $\pm$ 0.08 <sub>syst</sub>		
<b>Total Signal</b>	0.76 $\pm$ 0.10 <sub>syst</sub>	0.60 $\pm$ 0.08 <sub>syst</sub>		
<b>Data</b>	14	33		

High Mass

- *Heavy Dibosons ( $WZ, ZZ$ ):* The  $WZ$  and  $ZZ$  diboson contributions provide three physical leptons, with  $WZ$  being the dominant background in both trilepton signal regions. Both samples are Pythia-based, where the  $W$  is allowed to decay inclusively and the  $Z$  is forced to decay leptonically (electron, muon, or tau pairs)[3].
- $Z\gamma$ : The  $Z\gamma$  background in the trilepton analyses replaces the Drell Yan contribution of the dilepton analyses and is created by the Bauer generator. We acquire a third lepton from a Drell Yan process when either an initial or final state radiated photon undergoes a conversion and showers in the calorimeter for the third lepton. As such, the  $Z\gamma$  is the restriction of Drell Yan to those events which do radiate a photon for the purpose of working with a larger statistical sample.

- *Fakes(WW, Z+Jets)*: In the dilepton analysis, the Fakes category is measured from single high  $p_T$  lepton data (rather than MC) and assumed to have a  $W$ +jets event topology, where the one lepton is from the  $W$ -boson. From this data sample, events with one-lepton+denominator object are selected and then re-weighted based on the rates at which jets fake a lepton, measured from QCD samples—where “denominator-objects” are looser lepton objects that do not fully satisfy lepton ID, but considered candidates for a physical object that may fake a lepton.

Similarly, for the trilepton analyses we are interested in processes that produce two physical leptons+ one denominator object from the jets. Two high  $p_T$  lepton data is dominated by  $WW$  and  $Z$ +jets. First note that we do not consider simulated  $WW$  background as the dilepton analyses do to avoid double counting the process. Second, because the rate at which a jet is expected to fake a lepton is on the order of 1 – 5%, the rate at which such an event is expected to fake two leptons is drastically lower: 0.01 – 0.25%. As such, we consider the contribution of  $W$ +jets with one real lepton and two faked lepton to be negligible for the trilepton analyses and so label this category  $WW, Z$ +Jets instead of  $W$ +Jets, but “ $W$ +Jets” is still accounted for.

The actual rates for which a light jet fakes a lepton used in this analysis are estimated from jet triggered data and expounded further in CDF note [3]. These rates were determined in the  $H \rightarrow WW$  group’s dilepton analysis and we adopt the same values here.

- $t\bar{t}$ : The  $t\bar{t}$  process is the smallest background, but arguably the most complex. This process decays to two pairs of a  $b$ -jet accompanied by a  $W$  boson. For the case of trileptons, we consider the case of the two  $W$ ’s decaying leptonically. The third lepton signature is then due to one of the  $b$ -jets, which is supposed to produce a lepton candidate with higher probability than a light jet, but this rate is not precisely known.

Because of this, we cannot ignore the possible contribution of  $t\bar{t}$  in our Fakes background category where the lepton decayed from the  $b$ -jet is the fake lepton (denominator object). However, any  $t\bar{t}$  that might be included in the high  $p_T$  lepton data of the Fakes background is then scaled down by a fake rate determined for a sample of jets assumed to be mostly light—hence, the  $t\bar{t}$  contribution to the Fakes background is scaled down further than it should be since it’s jets are the heavy  $b$ -jets.

The standard MC  $t\bar{t}$  ntuple used by the  $H \rightarrow WW$  group requires reconstructed leptons to pass a matching criteria to either a generator-level lepton or photon (for the case of photon conversion). For our purposes in the trilepton analysis, we are interested in a third lepton whose signature is the result of those  $b$ -jets, so we have our own MC  $t\bar{t}$  sample that allows matching to  $b$ -jets as well as leptons and photons. The MC  $t\bar{t}$  sample accounts for such events that result in three fully identified leptons, as opposed to the 2 leptons+1 fake lepton signature of the Fakes

background.

Lastly, there is inevitably some overlap between the  $t\bar{t}$  that occurs implicitly in the Fakes data-based background and the MC sample. By measuring the difference between the 3-lepton bin of the default  $t\bar{t}$  sample (lepton match only to generator-level leptons or photons) with another  $t\bar{t}$  sample allowing matching to  $b$ -jets as well, we take half the percentage difference to be the systematic error (23%) accounting for overlap.

- *Correction to Simulation and Fake Rates:* To properly weight events from simulation and scale data-based backgrounds, we follow the same standard procedures that the rest of the  $H \rightarrow WW$  group as described on page 41 in CDF Note 9863.

#### 9.2.4 Signal Yields in the *NoZPeak* and *InZPeak* Regions

Although we have defined two trilepton signal regions to separately focus on the  $WH$  and  $ZH$  associated production channels, both regions do contain both signals and are summarized for all generated masses in table 9.

$m_H$ GeV	<i>NoZPeak</i>			<i>InZPeak</i>		
	$WH$	$ZH$	Total	$WH$	$ZH$	Total
110	0.05	0.02	0.07	0.002	0.06	0.06
120	0.15	0.05	0.20	0.004	0.15	0.15
130	0.28	0.09	0.37	0.008	0.29	0.30
140	0.40	0.12	0.52	0.01	0.41	0.42
145	0.44	0.14	0.58	0.02	0.45	0.47
150	0.47	0.14	0.61	0.02	0.48	0.50
155	0.50	0.16	0.66	0.02	0.51	0.53
160	0.53	0.16	0.69	0.02	0.51	0.53
165	0.50	0.15	0.65	0.02	0.49	0.52
170	0.45	0.14	0.59	0.02	0.46	0.48
175	0.40	0.13	0.53	0.02	0.42	0.44
180	0.35	0.11	0.46	0.02	0.38	0.40
190	0.24	0.08	0.32	0.01	0.27	0.28
200	0.18	0.06	0.24	0.01	0.22	0.23

Table 9: Signal Summary

### 9.3 Neural Net

The trilepton  $H \rightarrow WW$  analyses rely on the NeuroBayes neural network package to discriminate signal from background; we do not attempt the Matrix Element method in this study. We use 13 input variables for the  $WH$  analysis and 16 for the  $ZH$  analysis. The neural net results can be seen in figures 9, 10, 11, and 12.

Because the interaction topology under consideration involves three leptons and also because we do not separate the analyses by jet bin (aside from reserving the  $\text{NJet}=0$  bin for the *InZPeak* control region of the  $ZH$  analysis), the signatures of the signal regions under consideration involve many potentially complex variables whose discriminatory power must be explored. As such, a larger than usual quantity of discriminating variables are used to train the NeuroBayes neural nets and we have found no reason yet to believe that fewer variables would be any benefit.

Recall that the standard model Higgs boson is postulated as a scalar particle and so decays to two  $W$ -bosons having  $+1$  and  $-1$  spin, respectively. Leptonic  $W$ -boson decays have a  $V - A$  distribution, so one of the  $W$  bosons decays to a lepton projected forward along its momentum vector while the other decays its lepton backwards along its momentum vector. If the two Higgs- $W$ -bosons decay close to back-to-back in the experimental rest frame—which is not a terrible assumption for a high mass Higgs—then the two decayed leptons will tend to have a relatively close proximity. Indeed, we find that this is the case (see figure 18) for  $WH$  events since both Higgs- $W$ -bosons must decay leptonically. Also,  $\cancel{E}_T$  is an excellent discriminating variable for  $WH$  events since three leptonic decays of  $W$ 's implies at least three neutrinos carrying away undetected energy.

Likewise, a trilepton signal in a  $ZH$  event implies a hadronic decay of one of the two Higgs- $W$ -bosons while  $WZ$  and  $Z\gamma$  events do not tend to have jets. As such,  $\text{NJet}$  is an excellent discriminating variable for the  $ZH$  signal (see figure 24). Other variables that are excellent for discriminating  $ZH$  in the trilepton case are  $\cancel{E}_T$  ( $ZH$  may have fewer neutrinos than  $WH$ , but the distribution still tends to be higher than the backgrounds), Lead Jet  $E_T$  (jets from vector bosons tend to have higher energy than other sources of jets), and  $\Delta R$  between the  $W$ -lepton and the leading jet (that is, between the decay products of the two Higgs- $W$ -bosons).

*WH* Variable Descriptions/Details:

- $\Delta R$  b/w Opp. Sign Close Leptons: With three leptons there are three possible pairings of leptons. Events with all three leptons having the same sign are rejected from this analysis, so every event has two possible pairings of opposite-signed leptons. Of those two pairings, this variable is the  $\Delta R$  value of the pairing with lower  $\Delta R$  value.
- $\cancel{E}_T$ : Missing Transverse Energy
- $H_T$ : Sum of the transverse energies of all three leptons, the  $\cancel{E}_T$ , and all jets.

- Dimass b/w Opp. Sign Close by  $\phi$ : Dilepton invariant mass of the opposite-signed lepton pair that is closer in the  $\phi$  coordinate.
- $\Delta\phi(\text{Lep2}, \cancel{E}_T)$ : The magnitude of the difference in  $\phi$  between the 2<sup>nd</sup> lepton by  $p_T$  and the  $\cancel{E}_T$ .
- Inv. Mass(Lep3,  $\cancel{E}_T$ , Jets): Invariant mass of the vector sum of the 3<sup>rd</sup> lepton,  $\cancel{E}_T$ , and Jets.
- $m_T(\text{Leptons}, \cancel{E}_T, \text{Jets})$ : Transverse mass of the vector sum of all three leptons,  $\cancel{E}_T$ , and all jets.
- $p_T$  of the 2<sup>nd</sup> lepton by  $p_T$ .
- $\Delta R$  Opp. Sign Far Leptons: With three leptons there are three possible pairings of leptons. Events with all three leptons having the same sign are rejected from this analysis, so every event has two possible pairings of opposite-signed leptons. Of those two pairings, this variable is the  $\Delta R$  value of the pairing with higher  $\Delta R$  value.
- $m_T$  Trilepton Mass: Transverse mass of the vector sum of the three leptons.
- NJet: The number of jets in the event. For this use of NJet, all events with  $\text{NJet} \geq 2$  jets are thrown into the  $\text{NJet} = 2$  bin.
- $m_T$  (Lep3,  $\cancel{E}_T$ ): Transverse mass of the vector sum of the 3<sup>rd</sup> lepton and the  $\cancel{E}_T$ .
- Inv. Mass(Lep1, Lep2,  $\cancel{E}_T$ ): Invariant mass of the vector sum of the 1<sup>st</sup> lepton, 2<sup>nd</sup> lepton, and  $\cancel{E}_T$ .

*ZH* Variable Descriptions/Details:

- NJet: The number of jets in the event.
- $\cancel{E}_T$ : Missing Transverse Energy
- Lead Jet  $E_T$ : Transverse energy of the leading jet. Note that the control region for *InZPeak* is  $\text{NJet} = 0$ , so all events in the signal region must have at least one jet by definition. Also, for this use of NJet, all events with  $\text{NJet} \geq 2$  jets are thrown into the  $\text{NJet} = 2$  bin.
- $\Delta R(W\text{-Lep, Lead Jet})$ : The *InZPeak* region is defined by having one lepton paring (opposite signed, same flavor) near the  $Z$  boson mass. Denote the one other lepton not in this pairing as the  $W$ -lepton. This variable is then the  $\Delta R$  between the  $W$ -lepton and the leading jet.

- $\Delta\phi(\text{Leptons}, \cancel{E}_T)$ :  $\Delta\phi$  between the vector sum of the three leptons and the  $\cancel{E}_T$ .
- $H_T(\text{Leptons}, \cancel{E}_T, \text{Jets})$ : Sum of  $E_T$  of all three leptons,  $\cancel{E}_T$ , and all jets.
- $m_T(\text{Leptons}, \cancel{E}_T, \text{Jets})$ : Transverse mass of the vector sum of all three leptons,  $\cancel{E}_T$ , and all jets.
- $\Delta\phi(\text{Lep2}, \cancel{E}_T)$ : The magnitude of the difference in  $\phi$  between the 2<sup>nd</sup> lepton by  $p_T$  and the  $\cancel{E}_T$ .
- $\Delta R$  b/w Opp. Sign Close Leptons: With three leptons there are three possible pairings of leptons. Events with all three leptons having the same sign are rejected from this analysis, so every event has two possible pairings of opposite-signed leptons. Of those two pairings, this variable is the  $\Delta R$  value of the pairing with lower  $\Delta R$  value.
- Trimass: The invariant mass of the vector sum of the three leptons.
- Inv. Mass(Lep3,  $\cancel{E}_T$ , Jets): Invariant mass of the vector sum of the 3<sup>rd</sup> lepton,  $\cancel{E}_T$ , and Jets.
- Dimass( $W$ -Lep,  $\cancel{E}_T$ ): The *InZPeak* region is defined by having one lepton paring (opposite signed, same flavor) near the  $Z$  boson mass. Denote the one other lepton not in this pairing as the  $W$ -lepton. This variable is then the invariant mass of the vector sum of the  $W$ -lepton and the  $\cancel{E}_T$ .
- $m_T$  Jets: Transverse mass of the vector sum of all jets. Note that the control region for *InZPeak* is  $\text{NJet} = 0$ , so all events in the signal region must have at least one jet by definition.
- $m_T(W\text{-Lep}, \cancel{E}_T)$ : Transverse mass of the vector sum of the  $W$ -lepton and the  $\cancel{E}_T$ .
- $\Delta\phi(Z\text{-Leptons}, W\text{-Lepton})$ :  $\Delta R$  between the vector sum of the two leptons whose dimass is near the  $Z$ -boson mass, and the other lepton.
- $\Delta R$  Opp. Sign Far Leptons: With three leptons there are three possible pairings of leptons. Events with all three leptons having the same sign are rejected from this analysis, so every event has two possible pairings of opposite-signed leptons. Of those two pairings, this variable is the  $\Delta R$  value of the pairing with higher  $\Delta R$  value.

Variable( $WH$ )	110	120	130	140	145	150	155
$\Delta R$ b/w Opp. Sign Close Lept.	12.4	40.8	9.69	40.2	41.4	40.8	43.1
$\not{E}_T$	26.0	21.2	33.8	25.7	26.2	28.1	28.9
Dimass b/w Opp. Sign Close by $\phi$	41.0	14.9	29.7	9.52	8.14	12.7	11.6
$H_T$	3.38	3.82	16.1	11.9	13.1	9.14	9.38
$\Delta\phi(\text{Lep2}, \not{E}_T)$	5.77	6.48	7.60	6.67	6.47	7.74	8.94
$m_T(\text{Leptons}, \not{E}_T, \text{Jets})$	(0.38)	2.08	4.84	5.46	5.99	6.33	7.42
$p_T$ 2 <sup>nd</sup> Lepton	2.77	5.06	3.26	5.12	3.08	4.57	6.88
Inv. Mass(Lep3, $\not{E}_T$ , Jets)	2.05	2.46	4.34	4.51	4.57	7.84	6.64
$\Delta R$ Opp. Sign Far Lept.	9.24	11.0	12.6	9.93	10.9	6.31	6.67
NJet	7.24	7.30	3.64	3.16	3.27	3.04	3.11
$m_T$ Trilepton Mass	(0.52)	2.62	3.78	3.85	6.62	6.67	4.44
$m_T$ (Lep3, $\not{E}_T$ )	3.38	2.13	(0.80)	(0.04)	(0.90)	2.32	3.17
Inv. Mass(Lep1, Lep2, $\not{E}_T$ )	8.38	8.34	4.51	2.69	4.16	1.75	1.56
Variable( $WH$ )	160	165	170	175	180	190	200
$\Delta R$ b/w Opp. Sign Close Lept.	45.7	47.1	31.5	29.0	27.3	19.5	17.3
$\not{E}_T$	29.8	11.3	45.9	46.4	47.0	48.0	21.6
Dimass b/w Opp. Sign Close by $\phi$	12.4	10.9	8.61	8.11	7.31	6.78	5.14
$H_T$	10.5	11.3	6.05	13.4	16.4	22.7	49.7
$\Delta\phi(\text{Lep2}, \not{E}_T)$	9.49	8.81	9.19	9.41	7.70	7.37	6.58
$m_T(\text{Leptons}, \not{E}_T, \text{Jets})$	8.08	8.57	9.93	8.35	8.67	9.54	10.7
$p_T$ 2 <sup>nd</sup> Lepton	7.85	4.59	8.48	8.57	4.66	8.28	8.45
Inv. Mass(Lep3, $\not{E}_T$ , Jets)	6.99	7.63	12.7	10.0	8.67	8.72	7.34
$\Delta R$ Opp. Sign Far Lept.	6.30	5.65	5.79	5.18	5.25	5.54	5.01
NJet	4.58	3.09	3.67	3.36	3.50	2.72	2.25
$m_T$ Trilepton Mass	4.59	7.55	4.65	4.57	7.70	3.98	3.23
$m_T$ (Lep3, $\not{E}_T$ )	3.77	4.14	4.46	3.64	3.68	3.05	1.85
Inv. Mass(Lep1, Lep2, $\not{E}_T$ )	3.15	1.98	1.52	(0.90)	(0.77)	(0.26)	1.67

Table 10:  $WH$  Significance: The variables are ordered by their significance as discriminating variables for the NeuroBayes neural net trained at the 160 GeV signal. Values in parentheses (\*) indicate the input variable was not used for the given  $m_H$ .

Variable( $ZH$ )	110	120	130	140	145	150	155
NJet	23.6	29.7	33.2	37.6	39.6	41.1	43.2
$\cancel{E}_T$	8.07	9.35	13.4	22.7	23.3	23.6	24.8
Lead Jet $E_T$	3.76	7.23	14.5	12.0	16.3	17.3	17.9
$\Delta R(W\text{-Lep}, \text{Lead Jet})$	19.2	17.4	16.7	13.6	13.8	13.0	12.7
$\Delta\phi(\text{Leptons}, \cancel{E}_T)$	21.3	20.5	19.1	10.9	10.2	12.4	11.6
$m_T(\text{Leptons}, \cancel{E}_T, \text{Jets})$	3.50	1.05	5.96	5.86	4.93	3.93	9.26
$\Delta\phi(\text{Lep2}, \cancel{E}_T)$	4.42	3.64	4.54	5.31	4.81	4.85	5.60
$\Delta R$ b/w Opp. Sign Close Lept.	13.8	13.9	10.7	14.6	11.7	10.9	7.10
Trimass	11.6	9.50	9.14	6.83	6.96	6.96	6.35
Inv. Mass(Lep3, $\cancel{E}_T$ , Jets)	7.29	2.78	(0.23)	1.91	1.47	1.94	4.67
$H_T(\text{Leptons}, \cancel{E}_T, \text{Jets})$	(0.48)	(0.95)	2.68	6.38	7.14	6.93	5.81
$m_T$ Jets	(1.01)	2.38	(1.01)	(0.98)	(0.18)	2.36	2.49
Dimass( $W\text{-Lep}, \cancel{E}_T$ )	2.02	(0.07)	2.05	2.80	2.76	2.34	3.09
$m_T(W\text{-Lep}, \cancel{E}_T)$	6.55	4.46	(0.72)	1.78	3.44	3.99	3.56
$\Delta R$ Opp. Sign Far Lept.	2.82	3.25	2.60	2.40	2.36	2.61	1.83
$\Delta\phi(Z\text{-Leptons}, W\text{-Lepton})$	1.55	(1.82)	1.43	(1.19)	2.54	2.64	2.09
Variable( $ZH$ )	160	165	170	175	180	190	200
NJet	45.8	46.6	46.8	47.4	25.8	24.7	22.2
$\cancel{E}_T$	26.7	27.8	27.8	28.4	15.0	13.9	12.7
Lead Jet $E_T$	19.2	19.0	19.5	20.1	12.2	11.6	10.6
$\Delta R(W\text{-Lep}, \text{Lead Jet})$	13.2	12.7	12.1	11.0	7.84	5.53	4.48
$\Delta\phi(\text{Leptons}, \cancel{E}_T)$	12.0	13.2	12.1	11.0	9.72	7.55	6.82
$m_T(\text{Leptons}, \cancel{E}_T, \text{Jets})$	8.62	9.39	9.09	8.52	10.9	9.81	9.26
$\Delta\phi(\text{Lep2}, \cancel{E}_T)$	8.19	8.11	8.02	6.67	5.48	5.17	4.52
$\Delta R$ b/w Opp. Sign Close Lept.	6.54	6.06	5.23	4.95	4.52	3.63	2.81
Trimass	5.84	5.04	4.87	4.87	4.52	3.07	2.66
Inv. Mass(Lep3, $\cancel{E}_T$ , Jets)	5.84	6.64	6.60	6.23	6.81	6.93	7.32
$H_T(\text{Leptons}, \cancel{E}_T, \text{Jets})$	5.02	5.86	7.97	9.66	51.1	54.4	58.7
$m_T$ Jets	4.28	4.58	4.88	4.79	4.31	3.38	2.53
Dimass( $W\text{-Lep}, \cancel{E}_T$ )	4.08	4.22	4.68	4.54	3.88	3.98	3.25
$m_T(W\text{-Lep}, \cancel{E}_T)$	3.11	2.62	3.28	2.68	3.24	2.93	3.00
$\Delta R$ Opp. Sign Far Lept.	2.94	2.61	2.34	2.02	2.45	1.40	1.32
$\Delta\phi(Z\text{-Leptons}, W\text{-Lepton})$	2.60	2.59	2.94	1.98	2.07	1.32	1.35

Table 11:  $ZH$  Significance: The variables are ordered by their significance as discriminating variables for the NeuroBayes neural net trained at the 160 GeV signal. Values in parentheses (\*) indicate the input variable was not used for the given  $m_H$ .

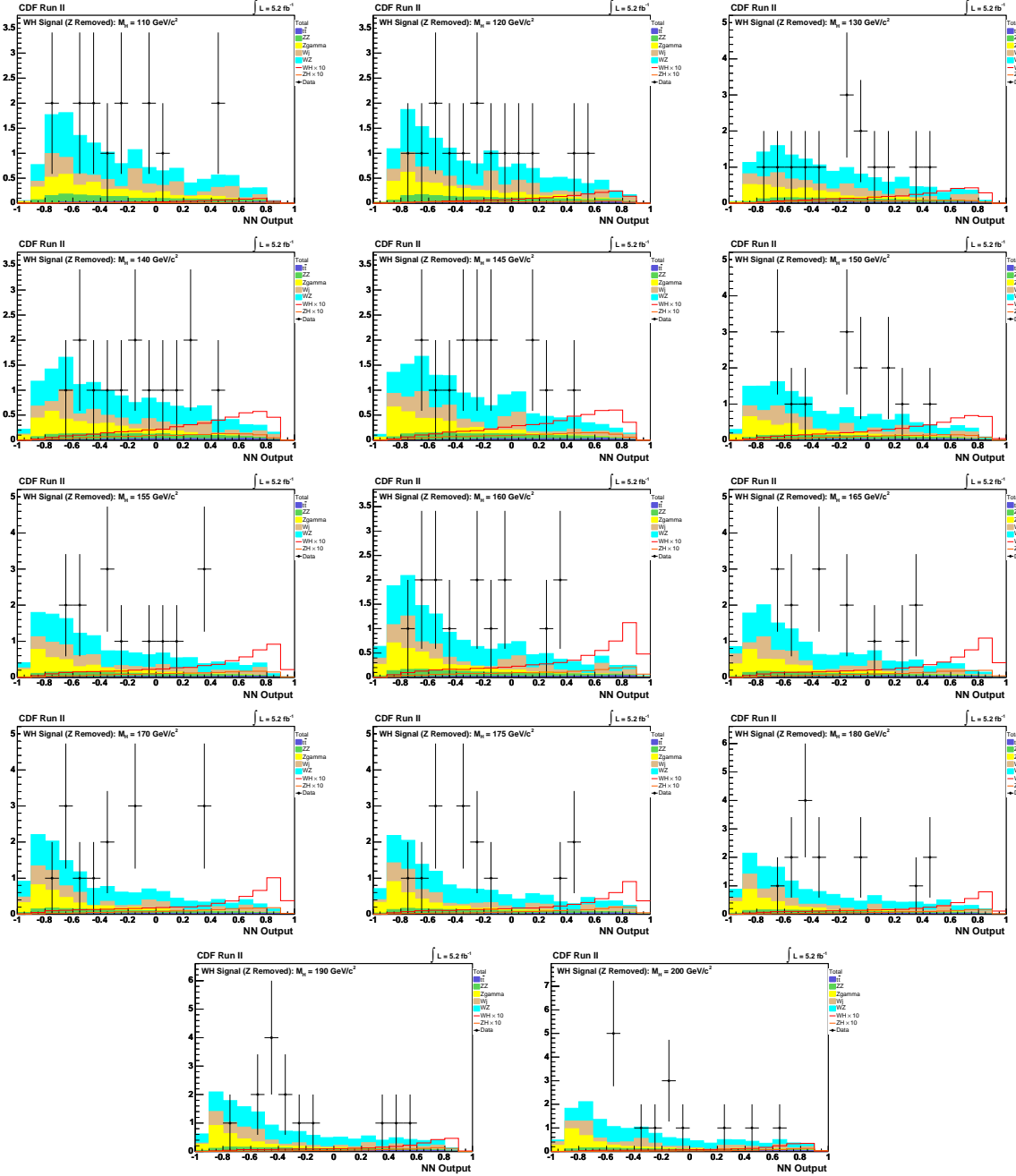


Figure 9: Trilepton  $WH$  NeuroBayes Neural Network output (linear scale)

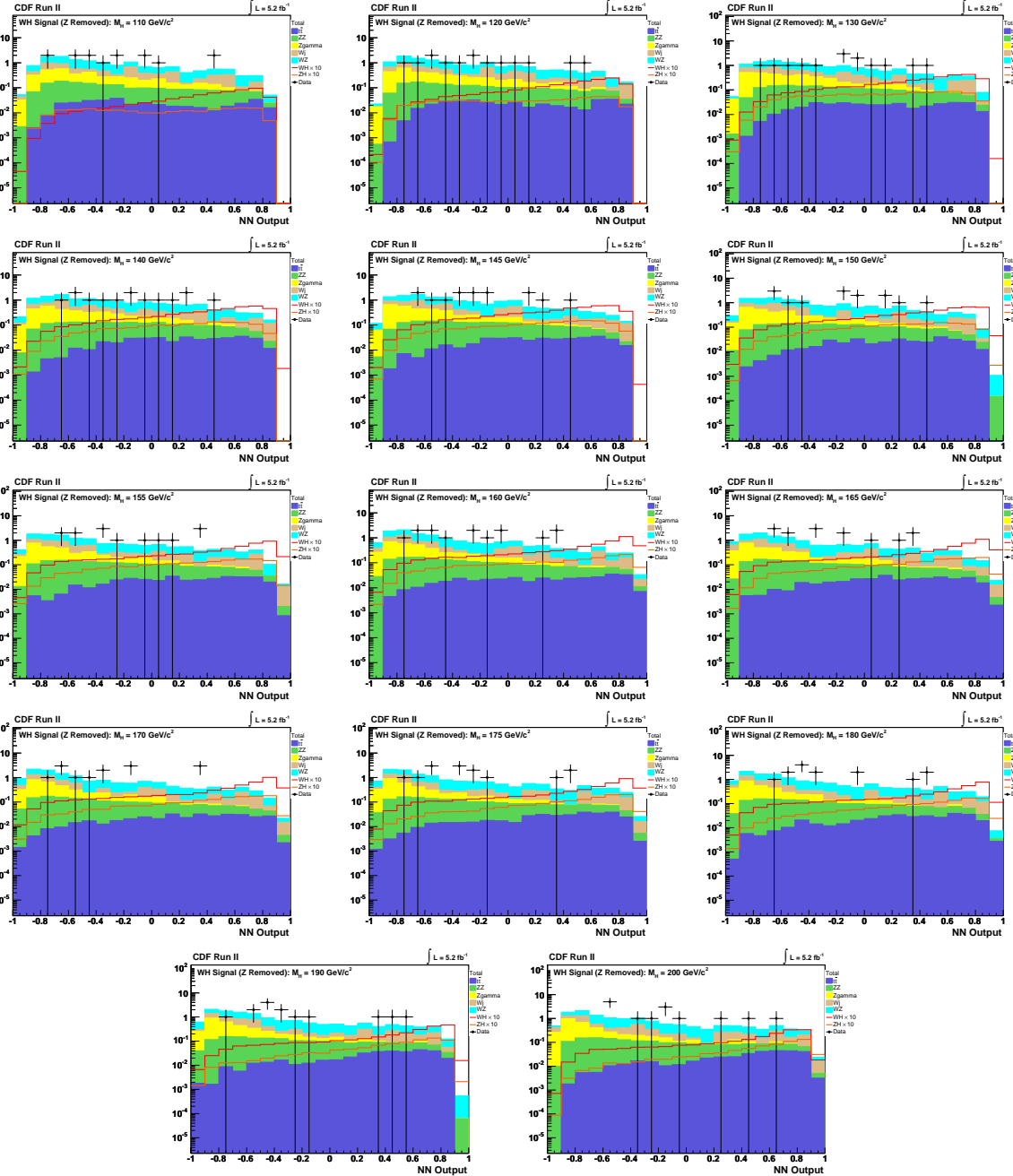


Figure 10: Trilepton  $WH$  NeuroBayes Neural Network output (logarithmic scale)

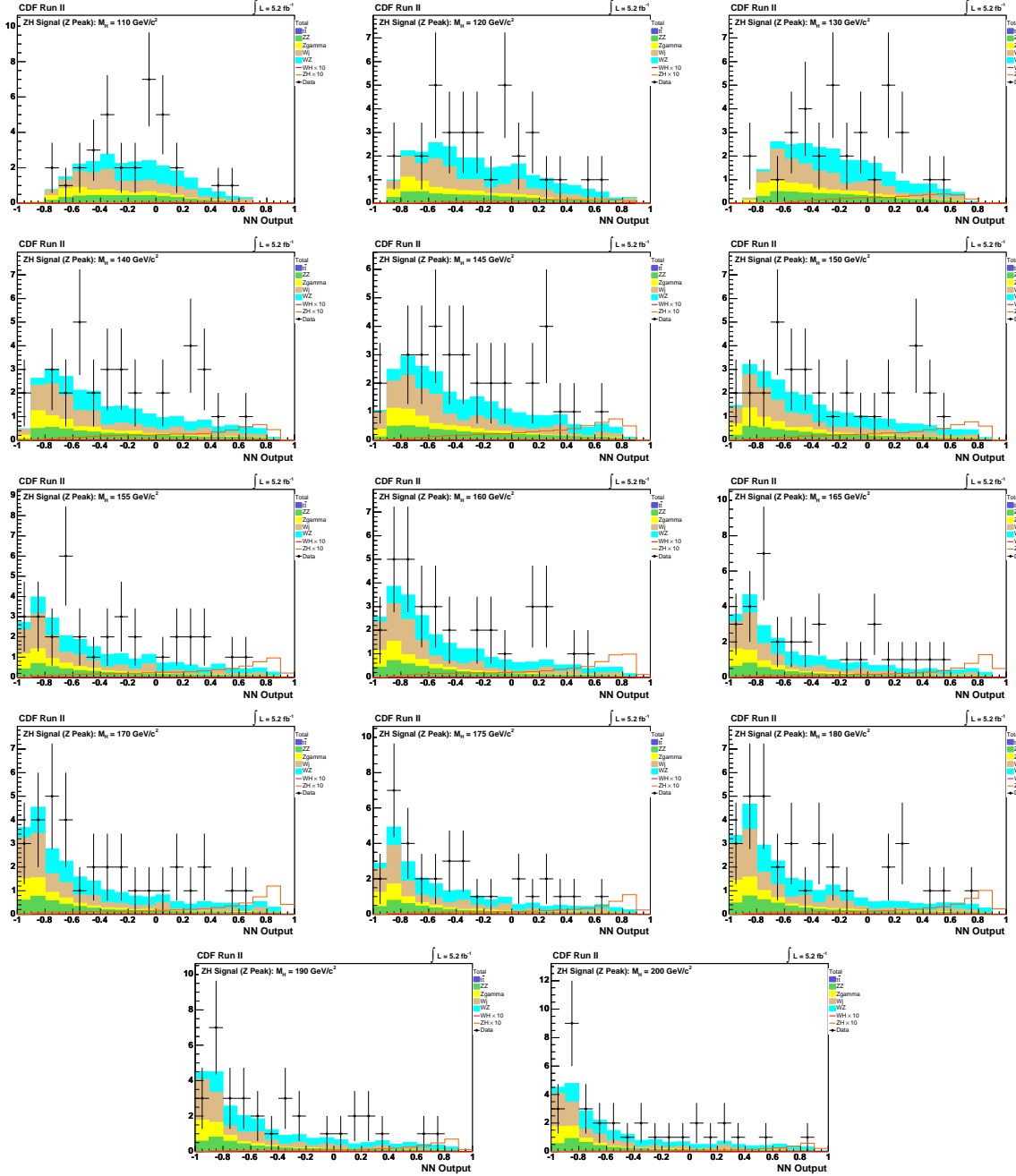


Figure 11: Trilepton  $ZH$  NeuroBayes Neural Network output (linear scale)

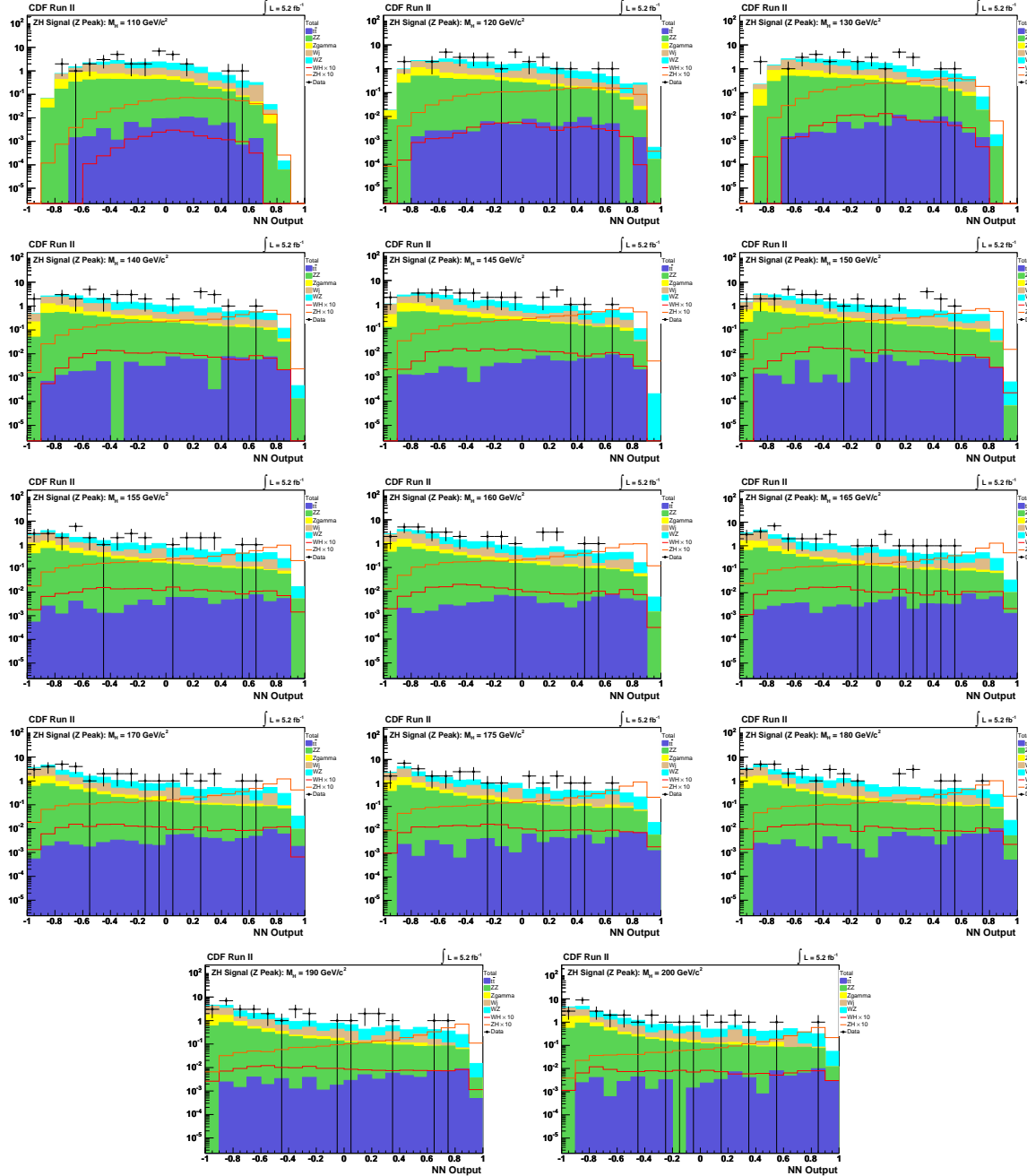


Figure 12: Trilepton  $ZH$  NeuroBayes Neural Network output (logarithmic scale)

## 9.4 Control Regions

The modeling of basic kinematic properties and the discriminating variables in the Monte Carlo simulation is tested by comparing the distributions of these variables in the final selected data. Ideally, the modeling of these variables is further tested by creating orthogonal "control regions" which are enhanced in specific major backgrounds and contain minimum possible signal contribution.

The control regions we choose for both the  $WH$  and  $ZH$  trilepton analyses contain minimal signal (see table 9.4) so cutting them out of the analyses drastically cuts down the background to discriminate against in addition to providing a verification of modelling.

They are:

- $WH$  Analysis Control Region:  $10.0 < \cancel{E}_T < 20.0$
- $ZH$  Analysis Control Region: Number of Jets= 0

The topology of  $WH$  associated production in the trilepton channel also contains at least three neutrinos (more if  $W \rightarrow \tau\nu_\tau \rightarrow l_{e,\mu}\nu_{e,\mu}\nu_\tau$  decays are involved), resulting in high missing energy values (see figure 18). The low  $\cancel{E}_T$  region is a natural choice for a control region in the  $WH$  analysis since it contains negligible signal contribution and is enriched in  $Z\gamma$  and Fakes backgrounds. Also including a  $\cancel{E}_T > 20$  cut for the  $WH$  signal region substantially enhances the signal to background ratio in the final signal region.

Similarly, the topology of  $ZH$  associated production lends to a preference for at least one or two jets (see figures 37 and 24) since one of the two Higgs- $W$ -bosons decays hadronically. Only  $\sim 10\%$  of the trilepton  $ZH$  signal is present in the  $NJet= 0$  bin, but much of it's most dominant background,  $WZ$ , is. Thus, the  $NJet= 0$  bin is a natural choice for the control region of the  $ZH$  trilepton analysis. Unfortunately, there are several nefarious difficulties that arise from this choice that must be discussed. First, three of the discriminating variables chosen in the neural network treatment discussed in section 9.6 are undefined when  $NJet= 0$  (though can be powerful discriminators among those events that do have at least one jet, serving as yet another argument for this choice of control region) and  $NJet$  must be excluded as a discriminating variable as well since the control region allows it only one possible value by definition (a variable cannot be used to discriminate background from signal when both background and signal must have identical values for that variable). The neural network result for the control region of  $ZH$  has the following removed from the list of discriminating variables:

- $NJet$
- $E_T$  of the leading jet
- $\Delta R$  between the  $W$ -lepton and the leading jet. Denote the two leptons with dilepton invariant mass  $\in [81.0, 101.0]$  GeV (the definition of the *InZPeak* region for the  $ZH$  analysis) as the  $Z$ -leptons, then the other lepton is denoted the  $W$ -lepton.

- Transverse mass of the vector sum of all jets

Further, with the  $t\bar{t}$  background being borderline negligible already, our monte carlo sample of  $t\bar{t}$  does not contain a single trilepton event in the  $ZH$  control region. Summarily, to obtain a neural network result for this *InZPeak* control region we had to retrain a neural network on the signal region ( $N\text{Jet} \geq 1$ ) excluding both the four aforementioned discriminating variables and the  $t\bar{t}$  background.

To support the claim that this neural network result for the *InZPeak* control region of the  $ZH$  analysis is valid, we first emphasize that the  $t\bar{t}$  contribution to the signal region is only 0.02 events expected in  $4.8\text{fb}^{-1}$  of data compared to a total background of  $20.9 \pm 2.64$ . As such, it's arguable that we could have removed this background from the analysis entirely without any noticeable difference. Second, we chose 16 discriminating variables for the signal region, so losing these four is a serious but not critical loss; the total correlation to target drops from 61.9% to 52.2%.

While this choice of control region poses challenges, we are rewarded with both a cut that excludes a large portion of the backgrounds with minimal signal loss and with three powerful discriminating variables that would be ill-defined otherwise.

CDF Run II Prebless			$\int \mathcal{L} = 5.3 \text{ fb}^{-1}$		
$(m_H = 165 \text{ GeV}/c^2)$	WH Signal Region	ZH Signal Region			
$WZ$	0.77 $\pm$ 0.11 <sub>syst</sub>	32.0 $\pm$ 6.19 <sub>syst</sub>			
$ZZ$	0.72 $\pm$ 0.10 <sub>syst</sub>	3.55 $\pm$ 0.55 <sub>syst</sub>			
$Z\gamma$	19.4 $\pm$ 3.31 <sub>syst</sub>	5.56 $\pm$ 1.17 <sub>syst</sub>			
Fakes ( $WW, Z + \text{Jets}$ )	7.58 $\pm$ 2.27 <sub>syst</sub>	9.43 $\pm$ 2.83 <sub>syst</sub>			
$t\bar{t}$	0.01 $\pm$ 0.002 <sub>syst</sub>	- $\pm$ -			
<b>Total Background</b>	28.4 $\pm$ 4.02 <sub>syst</sub>	50.5 $\pm$ 7.81 <sub>syst</sub>			
$WH$	0.025 $\pm$ 0.003 <sub>syst</sub>	0.06 $\pm$ 0.01 <sub>syst</sub>			
$ZH$	0.014 $\pm$ 0.002 <sub>syst</sub>	0.06 $\pm$ 0.01 <sub>syst</sub>			
<b>Total Signal</b>	0.038 $\pm$ 0.005 <sub>syst</sub>	0.12 $\pm$ 0.02 <sub>syst</sub>			
<b>Data</b>	31	49			

High Mass

We provide here the neural net score for the discriminating variables in the  $WH$  and  $ZH$  trilepton analyses control regions. The MC models the data well.

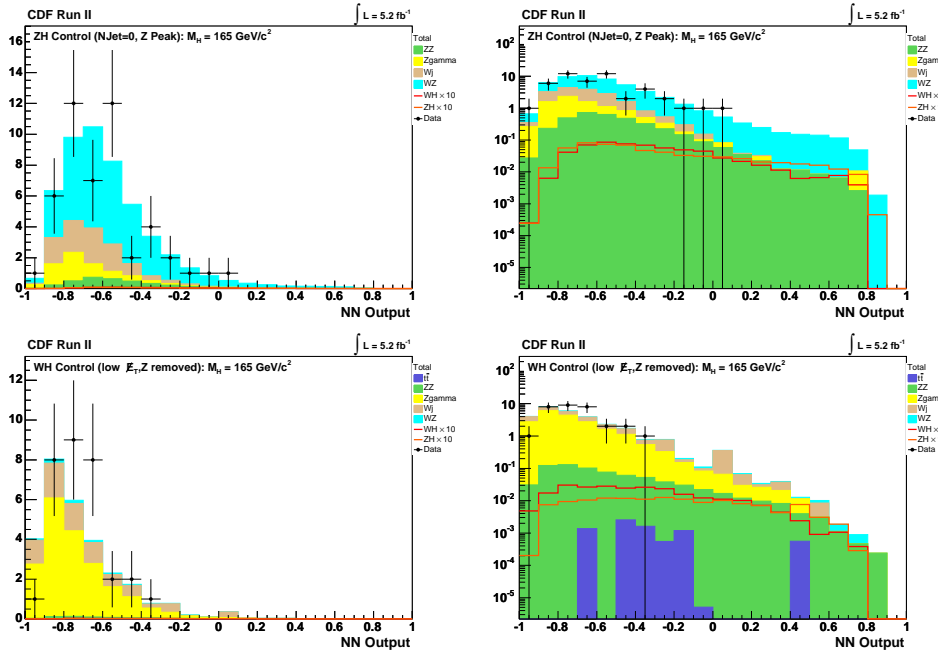


Figure 13:  $WH$  Control Region ( $10.0 \text{ GeV} < \cancel{E}_T < 20.0 \text{ GeV}$ ) and  $ZH$  Control Region ( $\text{NJet} = 0$ ) neural net results against samples trained on signal regions.

## 9.5 Systematic Errors

Systematic Uncertainty	WZ	ZZ	$Z\gamma$	$t\bar{t}$	Fakes	WH	ZH
Diboson Higher Order Diagrams	0.100	0.100		0.100			
$t\bar{t}$ Higher Order Diagrams							
Higgs Higher Order Diagrams						0.100	0.100
PDF Model	0.027	0.027		0.021		0.012	0.009
Lepton ID Efficiencies	0.020	0.020		0.020		0.020	0.020
Trigger Efficiencies	0.021	0.021		0.020		0.021	0.021
Light Jet Fake Rates					0.300		
$b$ -Jet Fake Rate*				0.23			
Luminosity	0.059	0.059		0.059		0.059	0.059
MC Run Dependence			0.050*				
Jet Energy Scale	0.098* <sup>a</sup>	0.053* <sup>a</sup>	0.086* <sup>a</sup>			0.084* <sup>a</sup>	0.011* <sup>a</sup>
$Z\gamma$ Higher Order Diagrams*			0.110*				
$W\gamma$ Scaling			0.110*				
$\sigma_{\text{Diboson}}$	0.060	0.060					
$\sigma_{t\bar{t}}$				0.100			
$\sigma_{\text{VH}}$						0.050	
$\sigma_{Z\gamma}^*$			0.050*				0.050

Table 12: Systematic Uncertainties: Standard values for systematics used in other  $H \rightarrow WW$  analyses are used wherever applicable.

<sup>a</sup> Only for the  $ZH$  analysis (*trilep-InZPeak* region) because the  $\text{NJet}=0$  bin is removed from the signal region and made a control region.

\* New to trilepton analysis, not in dilepton analysis.

The systematic uncertainties used are summarized in table 12. Most values used are standard to all  $H \rightarrow WW$  analyses, but since  $Z\gamma$  is a new background in this analysis—and a couple other reasons—there are several new systematics particular to this analysis.

- $Z\gamma$  (and  $W\gamma$ ) *Scaling*: Note that the  $W\gamma$  background is already scaled down by 17% in other  $H \rightarrow WW$  analyses due to known mismodelling of photon conversions. We are using the same scale factor for the  $Z\gamma$  contribution since the same photon conversion effect is assumed, as such we use the same systematic error associated with this scale factor. Also, we keep this systematic error correlated between the  $Z\gamma$  of the trilepton analyses and  $W\gamma$  of the dilepton analyses because of the common origin.
- $Z\gamma$  *Higher Order Diagrams*: We have for  $W\gamma$  in the dilepton analysis the  $W\gamma$  *higher order diagrams* systematic, which accounts for poor MC modeling beyond

leading order. Likewise, we assume the same error of 11% for a new  $Z\gamma$  *higher order diagrams* systematic since both are modelled by the Bauer MC generator.

- *b-Jet Fake Rate*: Although  $t\bar{t}$  is a small contribution to the background for these high  $m_H$  standard model Higgs boson in the trilepton case, we do have to account for the peculiar situation that our 3<sup>rd</sup> lepton is faked from a *b*-jet and the rate at which a *b*-jet fakes a lepton—as opposed to a light jet—is not well-known. Further, as a background with two real leptons and one faked, we cannot ignore the possible coverage of  $t\bar{t}$  in the data-based Fakes category. We know that the fake rates used in the Fakes category is based on jet samples populated mostly with light jets and presume that *b*-jets in particular are more likely than light jets to produce a signature that could fake a lepton. Hence, whatever  $t\bar{t}$  contribution that exists in the Fakes category is scaled down by the light jet dominated fake rate, meaning it is scaled down too far. To make up for the difference we use an MC  $t\bar{t}$  sample that allows reconstructed leptons to match to generator-level leptons, photons, or *b*-jets (typically, for these reconstructed MC leptons to be considered fully "found" they must pass a matching criterion to a generator-level lepton or photon only). Now, of course, we have the problem of possible double-counting of  $t\bar{t}$  between the MC and what implicit  $t\bar{t}$  contribution populates the Fakes category. To account for the double-counting possibility, we assign a systematic error defined to be one half the percentage difference between the MC  $t\bar{t}$  sample that allows leptons to match to generator-level leptons, photons, and *b*-jets; and the MC  $t\bar{t}$  sample that allows such matching to generator-level leptons and photons only. The systematic errors adopted are:

- *WH Analysis (trilep-NoZPeak region)*: 0.223
- *ZH Analysis (trilep-InZPeak region)*: 0.231

- *Jet Energy Scaling*: Jet energy scaling is modelled inclusively to all jet bins, so removing the zero-jet bin as a control region for the *ZH* analysis introduces a slight mismodelling for the signal region. To account for this, we re-run the analysis with different MC samples that have the jet energy scaling increased and decreased by one standard deviation.

If the jet energy scale is shifted down, then the jets of an event have lower energy, so event count fewer jets on average because fewer jets have enough energy to be considered above the energy threshold to be counted as such. Similarly, if the jet energy scale is shifted up, then the jets of an event have higher energy, so events count more jets on average because more jets have enough energy to be considered above the threshold energy to be counted.

Singe the *ZH* analysis signal region only has  $\text{NJet} \geq 1$  (the  $\text{NJet} = 0$  bin is the control region), the events from samples with jet energy scaled down have fewer jets

on average so more events are shifted out of the signal region and into the control region. Likewise, events with the jet energy scaled up will count more jets on average and shift events out of the control region and into the signal region. These shifts change the weighted count for the backgrounds for some given integrated luminosity. As such, we must assign a systematic error for each background corresponding to the error of the jet energy scaling.

We then take the average of the percent difference between each and the original samples. Differences necessitating systematic errors arose only for  $WZ$ ,  $ZZ$ , and  $Z\gamma$  samples, and only for the  $ZH$  analysis.

- $WZ$  ( $ZH$  Signal Region): 0.097
- $ZZ$  ( $ZH$  Signal Region): 0.052
- $Z\gamma$  ( $ZH$  Signal Region): 0.088

We explored the possibility of having a jet energy scaling **shape** systematic as well. That is, even if the total count of a particular process does not change appreciably, we must account for the possibility that the distribution of the process in the neural net output (the templates that serve as the inputs for calculating statistical limits) changes. The subsequent limits could be altered if a process is shifted towards or away from the signal region of the templates. To check, we used the shape systematic error for the limit calculation at the  $m_H = 165$  GeV mass point and compared the results to default values. The result is in table 13. We see that the shape systematic does not affect the limit results and is therefore not included in the analysis at this time.

$m_H = 165$ GeV bin	Exp. Limit $-1\sigma$	Median Exp. Limit	Exp. Limit $+1\sigma$
$WH$ Analysis, JES Shape Syst.	6.7	8.9	12.3
$WH$ Analysis, Standard	6.7	8.8	12.4
$ZH$ Analysis, JES Shape Syst.	9.4	12.5	17.7
$ZH$ Analysis, Standard	9.4	12.5	17.2
Trilepton Analyses, JES Shape Syst.	4.7	6.3	8.9
Trilepton Analyses, Standard	4.7	6.3	8.9

Table 13: Compare default limit values for the  $ZH$ ,  $WH$ , and combined trilepton analyses. we see that a jet energy scaling shape systematic is not necessary.

- *MC Run Dependence*: The  $Z\gamma$  stntuples used cover only periods 0 – 11, so we assign the customary MC run dependence systematics for such samples. This is determined by comparing a  $WW$  sample with partial run dependence (periods 0 – 7) with a fully run-dependent  $WW$  sample.

- *Lepton, Trigger ID, Luminosity, Parton Distribution Function Model:* Finally, note that we do not use systematic errors for the lepton, trigger ID, luminosity, and PDF model efficiencies because of the scale factor derived from the  $W\gamma$  control region in the dilepton analysis. Since we’re measuring the  $W\gamma$  normalization directly from data, that systematic should cover these effects. However, to be conservative—especially since we measure the scale factor in a control region with selection cuts that differ from our various signal regions—we keep the systematic uncertainties on the MC that are not related to normalization (higher-order kinematic effects, MC jet modelling).

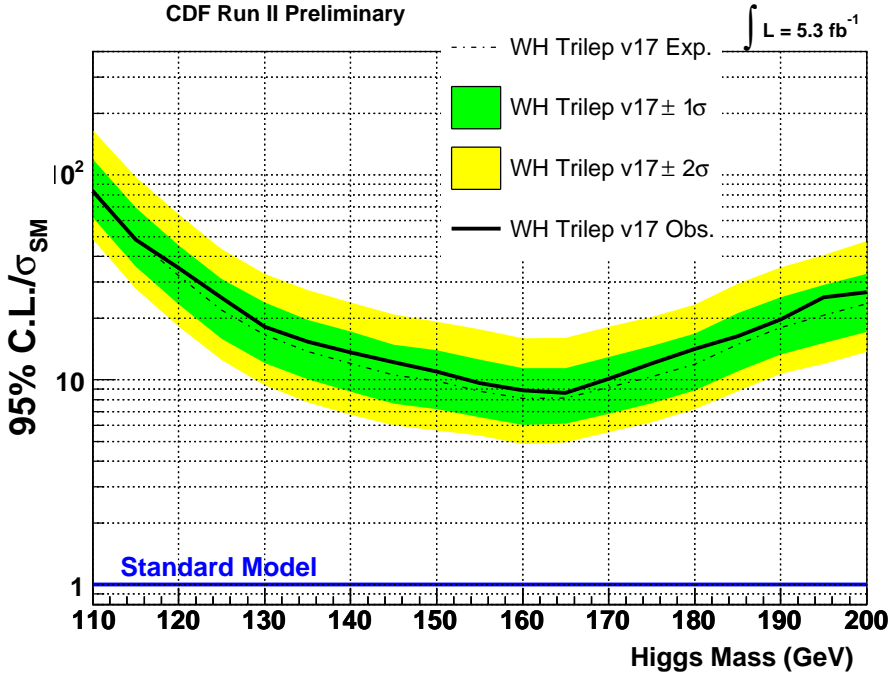


Figure 14: Trilepton *NoZPeak* Region Limits

## 9.6 Results

The results of this trilepton analysis present a significant contribution to the  $H \rightarrow WW$  combined result. We are poised to solidify and expand the window of standard model Higgs boson exclusion within  $163 < m_H < 166$  GeV [6]. In the 165 GeV bin, the  $WH$  analysis limits are set at 8.86 times the expected standard model limit; the  $ZH$  analysis is set at 12.6 times the expected standard model limit; and the combined trilepton analysis is set at 6.3 times the expected standard model limit. Finally, for the combined  $H \rightarrow WW$  analysis result, in the 165 GeV bin the expected limit drops from 1.21[4] to 1.15 while the observed limit drops from 1.23 to 1.08. As such, we are poised to begin excluding the standard model Higgs boson at 95% confidence level with CDF-only analyses in short order.

The limit calculations presented were computed with `HWWLimit` version of `MCLimit`. Expected limits for the  $ZH$ ,  $WH$ , and combined trileptons were calculated in each case with 1,000 iterations of 10,000 pseudoexperiments (1000 iterations of 1000 pseudoexperiments performed 10 times), while 500,000 iterations of 1 pseudoexperiment were performed for the observed results—as is standard. For greater precision, the combined  $HWW$  dilepton and trilepton result used 30,000 pseudoexperiments instead of 10,000 for the expected limits, and 5 pseudoexperiment (500,000 iterations each) instead of 1 for the observed limits.

Limits	110	120	130	140	145	150	155
$+2\sigma/\sigma_{\text{SM}}$	180	67.2	35.5	24.4	22.5	20.3	18.4
$+1\sigma/\sigma_{\text{SM}}$	130	48.3	25.3	17.7	16.0	14.5	13.1
<b>Median</b> $/\sigma_{\text{SM}}$	<b>91.6</b>	<b>34.1</b>	<b>17.9</b>	<b>12.5</b>	<b>11.4</b>	<b>10.4</b>	<b>9.35</b>
$-1\sigma/\sigma_{\text{SM}}$	67.9	25.1	13.2	9.23	8.40	7.76	7.05
$-2\sigma/\sigma_{\text{SM}}$	54.0	19.9	10.5	7.36	6.67	6.25	5.72
<b>Observed</b> $/\sigma_{\text{SM}}$	<b>94.4</b>	<b>36.9</b>	<b>19.9</b>	<b>16.5</b>	<b>13.9</b>	<b>13.8</b>	<b>12.2</b>
Limits	160	165	170	175	180	190	200
$+2\sigma/\sigma_{\text{SM}}$	16.9	17.2	19.8	22.1	25.3	27.1	49.3
$+1\sigma/\sigma_{\text{SM}}$	12.2	12.4	14.0	15.6	18.0	26.8	35.1
<b>Median</b> $/\sigma_{\text{SM}}$	<b>8.62</b>	<b>8.86</b>	<b>9.91</b>	<b>11.0</b>	<b>12.8</b>	<b>19.1</b>	<b>24.9</b>
$-1\sigma/\sigma_{\text{SM}}$	6.48	6.71	7.49	8.29	9.62	14.3	18.5
$-2\sigma/\sigma_{\text{SM}}$	5.29	5.60	6.17	6.85	7.90	11.7	15.0
<b>Observed</b> $/\sigma_{\text{SM}}$	<b>11.1</b>	<b>11.0</b>	<b>12.6</b>	<b>13.6</b>	<b>17.3</b>	<b>23.9</b>	<b>33.3</b>

Table 14:  $WH$  trilepton analysis limits for  $4.8\text{fb}^{-1}$ .

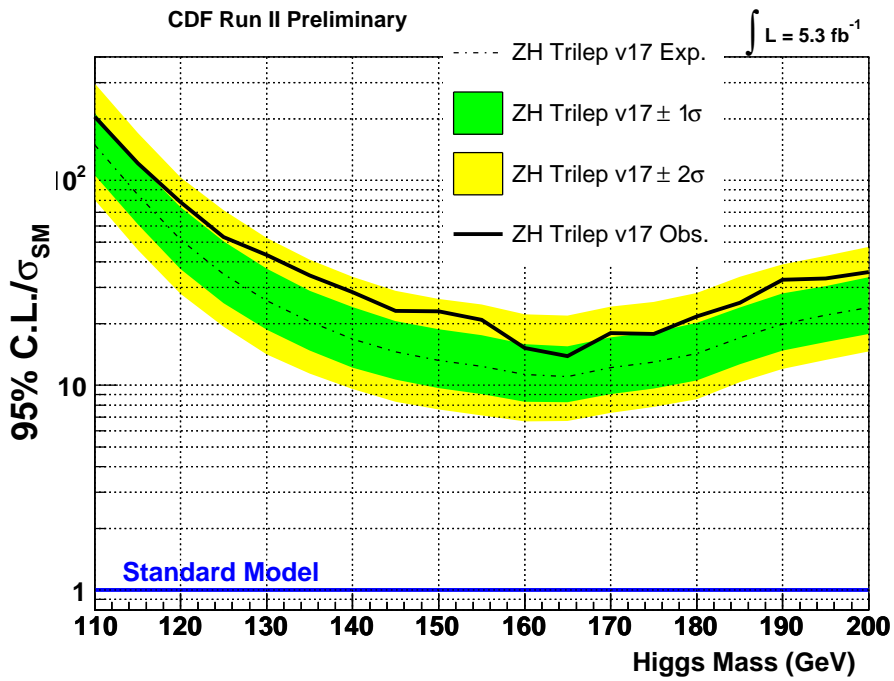


Figure 15: Trilepton *InZPeak* Region Limits

Limits	110	120	130	140	145	150	155
$+2\sigma/\sigma_{\text{SM}}$	327	112	57.0	37.3	32.6	29.7	26.7
$+1\sigma/\sigma_{\text{SM}}$	233	80.6	40.6	26.5	23.2	21.1	19.1
<b>Median</b> $/\sigma_{\text{SM}}$	<b>162</b>	<b>56.3</b>	<b>28.5</b>	<b>18.8</b>	<b>16.4</b>	<b>14.9</b>	<b>13.4</b>
$-1\sigma/\sigma_{\text{SM}}$	116	40.6	20.5	13.7	11.9	10.8	9.90
$-2\sigma/\sigma_{\text{SM}}$	88.0	31.1	15.7	10.6	9.37	8.54	7.86
<b>Observed</b> $/\sigma_{\text{SM}}$	<b>192</b>	<b>71.9</b>	<b>40.8</b>	<b>27.0</b>	<b>25.2</b>	<b>20.3</b>	<b>19.1</b>
Limits	160	165	170	175	180	190	200
$+2\sigma/\sigma_{\text{SM}}$	25.2	24.6	26.8	29.0	31.7	43.3	52.0
$+1\sigma/\sigma_{\text{SM}}$	17.8	17.6	19.1	20.6	22.4	30.8	37.0
<b>Median</b> $/\sigma_{\text{SM}}$	<b>12.6</b>	<b>12.6</b>	<b>13.5</b>	<b>14.6</b>	<b>16.0</b>	<b>21.9</b>	<b>26.4</b>
$-1\sigma/\sigma_{\text{SM}}$	9.27	9.44	10.1	10.9	11.9	16.3	19.8
$-2\sigma/\sigma_{\text{SM}}$	7.50	7.65	8.37	8.91	9.68	13.4	16.2
<b>Observed</b> $/\sigma_{\text{SM}}$	<b>17.0</b>	<b>15.8</b>	<b>17.8</b>	<b>18.7</b>	<b>22.1</b>	<b>32.8</b>	<b>34.5</b>

Table 15:  $ZH$  trilepton analysis limits for  $4.8\text{fb}^{-1}$ .

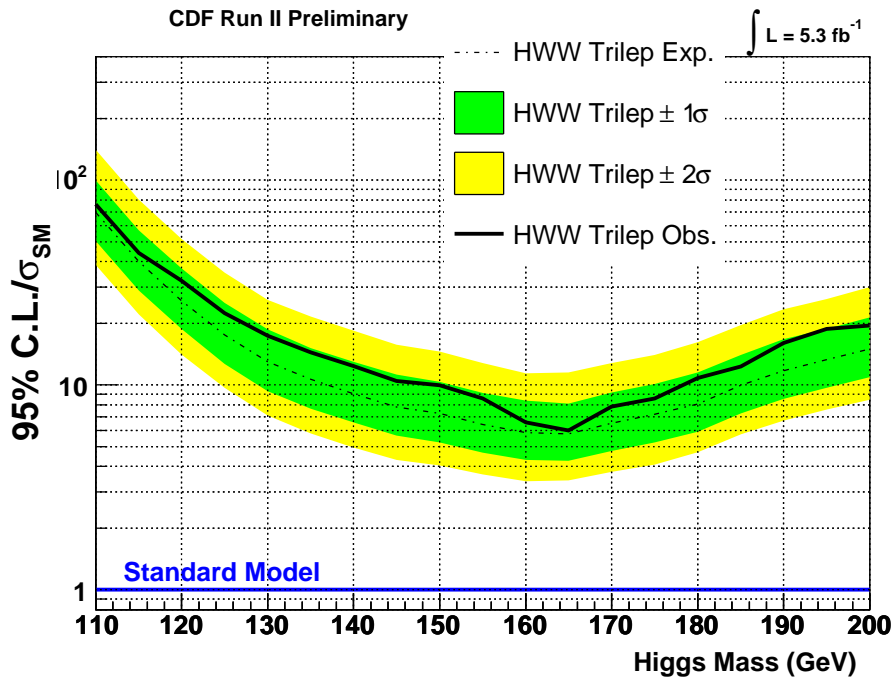


Figure 16: Trilepton Combined Limits

Limits	110	120	130	140	145	150	155
$+2\sigma/\sigma_{\text{SM}}$	151	55.0	28.3	19.2	16.9	15.8	13.6
$+1\sigma/\sigma_{\text{SM}}$	108	38.9	20.0	13.7	12.1	11.1	9.74
<b>Median</b> $/\sigma_{\text{SM}}$	<b>75.8</b>	<b>27.4</b>	<b>14.0</b>	<b>9.63</b>	<b>8.55</b>	<b>7.79</b>	<b>6.84</b>
$-1\sigma/\sigma_{\text{SM}}$	54.9	20.0	10.2	6.96	6.16	5.69	5.03
$-2\sigma/\sigma_{\text{SM}}$	42.0	15.2	7.81	5.31	4.79	4.45	3.97
<b>Observed</b> $/\sigma_{\text{SM}}$	<b>77.4</b>	<b>30.5</b>	<b>17.2</b>	<b>13.5</b>	<b>12.0</b>	<b>10.6</b>	<b>9.64</b>
Limits	160	165	170	175	180	190	200
$+2\sigma/\sigma_{\text{SM}}$	12.5	12.5	13.6	15.3	17.4	24.8	31.5
$+1\sigma/\sigma_{\text{SM}}$	8.93	8.91	9.87	10.9	12.4	17.7	22.4
<b>Median</b> $/\sigma_{\text{SM}}$	<b>6.33</b>	<b>6.31</b>	<b>6.95</b>	<b>7.72</b>	<b>8.73</b>	<b>12.6</b>	<b>15.8</b>
$-1\sigma/\sigma_{\text{SM}}$	4.65	4.68	5.16	5.70	6.47	9.27	11.6
$-2\sigma/\sigma_{\text{SM}}$	3.69	3.78	4.17	4.57	5.13	7.36	9.17
<b>Observed</b> $/\sigma_{\text{SM}}$	<b>8.33</b>	<b>7.61</b>	<b>8.90</b>	<b>9.52</b>	<b>12.4</b>	<b>18.1</b>	<b>22.0</b>

Table 16: Trilepton combined ( $WH$  and  $ZH$ ) analysis limits for  $4.8\text{fb}^{-1}$ .

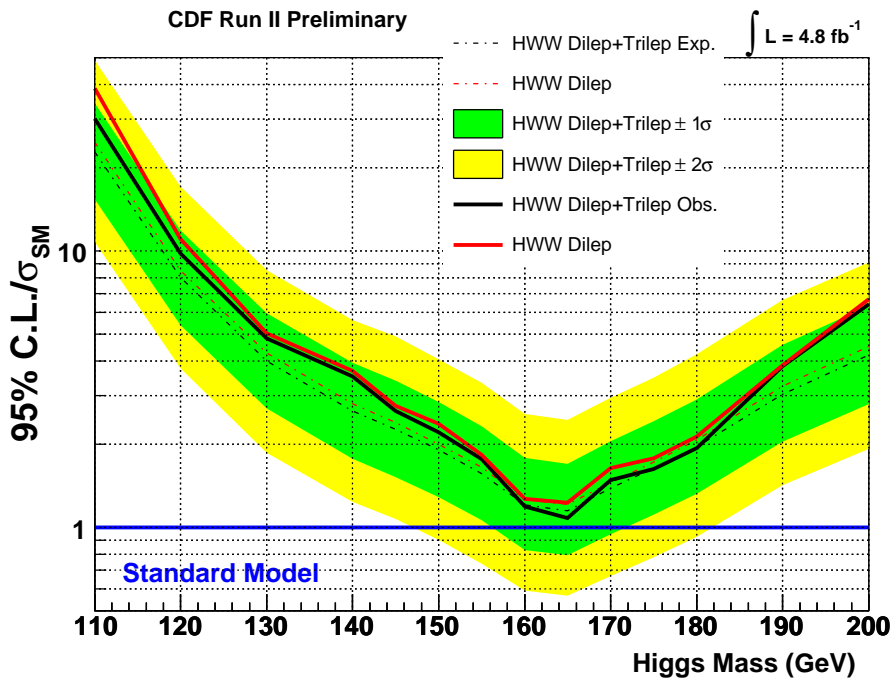


Figure 17: HWW+Trilepton Combined Limits

Limits	110	120	130	140	145	150	155
$+2\sigma/\sigma_{SM}$	49.0	17.1	8.52	5.62	4.91	4.06	3.34
$+1\sigma/\sigma_{SM}$	34.2	11.9	5.95	3.94	3.39	2.84	2.32
<b>Median</b> $/\sigma_{SM}$	<b>22.8</b>	<b>8.02</b>	<b>4.01</b>	<b>2.64</b>	<b>2.27</b>	<b>1.91</b>	<b>1.57</b>
$-1\sigma/\sigma_{SM}$	15.4	5.39	2.70	1.77	1.52	1.29	1.06
$-2\sigma/\sigma_{SM}$	10.8	3.76	1.86	1.24	1.08	0.90	0.74
<b>Observed</b> $/\sigma_{SM}$	<b>30.1</b>	<b>9.79</b>	<b>4.83</b>	<b>3.52</b>	<b>2.64</b>	<b>2.21</b>	<b>1.77</b>
Limits	160	165	170	175	180	190	200
$+2\sigma/\sigma_{SM}$	2.57	2.45	2.95	3.48	4.23	6.65	9.08
$+1\sigma/\sigma_{SM}$	1.79	1.70	2.05	2.42	2.91	4.57	6.33
<b>Median</b> $/\sigma_{SM}$	<b>1.21</b>	<b>1.15</b>	<b>1.39</b>	<b>1.64</b>	<b>1.96</b>	<b>3.03</b>	<b>4.20</b>
$-1\sigma/\sigma_{SM}$	0.83	0.79	0.94	1.11	1.32	2.04	2.80
$-2\sigma/\sigma_{SM}$	0.59	0.57	0.67	0.78	0.93	1.42	1.93
<b>Observed</b> $/\sigma_{SM}$	<b>1.19</b>	<b>1.08</b>	<b>1.49</b>	<b>1.63</b>	<b>1.94</b>	<b>3.83</b>	<b>6.41</b>

Table 17: HWW w/ Trileptons Combined Expected Sensitivity.

## 10 Conclusions

## References

- [1] Yao *et al.*, W. -M. *Review of Particle Physics* Particle Data Group, "J. Phys. G," vol. 33, (2006) p. 1-1232.
- [2] Benjamin, D. and and Kruse, M. and Oh, Seig and Yu, Geumbong and Bussey, P. and James, E. and Hidas, D. and Jindariani, S. and Rutherford, B. and Lysak, R. and Herndon, M. and Nett, J. and Pursley, J. and d'Errico, M. and Griso, S.P. and Lucchesi, D. and Robson, A. and St.Denis, R. and d'Errico, Maria and Lucchesi, Donatella and Canepa, Anadi *Search for  $H \rightarrow WW$  Production Using  $5.3 \text{ fb}^{-1}$*  (2010), CDF/PHYS/EXOTIC/CDFR/10086.
- [3] Benjamin, D. and and Kruse, M. and Bussey, P. and James, E. and Hidas, D. and Jindariani, S. and Rutherford, B. and Lysak, R. and Herndon, M. and Nett, J. and Pursley, J. and d'Errico, M. and Griso, S.P. and Lucchesi, D. and Robson, A. and St.Denis, R., *Updated Search for  $H \rightarrow WW$  Production Using Likelihood-Based Electron Selection*, (2009), CDF/PHYS/EXOTIC/CDFR/9863.
- [4] Benjamin, D. and and Kruse, M. and Bussey, P. and James, E. and Hidas, D. and Jindariani, S. and Rutherford, B. and Lysak, R. and Herndon, M. and Nett, J. and Pursley, J. and d'Errico, M. and Griso, S.P. and Lucchesi, D. and Robson, A. and St.Denis, R. *Search for  $H \rightarrow WW$  Production in the Low  $M_{ll}$  Region Using  $4.8 \text{ fb}^{-1}$*  (2009), CDF/PHYS/EXOTIC/CDFR/9864.
- [5] Pursley, J. *Search for Standard Model Higgs Boson in  $H \rightarrow WW$  Channel at CDF* Proceedings of the DPF-2009 Conference, Detroit, MI, July 27-31, 2009.
- [6] CDF Collaboration, *Combined CDF and D0 Upper Limits on Standard Model Higgs Boson Production with up to  $5.4 \text{ fb}^{-1}$  of Data* (2009), CDF/PHYS/EXOTIC/CDFR/9998.
- [7] CDF Collaboration, *Combined Upper Limit on Standard Model Higgs Boson Production* (2009), CDF/PHYS/EXOTIC/CDFR/9999.
- [8] Canelli, Florencia and Casal Larana, Bruno and Group, Craig and James, Eric and Lewis, Jonathon and Wright, Tom. *Muon Trigger Studies: Focusing on the Gaps* (2007) CDF/DOC/JET/PUBLIC/9106.
- [9] CDF Collaboration, *CDF Central Outer Tracker* (2001),
- [10] CDF Collaboration, ed. Lukens, P. *CDF Run II Technical Design Report* ((2003)), CDF/DOC/CDF/PUBLIC/6261.
- [11] Michael E. Peskin, Daniel V. Schroeder *An Introduction to Quantum Field Theory*. Westview Press, Perseus Books Group, 1995.

- [12] J.J. Sakurai *Modern Quantum Mechanics (Revised Edition)*. Addison-Wesley Publishing Company, Inc., 1994.
- [13] I. J. R. Aitchison and A. J. G. Hey *Gauge Theories in Particle Physics. Vol. 2: QCD and the Electroweak Theory*. Institute of Physics Publishing (Bristol and Philadelphia), 2004.
- [14] Halzen, Francis and Martin, Alan *Quarks and Leptons: An Introductory Course in Modern Particle Physics*. John Wiley & Sons, Inc., 1984.
- [15] Dummit, David and Foote, Richard *Abstract Algebra, 3rd. ed.* John Wiley & Sons, Inc., 2004.
- [16] *Journal of Physics G: Nuclear and Particle Physics*(vol.33). Institute of Physics Publishing, 2006.
- [17] Perkins, Donald H. *Introduction to High Energy Physics, 3rd ed.* Addison-Wesley Publishing Company, Inc. 1987.
- [18] [http://www.fnal.gov/pub/today/archive\\_2008/today08-06-18.html](http://www.fnal.gov/pub/today/archive_2008/today08-06-18.html)
- [19] <http://www.fnal.gov/pub/now/tevlum.html>
- [20] <http://www-bd.fnal.gov/public/antiproton.html#target>
- [21] <http://www-bd.fnal.gov/public/tevatron.html>
- [22] [http://www-d0.fnal.gov/runcoor/RUN/run2\\_lumi.html](http://www-d0.fnal.gov/runcoor/RUN/run2_lumi.html)
- [23] <http://www-bd.fnal.gov/public/maininj.html>
- [24] <http://www-cdf.fnal.gov/internal/upgrades/layer00/layer00.html>
- [25] [http://www-cdf.fnal.gov/internal/upgrades/svxii/svxii\\_home.html](http://www-cdf.fnal.gov/internal/upgrades/svxii/svxii_home.html)
- [26] <http://www-cdf.fnal.gov/internal/upgrades/isl/isl.html>
- [27] <http://www-cdf.fnal.gov/internal/upgrades/cot/>
- [28] [http://www.phy.duke.edu/ kotwal/detectorLectures/detector\\_lectures\\_Phil\\_Schlabach\\_1\\_muondet](http://www.phy.duke.edu/ kotwal/detectorLectures/detector_lectures_Phil_Schlabach_1_muondet)
- [29] [http://cdfdbb.fnal.gov:8520/cdfr2/databases?tdt=phy&tdv=PHYSICS\\_5\\_04\\_v-3&tdh=arg&tdl=sov&dates=&skip=&limit=all&rc=y&email=&type=tf-trg&do=r&nsrc=cdfonprd&fsrc=cdfofpr2&gsrc=cdfonprd&dcbk=FILECATALOG&calbk=PUB](http://cdfdbb.fnal.gov:8520/cdfr2/databases?tdt=phy&tdv=PHYSICS_5_04_v-3&tdh=arg&tdl=sov&dates=&skip=&limit=all&rc=y&email=&type=tf-trg&do=r&nsrc=cdfonprd&fsrc=cdfofpr2&gsrc=cdfonprd&dcbk=FILECATALOG&calbk=PUB)

## A Appendix

### A.1 Neural Net Input Variables

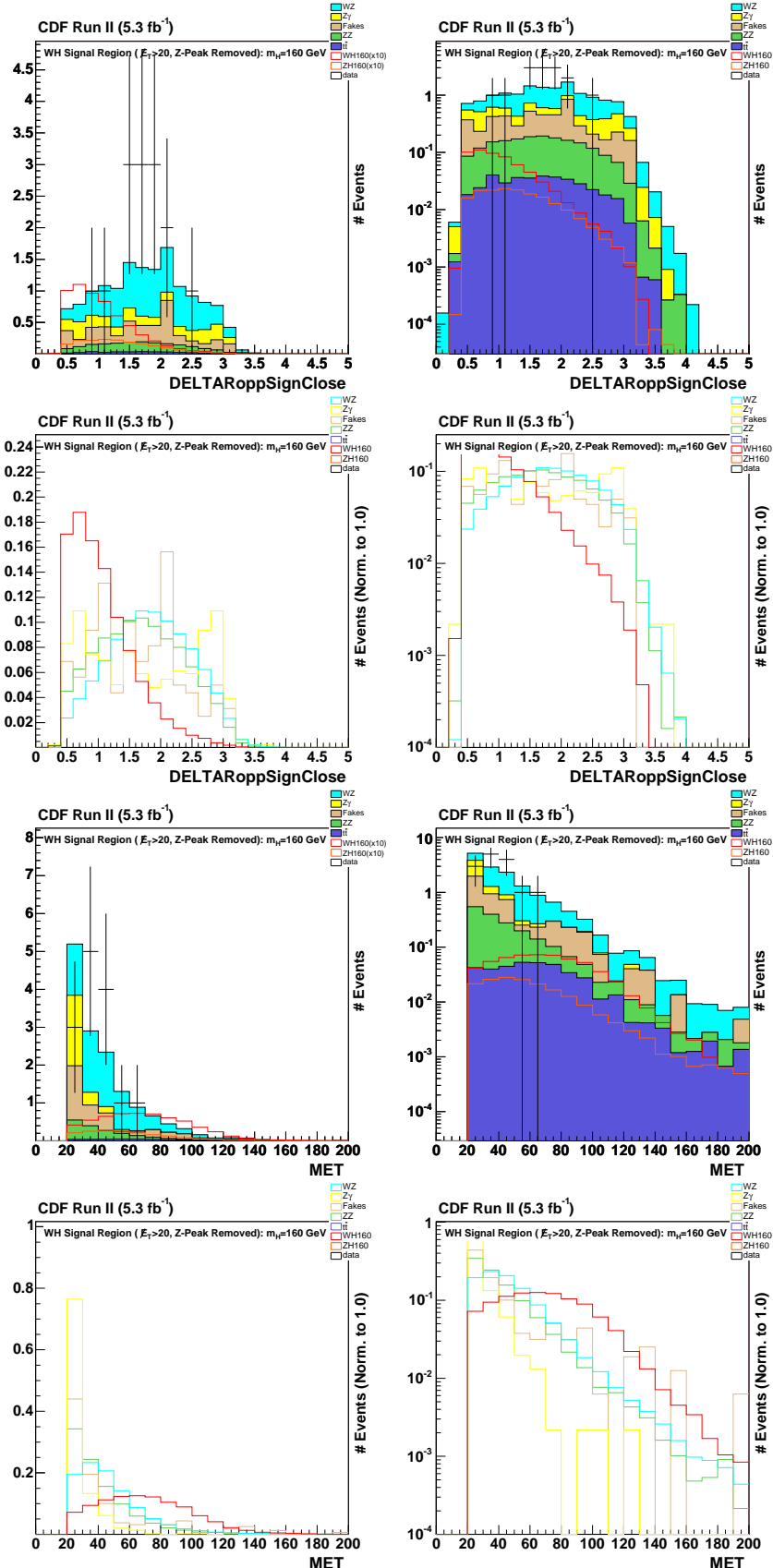


Figure 18: *NoZPeak* Signal Region ( $10.0 \text{ GeV} < \cancel{E}_T < 20.0 \text{ GeV}$ ):  $\Delta R$  Opp. Sign Close Leptons,  $\cancel{E}_T$ .

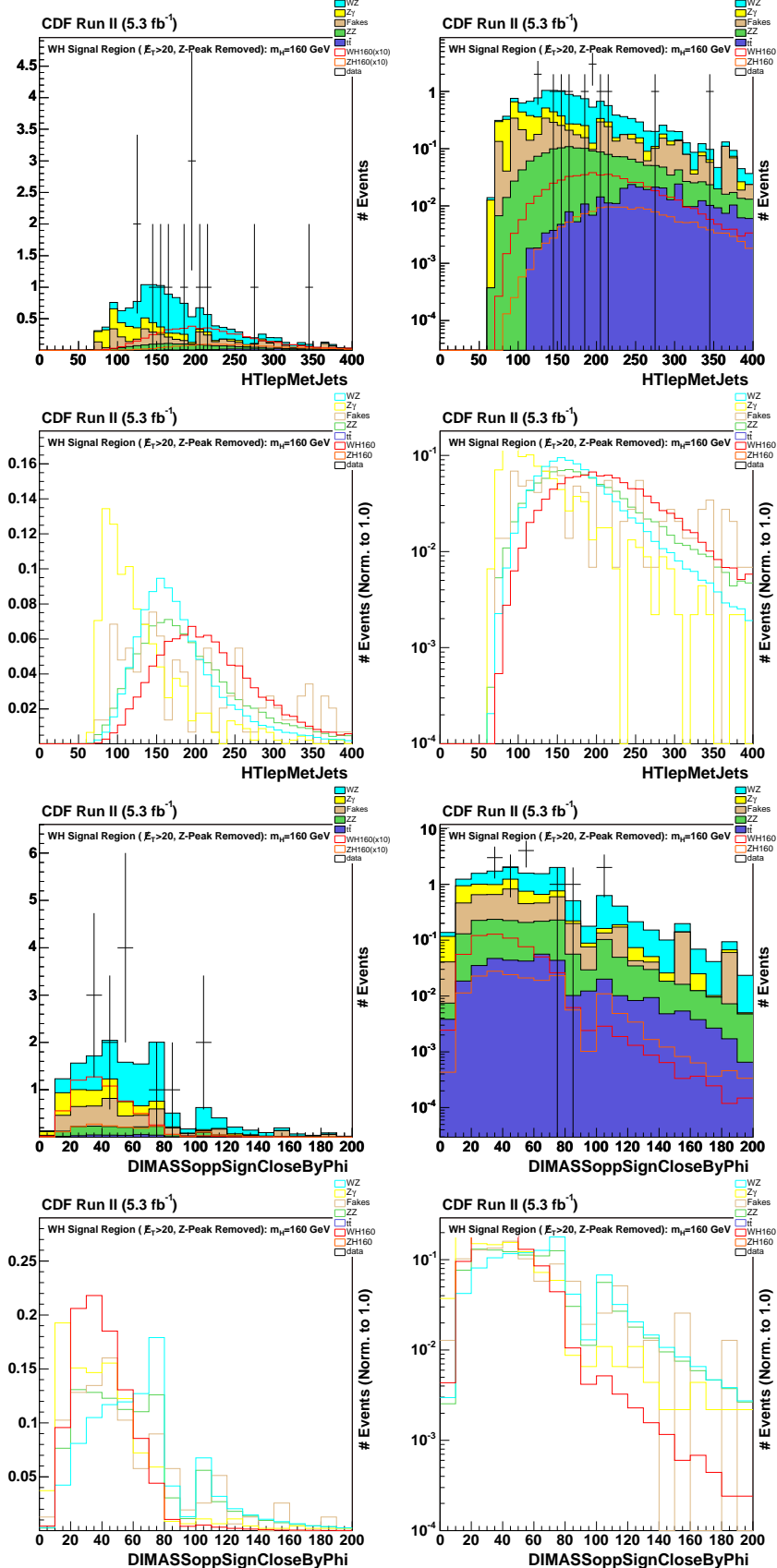


Figure 19: *NoZPeak* Signal Region ( $10.0 \text{ GeV} < \cancel{E}_T < 20.0 \text{ GeV}$ ):  $H_T$  (all leptons,  $\cancel{E}_T$ , all jets), Dimass Opp. Sign Leptons (closer pair in  $\phi$ ).

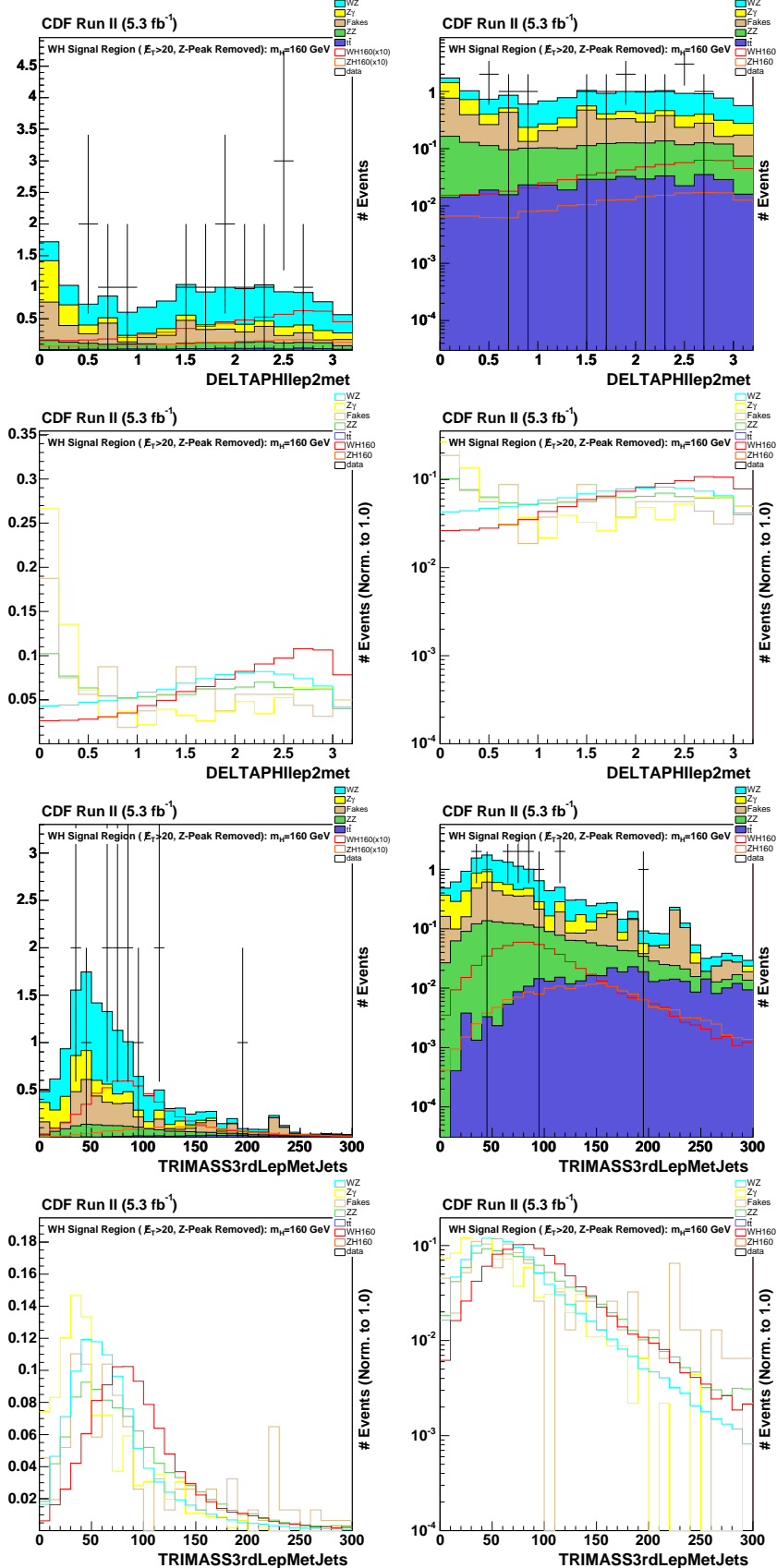


Figure 20: *NoZPeak* Signal Region ( $10.0 \text{ GeV} < \cancel{E}_T < 20.0 \text{ GeV}$ ):  $\Delta\phi$  between the 2<sup>nd</sup> lepton and  $\cancel{E}_T$ , Inv. mass of the 3<sup>rd</sup> lepton+ $\cancel{E}_T$ +Jets.

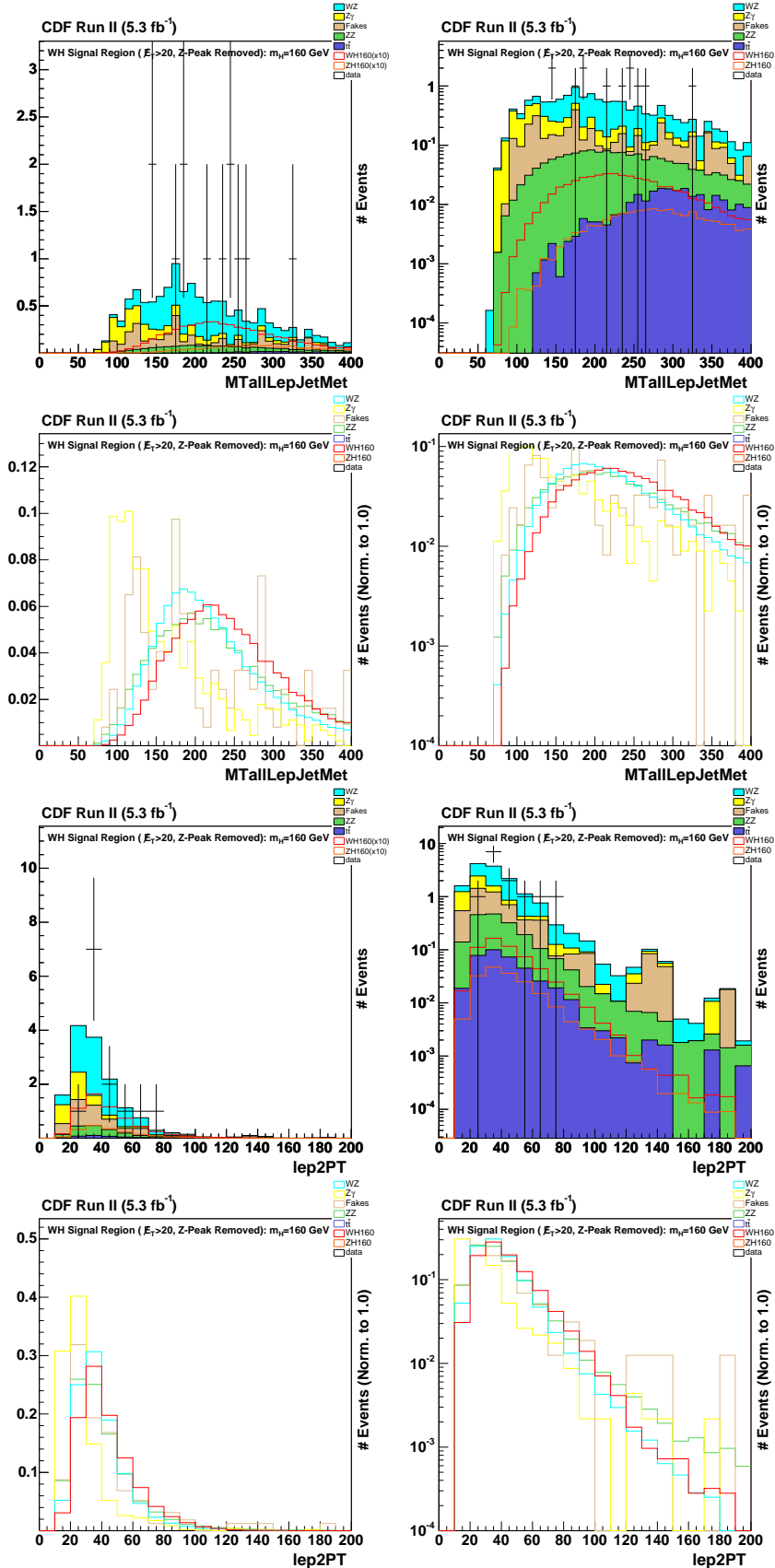


Figure 21: *NoZPeak* Signal Region ( $10.0 \text{ GeV} < \cancel{E}_T < 20.0 \text{ GeV}$ ):  $m_T(\text{Leptons}, \cancel{E}_T, \text{Jets})$ ,  $p_T$  of 2<sup>nd</sup> Lepton

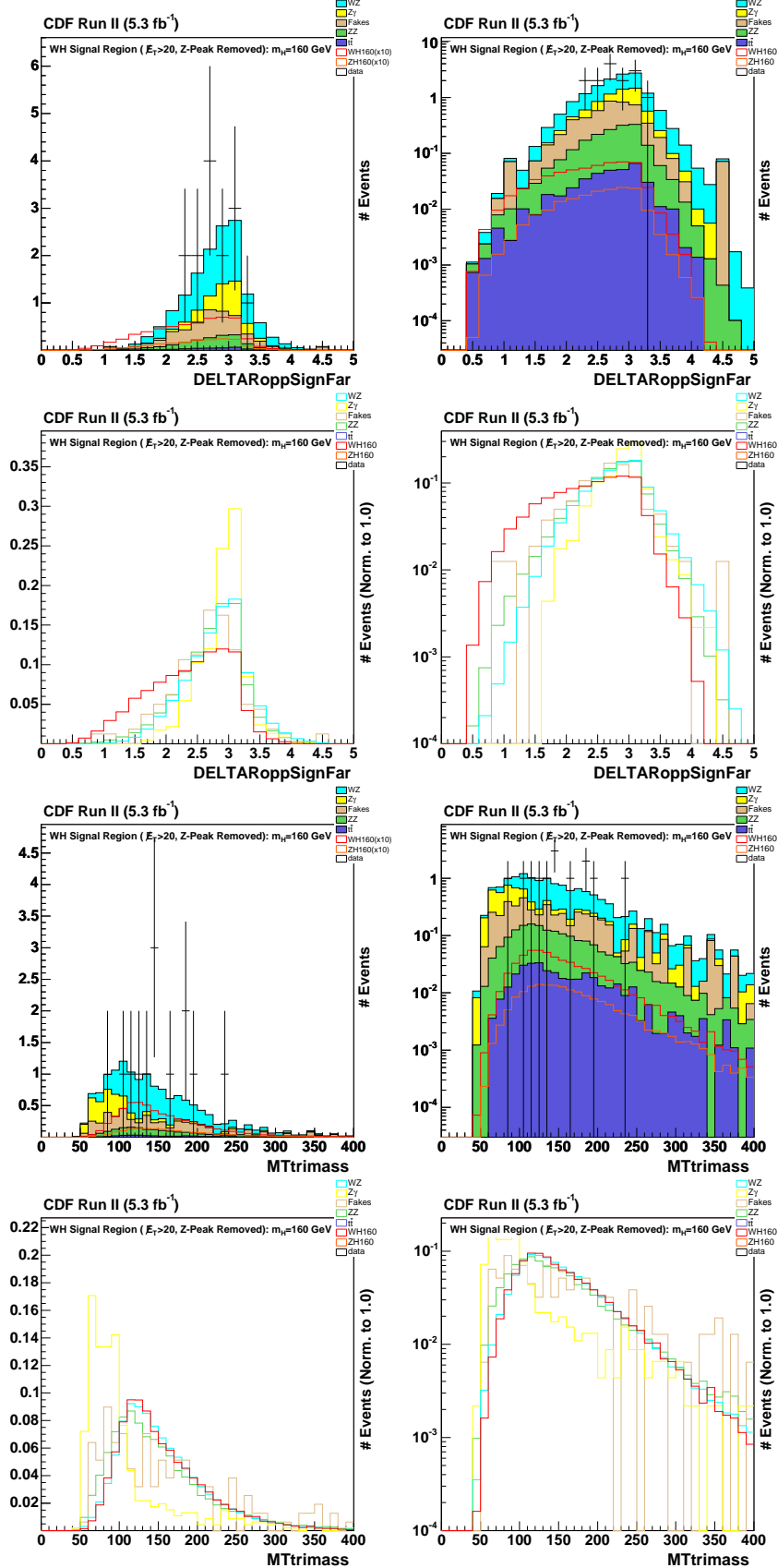


Figure 22: *NoZPeak* Signal Region ( $10.0 \text{ GeV} < \cancel{E}_T < 20.0 \text{ GeV}$ ):  $\Delta R$  Opp. Sign Far Leptons,  $m_T$  Trilepton Mass.

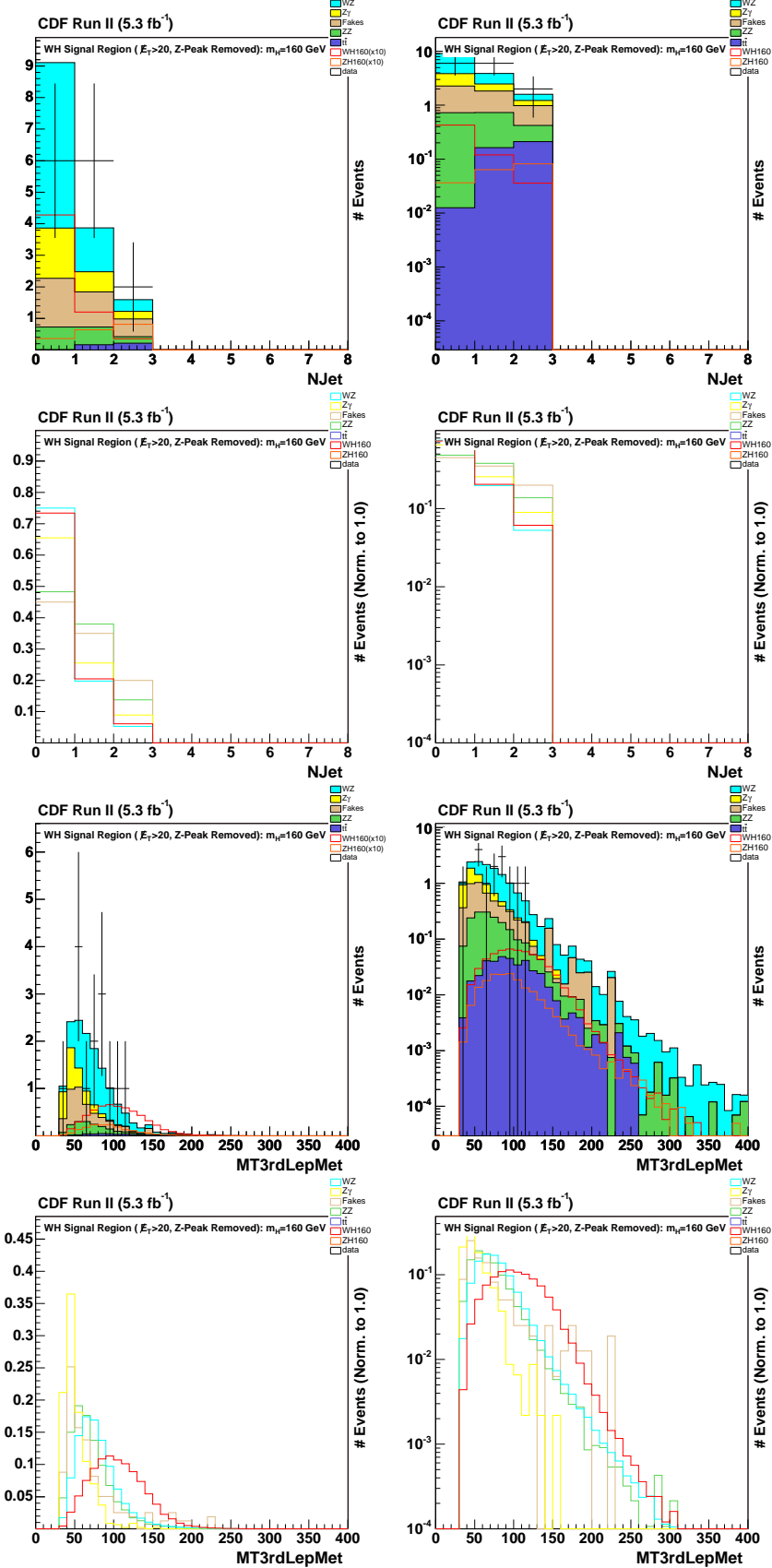


Figure 23: *NoZPeak* Signal Region ( $10.0 \text{ GeV} < \cancel{E}_T < 20.0 \text{ GeV}$ ): NJet (note that the 0-jet bin is not used in the analysis),  $m_T$  (Lep3,  $\cancel{E}_T$ ).

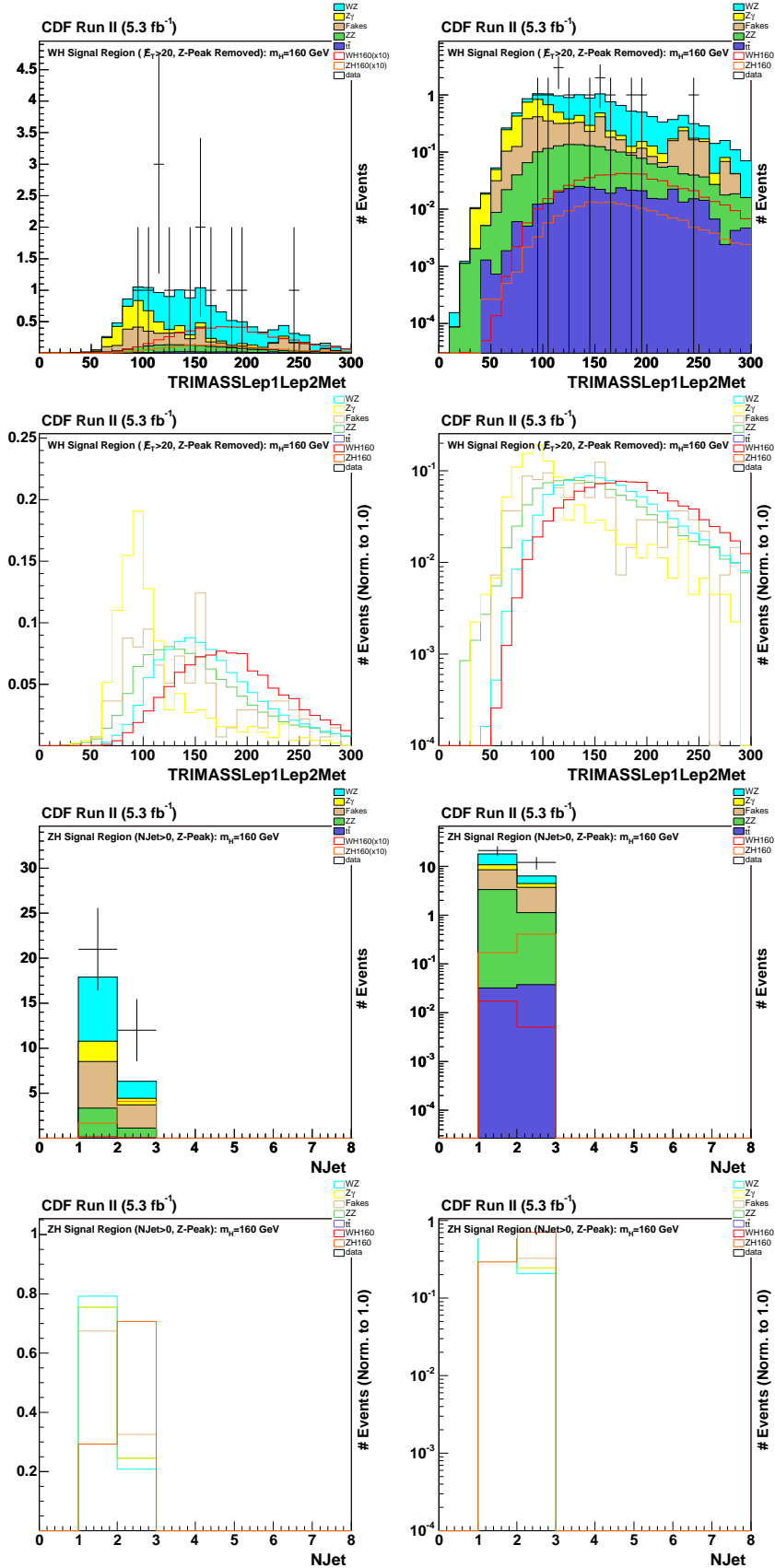


Figure 24: *NoZPeak* Signal Region ( $10.0 \text{ GeV} < \cancel{E}_T < 20.0 \text{ GeV}$ ): Inv. Mass(Lep1,Lep2, $\cancel{E}_T$ ). *InZPeak* Signal Region ( $\text{NJet} \neq 0$ ): NJet.

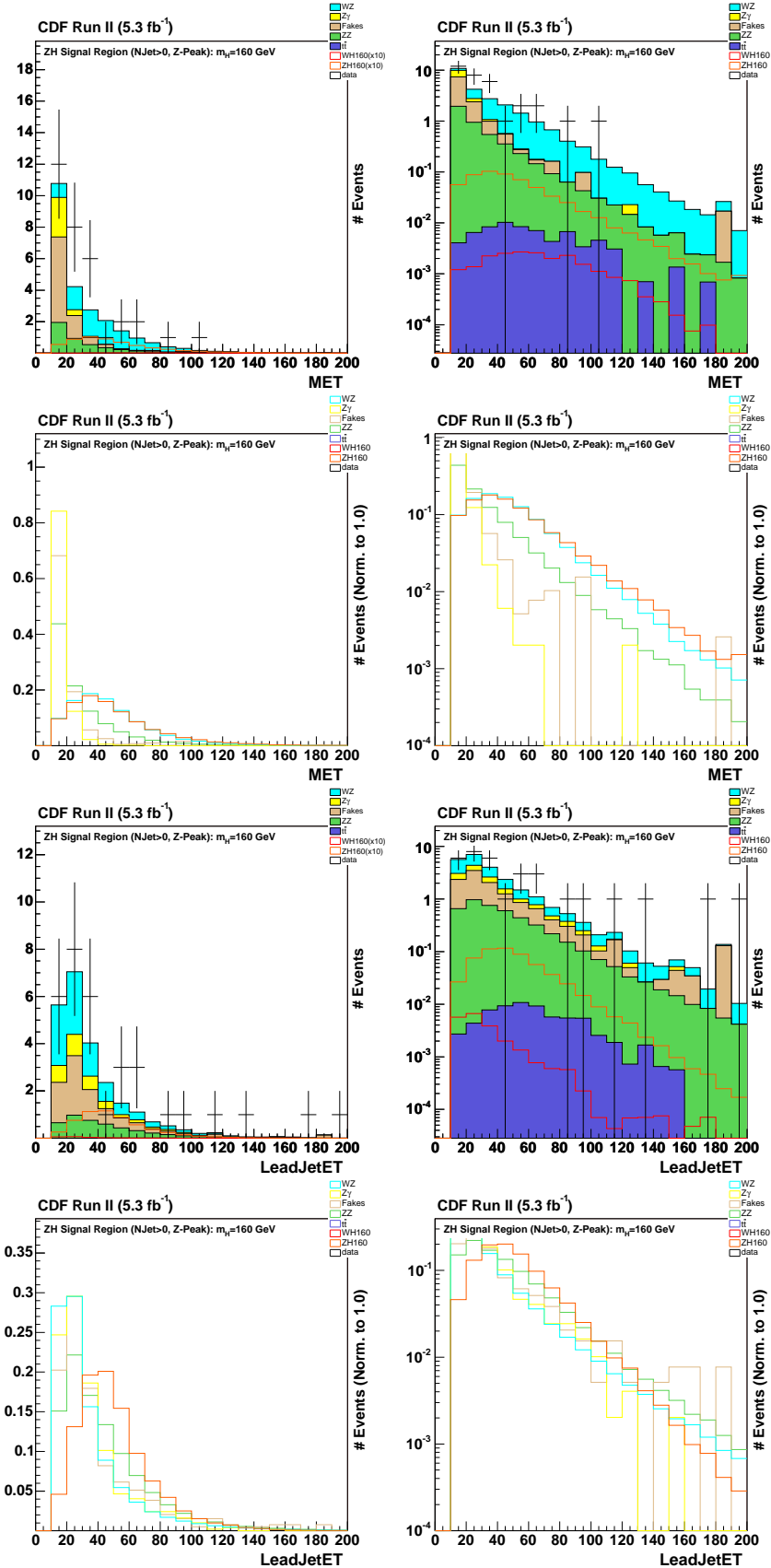


Figure 25: *InZPeak* Signal Region (NJet  $\neq 0$ ):  $\cancel{E}_T$ , Lead Jet  $E_T$ .  
90

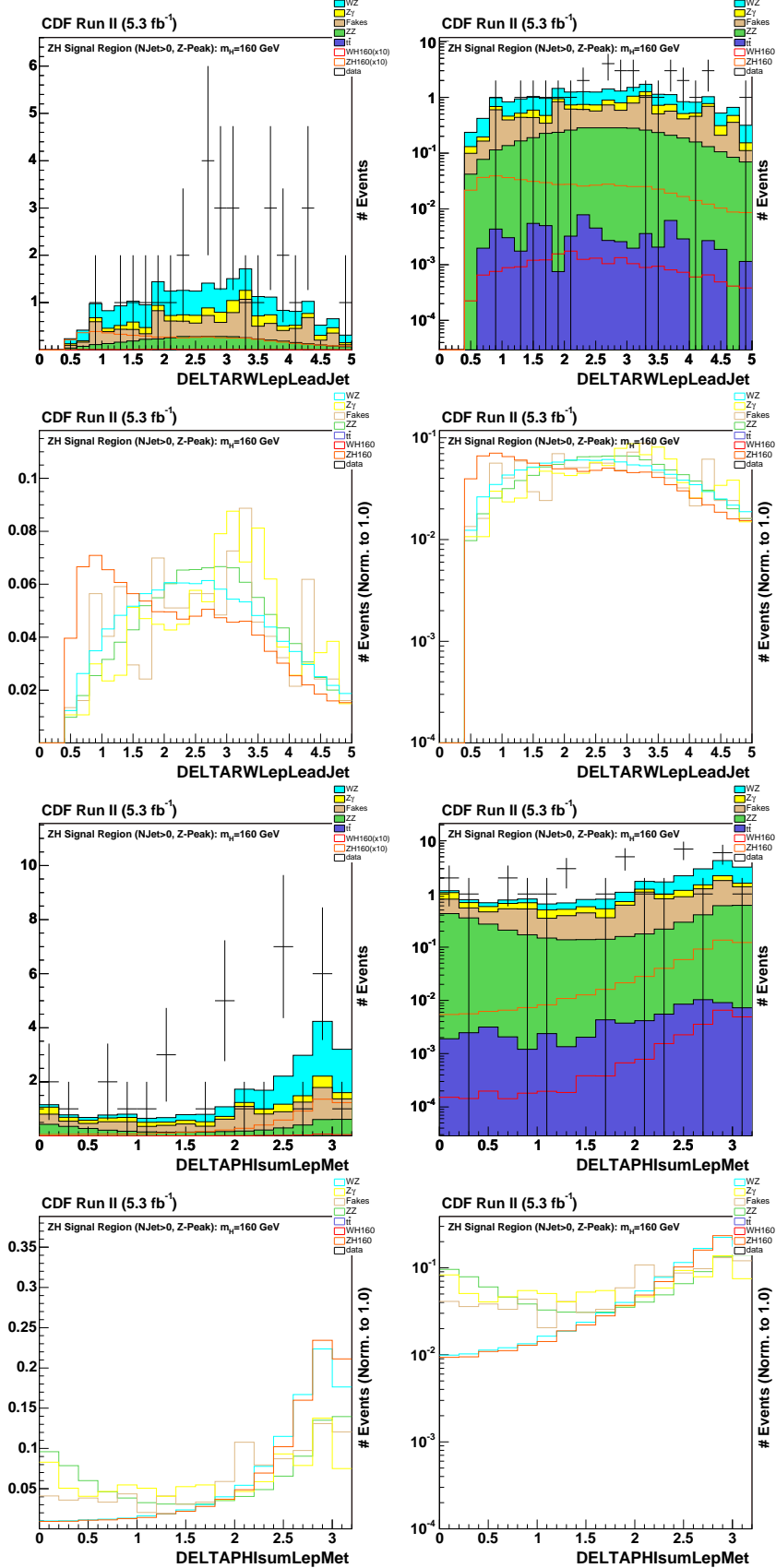


Figure 26: *InZPeak* Signal Region ( $N_{\text{Jet}} \neq 0$ ):  $\Delta R(W\text{-Lep}, \text{Lead Jet})$ ,  $\Delta\phi(\text{Leptons}, \vec{H}_T)$ .

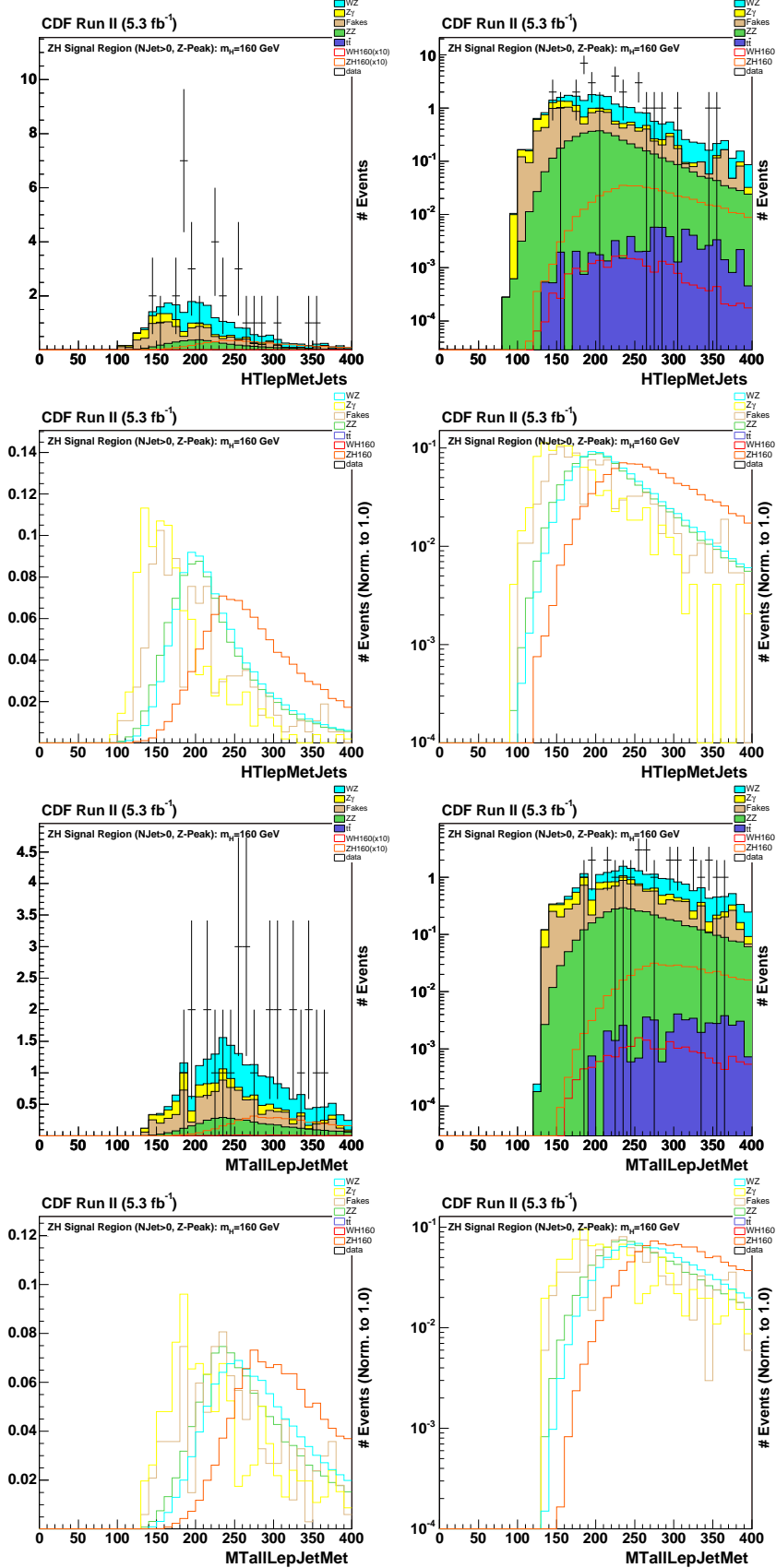


Figure 27: *InZPeak* Signal Region<sub>92</sub> ( $N_{\text{Jet}} \neq 0$ ):  $H_T(\text{Leptons}, \cancel{E}_T, \text{Jets})$ ,  $m_T(\text{Leptons}, \cancel{E}_T, \text{Jets})$ .

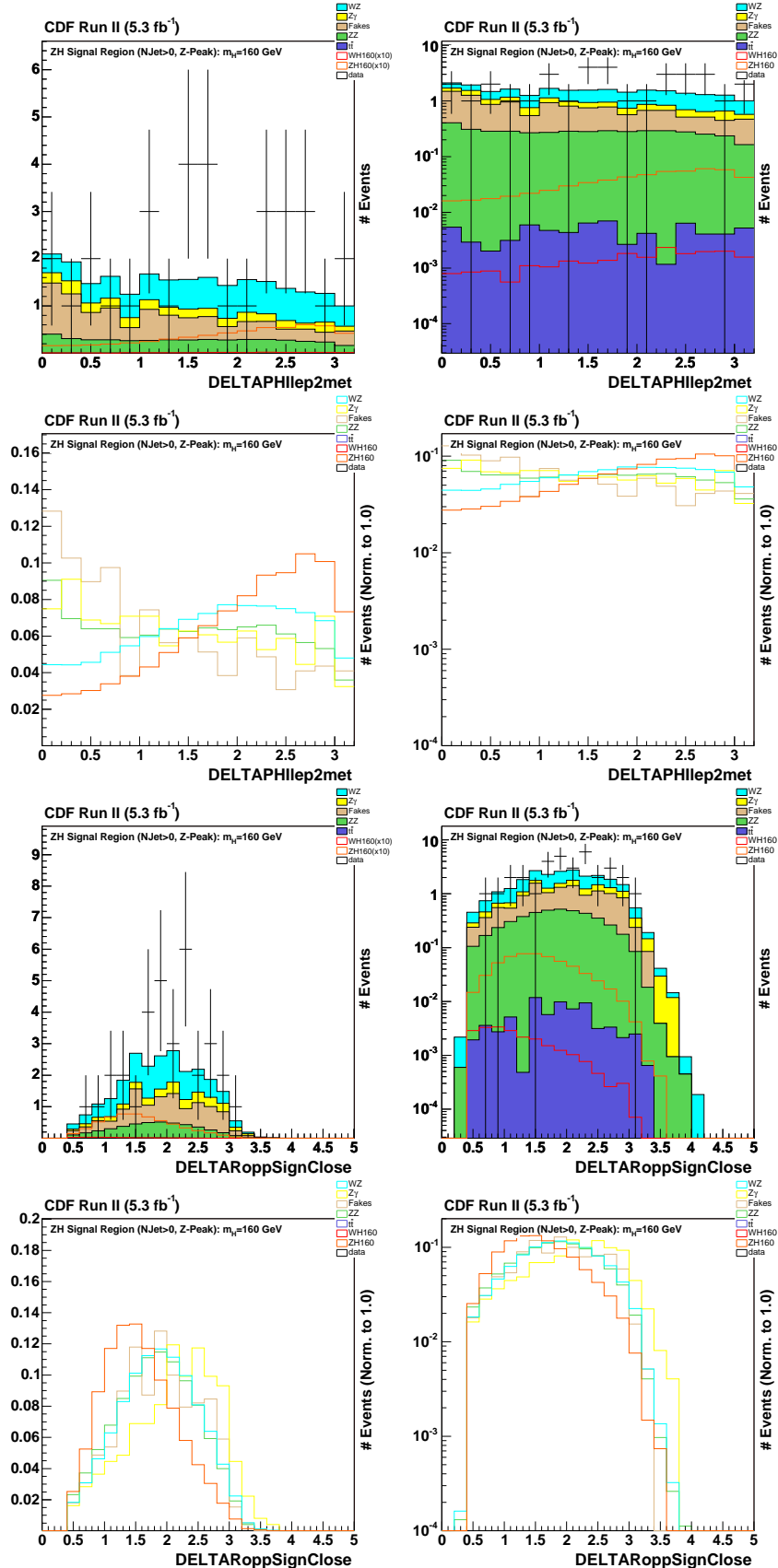


Figure 28: *InZPeak* Signal Region ( $N_{\text{Jet}} \neq 0$ ):  $\Delta\phi(\text{Lep2}, \vec{H}_T)$ ,  $\Delta R$  b/w Opp. Sign Close Leptons.

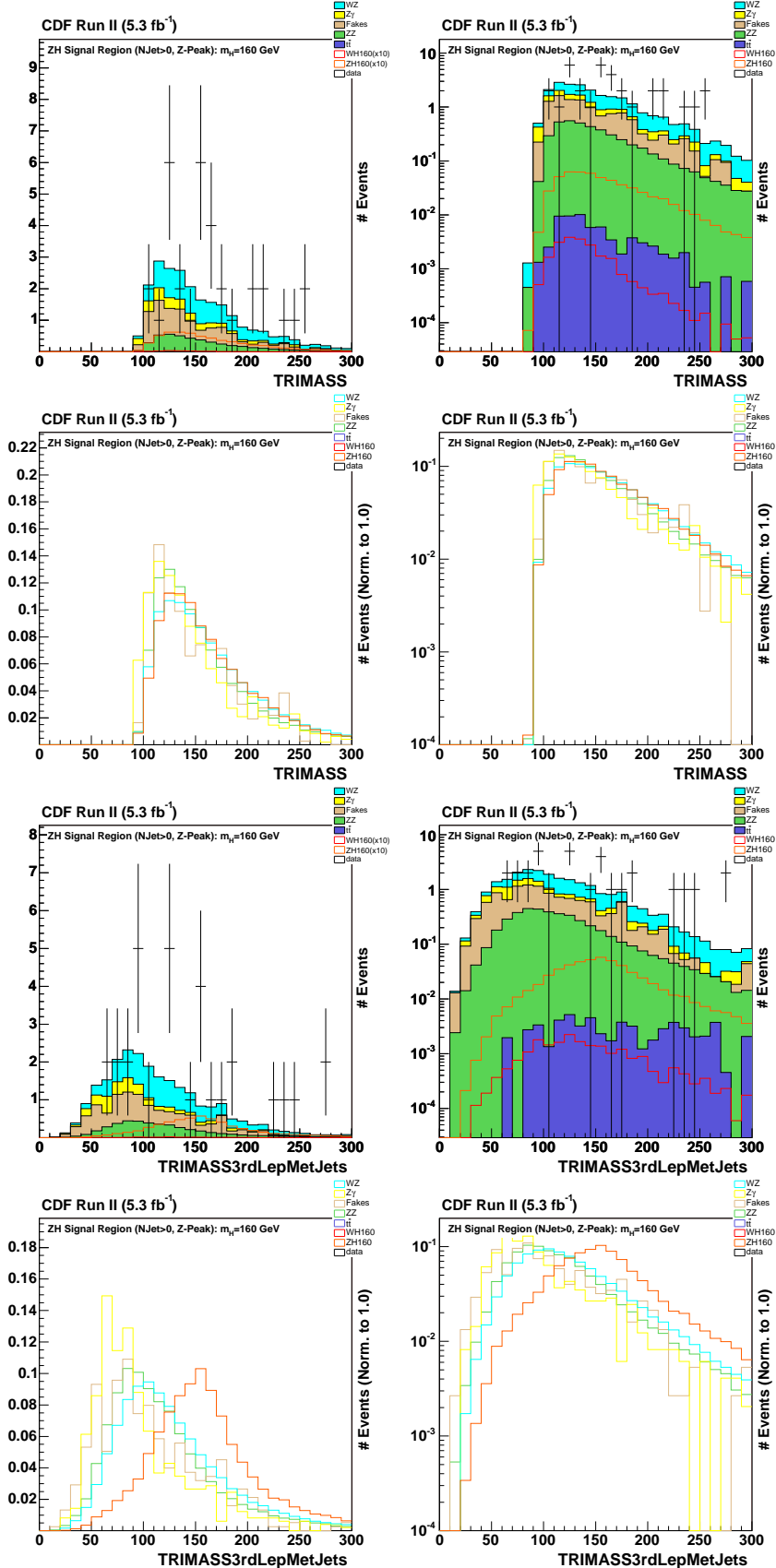


Figure 29:  $InZPeak$  Signal Region ( $N_{\text{Jet}} \neq 0$ ): Trilepton Invariant Mass, Inv. Mass( $\text{Lep3}, \cancel{E}_T, \text{Jets}$ ).

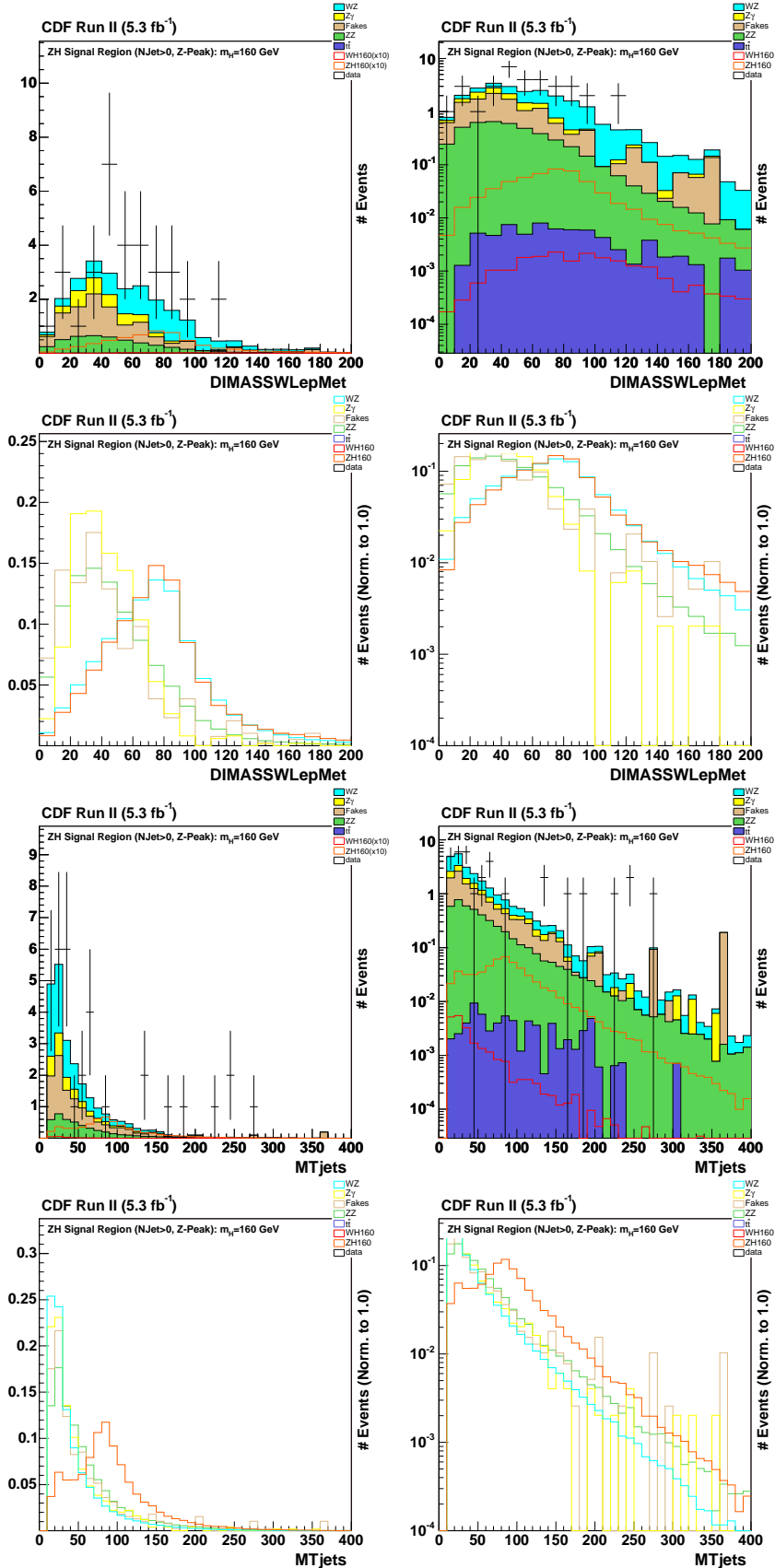


Figure 30:  $InZPeak$  Signal Region ( $N_{\text{Jet}} \neq 0$ ):  $\text{Dimass}(W\text{-Lep}, H_T)$ ,  $m_T$  Jets.

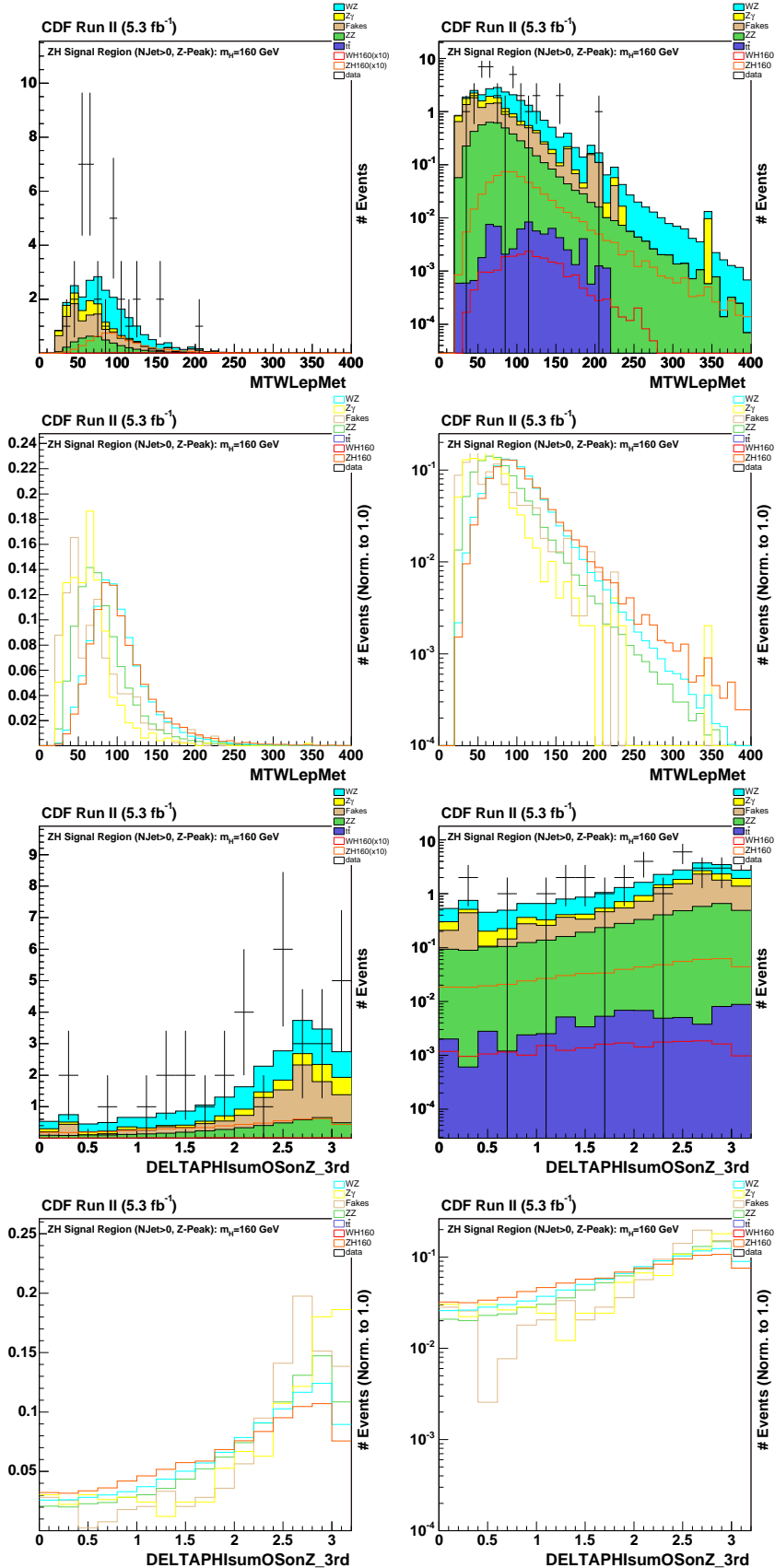


Figure 31:  $InZPeak$  Signal Region ( $\text{NJet}_{90\%} \neq 0$ ):  $m_T(W\text{-Lep}, \not{E}_T)$ ,  $\Delta\phi(Z\text{-Leptons}, W\text{-Lepton})$ .

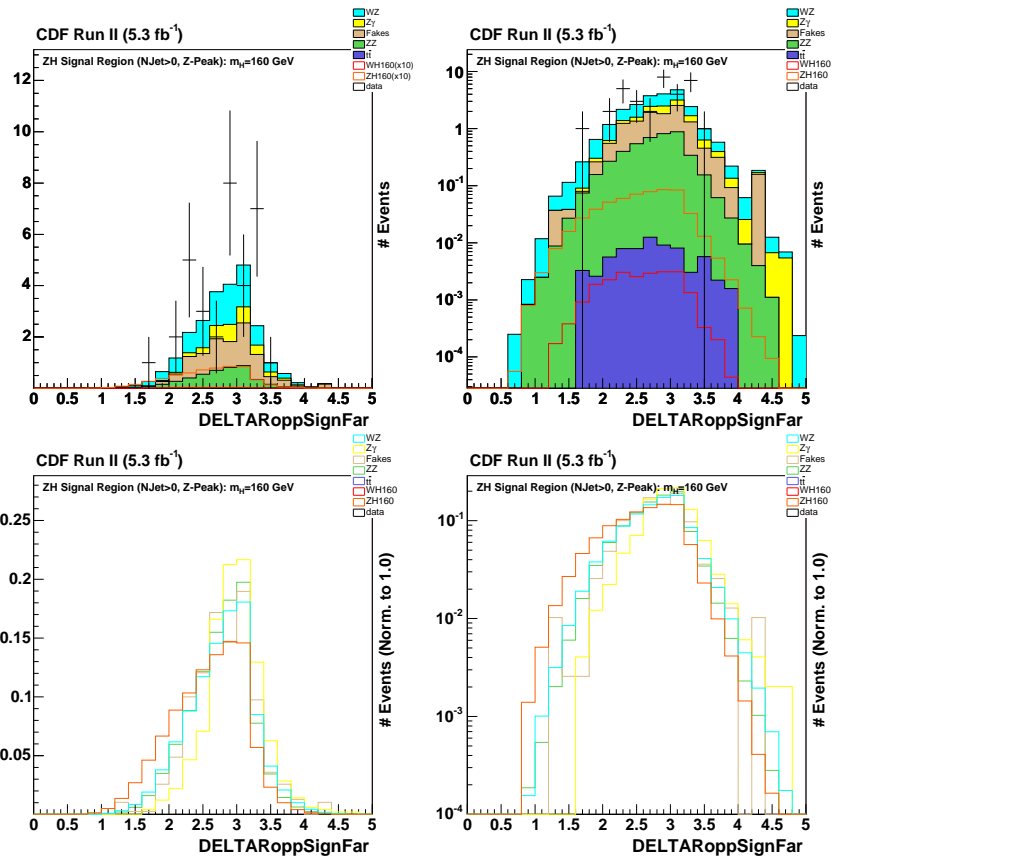


Figure 32: *InZPeak* Signal Region ( $N_{\text{Jet}} \neq 0$ ):  $\Delta R$  Opp. Sign Far Leptons.

## A.2 Input Variables in Control Regions

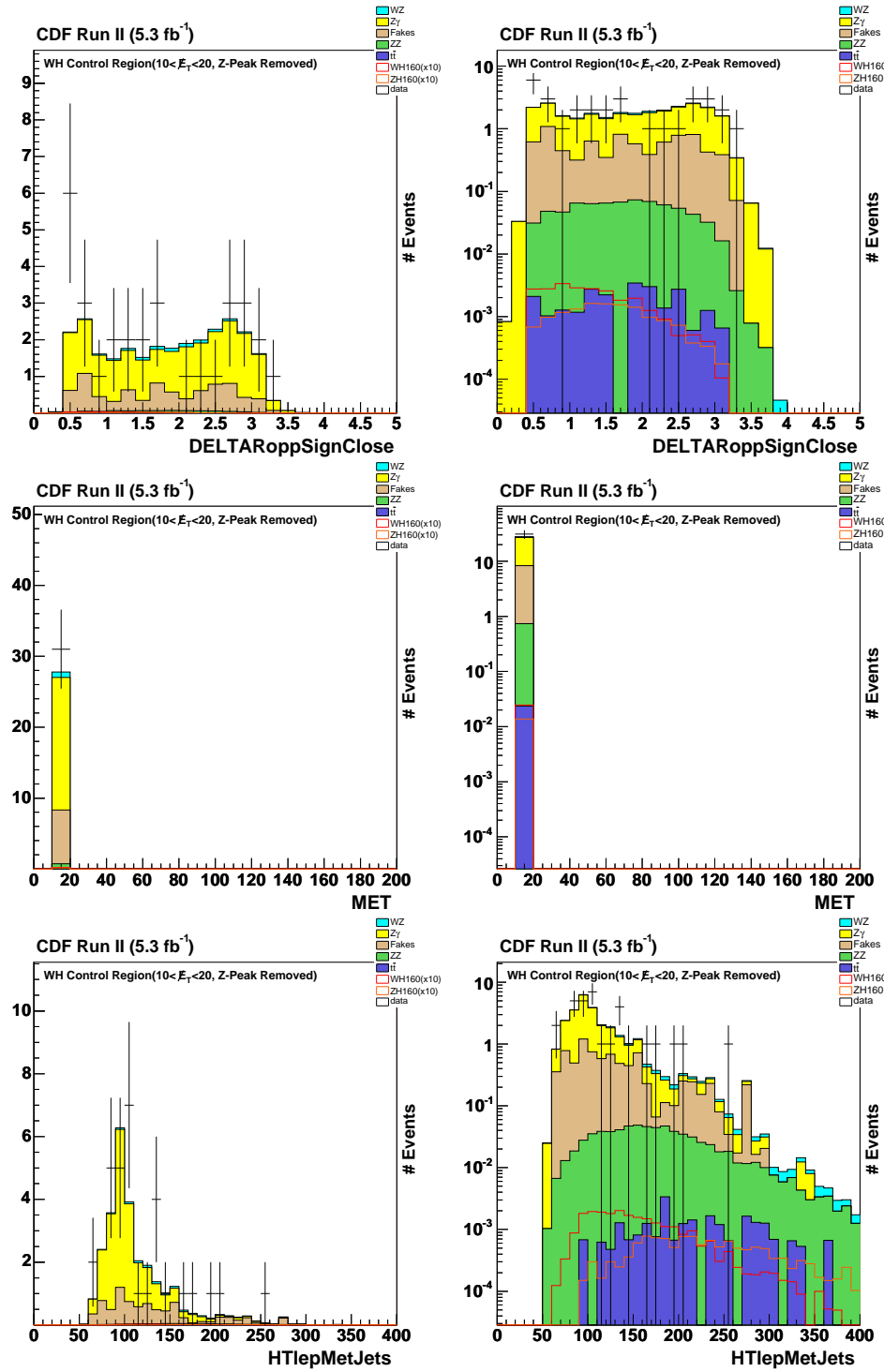


Figure 33: *NoZPeak* Control Region ( $10.0 \text{ GeV} < \cancel{E}_T < 20.0 \text{ GeV}$ ):  $\Delta R$  Opp. Sign Close Leptons,  $\cancel{E}_T$ ,  $H_T$ (all leptons),  $\cancel{E}_T$ , all jets).

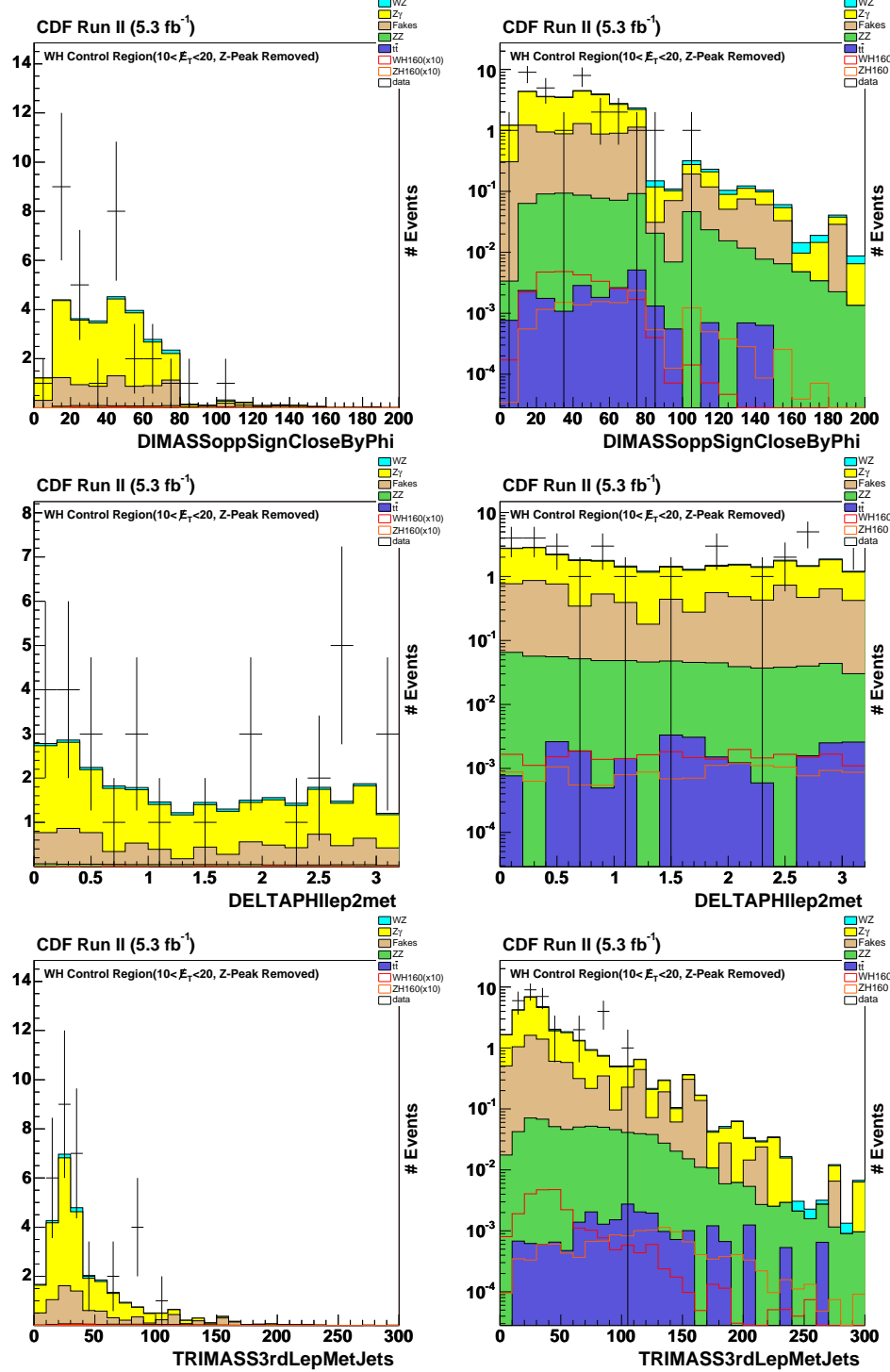


Figure 34: *NoZPeak* Control Region ( $10.0 \text{ GeV} < \cancel{E}_T < 20.0 \text{ GeV}$ ): Dimass Opp. Sign Leptons (closer pair in  $\phi$ ),  $\Delta\phi$  between the 2<sup>nd</sup> lepton and  $\cancel{E}_T$ , Inv. mass of the 3<sup>rd</sup> lepton+  $\cancel{E}_T$ +Jets.

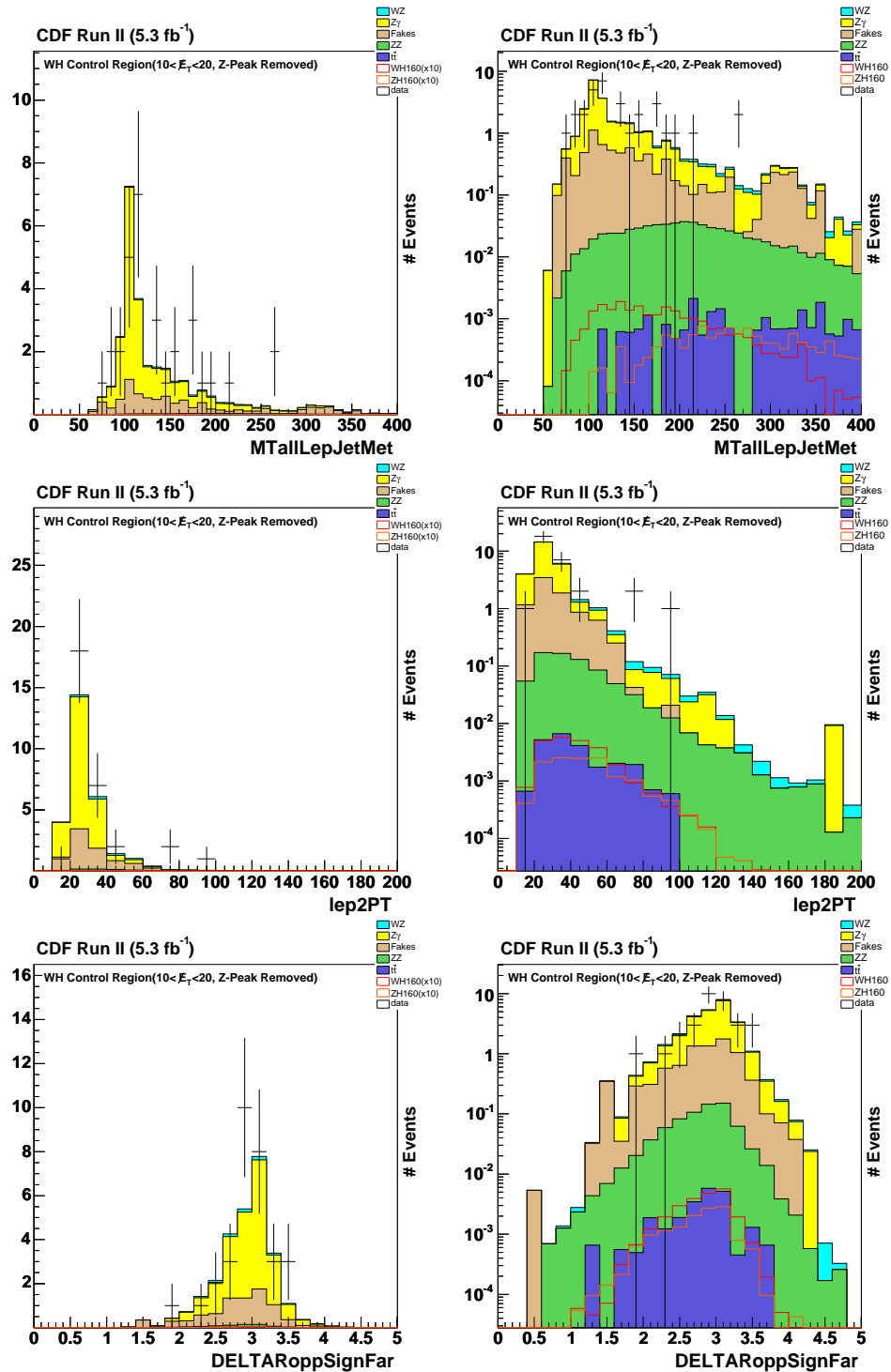


Figure 35: *NoZPeak* Control Region ( $10.0 \text{ GeV} < H_T < 20.0 \text{ GeV}$ ):  $m_T(\text{Leptons}, H_T, \text{Jets})$ ,  $p_T$  of 2<sup>nd</sup> Lepton,  $\Delta R$  Opp. Sign Far Leptons.

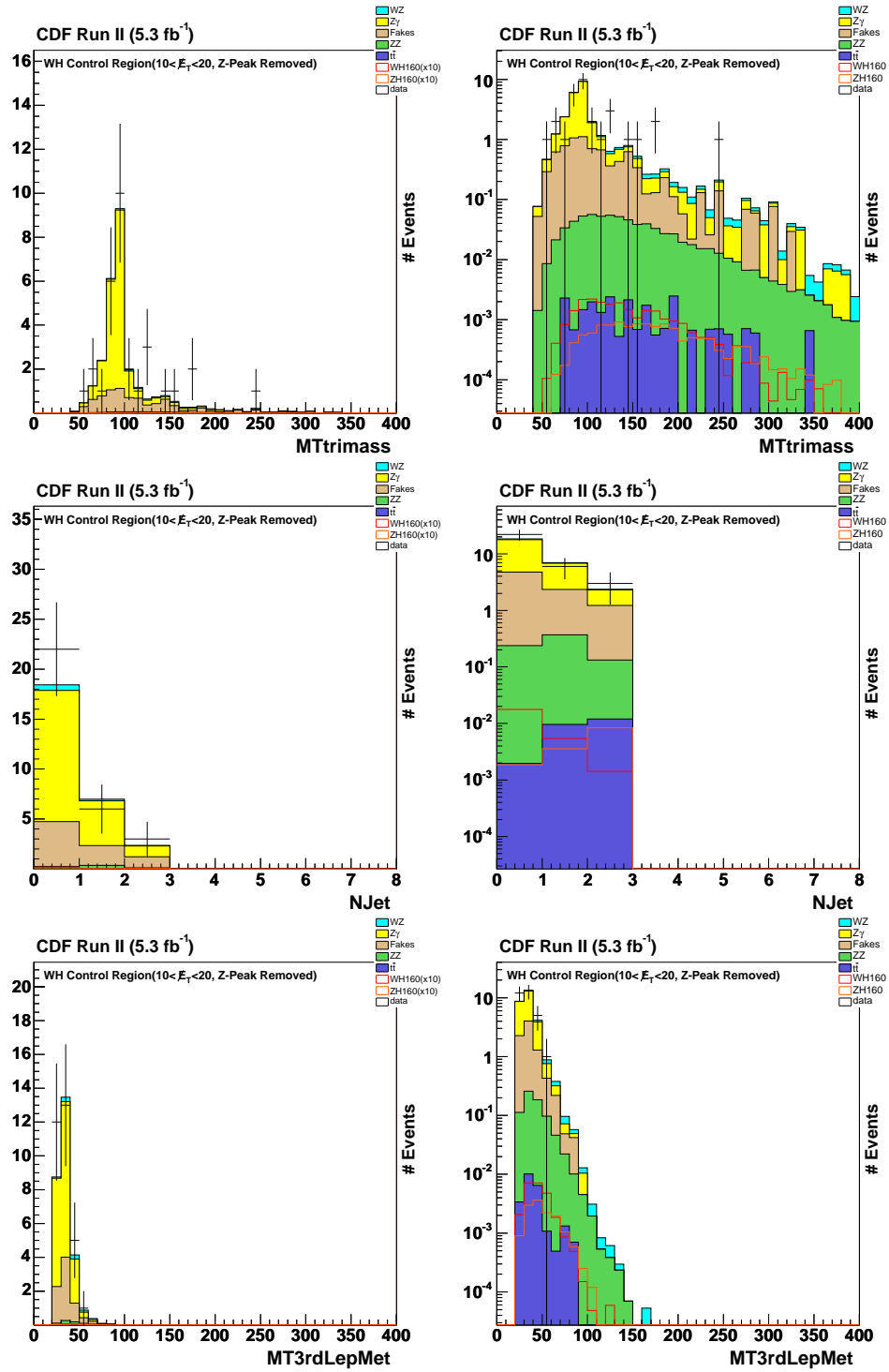


Figure 36: *NoZPeak* Control Region ( $10.0 \text{ GeV} < \cancel{E}_T < 20.0 \text{ GeV}$ ):  $m_T$  Trilepton Mass, NJet,  $m_T$  (Lep3,  $\cancel{E}_T$ ).

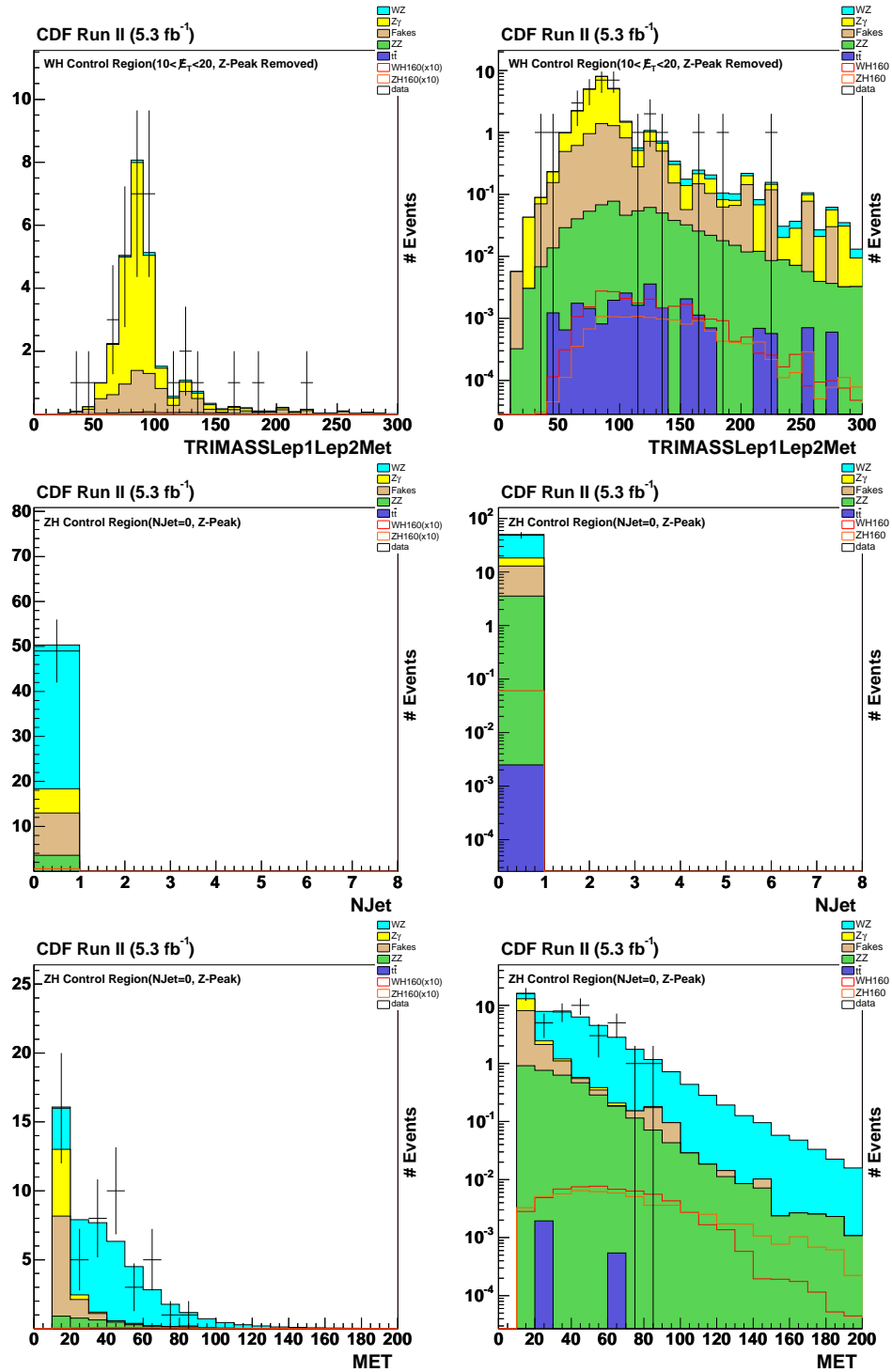


Figure 37: *NoZPeak* Control Region ( $10.0 \text{ GeV} < \cancel{E}_T < 20.0 \text{ GeV}$ ): Inv. Mass(Lep1,Lep2, $\cancel{E}_T$ ). *InZPeak* Control Region ( $\text{NJet}=0$ ): NJet,  $\cancel{E}_T$ .

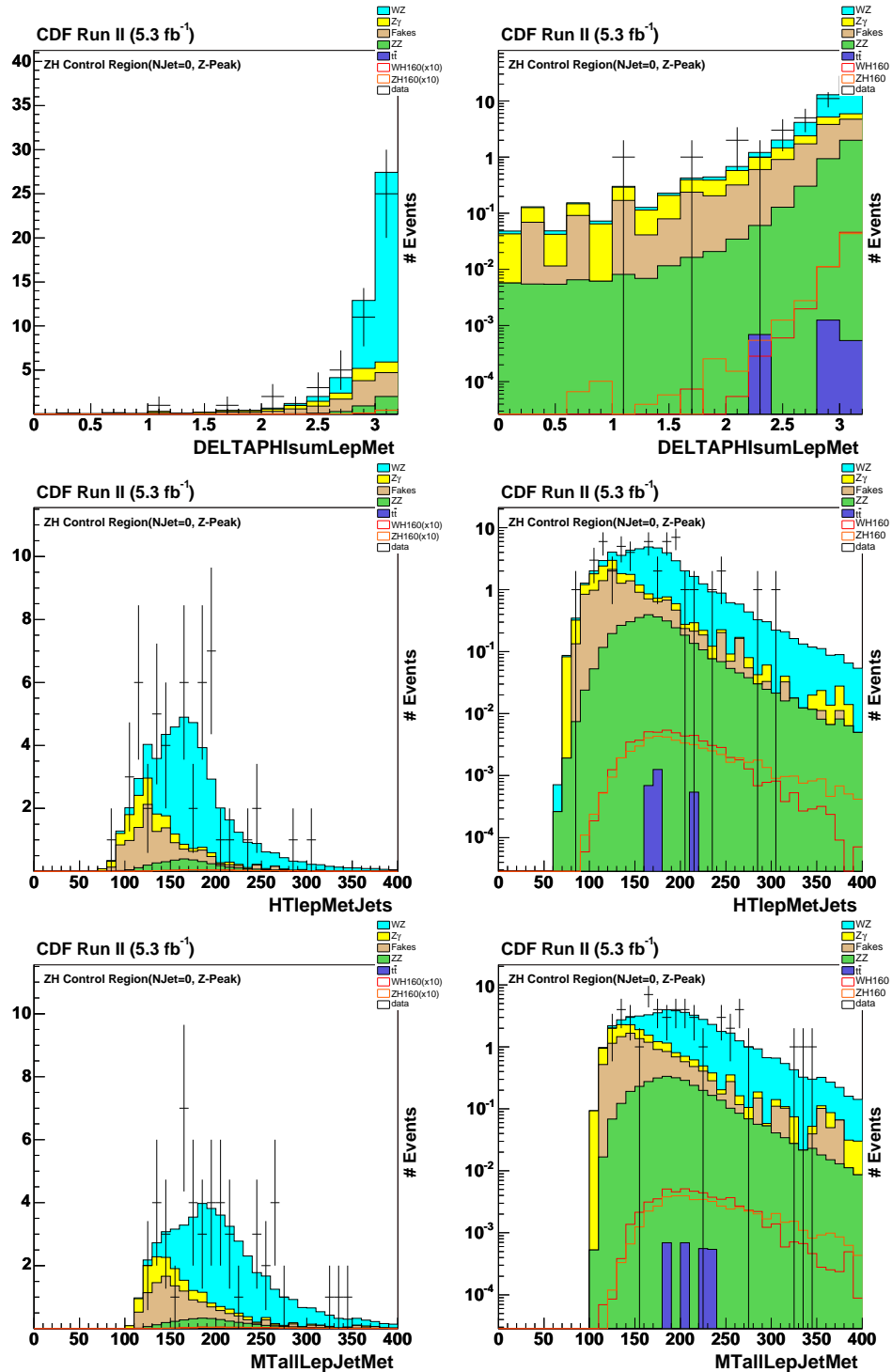


Figure 38: *InZPeak* Control Region (NJet=0):  $\Delta\phi(\text{Leptons}, \vec{E}_T)$ ,  $H_T(\text{Leptons}, \vec{E}_T, \text{Jets})$ ,  $m_T(\text{Leptons}, \vec{E}_T, \text{Jets})$

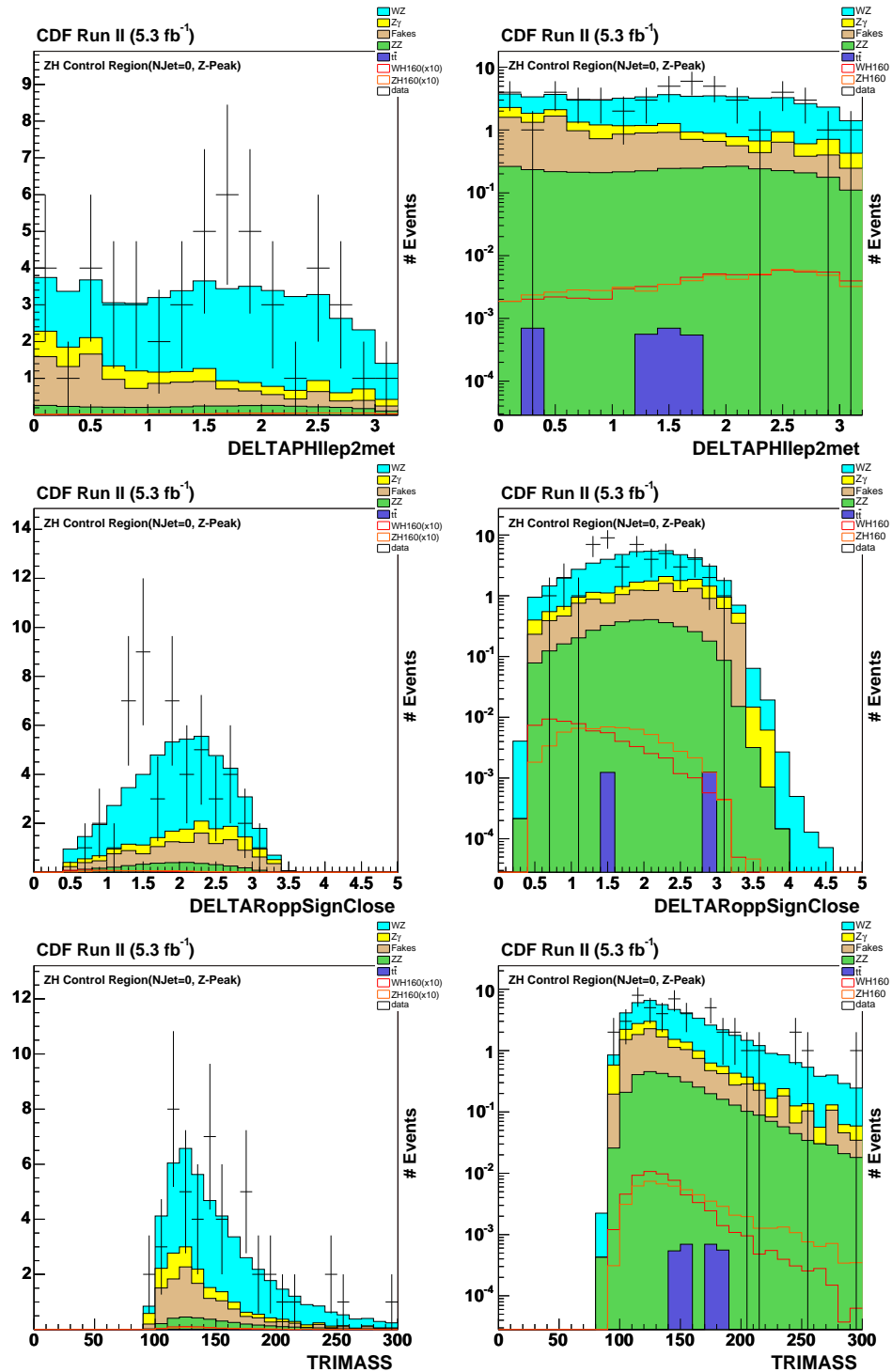


Figure 39: *InZPeak* Control Region (NJet=0):  $\Delta\phi(\text{Lep2}, \not{E}_T)$ ,  $\Delta R$  b/w Opp. Sign Close Lept, trilepton invariant mass.

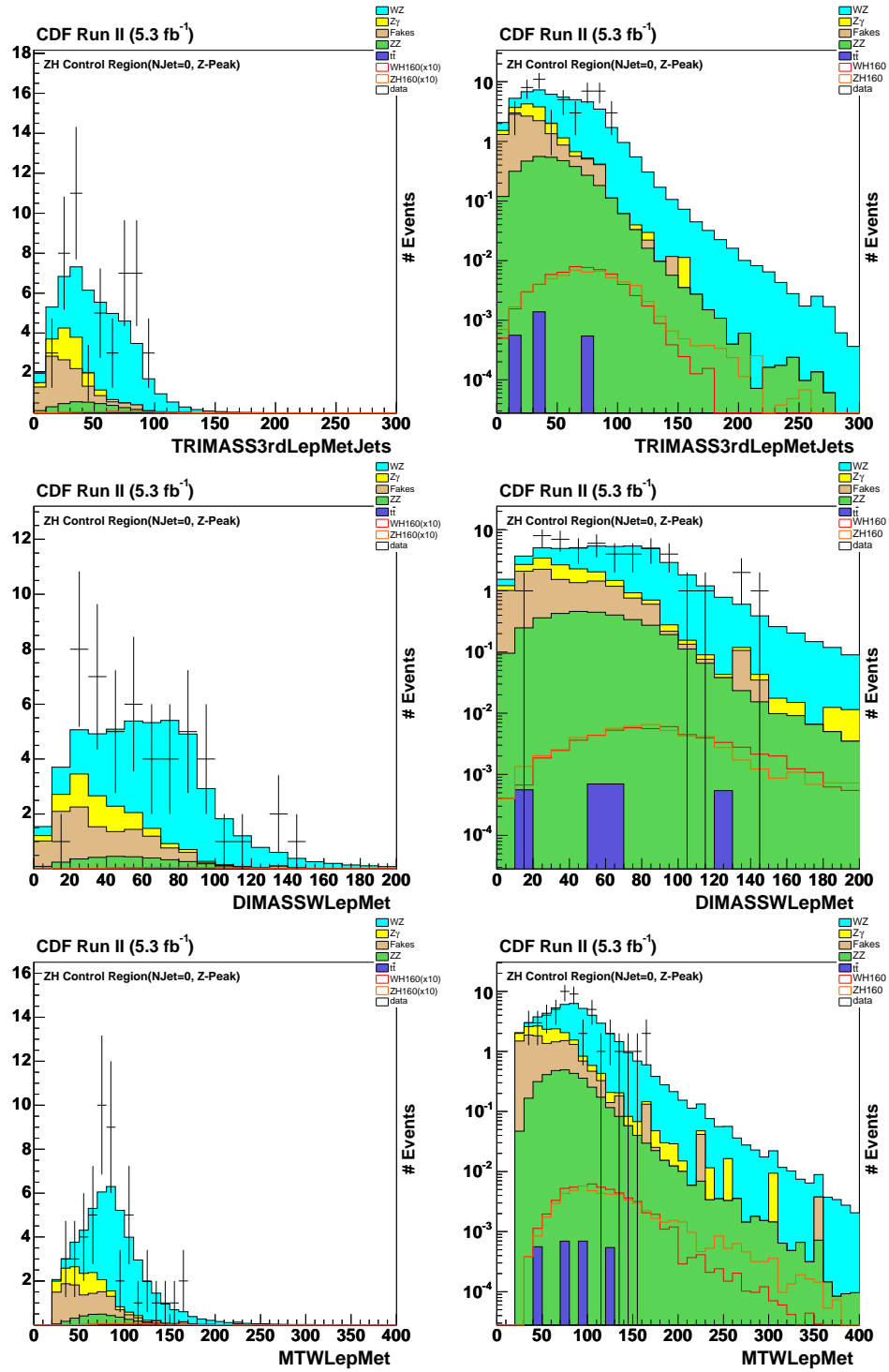


Figure 40: *InZPeak* Control Region (NJet=0): Inv. Mass(Lep3,  $\cancel{E}_T$ , Jets), Dimass( $W$ -Lep,  $\cancel{E}_T$ ),  $m_T(W$ -Lep,  $\cancel{E}_T$ ).

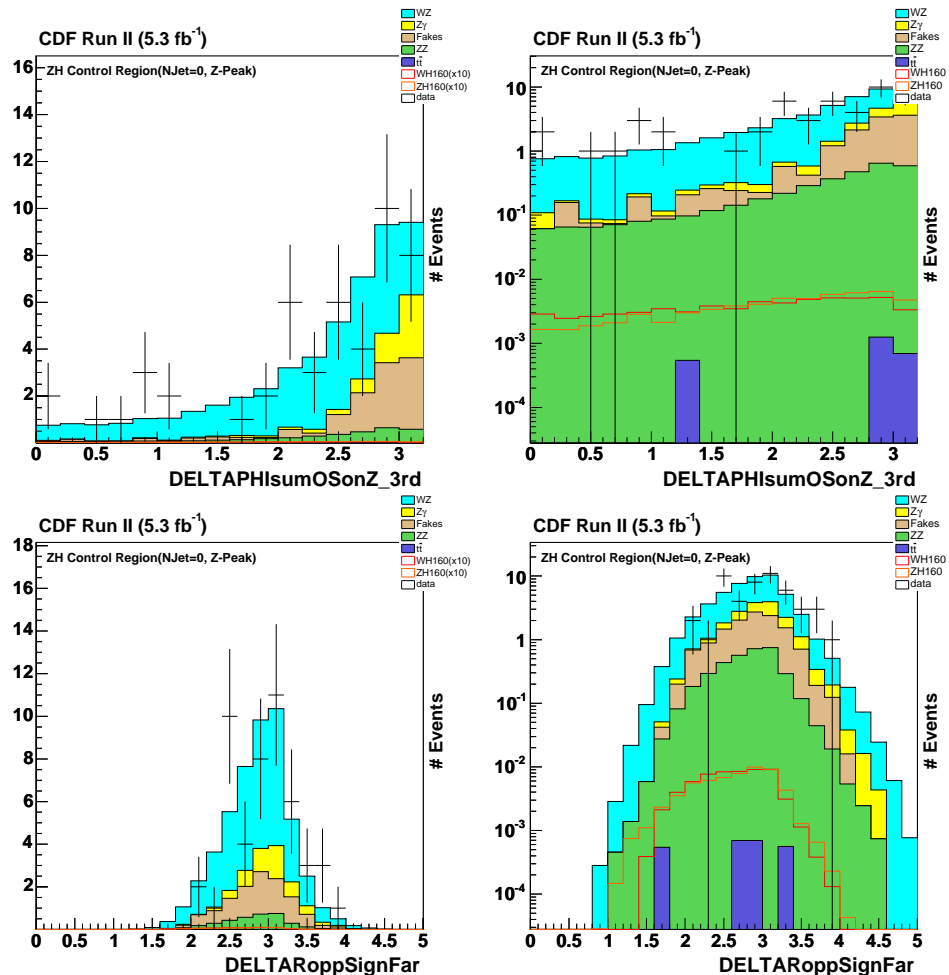


Figure 41: *InZPeak* Control Region (NJet=0):  $\Delta\phi(\text{Z-Leptons}, \text{W-Lepton})$ ,  $\Delta R$  Opp. Sign Far Leptons.

### A.3 $U(1)$ Global Symmetry Breaking

The Standard Model and its component quantum field theories are based on symmetries of particular groups. Equally important is the concept that symmetries of nature may be spontaneously broken with physical consequences. In this and the subsequent few sections of the appendix, we shall explore the concept of spontaneously broken symmetries because the idea is central to the function of the Higgs boson in the Standard Model.

In this section, we shall explore the concept of spontaneously broken  $U(1)$  symmetry for a complex scalar particle. An arbitrary complex field has real and imaginary components, by definition.[13]

$$\phi = \frac{1}{\sqrt{2}}(\phi_1 - i\phi_2) \quad (130)$$

Its complex conjugate is then:

$$\phi = \frac{1}{\sqrt{2}}(\phi_1 + i\phi_2) \quad (131)$$

We postulate the lagrangian for this particle:

$$\mathcal{L} = (\partial_\mu \phi)^\dagger (\partial^\mu \phi) - m_0^2 \phi^\dagger \phi - \frac{1}{4} \lambda (\phi^\dagger \phi)^2 \quad (132)$$

The first term has the typical form of kinetic energy, the second terms is the potential energy or “rest mass,” and the last term governs the possibility of an interaction. If  $m_0^2 > 0$ , then the lagrangian describes a complex scalar particle with mass  $m_0$ .

Denote the last two term as  $V(\phi) = m_0^2 \phi^\dagger \phi + \frac{1}{4} \lambda (\phi^\dagger \phi)^2$ , the potential. The task of determining the particle spectrum of the  $\phi$  field reduces to finding the minima of  $V(\phi)$  and calculating perturbative oscillations from it.

Recall that the  $U(1)$  symmetry group is the group of angular rotations in the complex plane. We say the lagrangian exhibits a  $U(1)$  global symmetry, or is “invariant” under  $U(1)$  transformations, because if we rotate the field  $\phi$  in the complex plane by some arbitrary angle  $\alpha$  in a manner not dependent on spacetime location

$$\phi \rightarrow \phi' = e^{i\alpha} \phi \quad (133)$$

then the lagrangian does not change

$$\mathcal{L} = (\partial_\mu \phi')^\dagger (\partial^\mu \phi') - m_0^2 \phi'^\dagger \phi' - \frac{1}{4} \lambda (\phi'^\dagger \phi')^2 \quad (134)$$

$$= (\partial_\mu \phi e^{i\alpha})^\dagger (\partial^\mu \phi e^{i\alpha}) - m_0^2 \phi^\dagger e^{-i\alpha} \phi e^{i\alpha} - \frac{1}{4} \lambda (\phi^\dagger e^{-i\alpha} \phi e^{i\alpha})^2 \quad (135)$$

$$= (\partial_\mu \phi)^\dagger (\partial^\mu \phi) - m_0^2 \phi^\dagger \phi - \frac{1}{4} \lambda (\phi^\dagger \phi)^2 \quad (136)$$

$$\quad (137)$$

Consequently, the physics implied by the lagrangian also does not change. It is important that the rotation is not dependent on spacetime coordinates because if it was, then the partial derivatives would act on the rotation, extra terms would arise, and the lagrangian would therefore not be invariant under the transformation.

Symmetries in physics imply conservation of some property. Invariance to spatial location implies conservation of momentum; Invariance to temporal location implies conservation of energy; etc. In this case, invariance to rotations in the complex plane implies conservation by charge, which can be derived by studying the lagrangian under an infinitesimal  $U(1)$  transformation  $\phi \rightarrow \phi' = (1 + i\alpha)\phi$ [14]. However, this is not the task at hand.

If we assume  $m_0^2 > 0$ , then the potential simply has a unique and stable extremum at the origin. The quantum theoretical prescription for calculating the particle state spectrum is to determine small harmonic oscillations about this minimum. The symmetry about the origin is stable and would remain unbroken.

If, however,  $m_0^2 < 0$ , then the potential still exhibits the same cylindrical symmetry, but the extremum at the origin is now a maximum and there is a minima ring that assumes the lowest value of the potential. The potential at the origin is unstable, and so it is natural for the symmetry to “break” by having such a state fall to one corresponding to the minima ring.

Determining the particle spectrum now requires choosing some point on the minima circle to perform the perturbative expansion. The minima manifold is found at

$$\frac{dV}{d(\phi^\dagger\phi)} = m_0^2 + \frac{\lambda}{4}2\phi^\dagger\phi = 0 \quad (138)$$

$$\phi^\dagger\phi = -\frac{2m_0^2}{\lambda} \quad (139)$$

$$v \equiv \sqrt{\phi_1^2 + \phi_2^2} = \sqrt{\frac{-4m_0^2}{\lambda}} \quad (140)$$

The new parameter  $v$  is then the radius of the circle.

One way to proceed is to expand about the point  $\phi_1 = v_1, \phi_2 = 0$ . Let

$$\phi(x) = \frac{1}{\sqrt{2}}(v + \eta(x) + i\xi(x)) \quad (141)$$

Then  $\eta(x)$  is a field perturbation in the  $\Re$  direction and the perturbation  $\xi(x)$  in the purely  $\Im$  direction. We find the consequent particle spectrum by putting this expression

of  $\phi(x)$  back into the lagrangian.

$$\mathcal{L} = (\partial_\mu \phi)^\dagger (\partial^\mu \phi) - m_0^2 \phi^\dagger \phi - \frac{1}{4} \lambda (\phi^\dagger \phi)^2 \quad (142)$$

$$= \frac{1}{2} (v + \partial_\mu \eta - i \partial_\mu \xi) (v + \partial^\mu \eta + i \partial^\mu \xi) - \frac{m_0^2}{2} (v + \eta - i \xi) (v + \eta + i \xi) \quad (143)$$

$$- \frac{1}{16} \lambda [(v + \eta - i \xi) (v + \eta + i \xi)]^2 \quad (144)$$

$$= \frac{1}{2} (\partial_\mu \xi)^2 + \frac{1}{2} (\partial_\mu \eta)^2 + m_0^2 \eta^2 + (\text{cubic and quartic terms}) \quad (145)$$

$$(146)$$

From the  $m_0^2 \eta^2$  term, we see the  $\eta$ -field perturbation is associated with a particle of mass  $m_\eta = \sqrt{-2m_0^2}$ . There is no mass term for the  $\xi$ -field. In attempting to generate a massive gauge boson, spontaneously broken gauge theory has provided its own massless particle.

Pictorially, notice that the  $\eta$ -perturbation (the one that does result in a massive particle) climbs up the potential well while the  $\xi$ -perturbation (the massless one) is directed tangent to the circular minima manifold. Perturbing up the potential well implies the existence of an associated massive particle state.

This suggests a possibly more appropriate choice of how to parameterize the field perturbations. Remember that the choice to expand about  $\phi_1 = v, \phi_2 = 0$  was arbitrary. Let's parameterize the perturbations in polar, rather than cartesian, coordinates. That way, we need not specify where on the minima manifold we expand around; the argument applies equivalently to all choices. One field perturbation will be in the radial direction, the other in the angular.

$$\phi(x) = \underbrace{\frac{\rho(x)}{\sqrt{2}}}_{\text{Radial Perturbation}} \cdot \underbrace{e^{\frac{i}{v} \theta(x)}}_{\text{Angular Perturbation}} \quad (147)$$

Since the minima manifold has a radius  $v$ ,  $\rho(x) = v + h(x)$  (spoiler alert: the letter “ $h$ ” is chosen for this perturbation off the potential minimum because this is a precursor to the Higgs boson).

Just as before, we put  $\phi(x)$  back into the lagrangian and see what the particle spectrum

looks like.

$$\mathcal{L} = (\partial_\mu \phi)^\dagger (\partial^\mu \phi) - m_0^2 \phi^\dagger \phi - \frac{1}{4} \lambda (\phi^\dagger \phi)^2 \quad (148)$$

$$= \frac{1}{\sqrt{2}} e^{-\frac{i}{v} \theta(x)} \left[ \partial_\mu \rho(x) - \frac{i}{v} \rho(x) \partial_\mu \theta(x) \right] \frac{1}{\sqrt{2}} e^{\frac{i}{v} \theta(x)} \left[ \partial^\mu \rho(x) + \frac{i}{v} \rho(x) \partial^\mu \theta(x) \right] \quad (149)$$

$$- \frac{1}{2} m_0^2 \rho^2(x) - \frac{1}{16} \lambda \rho^4(x) \quad (150)$$

$$= \frac{1}{2} \left[ (\partial_\mu \rho)(\partial^\mu \rho) + \frac{1}{v^2} \rho^2 (\partial_\mu \theta)(\partial^\mu \theta) \right] - \frac{1}{2} m_0^2 \rho^2 - \frac{1}{16} \lambda \rho^4 \quad (151)$$

$$= \frac{1}{2} (\partial_\mu h + v)(\partial^\mu h + v) + \frac{1}{2v^2} (h + v)^2 (\partial_\mu \theta)^2 - \frac{1}{2} m_0^2 (h^2 + 2vh + v^2) - \frac{1}{16} \lambda (h + v)^4 \quad (152)$$

$$= \frac{1}{2} (\partial_\mu h)^2 + v(\partial_\mu h) + \frac{1}{2} v^2 + \left( \frac{1}{2v^2} h^2 + \frac{1}{v^2} hv + \frac{1}{2v^2} v^2 \right) (\partial_\mu \theta)^2 \quad (153)$$

$$- \frac{1}{2} m_0^2 h^2 - m_0^2 vh - \frac{1}{2} m_0^2 v^2 - \frac{1}{16} \lambda (h + v)^4 \quad (154)$$

$$= \frac{1}{2} (\partial_\mu h)^2 + \frac{1}{2} (\partial_\mu \theta)^2 - \frac{1}{2} m_0^2 h^2 + \dots \quad (155)$$

$$(156)$$

Hence, choosing any arbitrary location on the minima manifold and calculating the particle spectrum via field perturbations, we have kinetic terms for both  $h(x)$  and  $\theta(x)$ , but a mass term only for  $h(x)$ . Also, given this parametrization of  $\phi(x)$ , the vacuum expectation value is

$$\langle 0 | \phi | 0 \rangle = \frac{v}{\sqrt{2}} \quad (157)$$

This is a situation where a symmetric field potential is spontaneously broken in nature and this breaking manifests in a physics different from the situation of the origin being a stable extremum, in which case the symmetry would not spontaneously break in nature.

## A.4 $U(1)$ Local Symmetry Breaking

The situation of global  $U(1)$  symmetry explored in section A.3 is a special case of the topic of this section, local  $U(1)$  symmetry. This scenario is also referred to as the “abelian [commutative] Higgs model.”[13] It is not the fully Standard Model version, but still a critical step toward understanding the Higgs sector of the Standard Model. For that reason, the detailed treatment presented in these sections A.3 through A.6 are included in this thesis.

Recall the postulated globally gauge invariant lagrangian from section A.3.

$$\mathcal{L} = (\partial_\mu \phi)^\dagger (\partial^\mu \phi) - m_0^2 \phi^\dagger \phi - \frac{1}{4} \lambda (\phi^\dagger \phi)^2 \quad (158)$$

To make this lagrangian invariant to local gauge transformations, we must replace the derivatives with “covariant derivatives” to keep the lagrangian invariant under transformation. The covariant derivative is not derived—we postulate the desired covariant derivative and consider its form to be justified by the fact that it works

$$\partial_\mu \rightarrow D_\mu = \partial_\mu + iqA_\mu \quad (159)$$

and include a kinetic term for the “gauge field”  $A_\mu$  that must be included to keep the lagrangian invariant under a local  $U(1)$  transformation.

$$\mathcal{L} = [(\partial^\mu + iqA^\mu)\phi]^\dagger [(\partial_\mu + iqA_\mu)\phi] - \frac{1}{4} F_{\mu\nu} F^{\mu\nu} - \frac{1}{4} \lambda (\phi^\dagger \phi)^2 - m_0^2 (\phi^\dagger \phi) \quad (160)$$

$$(161)$$

where  $F^{\mu\nu} = \partial^\mu A^\nu - \partial^\nu A^\mu$ . Notice this part is the form of the Maxwell lagrangian and  $A^\mu$  is analogous to the photon. We shall return to this point shortly.

This lagrangian is then invariant to a *local*  $U(1)$  field transformation

$$\phi(x) \rightarrow \phi'(x) = e^{-i\alpha(x)} \phi(x) \quad (162)$$

or, in infinitesimal form

$$\phi(x) \rightarrow \phi'(x) = (1 - i\alpha(x)) \phi(x) \quad (163)$$

We still do not know now the gauge field itself transforms. The point of this covariant derivative is to have  $D^\mu \phi$  transform the same way  $\phi$  does. So assume

$$D'^\mu \phi' = (1 - i\alpha(x)) D^\mu \phi \quad (164)$$

to be true and derive the transformation law for  $A_\mu$  from it.

$$(\partial^\mu + iqA'^\mu)\phi' = (1 - i\alpha(x))(\partial^\mu + iqA^\mu)\phi \quad (165)$$

Since this is an infinitesimal transformation, the transformation of  $A^\mu$  should have a general form  $A^\mu \rightarrow A'^\mu = A^\mu + \delta A^\mu$ . Note that both  $\alpha(x)$  and  $\delta A^\mu$  are infinitesimals, so any terms infinitesimal to the 2<sup>nd</sup> order or higher drop.

$$(\partial^\mu + iqA^\mu + iq\delta A^\mu)(1 - i\alpha(x))\phi = (1 - i\alpha(x))(\partial^\mu + iqA^\mu)\phi \quad (166)$$

$$(-i\partial^\mu\alpha(x) + iq\delta A^\mu)\phi = (-i\alpha(x)\partial^\mu)\phi \quad (167)$$

$$iq\delta A^\mu\phi = (i\partial^\mu\alpha(x) - i\alpha(x)\partial^\mu)\phi \quad (168)$$

$$q\delta A^\mu\phi = \partial^\mu(\alpha\phi) - \alpha(\partial^\mu\phi) \quad (169)$$

$$q\delta A^\mu\phi = (\partial^\mu\alpha)\phi \quad (170)$$

$$\delta A^\mu = \frac{1}{q}\partial^\mu\alpha \quad (171)$$

Hence, the gauge field transforms as

$$A^\mu(x) \rightarrow A'^\mu(x) = A^\mu(x) + \frac{1}{q}\partial^\mu\alpha(x) \quad (172)$$

Now we'll see how the gauge field  $A^\mu$  absorbs the massless boson  $\theta$  that was present in the treatment of the global  $U(1)$  case in section A.3.

Recalling the Maxwell term in the lagrangian, let's study the field equation for  $A^\mu$

$$\square A^\nu - \partial^\nu(\partial_\mu A^\mu) = j_\text{em}^\nu = iq(\phi^\dagger(\partial^\nu\phi) - (\partial^\nu\phi)^\dagger\phi) - 2q^2 A^\nu\phi^\dagger\phi \quad (173)$$

Now recall the  $U(1)$  field parametrization for spontaneous symmetry breaking

$$\phi(x) = \underbrace{\frac{v + h(x)}{\sqrt{2}}}_{\text{Radial Perturbation}} \cdot \underbrace{e^{-\frac{i}{v}\theta(x)}}_{\text{Angular Perturbation}} \quad (174)$$

The current becomes

$$j_\text{em}^\nu = iq \left[ \frac{1}{\sqrt{2}}(v + h)e^{\frac{i}{v}\theta(x)} \left( \frac{1}{\sqrt{2}}(v + (\partial^\nu h))e^{-\frac{i}{v}\theta(x)} \right) + \frac{1}{\sqrt{2}}(v + h) \left( \frac{-i}{v}(\partial^\nu\theta) \right) e^{-\frac{i}{v}\theta(x)} \right. \quad (175)$$

$$\left. - \left( \frac{1}{\sqrt{2}}(v + (\partial^\nu h))e^{\frac{i}{v}\theta(x)} \frac{1}{\sqrt{2}}(v + h) \frac{i}{v}(\partial^\nu\theta)e^{\frac{i}{v}\theta(x)} \right) \frac{1}{\sqrt{2}}(v + h)e^{-\frac{i}{v}\theta(x)} \right] \quad (176)$$

$$- 2q^2 A^\nu \cdot \frac{1}{2}(v + h)^2 \quad (177)$$

$$j_\text{em}^\nu = -\frac{iq}{2} \left[ (v + h)(v + \partial^\nu h) + (v + h)^2 \left( \frac{-i}{v}\partial^\nu\theta \right) \right. \quad (178)$$

$$\left. - (v + \partial^\nu h)(v + h) - (v + h)^2 \left( \frac{i}{v}\partial^\nu\theta \right) \right] \quad (179)$$

$$- q^2 A^\nu(v + h)^2 \quad (180)$$

$$(181)$$

$$j_{\text{em}}^\nu = -\frac{iq}{2} \left[ \frac{2i}{v} (v+h)^2 \partial^\nu \theta \right] - q^2 A^\nu (v+h)^2 \quad (182)$$

$$j_{\text{em}}^\nu = \frac{q}{v} (v+h)^2 \partial^\nu \theta - q^2 A^\nu (v+h)^2 \quad (183)$$

$$j_{\text{em}}^\nu = -v^2 q^2 \left( A^\nu - \frac{\partial^\nu \theta}{vq} \right) + \text{higher order terms} \quad (184)$$

Using only the linear term for the current, put it back into the field equation for  $A^\nu$

$$\square A^\nu - \partial^\nu (\partial_\mu A^\mu) = j_{\text{em}}^\nu \quad (185)$$

$$\square A^\nu - \partial^\nu (\partial_\mu A^\mu) = -v^2 q^2 \left( A^\nu - \frac{\partial^\nu \theta}{vq} \right) \quad (186)$$

Now recall that a gauge transformation on  $A^\mu$  has the form  $A^\mu(x) \rightarrow A'^\mu(x) + \frac{1}{q} \partial^\mu \alpha(x)$ , and notice that the right hand side already has this form. As such, define

$$A'^\nu = A^\nu - \frac{\partial^\nu \theta}{vq} \quad (187)$$

Then the field equation becomes

$$\square A'^\nu - \partial^\nu \partial_\mu A'^\mu = -v^2 q^2 A'^\nu \quad (188)$$

$$\boxed{(\square + v^2 q^2) A'^\nu - \partial^\nu \partial_\mu A'^\mu = 0} \quad (189)$$

Finally, we see that the field equation becomes a free massive vector field for a particle with mass  $vq$ . In particular, notice how the appropriate choice of gauge allowed the massless gauge field  $A^\nu$  to absorb the  $\theta$  (“Goldstone” boson) field term and become massive as a result.

Summarily, generalizing from global to local  $U(1)$  symmetry breaking required us to introduce a “gauge field”  $A^\nu$  in order to keep the lagrangian invariant, or symmetric, under  $U(1)$  transformations. After deriving the manner in which  $A^\nu$  itself transforms, we were able to choose a particular “gauge,” or  $U(1)$  transformation, that allows it to absorb the  $\theta$  field (perturbations along the angular direction of the circular minima manifold of the previous section). In the end, we no longer had a  $\theta$  field at all, but rather the gauge field  $A^\nu$  that became massive after absorbing the  $\theta$  field. What has just happened here is important for understanding how the Higgs boson is related to the photon and weak vector boson in the Standard Model theory.

## A.5 $SU(2)$ Global Symmetry Breaking

The “special unitary group”  $SU(2)$  transformations we will be considering in this section are similar to the  $U(1)$  case of sections A.3 and A.4, except that the rotation angle  $\alpha$  now becomes rank-2 matrices  $\vec{\alpha} \cdot \vec{\tau}$ .

To recap, global  $U(1)$  symmetry breaking lead to two fields: a massive field  $h(x)$  and a massless field  $\theta(x)$ . Extending to local  $U(1)$  symmetry required us to introduce a gauge boson  $A^\nu$  and we exploited the gauge symmetry to have  $A^\nu$  absorb the  $\theta(x)$  field and become massive. Now, we will see that by generalizing the same arguments to global  $SU(2)$  symmetry we will end up with another massive  $H(x)$  field and three  $\theta(x)$  fields instead of one.

Consider an  $SU(2)$  doublet of complex bosons

$$\phi = \begin{bmatrix} \phi^+ \\ \phi^0 \end{bmatrix} = \begin{bmatrix} \frac{1}{\sqrt{2}}(\phi_1 + i\phi_2) \\ \frac{1}{\sqrt{2}}(\phi_3 + i\phi_4) \end{bmatrix} \quad (190)$$

where  $\phi^+$  destroys positively charged particles and creates negatively charged particle, and  $\phi^0$  destroys neutral particles and creates neutral antiparticles.

Postulate the form of the lagrangian as a direct generalization of the previous two sections

$$\mathcal{L} = (\partial_\mu \phi)^\dagger (\partial^\mu \phi) - m_0^2 \phi^\dagger \phi - \frac{\lambda}{4} (\phi^\dagger \phi)^2 \quad (191)$$

where  $m_0^2 < 0$ . This lagrangian is not only invariant to  $SU(2)$  transformations, but also to the global  $U(1)$  transformations of section A.3. We treat the global  $SU(2)$  case here, so  $\alpha$  is not dependent on spacetime coordinate.

$$\phi \rightarrow \phi' = e^{-\frac{i}{2}\vec{\alpha} \cdot \vec{\tau}} \phi \quad \text{for } SU(2) \quad (192)$$

$$\phi \rightarrow \phi' = e^{-i\alpha} \phi \quad \text{for } U(1) \quad (193)$$

The minimum occurs at

$$\frac{\partial \mathcal{L}}{\partial (\phi^\dagger \phi)} = -m_0^2 - \frac{\lambda}{2} (\phi^\dagger \phi)_{\min} = 0 \quad (194)$$

$$(\phi^\dagger \phi)_{\min} = \frac{-2m_0^2}{\lambda} \equiv \frac{v^2}{2} \quad (195)$$

As before, we take the minimum to be the vacuum.

$$\langle 0 \mid \phi^\dagger \phi \mid 0 \rangle = \frac{v^2}{2} = \langle 0 \mid \phi_1^2 + \phi_2^2 + \phi_3^2 + \phi_4^2 \mid 0 \rangle \quad (196)$$

To obtain the particle spectrum we expand the fields  $\phi$  about the choice of vacuum. Again, rather than a single point, we have a whole space of minima to choose from. Let,

$$\langle 0 | \phi | 0 \rangle = \begin{bmatrix} 0 \\ \frac{v}{\sqrt{2}} \end{bmatrix} \quad (197)$$

Oscillations about this vacuum choice are parametrized by

$$\phi = e^{-\frac{i}{2}(\vec{\theta}(x) \cdot \vec{\tau})v} \begin{bmatrix} 0 \\ \frac{1}{\sqrt{2}}(v + H(x)) \end{bmatrix} \quad (198)$$

We have here three fields  $\vec{\theta}$  for possible “angular” oscillations associated with the  $SU(2)$  symmetry, and one radial field oscillation  $H(x)$ . We shall see now that only the  $H(x)$  field has nonzero mass, indicating that each  $\vec{\theta}$  field oscillates in a direction within the minima manifold, i.e. does not climb the potential just as in the global  $U(1)$  case. To do this, put  $\phi$  back into the lagrangian and look for mass terms.

$$\partial^\mu \phi = \begin{bmatrix} 0 \\ -\frac{i}{2v}((\partial^\mu \vec{\theta}) \cdot \vec{\tau})e^{-\frac{i}{2v}\vec{\theta} \cdot \vec{\tau}} \frac{1}{\sqrt{2}}(v + H) + e^{-\frac{i}{2v}\vec{\theta} \cdot \vec{\tau}} \frac{1}{\sqrt{2}}\partial^\mu H \end{bmatrix} \quad (199)$$

$$= e^{-\frac{i}{2v}\vec{\theta} \cdot \vec{\tau}} \begin{bmatrix} 0 \\ \frac{-i}{2\sqrt{2}v}((\partial^\mu \vec{\theta}) \cdot \vec{\tau})(v + H) + \frac{1}{\sqrt{2}}\partial^\mu H \end{bmatrix} \quad (200)$$

Similarly,

$$(\partial^\mu \phi)^\dagger = \begin{bmatrix} 0 & \frac{i}{2\sqrt{2}v}((\partial^\mu \vec{\theta}) \cdot \vec{\tau})(v + H) + \frac{1}{\sqrt{2}}\partial^\mu H \end{bmatrix} \quad (201)$$

Putting these terms into the lagrangian, we get:

$$\mathcal{L} = \frac{1}{8v^2}(\partial^\mu \vec{\theta} \cdot \vec{\tau})(\partial_\mu \vec{\theta} \cdot \vec{\tau})(v + H)^2 + \frac{1}{2}(\partial^\mu H)(\partial_\mu H) - \frac{m_0^2}{2}v^2 - \frac{m_0^2}{2}vH - \frac{m_0^2}{2}H^2 - \frac{\lambda}{4}(v + H)^4 \quad (202)$$

Mass terms with different fields multiplied govern the interaction between the fields. Notice now since  $\vec{\theta}(x)$  only appear in an exponent in the field  $\phi$ , it only has derivative terms in the lagrangian. Thus, the particles associated with the  $\vec{\theta}$  fields are massless. Only the  $H(x)$  has a mass term.

## A.6 $SU(2)$ Local Symmetry Breaking

Let's now generalize the  $SU(2)$  global invariance of the previous section to local invariance in the same manner we did for  $U(1)$  transformations in section A.4.

Local  $SU(2)$  gauge transformations have the form

$$\phi(x) \rightarrow \phi'(x) = e^{\frac{ig}{2}\vec{\tau} \cdot \vec{\alpha}(x)} \phi(x) \quad (203)$$

where the factor  $g$  is inserted to represent the coupling strength.

Just as in the case of electromagnetic interactions, no lagrangian for a free particle can be Lorentz invariant under this local gauge transformation. To make it Lorentz invariant, the derivative must be replaced by a covariant derivative. This way,  $D^\mu \phi$  transforms the same way  $\phi$  does, whereas  $\partial^\mu \phi$  does not. Just as in the  $U(1)$  case, this will necessarily involve the introduction of new gauge fields.

In the  $SU(2)$  case,

$$\partial^\mu \phi'(x) = e^{\frac{ig}{2}\vec{\tau} \cdot \vec{\alpha}(x)} (\partial^\mu \phi(x)) + \frac{ig}{2} \vec{\tau} \cdot (\partial^\mu \vec{\alpha}(x)) e^{\frac{ig}{2}\vec{\tau} \cdot \vec{\alpha}(x)} \phi(x) \quad (204)$$

where it is the second term that breaks the covariance.

The covariant derivative  $D^\mu$  must act like:

$$D^\mu \phi'(x) = e^{\frac{ig}{2}\vec{\tau} \cdot \vec{\alpha}(x)} \phi(x) D^\mu \phi(x) \quad (205)$$

The form of  $D^\mu$  is just postulated, then justified by the fact that it works.

$$D^\mu \equiv \partial^\mu + \frac{ig}{2} \vec{\tau} \cdot \vec{W}^\mu \quad (206)$$

where  $\vec{W}^\mu \equiv (W_1^\mu, W_2^\mu, W_3^\mu)$ , a slight precursor to the weak vector bosons.

The  $\vec{W}^\mu$  are the  $SU(2)$  gauge fields, analogous to the  $U(1)$  gauge field  $A^\mu$ , and the  $\vec{\tau}$  are the Pauli spin matrices.

$$\vec{\tau} \cdot \vec{W}^\mu = \begin{bmatrix} 0 & 1 \\ 1 & 0 \end{bmatrix} W_1^\mu + \begin{bmatrix} 0 & -i \\ i & 0 \end{bmatrix} W_2^\mu + \begin{bmatrix} 1 & 0 \\ 0 & -1 \end{bmatrix} W_3^\mu \quad (207)$$

$$= \begin{bmatrix} 0 & W_1^\mu \\ W_1^\mu & 0 \end{bmatrix} + \begin{bmatrix} 0 & -iW_2^\mu \\ iW_2^\mu & 0 \end{bmatrix} + \begin{bmatrix} W_3^\mu & 0 \\ 0 & -W_3^\mu \end{bmatrix} \quad (208)$$

$$= \begin{bmatrix} W_3^\mu & W_1^\mu - iW_2^\mu \\ W_1^\mu + iW_2^\mu & -W_3^\mu \end{bmatrix} \quad (209)$$

Remember that the three gauge fields  $\vec{W}^\mu$  are spacetime dependent.

Let's examine the  $SU(2)$  transformation in infinitesimal form

$$\phi' = \left( 1 + \frac{ig}{2} \vec{\tau} \cdot \vec{\epsilon}(x) \right) \phi \quad (210)$$

$$\partial \phi' = \left( 1 + \frac{ig}{2} \vec{\tau} \cdot \vec{\epsilon}(x) \right) \partial^\mu \phi + \frac{ig}{2} \vec{\tau} \cdot (\partial^\mu \vec{\epsilon}) \phi \quad (211)$$

We again see the noncovariant term. Let's use the covariant derivative instead.

$$D'^\mu \phi' = \left( 1 + \frac{ig}{2} \vec{\tau} \cdot \vec{\epsilon}(x) \right) D^\mu \phi \quad (212)$$

$$\left( \partial^\mu + \frac{ig}{2} \vec{\tau} \cdot \vec{W}'^\mu \right) \left[ 1 + \frac{ig}{2} \vec{\tau} \cdot \vec{\epsilon}(x) \right] \phi = \left[ 1 + \frac{ig}{2} \vec{\tau} \cdot \vec{\epsilon}(x) \right] \left( \partial^\mu + \frac{ig}{2} \vec{\tau} \cdot \vec{W}^\mu \right) \phi \quad (213)$$

So far, we do not know how the gauge fields  $W^\mu$  transform (notice that both  $\vec{W}'^\mu$  and  $\vec{W}^\mu$  appear). We proceed by assuming that the previous equality does, in fact, hold; and determine the transformation law for  $\vec{W}^\mu$  from it.

The previous equality involves an infinitesimal transformation, so the transformation of  $\vec{W}^\mu$  must look something like

$$\vec{W}^\mu \rightarrow \vec{W}'^\mu = \vec{W}^\mu + \delta \vec{W}^\mu \quad (214)$$

Let's start the algebra.

$$\left[ \partial^\mu + \frac{ig}{2} \vec{\tau} \cdot \vec{W}'^\mu \right] \left[ 1 + \frac{ig}{2} \vec{\tau} \cdot \vec{\epsilon}(x) \right] \phi = \left[ 1 + \frac{ig}{2} \vec{\tau} \cdot \vec{\epsilon}(x) \right] \left[ \partial^\mu + \frac{ig}{2} \vec{\tau} \cdot \vec{W}^\mu \right] \phi \quad (215)$$

$$\left[ \partial^\mu + \frac{ig}{2} \vec{\tau} \cdot \vec{W}^\mu + \frac{ig}{2} \vec{\tau} \cdot \delta \vec{W}^\mu \right] \left[ 1 + \frac{ig}{2} \vec{\tau} \cdot \vec{\epsilon}(x) \right] \phi = \left[ 1 + \frac{ig}{2} \vec{\tau} \cdot \vec{\epsilon}(x) \right] \left[ \partial^\mu + \frac{ig}{2} \vec{\tau} \cdot \vec{W}^\mu \right] \phi \quad (216)$$

$$\left[ \frac{ig}{2} \vec{\tau} \cdot \partial^\mu \vec{\epsilon} - \frac{1}{4} g^2 (\vec{\tau} \cdot \vec{W}^\mu) (\vec{\tau} \cdot \vec{\epsilon}) \frac{ig}{2} \vec{\tau} \cdot \delta \vec{W}^\mu \right] \phi = \left[ \frac{ig}{2} (\vec{\tau} \cdot \vec{\epsilon}) \partial^\mu - \frac{g^2}{4} (\vec{\tau} \cdot \vec{\epsilon}) (\vec{\tau} \cdot \vec{W}^\mu) \right] \phi \quad (217)$$

$$\frac{ig}{2} \vec{\tau} \cdot \partial^\mu (\vec{\epsilon} \phi) - \frac{1}{4} g^2 (\vec{\tau} \cdot \vec{W}^\mu) (\vec{\tau} \cdot \vec{\epsilon}) \phi + \frac{ig}{2} \vec{\tau} \cdot (\delta \vec{W}^\mu) \phi = \frac{ig}{2} \vec{\tau} \cdot (\vec{\epsilon} \partial^\mu \phi) - \frac{g^2}{4} (\vec{\tau} \cdot \vec{\epsilon}) (\vec{\tau} \cdot \vec{W}^\mu) \phi \quad (218)$$

$$\frac{ig}{2} \vec{\tau} \cdot (\delta \vec{W}^\mu) \phi = \frac{ig}{2} \vec{\tau} \cdot [\vec{\epsilon} (\partial^\mu \phi) - \partial^\mu (\vec{\epsilon} \phi)] + \frac{g^2}{4} \left[ (\vec{\tau} \cdot \vec{W}^\mu) (\vec{\tau} \cdot \vec{\epsilon}) - (\vec{\tau} \cdot \vec{\epsilon}) (\vec{\tau} \cdot \vec{W}^\mu) \right] \phi \quad (219)$$

$$\frac{ig}{2} \vec{\tau} \cdot (\delta \vec{W}^\mu) \phi = \frac{ig}{2} \vec{\tau} \cdot [-(\partial^\mu \vec{\epsilon}) \phi] + \frac{g^2}{4} \left[ (\vec{\tau} \cdot \vec{W}^\mu) (\vec{\tau} \cdot \vec{\epsilon}) - (\vec{\tau} \cdot \vec{\epsilon}) (\vec{\tau} \cdot \vec{W}^\mu) \right] \phi \quad (220)$$

$$ig \frac{\vec{\tau} \cdot (\delta \vec{W}^\mu)}{2} = -ig \frac{\vec{\tau} \cdot (\partial^\mu \vec{\epsilon}(x))}{2} + (ig)^2 \left[ \left( \frac{\vec{\tau} \cdot \vec{\epsilon}}{2} \right) \left( \frac{\vec{\tau} \cdot \vec{W}^\mu}{2} \right) - \left( \frac{\vec{\tau} \cdot \vec{W}^\mu}{2} \right) \left( \frac{\vec{\tau} \cdot \vec{\epsilon}}{2} \right) \right] \quad (221)$$

$$\vec{\tau} \cdot (\delta \vec{W}^\mu) = -\vec{\tau} \cdot (\partial^\mu \vec{\epsilon}) - \frac{g}{2} \left[ (\vec{\tau} \cdot \vec{\epsilon}) (\vec{\tau} \cdot \vec{W}^\mu) - (\vec{\tau} \cdot \vec{W}^\mu) (\vec{\tau} \cdot \vec{\epsilon}) \right] \quad (222)$$

$$(223)$$

Let's take a closer look at the terms inside the brackets alone.

$$[(\vec{\tau} \cdot \vec{\epsilon}) (\vec{\tau} \cdot \vec{W}^\mu) - (\vec{\tau} \cdot \vec{W}^\mu) (\vec{\tau} \cdot \vec{\epsilon})] = (\vec{\epsilon} \cdot \vec{W}^\mu + i\vec{\tau} \cdot \vec{\epsilon} \times \vec{W}^\mu) - (\vec{W}^\mu \cdot \vec{\epsilon} + i\vec{\tau} \cdot \vec{W}^\mu \times \vec{\epsilon}) \quad (224)$$

$$= i\vec{\tau} (\vec{\epsilon} \times \vec{W}^\mu - \vec{W}^\mu \times \vec{\epsilon}) \quad (225)$$

$$= i\vec{\tau} (\vec{\epsilon} \times \vec{W}^\mu - \vec{\epsilon} \times \vec{W}^\mu) \quad (226)$$

$$= 2i\vec{\tau} \cdot (\vec{\epsilon} \times \vec{W}^\mu) \quad (227)$$

Let's put this back into equation 222.

$$\vec{\tau} \cdot (\delta \vec{W}^\mu) = -\delta^\mu \vec{\epsilon}(x) - g [\vec{\epsilon}(x) \times \vec{W}^\mu] \quad (228)$$

$$(229)$$

This means the infinitesimal piece is

$$\delta \vec{W}^\mu = -\partial^\mu \vec{\epsilon}(x) - g [\vec{\epsilon}(x) \times \vec{W}^\mu] \quad (230)$$

$$(231)$$

Generalizing from global to local transformations introduces the extra  $\partial^\mu \vec{\epsilon}(x)$  term. Hence, the gauge fields for a local  $SU(2)$  gauge (phase) transform as

$$\vec{W}'^\mu = \vec{W}^\mu - \partial^\mu \vec{\epsilon}(x) - g [\vec{\epsilon}(x) \times \vec{W}^\mu] \quad (232)$$

$$(233)$$

Now that we know how the gauge field and the covariant derivative transform with an  $SU(2)$  gauge transformation, we can compute the consequences from our basic postulated lagrangian from equation 191, which can now be restated in  $SU(2)$  invariant form

$$\mathcal{L} = (D_\mu \phi)^\dagger (D^\mu \phi) - m_0^2 \phi^\dagger \phi - \frac{\lambda}{4} (\phi^\dagger \phi)^2 - \frac{1}{4} \vec{W}_{\mu\nu} \cdot \vec{W}^{\mu\nu} \quad (234)$$

where  $\vec{W}_{\mu\nu} \equiv \partial_\mu \vec{W}_\nu - \partial_\nu \vec{W}_\mu - g \vec{W}_\mu \times \vec{W}_\nu$ , where the last term is necessary because of the non-Abelian nature of the  $SU(2)$  group.

Note that if  $m_0^2 > 0$ , then we just have a system of four scalar particles of mass  $m_0$ . However, we are interested in the  $m_0^2 < 0$  case. Just as for the  $U(1)$  case, we want to find the minima of the potential and find an entire minima manifold.

$$\frac{\partial \mathcal{L}}{\partial (\phi^\dagger \phi)} = 0 \quad (235)$$

$$(\phi^\dagger \phi)_{\min} = -\frac{2m_0^2}{\lambda} = \frac{1}{2} (\phi_1^2 + \phi_2^2 + \phi_3^2 + \phi_4^2) \quad (236)$$

We must choose some particular point on the minima manifold upon which to expand and calculate the particle spectrum, so choose  $\phi_1 = \phi_2 = \phi_4 = 0$  and then we are left with

$$\frac{1}{2}\phi_3^2 = \frac{-2m_0^2}{\lambda} \quad (237)$$

$$\phi_3 = 2\sqrt{\frac{-m_0^2}{\lambda}} \equiv v \quad (238)$$

Then our complex field doublet at this minimum becomes

$$\phi_{\min} = \frac{1}{\sqrt{2}} \begin{bmatrix} \phi_1 + i\phi_2 \\ \phi_3 + i\phi_4 \end{bmatrix} = \frac{1}{\sqrt{2}} \begin{bmatrix} 0 \\ v \end{bmatrix} \quad (239)$$

Again, completely analogous to the  $U(1)$  case, we can parametrize perturbations about this minimum as

$$\phi(x) = \frac{\rho(x)}{\sqrt{2}} e^{\frac{i}{v} \vec{\tau} \cdot \vec{\theta}(x)} \quad , \text{ where} \quad (240)$$

$$\rho(x) = \begin{bmatrix} 0 \\ v + h(x) \end{bmatrix} \quad (241)$$

This can be seen more intuitively when looked at in infinitesimal form.

Nevertheless, we now have an  $SU(2)$  gauge invariant lagrangian with covariant derivatives and we know how the introduced gauge fields  $\vec{W}^\mu$  change with an  $SU(2)$  transformation. As such, the massless  $\vec{\theta}(x)$  fields can be gauged away and we are left with massive  $\vec{W}^\mu$  and  $h$  fields, another example of the Higgs mechanism.

For Standard Model physics, we will be combining this effect for both the  $U(1)$  and  $SU(2)$  cases to get the massive weak vector bosons and the photon—the higgs will be a necessary consequence. More details will be worked out in sections A.7, A.8, and A.10.

## A.7 The Higgs Mechanism in the $SU(2) \times U(1)$ Local Spontaneous Symmetry Breaking

Recall that we had a scalar  $SU(2)$  doublet

$$\phi = \begin{bmatrix} \phi^+ \\ \phi^0 \\ \phi^- \end{bmatrix} \quad (242)$$

whose lagrangian is

$$\mathcal{L} = (\partial_\mu \phi)^\dagger (\partial^\mu \phi) - m_0^2 \phi^\dagger \phi - \frac{\lambda}{4} (\phi^\dagger \phi)^2 \quad (243)$$

This lagrangian is invariant to  $U(1)$  global transformations

$$\phi \rightarrow \phi' = e^{-i\alpha} \phi \quad (244)$$

and global  $SU(2)$  transformations

$$\phi \rightarrow \phi' = e^{-\frac{i}{2}\vec{\alpha} \cdot \vec{\tau}} \phi \quad (245)$$

For a theory that is invariant to local transformations we must introduce three  $SU(2)$  gauge fields (see section A.6) and one  $U(1)$  gauge field (see section A.4). Denote them here as  $W_i^\mu(x)$  for  $i = 1, 2, 3$  and  $B^\mu(x)$ , respectively. Also, the derivatives must be replaced with a covariant derivative for both  $U(1)$  and  $SU(2)$ .

$$D^\mu \phi = \left( \partial^\mu + \underbrace{\frac{ig}{2} \vec{\tau} \cdot \vec{W}^\mu}_{SU(2)\text{piece}} + \underbrace{\frac{ig'}{2} B^\mu}_{U(1)\text{piece}} \right) \phi \quad (246)$$

Kinetic terms for the new gauge fields must also be included.

$$\vec{F}^{\mu\nu} = \partial^\mu \vec{W}^\nu - \partial^\nu \vec{W}^\mu - g \vec{W}^\mu \times \vec{W}^\nu \quad (247)$$

$$G^{\mu\nu} = \partial^\mu B^\nu - \partial^\nu B^\mu \quad (248)$$

So the new full lagrangian is

$$\mathcal{L} = (D_\mu \phi)^\dagger (D^\mu \phi) + m_0^2 \phi^\dagger \phi - \frac{\lambda}{4} (\phi^\dagger \phi)^2 - \frac{1}{4} \vec{F}_{\mu\nu} \cdot \vec{F}^{\mu\nu} - \frac{1}{4} G_{\mu\nu} G^{\mu\nu} \quad (249)$$

$$(250)$$

We already looked at spontaneous symmetry breaking for the  $U(1)$  and  $SU(2)$  cases individually, now we want to do so for the product group  $SU(2) \times U(1)$  in such a way that we are left with three massive gauge bosons ( $W^\pm, Z$ ) and one massless gauge boson

(the photon  $\gamma$ ). Being massless, the photon corresponds to some symmetry that is left unbroken. Weinberg suggested [13]

$$\langle 0 | \phi | 0 \rangle = \begin{bmatrix} 0 \\ \frac{\sqrt{2}m_0}{\sqrt{\lambda}} \end{bmatrix} \equiv \begin{bmatrix} 0 \\ \frac{v}{\sqrt{2}} \end{bmatrix} \quad (251)$$

This choice leaves the vacuum invariant to a transformation of  $U(1) +$  third component of  $SU(2)$ . That is,

$$(1 + \tau_3)\langle 0 | \phi | 0 \rangle = (1 + \tau_3) \begin{bmatrix} 0 \\ \frac{v}{\sqrt{2}} \end{bmatrix} = \begin{bmatrix} 2 & 0 \\ 0 & 0 \end{bmatrix} \begin{bmatrix} 0 \\ \frac{2}{\sqrt{2}} \end{bmatrix} = \begin{bmatrix} 0 \\ 0 \end{bmatrix} \quad (252)$$

where the  $\vec{\tau}$  are the Pauli matrices. This is also why we eventually find the electric charge to be expressed in terms of weak hypercharge  $Y$  and third component of isospin  $t_3$ :  $Q = \frac{Y}{2} + t_3$  [14]. We are about to see that this interplay between the  $U(1)$  symmetry (corresponding to  $Y$ ) and the third component of  $SU(2)$  symmetry (corresponding to  $t_3$ ) manifests as a mixing of the  $W_3^\mu$  and  $B^\mu$  gauge fields to yield the photon field  $A^\mu$  and the neutral weak vector boson  $Z$ .

To consider oscillations about the vacuum, parametrize the degrees of freedom by

$$\phi = e^{-\frac{i}{2v}\vec{\theta}(x) \cdot \vec{\tau}} \begin{bmatrix} 0 \\ \frac{1}{\sqrt{2}}(v + H(x)) \end{bmatrix} \quad (253)$$

However, recall that the three  $\vec{\theta}$  field perturbations, which would become Goldstone bosons, disappear if we make the appropriate gauge transformation. So we effectively use

$$\phi = \begin{bmatrix} 0 \\ \frac{1}{\sqrt{2}}(v + H(x)) \end{bmatrix} \quad (254)$$

The consequences for the lagrangian are (details of how the following form of the lagrangian are calculated are in section A.10)

$$\mathcal{L} = \frac{1}{2}(\partial_\mu H)(\partial^\mu H) + \frac{m_0^2}{2}(v + H)^2 - \frac{\lambda}{16}(v + H)^4 - \frac{1}{4}\vec{F}_{\mu\nu} \cdot \vec{F}^{\mu\nu} - \frac{1}{4}G_{\mu\nu}G^{\mu\nu} \quad (255)$$

$$\mathcal{L} = \frac{1}{2}(\partial_\mu H)(\partial^\mu H) + \frac{m_0^2}{2}(v + H)^2 - \frac{\lambda}{16}(v + H)^4 \quad (256)$$

$$- \frac{1}{4}(\partial_\mu W_{1\nu} - \partial_\nu W_{1\mu})(\partial^\mu W_1^\nu - \partial^\nu W_1^\mu) + \frac{1}{8}g^2v^2W_{1\nu}W_1^\nu \quad (257)$$

$$- \frac{1}{4}(\partial_\mu W_{2\nu} - \partial_\nu W_{2\mu})(\partial^\mu W_2^\nu - \partial^\nu W_2^\mu) + \frac{1}{8}g^2v^2W_{2\nu}W_2^\nu \quad (258)$$

$$- \frac{1}{4}(\partial_\mu W_{3\nu} - \partial_\nu W_{3\mu})(\partial^\mu W_3^\nu - \partial^\nu W_3^\mu) - \frac{1}{4}G_{\mu\nu}G^{\mu\nu} \quad (259)$$

$$+ \frac{1}{8}v^2(gW_{3\mu} - g'B_\mu)(gW_3^\mu - g'B^\mu) + \text{Higgs interactions} \quad (260)$$

The second and third lines show that the  $W_1$  and  $W_2$  gauge fields are massive and have the same mass  $m_W = \frac{gv}{2}$ . These are the  $W^+, W^-$  vector gauge bosons in electroweak theory. The Higgs interaction terms are being ignored here because we are focusing on the generation of the Standard Model gauge bosons in this section. In section A.10, I will go through the details of deriving the full version of this and discuss the interactions between the Higgs and gauge bosons that are produced. The Higgs boson decaying to gauge bosons is precisely the kind of interaction that this dissertation explores experimentally.

The last two lines show that the gauge fields  $W_3$  and  $B$  are mixed. The key clue is to notice in the last line it is the combination  $(gW_3^\mu - g'B^\mu)$  that has a mass. Introduce the linear combinations

$$Z^\mu \equiv W_3^\mu \cos \theta_W - B^\mu \sin \theta_W \quad (261)$$

$$A^\mu \equiv W_3^\mu \sin \theta_W + B^\mu \cos \theta_W \quad (262)$$

where

$$\cos \theta_W = \frac{g}{\sqrt{g^2 + g'^2}} \quad (263)$$

$$\sin \theta_W = \frac{g'}{\sqrt{g^2 + g'^2}} \quad (264)$$

Or, if we invert them

$$B^\mu = A^\mu \cos \theta_W - Z^\mu \sin \theta_W \quad (265)$$

$$W_3^\mu = A^\mu \sin \theta_W + Z^\mu \cos \theta_W \quad (266)$$

Using this, we can write the last two lines of the lagrangian in terms of  $A^\mu$  and  $Z^\mu$ ,

instead of  $B^\mu$  and  $W_3^\mu$ .

$$-\frac{1}{4}(\partial_\mu W_{3\nu} - \partial_\nu W_{3\mu})(\partial^\mu W_3^\nu - \partial^\nu W_3^\mu) - \frac{1}{4}G_{\mu\nu}G^{\mu\nu} + \frac{v^2}{8}(gW_{3\mu} - g'B_\mu)(gW_3^\mu - g'B^\mu) \quad (267)$$

$$= -\frac{1}{4}(\partial_\mu(Z_\nu \cos \theta_W + A_\nu \sin \theta_W) - \partial_\nu(Z_\mu \cos \theta_W + A_\mu \sin \theta_W)) \quad (268)$$

$$\cdot (\partial^\mu(Z^\nu \cos \theta_W + A^\nu \sin \theta_W) - \partial^\nu(Z^\mu \cos \theta_W + A^\mu \sin \theta_W)) \quad (269)$$

$$- \frac{1}{4}(\partial_\mu(A_\nu \cos \theta_W - Z_\nu \sin \theta_W) - \partial_\nu(A_\mu \cos \theta_W - Z_\mu \sin \theta_W)) \quad (270)$$

$$\cdot (\partial^\mu(A^\nu \cos \theta_W - Z^\nu \sin \theta_W) - \partial^\nu(A^\mu \cos \theta_W - Z^\mu \sin \theta_W)) \quad (271)$$

$$+ \frac{1}{8}v^2(g(Z_\mu \cos \theta_W + A_\mu \sin \theta_W) - g'(A_\mu \cos \theta_W - Z_\mu \sin \theta_W)) \quad (272)$$

$$\cdot (g(Z^\mu \cos \theta_W + A^\mu \sin \theta_W) - g'(A^\mu \cos \theta_W - Z^\mu \sin \theta_W)) \quad (273)$$

$$= -\frac{1}{4}((\partial_\mu Z_\nu - \partial_\nu Z_\mu) \cos \theta_W + (\partial_\mu A_\nu - \partial_\nu A_\mu) \sin \theta_W) \quad (274)$$

$$\cdot ((\partial^\mu Z^\nu - \partial^\nu Z^\mu) \cos \theta_W + (\partial^\mu A^\nu - \partial^\nu A^\mu) \sin \theta_W) \quad (275)$$

$$- \frac{1}{4}((\partial_\mu A_\nu - \partial_\nu A_\mu) \cos \theta_W - (\partial_\mu Z_\nu - \partial_\nu Z_\mu) \sin \theta_W) \quad (276)$$

$$\cdot ((\partial^\mu A^\nu - \partial^\nu A^\mu) \cos \theta_W - (\partial^\mu Z^\nu - \partial^\nu Z^\mu) \sin \theta_W) \quad (277)$$

$$+ \frac{1}{8}v^2(Z_\mu(g \cos \theta_W + g' \sin \theta_W) + A_\mu(g \sin \theta_W - g' \cos \theta_W)) \quad (278)$$

$$\cdot (Z^\mu(g \cos \theta_W + g' \sin \theta_W) + A^\mu(g \sin \theta_W - g' \cos \theta_W)) \quad (279)$$

Define  $\mathcal{F}_{\mu\nu} \equiv \partial_\mu A_\nu - \partial_\nu A_\mu$  and  $Z_{\mu\nu} \equiv \partial_\mu Z_\nu - \partial_\nu Z_\mu$ .

$$= -\frac{1}{4}(Z_{\mu\nu} \cos \theta_W + \mathcal{F}_{\mu\nu} \sin \theta_W)(Z^{\mu\nu} \cos \theta_W + \mathcal{F}^{\mu\nu} \sin \theta_W) \quad (280)$$

$$- \frac{1}{4}(\mathcal{F}_{\mu\nu} \cos \theta_W - Z_{\mu\nu} \sin \theta_W)(\mathcal{F}^{\mu\nu} \cos \theta_W - Z^{\mu\nu} \sin \theta_W) \quad (281)$$

$$\frac{1}{8}v^2 \left( Z_\mu \frac{g^2 + g'^2}{\sqrt{g^2 + g'^2}} + A_\mu \frac{gg' - g'g}{\sqrt{g^2 + g'^2}} \right) \cdot \left( Z^\mu \frac{g^2 + g'^2}{\sqrt{g^2 + g'^2}} + A^\mu \frac{gg' - g'g}{\sqrt{g^2 + g'^2}} \right) \quad (282)$$

$$= -\frac{1}{4}(Z_{\mu\nu}Z^{\mu\nu} + \mathcal{F}_{\mu\nu}\mathcal{F}^{\mu\nu}) + \frac{1}{8}v^2Z_\mu Z^\mu(g^2 + g'^2) \quad (283)$$

Hence, we have unmixed the two fields. They become the  $Z$  boson and the photon.

$$m_Z = \frac{1}{2}v^2\sqrt{g^2 + g'^2} = \frac{m_W}{\cos \theta_W} \quad (284)$$

$$m_A = 0 \quad (285)$$

Now that we have our lagrangian in a usable form, we can finally start calculating the characteristics of Standard Model particles.

## A.8 The $SU(2)_L \times U(1)_Y$ Local Gauge Invariant Lagrangian and the [massless] Fermions

We know now from section A.7 what our postulated lagrangian should look like in order to be both  $U(1)$  and  $SU(2)$  invariant, which necessarily involved the weak vector bosons and the photon. Let's look at  $SU(2) \times U(1)$  gauge invariance for the first generation of quarks; the calculation is identical for the higher generations. The calculation for the lepton generations is also very similar and so not repeated in this dissertation.

The Higgs mechanism is *not* included here so the quarks will still be massless; that will be dealt with in section A.9. Instead, we will deal with fermions that appear as a left-handed doublet and right-handed singlets for both particles. In the end, we will have computed the lagrangian that tells us how these fermions interact with each other, the weak vector gauge bosons, and the photon. The mass terms will, in the absence of the Higgs mechanism, be also absent for this section.

Suppose we have the (fermion) quark doublet

$$q = \begin{bmatrix} u \\ d \end{bmatrix} \quad (286)$$

and recall that

$$\psi_L = \left( \frac{1 - \gamma_5}{2} \right) \psi \quad (287)$$

$$\psi_R = \left( \frac{1 + \gamma_5}{2} \right) \psi \quad (288)$$

are relations distinguishing the left and right handed components.

As always, we must postulate a lagrangian. In the sections exploring  $U(1)$  and  $SU(2)$  symmetries, we used generalizations of the Klein-Gordon equation's lagrangian for scalar particles. Now we want to look at spin-1/2 fermions, so we must use the Dirac lagrangian in our gauge invariant form. This is why I want to explore the case of massless fermions before adding in mass generation from the Higgs mechanism.[14]

Recall the Dirac lagrangian

$$\mathcal{L} = i\bar{\psi}\gamma_\mu\partial^\mu\psi - m\bar{\psi}\psi \quad (289)$$

Now we want a massless version for a fermion doublet:

$$\mathcal{L} = \bar{q}i\mathcal{D}q \quad (290)$$

$$\mathcal{L} = \bar{q}_L i\mathcal{D}_L q_L + \bar{u}_R i\mathcal{D}_R u_R + \bar{d}_R i\mathcal{D}_R d_R \quad (291)$$

where the covariant derivative for the doublet  $\mathcal{D}_L$  is  $SU(2) \times U(1)$  invariant, and  $\mathcal{D}_R$  is

only  $U(1)$  invariant for the singlet:

$$D_L^\rho = \partial^\rho + \frac{ig}{2} \vec{\tau} \cdot \vec{W}^\rho + \frac{ig'Y}{2} B^\rho \quad (292)$$

$$D_R^\rho = \partial^\rho + \frac{ig'Y}{2} B^\rho \quad (293)$$

### A.8.1 The $\mathcal{L}_R$ terms

$$\mathcal{L}_R = \bar{u}_R i \not{D} u_R + \bar{d}_R i \not{D} d_R \quad (294)$$

$$= \bar{u}_R i \gamma_\rho \left( \partial^\rho - \frac{ig'Y}{2} B^\rho \right) u_R + \bar{d}_R i \gamma_\rho \left( \partial^\rho - \frac{ig'Y}{2} B^\rho \right) d_R \quad (295)$$

$$= i \bar{u}_R \gamma_\rho (\partial^\rho u_R) - \frac{g'Y}{2} \bar{u}_R \gamma_\rho B^\rho u_R + i \bar{d}_R \gamma_\rho (\partial^\rho d_R) - \frac{g'Y}{2} \bar{d}_R \gamma_\rho B^\rho d_R \quad (296)$$

$$= i u_R^\dagger \gamma_0 \gamma_\rho (\partial^\rho u_R) - \frac{g'Y}{2} u_R^\dagger \gamma_0 \gamma_\rho B^\rho u_R + i d_R^\dagger \gamma_0 \gamma_\rho (\partial^\rho d_R) - \frac{g'Y}{2} d_R^\dagger \gamma_0 \gamma_\rho B^\rho d_R \quad (297)$$

$$= i u^\dagger \left( \frac{1+\gamma_5}{2} \right) \gamma_0 \gamma_\rho \left( \frac{1+\gamma_5}{2} \right) (\partial^\rho u) - \frac{g'Y}{2} u^\dagger \left( \frac{1+\gamma_5}{2} \right) \gamma_0 \gamma_\rho B^\rho \left( \frac{1+\gamma_5}{2} \right) u \quad (298)$$

$$+ i d^\dagger \left( \frac{1+\gamma_5}{2} \right) \gamma_0 \gamma_\rho \left( \frac{1+\gamma_5}{2} \right) (\partial^\rho d) - \frac{g'Y}{2} d^\dagger \left( \frac{1+\gamma_5}{2} \right) \gamma_0 \gamma_\rho B^\rho \left( \frac{1+\gamma_5}{2} \right) d \quad (299)$$

$$(300)$$

Use the fact that  $\gamma_5$  anticommutes with the other  $\gamma_\mu$ 's, so  $\{\gamma_5, \gamma_\mu\} = 0 \Rightarrow \left(\frac{1+\gamma_5}{2}\right) \gamma_\mu = \left(\frac{\gamma_\mu + \gamma_5 \gamma_\mu}{2}\right) = \left(\frac{\gamma_\mu + (-\gamma_\mu \gamma_5)}{2}\right) = \gamma_\mu \left(\frac{1-\gamma_5}{2}\right)$ . Also, note that after  $\left(\frac{1+\gamma_5}{2}\right)$  commutes past  $\gamma_0 \gamma_\rho$ ,  $\left(\frac{1+\gamma_5}{2}\right) \left(\frac{1+\gamma_5}{2}\right) = \left(\frac{1+\gamma_5}{2}\right)$ .

$$\Rightarrow \mathcal{L}_R = i \bar{u} \gamma_\rho \left( \frac{1+\gamma_5}{2} \right) (\partial^\rho u) - \frac{g'Y}{2} \bar{u} \gamma_\rho B^\rho \left( \frac{1+\gamma_5}{2} \right) u \quad (301)$$

$$+ i \bar{d} \gamma_\rho \left( \frac{1+\gamma_5}{2} \right) (\partial^\rho d) - \frac{g'Y}{2} \bar{d} \gamma_\rho B^\rho \left( \frac{1+\gamma_5}{2} \right) d \quad (302)$$

We will return to these terms later.

### A.8.2 The $\mathcal{L}_L$ terms

$$\mathcal{L}_L = \bar{q}_L i \not{D} q_L \quad (303)$$

As before, note that  $\bar{u}_L = u^\dagger \left( \frac{1-\gamma_5}{2} \right) \gamma_0$  and also that

$$\bar{q}_L = \overline{\begin{bmatrix} u_L \\ d_L \end{bmatrix}} = [\bar{u}_L \quad \bar{d}_L] \quad (304)$$

$$\mathcal{L}_L = [\bar{u}_L \quad \bar{d}_L] i\gamma_\rho D^\rho \begin{bmatrix} u_L \\ d_L \end{bmatrix} \quad (305)$$

$$= [\bar{u}_L \quad \bar{d}_L] i\gamma_\rho \left( \partial^\rho + \frac{ig}{2} \vec{\tau} \cdot \vec{W}^\rho + \frac{ig'Y}{2} B^\rho \right) \begin{bmatrix} u_L \\ d_L \end{bmatrix} \quad (306)$$

$$= \underbrace{i [\bar{u}_L \quad \bar{d}_L] \gamma_\rho \partial^\rho \begin{bmatrix} u_L \\ d_L \end{bmatrix}}_{\text{II.A}} - \underbrace{\frac{g}{2} [\bar{u}_L \quad \bar{d}_L] \gamma_\rho \vec{\tau} \cdot \vec{W}^\rho \begin{bmatrix} u_L \\ d_L \end{bmatrix}}_{\text{II.B}} - \underbrace{\frac{g'Y}{2} \gamma_\rho B^\rho \begin{bmatrix} u_L \\ d_L \end{bmatrix}}_{\text{II.C}} \quad (307)$$

### II.A The Derivative Terms

$$i [\bar{u}_L \quad \bar{d}_L] \gamma_\rho \partial^\rho \begin{bmatrix} u_L \\ d_L \end{bmatrix} = i [\bar{u}_L \quad \bar{d}_L] \begin{bmatrix} \partial u_L \\ \partial d_L \end{bmatrix} \quad (308)$$

$$= i\bar{u}_L \partial u_L + i\bar{d}_L \partial d_L \quad (309)$$

$$= iu^\dagger \left( \frac{1 - \gamma_5}{2} \right) \gamma_0 \gamma_\rho \left( \frac{1 - \gamma_5}{2} \right) (\partial^\rho u) + id^\dagger \left( \frac{1 - \gamma_5}{2} \right) \gamma_0 \gamma_\rho \left( \frac{1 - \gamma_5}{2} \right) (\partial^\rho d) \quad (310)$$

$$= iu^\dagger \gamma_0 \left( \frac{1 + \gamma_5}{2} \right) \gamma_\rho \left( \frac{1 - \gamma_5}{2} \right) (\partial^\rho u) + id^\dagger \gamma_0 \left( \frac{1 + \gamma_5}{2} \right) \gamma_\rho \left( \frac{1 - \gamma_5}{2} \right) (\partial^\rho d) \quad (311)$$

$$= iu^\dagger \gamma_0 \gamma_\rho \left( \frac{1 - \gamma_5}{2} \right)^2 (\partial^\rho u) + id^\dagger \gamma_0 \gamma_\rho \left( \frac{1 - \gamma_5}{2} \right)^2 (\partial^\rho d) \quad (312)$$

$$= iu^\dagger \gamma_0 \gamma_\rho \left( \frac{1 - \gamma_5}{2} \right) (\partial^\rho u) + id^\dagger \gamma_0 \gamma_\rho \left( \frac{1 - \gamma_5}{2} \right) (\partial^\rho d) \quad (313)$$

$$= i\bar{u} \gamma_\rho \left( \frac{1 - \gamma_5}{2} \right) (\partial^\rho u) + i\bar{d} \gamma_\rho \left( \frac{1 - \gamma_5}{2} \right) (\partial^\rho d) \quad (314)$$

### II.B The $W, W^\dagger, W_3$ Terms

The key here is to express

$$\frac{1}{2} \vec{\tau} \cdot \vec{W}^\mu = \frac{1}{2} [\tau_1 W_1^\mu + \tau_2 W_2^\mu + \tau_3 W_3^\mu] \quad (315)$$

$$= \frac{1}{\sqrt{2}} \left[ \tau_+ \left( \frac{W_1^\mu - iW_2^\mu}{\sqrt{2}} \right) \tau_- \left( \frac{W_1^\mu + iW_2^\mu}{\sqrt{2}} \right) \right] + \frac{1}{2} \tau_3 W_3^\mu \quad (316)$$

$$= \frac{1}{\sqrt{2}} [\tau_+ W^\mu + \tau_- W_\mu^\dagger] + \frac{1}{2} \tau_3 W_3^\mu \quad (317)$$

Where we denote

$$\tau_+ \equiv \frac{1}{2}(\tau_1 + i\tau_2) = \frac{1}{2} \begin{bmatrix} 0 & 1 \\ 1 & 0 \end{bmatrix} + i \begin{bmatrix} 0 & -i \\ i & 0 \end{bmatrix} = \frac{1}{2} \begin{bmatrix} 0 & 2 \\ 0 & 0 \end{bmatrix} = \begin{bmatrix} 0 & 1 \\ 0 & 0 \end{bmatrix} \quad (318)$$

$$\tau_- \equiv \frac{1}{2}(\tau_1 - i\tau_2) = \frac{1}{2} \begin{bmatrix} 0 & 1 \\ 1 & 0 \end{bmatrix} - i \begin{bmatrix} 0 & -i \\ i & 0 \end{bmatrix} = \frac{1}{2} \begin{bmatrix} 0 & 0 \\ 2 & 0 \end{bmatrix} = \begin{bmatrix} 0 & 0 \\ 1 & 0 \end{bmatrix} \quad (319)$$

$$W^\mu \equiv \frac{W_1^\mu - iW_2^\mu}{\sqrt{2}} \quad (320)$$

$$W^{\mu\dagger} \equiv \frac{W_1^\mu + iW_2^\mu}{\sqrt{2}} \quad (321)$$

The reason we want to do this is for the following:

$$\frac{1}{\sqrt{2}}\tau_+ W^\mu \begin{bmatrix} u_L \\ d_L \end{bmatrix} = \frac{1}{\sqrt{2}} \begin{bmatrix} 0 & W^\mu \\ 0 & 0 \end{bmatrix} \begin{bmatrix} u_L \\ d_L \end{bmatrix} = \frac{1}{\sqrt{2}} \begin{bmatrix} W^\mu d_L \\ 0 \end{bmatrix} = \frac{W^\mu}{\sqrt{2}} \begin{bmatrix} d_L \\ 0 \end{bmatrix} \quad (322)$$

$$\frac{1}{\sqrt{2}}\tau_+ W^{\mu\dagger} \begin{bmatrix} u_L \\ d_L \end{bmatrix} = \frac{1}{\sqrt{2}} \begin{bmatrix} 0 & 0 \\ W^{\mu\dagger} & 0 \end{bmatrix} \begin{bmatrix} u_L \\ d_L \end{bmatrix} = \frac{1}{\sqrt{2}} \begin{bmatrix} 0 \\ W^{\mu\dagger} u_L \end{bmatrix} = \frac{W^{\mu\dagger}}{\sqrt{2}} \begin{bmatrix} 0 \\ u_L \end{bmatrix} \quad (323)$$

Notice how the  $u_L$  and  $d_L$  fields switch positions in the vector. This is what will subsequently allow interactions between these fields via the gauge bosons  $W^\mu$ .

Lastly,

$$\frac{1}{2}\tau_3 W_3^\mu \begin{bmatrix} u_L \\ d_L \end{bmatrix} = \frac{1}{2} \begin{bmatrix} 1 & 0 \\ 0 & -1 \end{bmatrix} \begin{bmatrix} W_3^\mu u_L \\ W_3^\mu d_L \end{bmatrix} = \frac{1}{2} \begin{bmatrix} W_3^\mu u_L \\ -W_3^\mu d_L \end{bmatrix} = \frac{W_3^\mu}{2} \begin{bmatrix} u_L \\ -d_L \end{bmatrix} \quad (324)$$

Now we are ready to return to the term II.B from the lagrangian.

$$\frac{g}{2} [\bar{u}_L \quad \bar{d}_L] \gamma_\rho \vec{W}^\rho \begin{bmatrix} u_L \\ d_L \end{bmatrix} \quad (325)$$

$$= g [\bar{u}_L \quad \bar{d}_L] \gamma_\rho \left( \frac{1}{2}\tau_+(W_1^\rho - iW_2^\rho) + \frac{1}{2}\tau_-(W_1^\rho + iW_2^\rho) + \frac{1}{2}\tau_3 W_3^\rho \right) \begin{bmatrix} u_L \\ d_L \end{bmatrix} \quad (326)$$

$$= g [\bar{u}_L \quad \bar{d}_L] \gamma_\rho \left( \frac{1}{\sqrt{2}}\tau_+ W^\rho + \frac{1}{\sqrt{2}}\tau_- W^{\rho\dagger} + \frac{1}{2}\tau_3 W_3^\rho \right) \begin{bmatrix} u_L \\ d_L \end{bmatrix} \quad (327)$$

$$= g [\bar{u}_L \quad \bar{d}_L] \gamma_\rho \left( \frac{1}{\sqrt{2}}W^\rho \begin{bmatrix} d_L \\ 0 \end{bmatrix} + \frac{1}{\sqrt{2}}W^{\rho\dagger} \begin{bmatrix} 0 \\ u_L \end{bmatrix} + \frac{1}{2}W_3^\rho \begin{bmatrix} u_L \\ -d_L \end{bmatrix} \right) \quad (328)$$

$$= \frac{1}{\sqrt{2}}g [\bar{u}_L \quad \bar{d}_L] \begin{bmatrix} W^\rho d_L \\ 0 \end{bmatrix} \frac{1}{\sqrt{2}}g [\bar{u}_L \quad \bar{d}_L] \begin{bmatrix} 0 \\ W^{\rho\dagger} u_L \end{bmatrix} \frac{1}{2}g [\bar{u}_L \quad \bar{d}_L] \begin{bmatrix} W_3^\rho u_L \\ -W_3^\rho d_L \end{bmatrix} \quad (329)$$

$$= \frac{1}{\sqrt{2}}g\bar{u}_L W^\rho d_L + \frac{1}{\sqrt{2}}g\bar{d}_L W^{\rho\dagger} u_L + \frac{1}{2}g\bar{u}_L W_3^\rho u_L + \frac{1}{2}g\bar{d}_L (-W_3^\rho d_L) \quad (330)$$

$$= \frac{1}{\sqrt{2}}g\bar{u}_L W^\rho d_L + \frac{1}{\sqrt{2}}g\bar{d}_L W^{\rho\dagger} u_L + \frac{1}{2}g\bar{u}_L W_3^\rho u_L + \frac{1}{2}g\bar{d}_L (-W_3^\rho d_L) \quad (331)$$

$$\frac{g}{2} [\bar{u}_L \quad \bar{d}_L] \gamma_\rho \vec{\tau} \cdot \vec{W}^\rho \begin{bmatrix} u_L \\ d_L \end{bmatrix} \quad (332)$$

$$= \frac{1}{\sqrt{2}} g u_L^\dagger \gamma_0 \gamma_\rho W^\rho d_L + \frac{1}{\sqrt{2}} g d_L^\dagger \gamma_0 \gamma_\rho W^{\rho\dagger} u_L + \frac{1}{2} g u_L^\dagger \gamma_0 \gamma_\rho W_3^\rho u_L - \frac{1}{2} g d_L^\dagger \gamma_0 \gamma_\rho W_3^\rho d_L \quad (333)$$

$$= \frac{1}{\sqrt{2}} g u^\dagger \left( \frac{1 - \gamma_5}{2} \right) \gamma_0 \gamma_\rho W^\rho \left( \frac{1 - \gamma_5}{2} \right) d + \frac{1}{\sqrt{2}} g d^\dagger \left( \frac{1 - \gamma_5}{2} \right) \gamma_0 \gamma_\rho W^{\rho\dagger} \left( \frac{1 - \gamma_5}{2} \right) u \quad (334)$$

$$+ \frac{1}{2} g u^\dagger \left( \frac{1 - \gamma_5}{2} \right) \gamma_0 \gamma_\rho W_3^\rho \left( \frac{1 - \gamma_5}{2} \right) u - \frac{1}{2} g d^\dagger \left( \frac{1 - \gamma_5}{2} \right) \gamma_0 \gamma_\rho W_3^\rho \left( \frac{1 - \gamma_5}{2} \right) d \quad (335)$$

$$= \frac{1}{\sqrt{2}} g \bar{u} \gamma_\rho W^\rho \left( \frac{1 - \gamma_5}{2} \right) d + \frac{1}{\sqrt{2}} g \bar{d} \gamma_\rho W^{\rho\dagger} \left( \frac{1 - \gamma_5}{2} \right) u \quad (336)$$

$$+ \frac{1}{2} g \bar{u} \gamma_\rho W_3^\rho \left( \frac{1 - \gamma_5}{2} \right) u - \frac{1}{2} g \bar{d} \gamma_\rho W_3^\rho \left( \frac{1 - \gamma_5}{2} \right) d \quad (337)$$

It is important to note that while these terms do describe quark interactions, the vertex factors here are not in their final Standard Model form. There are still the CKM matrix elements that govern the strength of the interactions to deal with. The proper form with the CKM matrix elements follows directly from the presence of the Higgs field and is therefore excluded from this section. That problem requires separate treatment.

### II.C The $B^\rho$ Field Terms

$$[\bar{u}_L \quad \bar{d}_L] \frac{g' Y}{2} \gamma_\rho B^\rho \begin{bmatrix} u_L \\ d_L \end{bmatrix} \quad (338)$$

$$= \frac{g' Y}{2} [\bar{u}_L \quad \bar{d}_L] \begin{bmatrix} \not{B} u_L \\ \not{B} d_L \end{bmatrix} \quad (339)$$

$$= \frac{g' Y}{2} [\bar{u}_L \not{B} u_L + \bar{d}_L \not{B} d_L] \quad (340)$$

$$= \frac{g' Y}{2} [u_L^\dagger \gamma_0 \gamma_\rho B^\rho u_L + d_L^\dagger \gamma_0 \gamma_\rho B^\rho d_L] \quad (341)$$

$$= \frac{g' Y}{2} \left[ u^\dagger \left( \frac{1 - \gamma_5}{2} \right) \gamma_0 \gamma_\rho B^\rho \left( \frac{1 - \gamma_5}{2} \right) u + d^\dagger \left( \frac{1 - \gamma_5}{2} \right) \gamma_0 \gamma_\rho B^\rho \left( \frac{1 - \gamma_5}{2} \right) d \right] \quad (342)$$

$$= \frac{g' Y}{2} \left[ \bar{u} \gamma_\rho \left( \frac{1 - \gamma_5}{2} \right) B^\rho u + \bar{d} \gamma_\rho \left( \frac{1 - \gamma_5}{2} \right) B^\rho d \right] \quad (343)$$

#### A.8.3 Find the $Z$ -boson and Photon Interactions

The next task is to mix these terms with the  $W_3^\mu$  terms from before to yield the photon and  $Z$ -boson interactions with the quarks. Note that the work of mixing these fields into

$A^\mu$  and  $Z^\mu$  was done in A.7. So we are going to collect the  $B^\rho$  and  $W_3^\rho$  terms from II.A, II.B, and II.C, then switch to expressing those terms with  $A^\mu$  and  $Z^\mu$  instead. This will yield quark interactions with the photon and  $Z$ -boson. Afterward, we will collect all the terms of the lagrangian and express it in a manner that elucidates the electroweak physics of quarks.

$$-\frac{g'Y}{2}\bar{u}\gamma_\rho B^\rho \left(\frac{1+\gamma_5}{2}\right)u - \frac{g'Y}{2}\bar{d}\gamma_\rho B^\rho \left(\frac{1+\gamma_5}{2}\right)d \quad (344)$$

$$-\frac{1}{2}g\bar{u}\gamma_\rho W_3^\rho \left(\frac{1-\gamma_5}{2}\right)u + \frac{1}{2}g\bar{d}\gamma_\rho W_3^\rho \left(\frac{1-\gamma_5}{2}\right)d \quad (345)$$

$$-\frac{g'Y}{2}\bar{u}\gamma_\rho \left(\frac{1-\gamma_5}{2}\right)B^\rho u - \frac{g'Y}{2}\bar{d}\gamma_\rho \left(\frac{1-\gamma_5}{2}\right)B^\rho d \quad (346)$$

$$= -\frac{g'Y}{2}\bar{u}\gamma_\rho \left(\frac{1+\gamma_5}{2}\right)u(-Z^\rho \sin \theta_W + A^\rho \cos \theta_W) \quad (347)$$

$$- \frac{g'Y}{2}\bar{d}\gamma_\rho \left(\frac{1+\gamma_5}{2}\right)d(-Z^\rho \sin \theta_W + A^\rho \cos \theta_W) \quad (348)$$

$$- \frac{g}{2}\bar{u}\gamma_\rho \left(\frac{1-\gamma_5}{2}\right)u(Z^\rho \cos \theta_W + A^\rho \sin \theta_W) \quad (349)$$

$$+ \frac{g}{2}\bar{d}\gamma_\rho \left(\frac{1-\gamma_5}{2}\right)d(Z^\rho \cos \theta_W + A^\rho \sin \theta_W) \quad (350)$$

$$- \frac{g'Y}{2}\bar{u}\gamma_\rho \left(\frac{1-\gamma_5}{2}\right)u(-Z^\rho \sin \theta_W + A^\rho \cos \theta_W) \quad (351)$$

$$- \frac{g'Y}{2}\bar{d}\gamma_\rho \left(\frac{1-\gamma_5}{2}\right)d(-Z^\rho \sin \theta_W + A^\rho \cos \theta_W) \quad (352)$$

Use  $Y = 1/3$  for  $u_L$ ;  $Y = 4/3$  for  $u_R$ ;  $Y = 1/3$  for  $d_L$ ; and  $Y = -2/3$  for  $d_R$  [13].

$$= -\frac{2g'}{3}\bar{u}\gamma_\rho\left(\frac{1+\gamma_5}{2}\right)u(-Z^\rho \sin \theta_W + A^\rho \cos \theta_W) \quad (353)$$

$$+ \frac{g'}{3}\bar{d}\gamma_\rho\left(\frac{1+\gamma_5}{2}\right)d(-Z^\rho \sin \theta_W + A^\rho \cos \theta_W) \quad (354)$$

$$- \frac{g}{2}\bar{u}\gamma_\rho\left(\frac{1-\gamma_5}{2}\right)u(Z^\rho \cos \theta_W + A^\rho \sin \theta_W) \quad (355)$$

$$+ \frac{g}{2}\bar{d}\gamma_\rho\left(\frac{1-\gamma_5}{2}\right)d(Z^\rho \cos \theta_W + A^\rho \sin \theta_W) \quad (356)$$

$$- \frac{g'}{6}\bar{u}\gamma_\rho\left(\frac{1-\gamma_5}{2}\right)u(-Z^\rho \sin \theta_W + A^\rho \cos \theta_W) \quad (357)$$

$$- \frac{g'}{6}\bar{d}\gamma_\rho\left(\frac{1-\gamma_5}{2}\right)d(-Z^\rho \sin \theta_W + A^\rho \cos \theta_W) \quad (358)$$

$$= \frac{2g'}{3}\bar{u}\gamma_\rho\left(\frac{1+\gamma_5}{2}\right)u(Z^\rho \sin \theta_W) - \frac{2g'}{3}\bar{u}\gamma_\rho\left(\frac{1+\gamma_5}{2}\right)u(A^\rho \cos \theta_W) \quad (359)$$

$$- \frac{g'}{3}\bar{d}\gamma_\rho\left(\frac{1+\gamma_5}{2}\right)d(Z^\rho \sin \theta_W) + \frac{g'}{3}\bar{d}\gamma_\rho\left(\frac{1+\gamma_5}{2}\right)d(A^\rho \cos \theta_W) \quad (360)$$

$$+ \bar{u}\gamma_\rho\left(\frac{1-\gamma_5}{2}\right)uZ^\rho\left(-\frac{1}{2}g \cos \theta_W + \frac{1}{6}g' \sin \theta_W\right) \quad (361)$$

$$+ \bar{u}\gamma_\rho\left(\frac{1-\gamma_5}{2}\right)uA^\rho\left(-\frac{1}{2}g \sin \theta_W - \frac{1}{6}g' \cos \theta_W\right) \quad (362)$$

$$+ \bar{d}\gamma_\rho\left(\frac{1-\gamma_5}{2}\right)dZ^\rho\left(\frac{1}{2}g \cos \theta_W + \frac{1}{6}g' \sin \theta_W\right) \quad (363)$$

$$+ \bar{d}\gamma_\rho\left(\frac{1-\gamma_5}{2}\right)dA^\rho\left(\frac{1}{2}g \sin \theta_W - \frac{1}{6}g' \cos \theta_W\right) \quad (364)$$

$$(365)$$

Now use  $g' = g \frac{\sin \theta_W}{\cos \theta_W}$  in all terms.

$$= \frac{2}{3} \bar{u} \gamma_\rho \left( \frac{1 + \gamma_5}{2} \right) u Z^\rho \left( g \frac{\sin \theta_W}{\cos \theta_W} \sin \theta_W \right) \quad (366)$$

$$- \frac{2}{3} \bar{u} \gamma_\rho \left( \frac{1 + \gamma_5}{2} \right) u A^\rho (g \sin \theta_W) \quad (367)$$

$$- \frac{1}{3} \bar{d} \gamma_\rho \left( \frac{1 + \gamma_5}{2} \right) d Z^\rho \left( g \frac{\sin \theta_W}{\cos \theta_W} \sin \theta_W \right) \quad (368)$$

$$+ \frac{1}{3} \bar{d} \gamma_\rho \left( \frac{1 + \gamma_5}{2} \right) d A^\rho g \sin \theta_W \quad (369)$$

$$\bar{u} \gamma_\rho \left( \frac{1 - \gamma_5}{2} \right) u Z^\rho \left( -\frac{1}{2} g \cos \theta_W + \frac{1}{6} g \frac{\sin \theta_W}{\cos \theta_W} \sin \theta_W \right) \quad (370)$$

$$\bar{u} \gamma_\rho \left( \frac{1 - \gamma_5}{2} \right) u A^\rho \left( -\frac{1}{2} g \sin \theta_W - \frac{1}{6} g \sin \theta_W \right) \quad (371)$$

$$\bar{d} \gamma_\rho \left( \frac{1 - \gamma_5}{2} \right) u Z^\rho \left( \frac{1}{2} g \cos \theta_W + \frac{1}{6} g \frac{\sin \theta_W}{\cos \theta_W} \sin \theta_W \right) \quad (372)$$

$$\bar{d} \gamma_\rho \left( \frac{1 - \gamma_5}{2} \right) d A^\rho \left( \frac{1}{2} g \sin \theta_W - \frac{1}{6} g \sin \theta_W \right) \quad (373)$$

$$(374)$$

$$= \frac{2g}{3} \bar{u} \gamma_\rho \left( \frac{1 + \gamma_5}{2} \right) u Z^\rho \left( \frac{\sin^2 \theta_W}{\cos \theta_W} \right) - \frac{2g}{3} \bar{u} \gamma_\rho \left( \frac{1 + \gamma_5}{2} \right) u A^\rho \sin \theta_W \quad (375)$$

$$- \frac{g}{3} \bar{d} \gamma_\rho \left( \frac{1 + \gamma_5}{2} \right) d Z^\rho \left( \frac{\sin^2 \theta_W}{\cos \theta_W} \right) + \frac{g}{3} \bar{d} \gamma_\rho \left( \frac{1 + \gamma_5}{2} \right) d A^\rho \sin \theta_W \quad (376)$$

$$+ \frac{g}{2 \cos \theta_W} \bar{u} \gamma_\rho \left( \frac{1 - \gamma_5}{2} \right) u Z^\rho \left( -\cos^2 \theta_W + \frac{1}{3} \sin^2 \theta_W \right) \quad (377)$$

$$- \frac{2g}{3} \bar{u} \gamma_\rho \left( \frac{1 - \gamma_5}{2} \right) u A^\rho \sin \theta_W \quad (378)$$

$$+ \frac{g}{2 \cos \theta_W} \bar{d} \gamma_\rho \left( \frac{1 - \gamma_5}{2} \right) d Z^\rho \left( \cos^2 \theta_W + \frac{1}{3} \sin^2 \theta_W \right) \quad (379)$$

$$+ \frac{g}{3} \bar{d} \gamma_\rho \left( \frac{1 - \gamma_5}{2} \right) d A^\rho \sin \theta_W \quad (380)$$

Use these trigonometric relations,

$$-\cos^2 \theta_W + \frac{1}{3} \sin^2 \theta_W = -1 + \frac{4}{3} \sin^2 \theta_W \quad (381)$$

$$\cos^2 \theta_W + \frac{1}{3} \sin^2 \theta_W = 1 - \frac{2}{3} \sin^2 \theta_W \quad (382)$$

$$\left( \frac{1 - \gamma_5}{2} \right) + \left( \frac{1 + \gamma_5}{2} \right) = 1 \quad (383)$$

and the electric charge defined as  $e_0 = g \sin \theta_W$  in recollecting all the terms of the lagrangian, which now has the form:

$$\mathcal{L} = i\bar{u}\gamma_\rho \left( \frac{1 + \gamma_5}{2} \right) (\partial^\rho u) + i\bar{d}\gamma_\rho \left( \frac{1 + \gamma_5}{2} \right) (\partial^\rho d) + i\bar{u}\gamma_\rho \left( \frac{1 - \gamma_5}{2} \right) (\partial^\rho u) + i\bar{d}\gamma_\rho \left( \frac{1 - \gamma_5}{2} \right) (\partial^\rho d) \quad (384)$$

$$+ \frac{1}{\sqrt{2}} g\bar{u}\gamma_\rho W^\rho \left( \frac{1 - \gamma_5}{2} \right) d + \frac{1}{\sqrt{2}} g\bar{d}\gamma_\rho W^{\rho\dagger} \left( \frac{1 - \gamma_5}{2} \right) u \quad (385)$$

$$+ \frac{g}{2 \cos \theta_W} Z^\rho \left[ \bar{u}\gamma_\rho \left( \frac{1 + \gamma_5}{2} \right) u \left( \frac{4}{3} \sin^2 \theta_W \right) - \bar{d}\gamma_\rho \left( \frac{1 + \gamma_5}{2} \right) d \left( \frac{2}{3} \sin^2 \theta_W \right) \right] \quad (386)$$

$$+ \bar{u}\gamma_\rho \left( \frac{1 - \gamma_5}{2} \right) u \left( -1 + \frac{4}{3} \sin^2 \theta_W \right) - \bar{d}\gamma_\rho \left( \frac{1 - \gamma_5}{2} \right) d \left( -1 + \frac{2}{3} \sin^2 \theta_W \right) \right] \quad (387)$$

$$- \frac{2e_0}{3} \bar{u}\gamma_\rho u A^\rho + \frac{e_0}{3} \bar{d}\gamma_\rho d A^\rho \quad (388)$$

$$(389)$$

## A.9 The Higgs Mechanism and Fermion Mass Generation

Recall from section A.8 that the kinetic part of a free Dirac fermion does not mix the left and right components of the field:

$$\bar{\psi} \gamma_\mu \partial^\mu \psi = \bar{\psi}_R \gamma_\mu \partial^\mu \psi_R + \bar{\psi}_L \gamma_\mu \partial^\mu \psi_L \quad (390)$$

Because of this, we can gauge the left and right handed components differently. Weak interactions are parity violating in the Standard Model and the  $SU(2)_L$  covariant derivative acts only on the left-handed term. However, a Dirac mass term has the form

$$-m (\bar{\psi}_L \psi_R + \bar{\psi}_R \psi_L) \quad (391)$$

when we write the left and right handed components separately. So the components are coupled, meaning any such mass term breaks  $SU(2)_L$  gauge invariance.

In a theory with spontaneous symmetry breaking, there is a way of giving mass to fermions without explicitly introducing gauge invariance breaking mass terms in the lagrangian. Consider the electron  $SU(2)_L$  doublet

$$l = \begin{bmatrix} \nu \\ e \end{bmatrix}_L \quad (392)$$

the Higgs doublet

$$\phi = \begin{bmatrix} \phi^+ \\ \phi^0 \end{bmatrix} \quad (393)$$

$$\phi^+ = \frac{1}{\sqrt{2}}(\phi_1 - i\phi_2) \quad (394)$$

$$\phi^0 = \frac{1}{\sqrt{2}}(\phi_3 - i\phi_4) \quad (395)$$

and the right handed electron singlet in a Yukawa model.

$$\mathcal{L}_e = -g_e \bar{l}_L \phi e_R - g_e \bar{e}_R \phi^\dagger l_L \quad (396)$$

It is important to notice that the structure of these terms has two  $SU(2)_L$  doublets multiplied to form an  $SU(2)_L$  scalar ( $\bar{l}_L \phi, \phi^\dagger l$ ), and that scalar multiplies the  $SU(2)_L$  scalar R-component. So this lagrangian is  $SU(2)_L$  invariant and the symmetry is preserved.[13]

Recall from section A.7 that the vacuum expectation value of the Higgs doublet assumes the value

$$\langle 0 | \phi | 0 \rangle = \begin{bmatrix} 0 \\ \frac{v}{\sqrt{2}} \end{bmatrix} \quad (397)$$

but that section dealt with a scalar Klein-Gordon particle. The consequence for a fermion doublet in this lagrangian is

$$\mathcal{L}_e = -g_e \bar{l}_L \phi e_R - g_e \bar{e}_R \phi^\dagger l_L \quad (398)$$

$$= -g_e \begin{bmatrix} \nu_L \\ e_L \end{bmatrix} \phi e_R - g_e \bar{e}_R \phi^\dagger \begin{bmatrix} \nu_L \\ e_L \end{bmatrix} \quad (399)$$

$$= -g_e [\bar{\nu}_L \quad \bar{e}_L] \begin{bmatrix} \phi^+ \\ \phi^0 \end{bmatrix} e_R - g_e \bar{e}_R [\phi^+ \quad \phi^0] \begin{bmatrix} \nu_L \\ e_L \end{bmatrix} \quad (400)$$

$$= -g_e (\bar{\nu}_L \phi^+ + \bar{e}_L \phi^0) e_R - g_e \bar{e}_R (\phi^+ \nu_L + \phi^0 e_L) \quad (401)$$

$$= -g_e [\bar{\nu}_L \phi^+ e_R + \bar{e}_L \phi^0 e_R + \bar{e}_R \phi^+ \nu_L + \bar{e}_R \phi^0 e_L] \quad (402)$$

Take on the vacuum expectation values.

$$\langle 0 | \mathcal{L}_e | 0 \rangle = -g_e \left[ \bar{\nu}_L \underbrace{\langle 0 | \phi^+ | 0 \rangle}_{=0} e_R + \bar{e}_L \underbrace{\langle 0 | \phi^0 | 0 \rangle}_{\frac{v}{\sqrt{2}}} e_R + \bar{e}_R \underbrace{\langle 0 | \phi^+ | 0 \rangle}_{=0} \nu_L + \bar{e}_R \underbrace{\langle 0 | \phi^0 | 0 \rangle}_{\frac{v}{\sqrt{2}}} e_L \right] \quad (403)$$

$$= -\frac{g_e v}{\sqrt{2}} [\bar{e}_L e_R + \bar{e}_R e_L] \quad (404)$$

This is exactly a Dirac mass with  $m_e = \frac{g_e v}{\sqrt{2}}$ . That was precisely the vacuum. Now let's see that if we consider also oscillations about the vacuum we generate a coupling between the electron and the Higgs field. In the last line, use  $v + H$  instead of just  $v$ .

$$\langle 0 | \mathcal{L}_e | 0 \rangle = -\frac{g_e v}{\sqrt{2}} [\bar{e}_L (v + H) e_R + \bar{e}_R (v + H) e_L] \quad (405)$$

$$= -\frac{g_e v}{\sqrt{2}} [v \bar{e}_L e_R + \bar{e}_L H e_R + v \bar{e}_R e_L + \bar{e}_R H e_L] \quad (406)$$

$$= -\frac{g_e v}{\sqrt{2}} \left[ v e^\dagger \left( \frac{1 - \gamma_5}{2} \right) \gamma_0 \left( \frac{1 + \gamma_5}{2} \right) e + e^\dagger \left( \frac{1 - \gamma_5}{2} \right) \gamma_0 H \left( \frac{1 + \gamma_5}{2} \right) e \right] \quad (407)$$

$$+ v e^\dagger \left( \frac{1 + \gamma_5}{2} \right) \gamma_0 \left( \frac{1 - \gamma_5}{2} \right) e + e^\dagger \left( \frac{1 + \gamma_5}{2} \right) \gamma_0 H \left( \frac{1 - \gamma_5}{2} \right) e \right] \quad (408)$$

$$= -\frac{g_e v}{\sqrt{2}} \left[ v \bar{e} \left( \frac{1 + \gamma_5}{2} \right) e + \bar{e} H e \left( \frac{1 + \gamma_5}{2} \right) + v \bar{e} \left( \frac{1 - \gamma_5}{2} \right) e + \bar{e} H e \left( \frac{1 - \gamma_5}{2} \right) \right] \quad (409)$$

$$= -\frac{g_e v}{\sqrt{2}} \left[ \underbrace{v \bar{e} e}_{\text{Dirac electron mass}} + \underbrace{\bar{e} H e}_{\text{electron-Higgs coupling}} \right] \quad (410)$$

Notice for the coupling term

$$\left(\frac{-g_e}{\sqrt{2}}\right)\bar{e}He = \left(-\frac{m_e}{v}\right)\bar{e}He = \left(-\frac{gm_e}{2m_W}\right)\bar{e}He \quad (411)$$

So in addition to interactions of the form  $f\bar{f} \rightarrow (\gamma \text{ or } Z^0) \rightarrow W^+W^-$  we also have the possibility  $f\bar{f} \rightarrow H \rightarrow W^+W^-$ . The presence of the fermion mass in the coupling to the Higgs is significant.

We must now recall that if an  $SU(2)$  doublet transforms as

$$l' = e^{\frac{i}{2}\vec{\alpha}\cdot\vec{\tau}}l \quad (412)$$

then the charge conjugate states

$$i\tau_2 \begin{bmatrix} u^* \\ d^* \end{bmatrix} \quad (413)$$

transform the same way. So then the charge conjugate of the Higgs field is

$$\phi_c = i\tau_2\phi^* \quad (414)$$

$$= i \begin{bmatrix} 0 & -i \\ i & 0 \end{bmatrix} \begin{bmatrix} \phi^+ \\ \phi^0 \end{bmatrix}^* \quad (415)$$

$$= \begin{bmatrix} 0 & 1 \\ -1 & 0 \end{bmatrix} \begin{bmatrix} \frac{1}{\sqrt{2}}(\phi_1 - i\phi_2)^* \\ \frac{1}{\sqrt{2}}(\phi_3 - i\phi_4)^* \end{bmatrix} \quad (416)$$

$$= \begin{bmatrix} 0 & 1 \\ -1 & 0 \end{bmatrix} \begin{bmatrix} \frac{1}{\sqrt{2}}(\phi_1 + i\phi_2) \\ \frac{1}{\sqrt{2}}(\phi_3 + i\phi_4) \end{bmatrix} \quad (417)$$

$$= \begin{bmatrix} \frac{1}{\sqrt{2}}(\phi_3 + i\phi_4) \\ -\frac{1}{\sqrt{2}}(\phi_1 + i\phi_2) \end{bmatrix} \quad (418)$$

$$\equiv \begin{bmatrix} \phi^{0\dagger} \\ -\phi^- \end{bmatrix} \quad (419)$$

$\phi_c$  is also an  $SU(2)$  doublet which transforms the same way  $\phi$  does.

Note that in the use of the  $\phi$  Higgs doublet we could not use the terms  $\bar{l}_L\phi\nu_R$  or  $\bar{\nu}_R\phi^\dagger l_L$  in the lagrangian ( $\nu_R$  has replaced  $e_R$ ) because it leads to unphysical terms  $\bar{e}_L\nu_R$  and  $\bar{\nu}_R e_L$ . With the Higgs conjugate field doublet  $\phi_c$  we may include  $\bar{l}_L\phi_c\nu_R$  and  $\bar{\nu}_R\phi_c^\dagger l_L$  terms (but not  $\bar{l}_L\phi_c e_R$  and  $\bar{e}_R\phi_c^\dagger l_L$  terms for the same reasons just discussed) which yield

Dirac masses for the neutrinos as well as Higgs interactions. Observe,

$$\mathcal{L}_\nu = -g_\nu \left[ \bar{l}_L \phi \nu_R + \bar{\nu}_R \phi^\dagger l_L \right] \quad (420)$$

$$= -g_\nu \left[ \begin{bmatrix} \bar{\nu}_L & \bar{e}_L \end{bmatrix} \begin{bmatrix} \phi^{0\dagger} \\ -\phi^- \end{bmatrix} \nu_R + \begin{bmatrix} \phi^0 & -\phi^{-\dagger} \end{bmatrix} \begin{bmatrix} \nu_L \\ e_L \end{bmatrix} \right] \quad (421)$$

$$= -g_\nu \left[ \left( \bar{\nu}_L \phi^{0\dagger} - \bar{e}_L \phi^- \right) \nu_R + \bar{\nu}_R \left( \phi^0 \nu_L - \phi^{-\dagger} e_L \right) \right] \quad (422)$$

$$= -g_\nu \left[ \bar{\nu}_L \phi^{0\dagger} \nu_R - \bar{e}_L \phi^- \nu_R + \bar{\nu}_R \phi^0 \nu_L - \bar{\nu}_R \phi^{-\dagger} e_L \right] \quad (423)$$

Take the vacuum expectation value and all  $\phi^-$  terms vanish. The  $\phi^0$  factors become  $\frac{1}{\sqrt{2}}(v + H)$  again.

$$\langle 0 | \mathcal{L}_\nu | 0 \rangle = -\frac{g_\nu}{\sqrt{2}} \left[ \bar{\nu}_L (v + H) \nu_R + \bar{\nu}_R (v + H) \nu_L \right] \quad (424)$$

$$= -\frac{g_\nu}{\sqrt{2}} \left[ \underbrace{v \bar{\nu}_L \nu_R + v \bar{\nu}_R \nu_L}_{\text{Dirac Mass}} + \underbrace{\bar{\nu}_L H \nu_R + \bar{\nu}_R H \nu_L}_{\nu\text{-Higgs Interaction}} \right] \quad (425)$$

$$= -\frac{g_\nu}{\sqrt{2}} \left[ v \bar{\nu} \nu + \bar{\nu} H \nu \right] \quad (426)$$

Summarily, to give the electron-neutrino  $SU(2)$  doublet mass (as well as the other lepton and quark doublets), we are adding more terms to the lagrangian derived at the end of section A.8 of the form:

$$\mathcal{L}_{f,\text{Higgs}} = \sum_{l=e,\mu,\tau} \left[ -\frac{g_l}{\sqrt{2}} \left[ v \bar{l} l + \bar{l} H l \right] - \frac{g_{\nu_l}}{\sqrt{2}} \left[ v \bar{\nu}_l \nu_l + \bar{\nu}_l H \nu_l \right] \right] \quad (427)$$

for the three lepton generations and similar terms for the three quark doublets. Because of the Higgs mechanism, we now have sensible masses for Standard Model particles.

## A.10 The Higgs Sector in Standard Model Electroweak Physics

Let's refer back to section A.7, line 256. We shall now see the details of how we go from the postulated  $SU(2) \times U(1)$  invariant lagrangian for a scalar particle to a form that determines the physics it implies.

Recall the lagrangian for the (scalar) Higgs sector is

$$\mathcal{L} = (D_\mu \phi)^\dagger (D^\mu \phi) + m_0^2 \phi^\dagger \phi - \frac{\lambda}{4} (\phi^\dagger \phi)^2 - \frac{1}{4} \vec{F}_{\mu\nu} \cdot \vec{F}^{\mu\nu} - \frac{1}{4} G_{\mu\nu} G^{\mu\nu} \quad (428)$$

$$(429)$$

for

$$\vec{F}^{\mu\nu} = \partial^\mu \vec{W}^\nu - \partial^\nu \vec{W}^\mu - g \vec{W}^\mu \times \vec{W}^\nu \quad (430)$$

$$G^{\mu\nu} = \partial^\mu B^\nu - \partial^\nu B^\mu \quad (431)$$

$$D^\mu \phi = \left( \partial^\mu + \underbrace{\frac{ig}{2} \vec{\tau} \cdot \vec{W}^\mu}_{SU(2)\text{piece}} + \underbrace{\frac{ig'}{2} B^\mu}_{U(1)\text{piece}} \right) \phi \quad (432)$$

Consider only the first term for now.

$$(D^\mu \phi)^\dagger (D^\mu \phi) = \left( \partial_\mu \phi + \frac{ig}{2} \vec{\tau} \cdot \vec{W}_\mu \phi + \frac{ig'Y}{2} B_\mu \phi \right)^\dagger \left( \partial^\mu \phi + \frac{ig}{2} \vec{\tau} \cdot \vec{W}^\mu \phi + \frac{ig'Y}{2} B^\mu \phi \right) \quad (433)$$

$$= (\partial_\mu \phi)^\dagger (\partial^\mu \phi) \quad (434)$$

$$+ (\partial_\mu \phi)^\dagger \left( \frac{ig}{2} \vec{\tau} \cdot \vec{W}^\mu \phi + \frac{ig'Y}{2} B^\mu \phi \right) + \left( \frac{ig}{2} \vec{\tau} \cdot \vec{W}_\mu \phi + \frac{ig'Y}{2} B_\mu \phi \right)^\dagger (\partial^\mu \phi) \quad (435)$$

$$+ \left[ \frac{ig}{2} \vec{\tau} \cdot \vec{W}_\mu \phi + \frac{ig'Y}{2} B_\mu \phi \right]^\dagger \left[ \frac{ig}{2} \vec{\tau} \cdot \vec{W}^\mu \phi + \frac{ig'Y}{2} B^\mu \phi \right] \quad (436)$$

Now let's work on the last line of this. Note that in my expression of the Higgs doublet

I'll be skipping straight to vacuum expectation values.

$$\frac{ig}{2}\vec{\tau} \cdot \vec{W}_\mu \phi + \frac{ig'Y}{2}B_\mu \phi = \frac{ig}{2} \left[ \begin{bmatrix} 0 & 1 \\ 1 & 0 \end{bmatrix} W_{1\mu} + \begin{bmatrix} 0 & -i \\ i & 0 \end{bmatrix} W_{2\mu} + \begin{bmatrix} 1 & 0 \\ 0 & -1 \end{bmatrix} W_{3\mu} \right] \left[ \begin{bmatrix} 0 \\ \frac{1}{\sqrt{2}}(v + H) \end{bmatrix} \right] \quad (437)$$

$$+ \frac{ig'Y}{2}B_\mu \left[ \begin{bmatrix} 0 \\ \frac{1}{\sqrt{2}}(v + H) \end{bmatrix} \right] \quad (438)$$

$$= \frac{ig}{2} \left[ \begin{bmatrix} \frac{1}{\sqrt{2}}W_{1\mu}(v + H) \\ 0 \end{bmatrix} + \begin{bmatrix} \frac{-i}{\sqrt{2}}W_{2\mu}(v + H) \\ 0 \end{bmatrix} + \begin{bmatrix} 0 \\ \frac{-1}{\sqrt{2}}W_{3\mu}(v + H) \end{bmatrix} \right] \quad (439)$$

$$+ \left[ \begin{bmatrix} 0 \\ \frac{ig'Y}{2\sqrt{2}}B_\mu(v + H) \end{bmatrix} \right] \quad (440)$$

$$= \left[ \begin{bmatrix} \frac{ig}{2\sqrt{2}}W_{1\mu}(v + H) + \frac{g}{2\sqrt{2}}W_{2\mu}(v + H) \\ \frac{-ig}{2\sqrt{2}}W_{3\mu}(v + H) + \frac{ig'Y}{2\sqrt{2}}B_\mu(v + H) \end{bmatrix} \right] \quad (441)$$

$$= \left[ \begin{bmatrix} \frac{ig}{2}(W_{1\mu} - iW_{2\mu})\frac{1}{\sqrt{2}}(v + H) \\ -\frac{ig}{2}W_{3\mu}\frac{1}{\sqrt{2}}(v + H) + \frac{ig'Y}{2}B_\mu\frac{1}{\sqrt{2}}(v + H) \end{bmatrix} \right] \quad (442)$$

Next, multiply this by it's Hermitian conjugate from the left:

$$\left[ -\frac{ig}{2}(W_{1\mu} + iW_{2\mu})\frac{1}{\sqrt{2}}(v + H) \quad \frac{ig}{2}W_{3\mu}\frac{1}{\sqrt{2}}(v + H) - \frac{ig'Y}{2}B_\mu\frac{1}{\sqrt{2}}(v + H) \right] \quad (443)$$

$$\left[ \begin{bmatrix} \frac{ig}{2}(W_1^\mu - iW_2^\mu)\frac{1}{\sqrt{2}}(v + H) \\ -\frac{ig}{2}W_3^\mu\frac{1}{\sqrt{2}}(v + H) + \frac{ig'Y}{2}B^\mu\frac{1}{\sqrt{2}}(v + H) \end{bmatrix} \right] \quad (444)$$

$$= \frac{g^2}{4}|W_1 - iW_2|^2 \frac{1}{2}(v + H)^2 + \frac{g^2}{4}|W_3|^2 \frac{1}{2}(v + H)^2 - \frac{gg'Y}{4}W_{3\mu}B^\mu\frac{1}{2}(v + H)^2 \quad (445)$$

$$- \frac{gg'Y}{4}W_3^\mu B_\mu\frac{1}{2}(v + H)^2 + \frac{g'^2Y^2}{4}|B|^2\frac{1}{2}(v + H)^2 \quad (446)$$

$$= \frac{g^2}{4}W_\mu^\dagger W^\mu v^2 + \frac{g^2}{2}W_\mu^\dagger W_\mu vH + \frac{g^2}{4}W_\mu^\dagger W^\mu H + \frac{g^2}{8}|W_3|^2 v^2 + \frac{g^2}{4}|W_3|^2 vH + \frac{g^2}{8}|W_3|^2 H^2 \quad (447)$$

$$- \frac{gg'Y}{4}W_{3\mu}B^\mu v^2 - \frac{gg'Y}{2}W_{3\mu}B^\mu vH - \frac{gg'Y}{2}W_{3\mu}B^\mu H^2 \quad (448)$$

$$+ \frac{g'^2Y^2}{8}|B|^2 v^2 + \frac{g'^2Y^2}{4}|B|^2 vH + \frac{g'^2Y^2}{8}|B|^2 H^2 \quad (449)$$

Now we have mass terms for the gauge boson fields and interaction terms among the gauge and Higgs bosons. With that done, let's go back and deal with the terms from lines

434 and 435.

$$(\partial_\mu \phi)^\dagger (\partial^\mu \phi) = \begin{bmatrix} 0 & \frac{1}{\sqrt{2}}(\partial_\mu v + \partial_\mu H) \end{bmatrix} \begin{bmatrix} 0 \\ \frac{1}{\sqrt{2}}(\partial_\mu v + \partial_\mu H) \end{bmatrix} = \frac{1}{2}(\partial_\mu H)(\partial^\mu H) \quad (450)$$

$$(\partial_\mu \phi)^\dagger \left( \frac{ig}{2} \vec{\tau} \cdot \vec{W}^\mu \phi + \frac{ig'Y}{2} B^\mu \phi \right) = -\frac{ig}{4}(\partial_\mu H)W_3^\mu(v+H) + \frac{ig'Y}{2}(\partial_\mu H)B^\mu(v+H) \quad (451)$$

$$\left( \frac{ig}{2} \vec{\tau} \cdot \vec{W}^\mu \phi + \frac{ig'Y}{2} B^\mu \phi \right)^\dagger (\partial^\mu \phi) = \frac{ig}{4}W_{3\mu}(v+H)(\partial^\mu H) - \frac{ig'Y}{4}B_\mu(v+H)(\partial^\mu H) \quad (452)$$

We are now ready to put the first term of the lagrangian back together.

$$(D_\mu \phi)^\dagger (D^\mu \phi) = \frac{1}{2}(\partial_\mu H)(\partial^\mu H) - \frac{ig}{4}(\partial_\mu H)W_3^\mu(v+H) + \frac{ig'Y}{4}(\partial_\mu H)B^\mu(v+H) \quad (453)$$

$$+ \frac{ig}{4}W_{3\mu}(v+H)(\partial^\mu H) - \frac{ig'Y}{4}B_\mu(v+H)(\partial^\mu H) \quad (454)$$

$$+ \frac{g^2}{4}W_\mu^\dagger W^\mu v^2 + \frac{g^2}{2}W_\mu^\dagger W^\mu vH + \frac{g^2}{4}W_\mu^\dagger W^\mu H^2 \quad (455)$$

$$+ \frac{g^2}{8}|W_3|^2 v^2 + \frac{g^2}{4}|W_3|^2 vH + \frac{g^2}{8}|W_3|^2 H^2 \quad (456)$$

$$- \frac{gg'Y}{4}W_{3\mu}B^\mu v^2 - \frac{gg'Y}{4}W_{3\mu}B^\mu vH - \frac{gg'Y}{4}W_{3\mu}B^\mu H^2 \quad (457)$$

$$+ \frac{g'^2Y}{8}|B|^2 v^2 + \frac{g'^2Y}{4}|B|^2 vH + \frac{g'^2Y}{8}|B|^2 H^2 \quad (458)$$

And the  $SU(2)$  gauge fields kinetic terms:

$$\vec{F}_{\mu\nu} \cdot \vec{F}^{\mu\nu} = (\partial_\mu \vec{W}_\nu - \partial_\nu \vec{W}_\mu - g \vec{W}_\mu \times \vec{W}_\nu) \cdot (\partial^\mu \vec{W}^\nu - \partial^\nu \vec{W}^\mu - g \vec{W}^\mu \times \vec{W}^\nu) \quad (459)$$

$$= (\partial_\mu \vec{W}_\nu - \partial_\nu \vec{W}_\mu) \cdot (\partial^\mu \vec{W}^\nu - \partial^\nu \vec{W}^\mu) - g(\partial_\mu \vec{W}_\nu - \partial_\nu \vec{W}_\mu) \cdot (\vec{W}^\mu \times \vec{W}^\nu) \quad (460)$$

$$- g(\vec{W}_\mu \times \vec{W}_\nu) \cdot (\partial^\mu \vec{W}^\nu - \partial^\nu \vec{W}^\mu) + g^2(\vec{W}_\mu \times \vec{W}_\nu) \cdot (\vec{W}^\mu \times \vec{W}^\nu) \quad (461)$$

$$= (\partial_\mu \vec{W}_\nu - \partial_\nu \vec{W}_\mu) \cdot (\partial^\mu \vec{W}^\nu - \partial^\nu \vec{W}^\mu) - 2g(\vec{W}_\mu \times \vec{W}_\nu) \cdot (\partial^\mu \vec{W}^\nu - \partial^\nu \vec{W}^\mu) \quad (462)$$

$$+ g^2 \left[ |W_\mu|^2 |W_\nu|^2 - |\vec{W}_\mu \cdot \vec{W}_\nu|^2 \right] \quad (463)$$

$$(464)$$

Now we're ready to put the lagrangian back together. After a little algebra:

$$\mathcal{L} = \underbrace{\frac{1}{2}(\partial_\mu H)(\partial^\mu H) + \frac{1}{2}m_0^2(v + H)^2 - \frac{\lambda}{16}(v + H)^4}_{\text{Higgs kinetic, mass, and self-interaction terms}} \quad (465)$$

$$- \underbrace{\frac{1}{4}(\partial_\mu W_{1\nu} - \partial_\nu W_{1\mu})(\partial^\mu W_1^\nu - \partial^\nu W_1^\mu) - \frac{1}{4}(\partial_\mu W_{2\nu} - \partial_\nu W_{2\mu})(\partial^\mu W_2^\nu - \partial^\nu W_2^\mu)}_{W^\pm \text{ kinetic terms}} \quad (466)$$

$$- \frac{1}{4}(\partial_\mu W_{3\nu} - \partial_\nu W_{3\mu})(\partial^\mu W_3^\nu - \partial^\nu W_3^\mu) - \frac{1}{4}G_{\mu\nu}G^{\mu\nu} \quad (467)$$

$$+ \underbrace{\frac{1}{8}v^2(gW_{3\mu} - g'YB_\mu)(gW_3^\mu - g'YB^\mu)}_{\text{Terms that become the } Z\text{-boson and photon}} \quad (468)$$

$$+ \frac{g^2v^2}{4}W_\mu^\dagger W^\mu + \frac{g^2v}{2}W_\mu^\dagger W^\mu H + \frac{g^2}{4}W_\mu^\dagger W^\mu H^2 + \frac{g^2v}{4}|W_3|^2H + \frac{g^2}{8}|W_3|^2H^2 \quad (469)$$

$$- \underbrace{\frac{gg'Yv}{2}W_{3\mu}B^\mu H - \frac{gg'Y}{2}W_{3\mu}B^\mu H^2 + \frac{g'^2Y^2v}{4}|B|^2H + \frac{g'^2Y^2}{8}|B|^2H^2}_{W^\pm \text{ mass, trilinear, quadrilinear couplings with the Higgs}} \quad (470)$$

$$\underbrace{\frac{1}{2}g(\vec{W}_\mu \times \vec{W}_\nu) \cdot (\partial^\mu \vec{W}^\mu - \partial^\nu \vec{W}^\mu) - \frac{1}{4}g^2 \left[ |W_\mu|^2 |W_\nu|^2 - |\vec{W}_\mu \cdot \vec{W}_\nu|^2 \right]}_{\text{Quadrilinear couplings among the gauge bosons}} \quad (471)$$

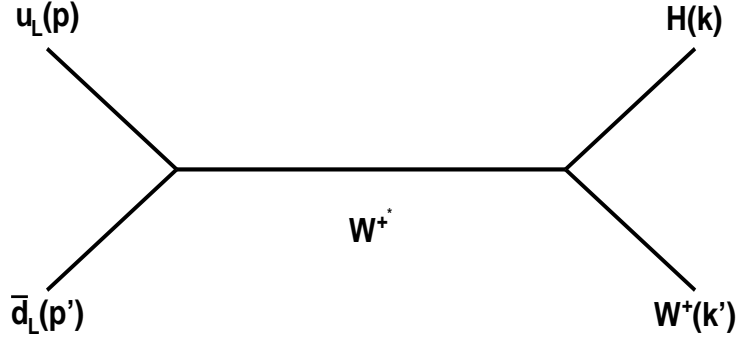


Figure 42: Associated Production with a  $W$  boson

### A.11 $WH$ Production Amplitude

The Tevatron consists of a proton beam colliding with an antiproton beam. So let's consider this interaction when an up quark interacts with an anti-down quark; the interaction of an anti-up quark with a down quark follows analogously. The full Lagrangian for the interaction is the sum of the Higgs Sector of the Standard Model Lagrangian with the Lagrangian for a quark doublet.

$$\mathcal{L} = \underbrace{\frac{1}{2} (\partial_\mu H) (\partial^\mu H) + \frac{1}{2} \mu^2 H^2 + \frac{g^2 v^2}{4} W_\mu^\dagger W^\mu + \frac{g^2 v}{2} W_\mu^\dagger W^\mu H}_{\text{Higgs Sector}} \quad (472)$$

$$\underbrace{-\frac{1}{4} \sum_{i=1,2} (\partial_\mu W_{i\nu} - \partial_\nu W_{i\mu}) (\partial^\mu W_i^\nu - \partial^\nu W_i^\mu)}_{\text{W boson kinetic terms}} \quad (473)$$

$$\underbrace{+i\bar{u}\gamma_\rho \left(\frac{1-\gamma_5}{2}\right) \partial^\rho u + i\bar{d}\gamma_\rho \left(\frac{1-\gamma_5}{2}\right) \partial^\rho d + \frac{gV_{ud}}{\sqrt{2}} \bar{d}\gamma_\rho W^{\dagger\rho} \left(\frac{1-\gamma_5}{2}\right) u}_{\text{Quark Doublet}} \quad (474)$$

To calculate the cross section for this interaction, I want the interaction Lagrangian, which is found by just collecting the interaction terms in the above Lagrangian.

$$\mathcal{L}_I = \frac{g^2 v}{2} W_\mu^\dagger W^\mu H + \frac{gV_{ud}}{\sqrt{2}} \bar{d}\gamma_\rho W^{\dagger\rho} \left(\frac{1-\gamma_5}{2}\right) u \quad (475)$$

I would like to change the form of the coefficients to be expressed in terms of the  $W$  mass and electric charge. Using  $m_W = \frac{gv}{2}$  and  $e_0 = g \sin \theta_W$ ,

$$\mathcal{L}_I = \frac{2m_W^2}{v} W_\mu^\dagger W^\mu H + \frac{e_0 V_{ud}}{\sqrt{2} \sin \theta_W} \bar{d} \gamma_\rho W^{\rho\dagger} \left( \frac{1 - \gamma_5}{2} \right) u \quad (476)$$

Later, I'll re-express the leftover  $v$  in terms of the Fermi Coupling Constant  $G_F = \sqrt{2}/2v^2$ . This way, I'll be able to express the cross section in terms of measured quantities.

From the interaction Lagrangian density I need the interaction Hamiltonian density.

$$\mathcal{H}_I(x) = \pi(x) \dot{\Phi}(x) - \mathcal{L}_I(x) \quad (477)$$

where  $\Phi(x)$  is a position-space field and  $\pi(x)$  is its conjugate momentum field. However, in this case there are no time-derivatives of fields in the interaction Lagrangian density. So it is simply

$$\mathcal{H}_I(x) = -\mathcal{L}(x) \quad (478)$$

$$= -\underbrace{\frac{2m_W^2}{v} W_\mu^\dagger W^\mu H}_{\mathcal{H}_{IH}(x)} - \underbrace{\frac{e_0 V_{ud}}{\sqrt{2} \sin \theta_W} \bar{d} \gamma_\rho W^{\rho\dagger} \left( \frac{1 - \gamma_5}{2} \right) u}_{\mathcal{H}_{Iq}(x)} \quad (479)$$

$$\Rightarrow \mathcal{H}_I(x) = \mathcal{H}_{IH}(x) + \mathcal{H}_{Iq}(x) \quad (480)$$

The scattering matrix for this interaction is[11]

$$\langle k'; k | S | p'; p \rangle = \langle k'; k | 1 | p'; p \rangle + i \langle k'; k | T | p'; p \rangle \quad (481)$$

where we recall that the scattering matrix is defined as the time-evolution operator as  $t \rightarrow \infty$ .

$$\langle k'; k | S | p'; p \rangle = \lim_{t \rightarrow \infty} \langle k'; k | e^{iH(2t)} | p'; p \rangle \quad (482)$$

The interaction component here is what I want to calculate. From (4.90) Peskin and Schroeder[11]

$$i \langle k'; k | T | p'; p \rangle = \lim_{t \rightarrow \infty (1-i\varepsilon)} \langle k'; k | T \exp \left[ -i \int_{-t}^t dt' H_I(t') \right] | p'; p \rangle \quad (483)$$

That exponential expands as (from (4.22) Peskin and Schroeder[11]):

$$T \exp \left[ -i \int_{-t}^t dt' H_I(t') \right] = 1 + (-i) \int_{-t}^t dt_1 H_I(t_1) + \frac{(-i)^2}{2!} \int_{-t}^t \int_{-t}^t dt_1 dt_2 T [H_I(t_1) H_I(t_2)] + \dots \quad (484)$$

As we are beginning and ending with two particle states, the second order term is the first that can contribute to this interaction, and any higher-order terms contain loops that we do not address here. The interaction part of the scattering matrix element becomes

$$i\langle k'; k | T | p'; p \rangle \cong \langle k'; k | \frac{(-i)^2}{2!} \iint_{-t}^t dt_1 dt_2 T [H_I(x_1)H_I(x_2)] | p'; p \rangle \quad (485)$$

where  $H_I(x) = \int d^3\vec{x} \mathcal{H}_I(x) = \int d^3\vec{x} [\mathcal{H}_{IH}(x) + \mathcal{H}_{Iq}(x)]$ , and in the Hamiltonian I replaced the variable  $t$  with full spacetime variable  $x = (t, x_1, x_2, x_3)$  because all components now come into play.

$$= \langle k'; k | \frac{(-i)^2}{2} \iint dt_1 dt_2 T \left[ \int d^3\vec{x}_1 \mathcal{H}_I(x_1) \int d^3\vec{x}_2 \mathcal{H}_I(x_2) \right] | p'; p \rangle \quad (486)$$

$$= \langle k'; k | \frac{(-i)^2}{2} T \left[ \int d^4x_1 \mathcal{H}_I(x_1) \int d^4x_2 \mathcal{H}_I(x_2) \right] \quad (487)$$

$$= \frac{(-i)^2}{2} \iint d^4x_1 d^4x_2 \langle k'; k | T [\mathcal{H}_I(x_1)\mathcal{H}_I(x_2)] | p'; p \rangle \quad (488)$$

$$= \frac{(-i)^2}{2} \iint d^4x_1 d^4x_2 \langle k'; k | T [\mathcal{H}_{IH}(x_1)\mathcal{H}_{IH}(x_2) + \mathcal{H}_{IH}(x_1)\mathcal{H}_{Iq}(x_2) + \mathcal{H}_{Iq}(x_1)\mathcal{H}_{IH}(x_2) + \mathcal{H}_{Iq}(x_1)\mathcal{H}_{Iq}(x_2)] | p'; p \rangle \quad (489)$$

$$+ \mathcal{H}_{Iq}(x_1)\mathcal{H}_{IH}(x_2) + \mathcal{H}_{Iq}(x_1)\mathcal{H}_{Iq}(x_2)] | p'; p \rangle \quad (490)$$

Since I have an interaction that involves both the quark doublet and the Higgs, the  $\mathcal{H}_{IH}(x_1)\mathcal{H}_{IH}(x_2)$  and  $\mathcal{H}_{Iq}(x_1)\mathcal{H}_{Iq}(x_2)$  terms do not contribute.

$$= \frac{(-i)^2}{2} \iint d^4x_1 d^4x_2 \langle k'; k | T [\mathcal{H}_{IH}(x_1)\mathcal{H}_{Iq}(x_2) + \mathcal{H}_{Iq}(x_1)\mathcal{H}_{IH}(x_2) + \mathcal{H}_{Iq}(x_1)\mathcal{H}_{Iq}(x_2)] | p'; p \rangle \quad (491)$$

Next, I have to calculate these two time-ordered products inside the brackets. Using terms from expression 480 above,

$$T [\mathcal{H}_{Iq}(x_1)\mathcal{H}_{IH}(x_2)] = \frac{2e_0 m_W^2 V_{ud}}{v \sqrt{2} \sin \theta_W} T \left[ W_\mu^\dagger(x_1) W^\mu(x_1) H(x_1) \bar{d}(x_2) W^\dagger(x_2) \left( \frac{1 - \gamma_5}{2} \right) u(x_2) \right] \quad (492)$$

$$= \frac{2e_0 m_W^2 V_{ud}}{v \sqrt{2} \sin \theta_W} N [W_\mu^\dagger(x_1) W^\mu(x_1) H(x_1) \bar{d}(x_2) W^\dagger(x_2) \left( \frac{1 - \gamma_5}{2} \right) u(x_2)] \quad (493)$$

$$+ \text{all contractions}] \quad (494)$$

The  $N$  operator indicates we explore all possible combination of field contractions, most of which vanish as irrelevant. Field contractions will be expressed notationally as  $\overline{A(x)B(x)C(x)}$

to contract field  $A$  with field  $C$ .

$$= \frac{2e_0 m_W^2 V_{ud}}{v\sqrt{2} \sin \theta_W} N [W_\mu^\dagger(x_1) W^\mu(x_1) H(x_1) \bar{d}(x_2) W^\dagger(x_2) \left( \frac{1 - \gamma_5}{2} \right) u(x_2)] \quad (495)$$

$$+ \overline{W_\mu^\dagger(x_1) W^\mu(x_1)} H(x_1) \bar{d}(x_2) W^\dagger(x_2) \left( \frac{1 - \gamma_5}{2} \right) u(x_2) \quad (496)$$

$$+ \overline{W_\mu^\dagger(x_1) W^\mu(x_1) H(x_1)} \bar{d}(x_2) W^\dagger(x_2) \left( \frac{1 - \gamma_5}{2} \right) u(x_2) \quad (497)$$

$$+ \overline{W_\mu^\dagger(x_1) W^\mu(x_1) H(x_1) \bar{d}(x_2)} W^\dagger(x_2) \left( \frac{1 - \gamma_5}{2} \right) u(x_2) \quad (498)$$

$$+ \overline{W_\mu^\dagger(x_1) W^\mu(x_1) H(x_1) \bar{d}(x_2) W^\dagger(x_2)} \left( \frac{1 - \gamma_5}{2} \right) u(x_2) \quad (499)$$

$$+ \overline{W_\mu^\dagger(x_1) W^\mu(x_1) H(x_1) \bar{d}(x_2) W^\dagger(x_2)} \left( \frac{1 - \gamma_5}{2} \right) u(x_2) \quad (500)$$

$$+ W_\mu^\dagger(x_1) \overline{W^\mu(x_1) H(x_1)} \bar{d}(x_2) W^\dagger(x_2) \left( \frac{1 - \gamma_5}{2} \right) u(x_2) \quad (501)$$

$$+ W_\mu^\dagger(x_1) \overline{W^\mu(x_1) H(x_1) \bar{d}(x_2)} W^\dagger(x_2) \left( \frac{1 - \gamma_5}{2} \right) u(x_2) \quad (502)$$

$$+ W_\mu^\dagger(x_1) \overline{W^\mu(x_1) H(x_1) \bar{d}(x_2) W^\dagger(x_2)} \left( \frac{1 - \gamma_5}{2} \right) u(x_2) \quad (503)$$

$$+ W_\mu^\dagger(x_1) \overline{W^\mu(x_1) H(x_1) \bar{d}(x_2) W^\dagger(x_2)} \left( \frac{1 - \gamma_5}{2} \right) u(x_2) \quad (504)$$

$$+ W_\mu^\dagger(x_1) W^\mu(x_1) \overline{H(x_1) \bar{d}(x_2)} W^\dagger(x_2) \left( \frac{1 - \gamma_5}{2} \right) u(x_2) \quad (505)$$

$$+ W_\mu^\dagger(x_1) W^\mu(x_1) \overline{H(x_1) \bar{d}(x_2) W^\dagger(x_2)} \left( \frac{1 - \gamma_5}{2} \right) u(x_2) \quad (506)$$

$$+ W_\mu^\dagger(x_1) W^\mu(x_1) H(x_1) \overline{\bar{d}(x_2) W^\dagger(x_2)} \left( \frac{1 - \gamma_5}{2} \right) u(x_2) \quad (507)$$

$$+ W_\mu^\dagger(x_1) W^\mu(x_1) H(x_1) \overline{\bar{d}(x_2) W^\dagger(x_2)} \left( \frac{1 - \gamma_5}{2} \right) u(x_2) \quad (508)$$

$$+ W_\mu^\dagger(x_1) W^\mu(x_1) H(x_1) \overline{\bar{d}(x_2) W^\dagger(x_2)} \left( \frac{1 - \gamma_5}{2} \right) u(x_2) \quad (509)$$

$$+ W_\mu^\dagger(x_1) W^\mu(x_1) H(x_1) \overline{\bar{d}(x_2) W^\dagger(x_2)} \left( \frac{1 - \gamma_5}{2} \right) u(x_2) \quad (510)$$

$$+ \text{terms with more than one contraction}] \quad (511)$$

There are some important characteristics to note which will greatly simplify this mess:

- Since we are dealing only with the tree-level production process, terms with more than one contraction are automatically irrelevant.
- Contracted fields at the same spacetime coordinate constitute loops so they are not involved in tree-level interactions.
- Contractions between fields of different types vanish. Physically, the contracted fields are the propagator in the feynman diagram.
- If there are no contractions of a particular field at  $x_1$  with a field at  $x_2$ , then there is no interaction between the initial and final states.
- The initial and final particle fields must be uncontracted. They contract with the initial and final state vectors later.

Hence, the only term left is the one that contracts  $W^\mu(x_1)$  to  $W^{\nu\dagger}(x_2)$  in expression 499— this establishes the physical propagation of a  $W$ -boson field from spacetime coordinate  $x_1$  to  $x_2$ . Notice that this is the only transition from initial to final states possible at tree-level.

Taking a step back to expression 491, here's where we are:

$$i\langle k'; k | T | p'; p \rangle = \frac{(-i)^2 e_0 m_W^2 V_{ud}}{v \sqrt{2} \sin \theta_W} \times \quad (512)$$

$$\iint d^4 x_1 d^4 x_2 \langle k'; k | [W_\mu^\dagger(x_1) \overline{W^\mu(x_1) H(x_1) \bar{d}(x_2) \gamma_\rho W^{\rho\dagger}(x_2)} \left( \frac{1 - \gamma_5}{2} \right) u(x_2) \quad (513)$$

$$+ \bar{d}(x_1) \gamma_\rho \overline{W^{\rho\dagger}(x_1) \left( \frac{1 - \gamma_5}{2} \right) u(x_1) W_\mu^\dagger(x_2) W^\mu(x_2) H(x_2)}] | p'; p \rangle \quad (514)$$

$$i\langle k'; k | T | p'; p \rangle = \frac{(-i)^2 e_0 m_W^2 V_{ud}}{v \sqrt{2} \sin \theta_W} \times \quad (515)$$

$$\iint d^4 x_1 d^4 x_2 \langle k'; k | W_\mu^\dagger(x_1) \overline{W^\mu(x_1) H(x_1) \bar{d}(x_2) \gamma_\rho W^{\rho\dagger}(x_2)} \left( \frac{1 - \gamma_5}{2} \right) u(x_2) | p'; p \rangle \quad (516)$$

$$+ \frac{(-i)^2 e_0 m_W^2 V_{ud}}{v \sqrt{2} \sin \theta_W} \times \quad (517)$$

$$\iint d^4 x_1 d^4 x_2 \langle k'; k | \bar{d}(x_1) \gamma_\rho \overline{W^{\rho\dagger}(x_1) \left( \frac{1 - \gamma_5}{2} \right) u(x_1) W_\mu^\dagger(x_2) W^\mu(x_2) H(x_2)}] | p'; p \rangle \quad (518)$$

The two terms cover two Feynman diagrams:

- $u$  and  $\bar{d}$  quarks interact at spacetime coordinate  $x_1$  to become a virtual  $W^+$ , which then radiates a Higgs boson at spacetime coordinate  $x_2$ .
- The same situation with spacetime coordinates  $x_1$  and  $x_2$  reversed.

The uncontracted terms now contract with the initial and final state vectors, corresponding physically to the incoming and outgoing particles of the Feynman diagram. They contract as follows:

$$\overline{\langle k' | W_\mu^\dagger(x)} = \langle 0 | \epsilon_\mu^{s*}(k') e^{ik' \cdot x} \quad (519)$$

$$\overline{\langle k | H(x)} = \langle 0 | e^{ik \cdot x} \quad (520)$$

$$\overline{\langle \bar{d}(x) | p' \rangle} = e^{-ip' \cdot x} \bar{d}^{r_1}(p') | 0 \rangle \quad (521)$$

$$\overline{\langle u(x) | p \rangle} = e^{-ip \cdot x} u^{r_2}(p) | 0 \rangle \quad (522)$$

where  $r_1, r_2$  are the fermion spins.

In position-space, the  $W$  propagator includes an integral over the momentum  $q$ :

$$\overline{W^{\rho\dagger}(x_1) W^\mu(x_2)} = \int \frac{d^4 q}{(2\pi)^4} i \left[ \frac{-g^{\mu\rho} + \frac{q^\mu q^\rho}{m_W^2}}{q^2 - m_W^2 + i\varepsilon} \right] e^{-iq \cdot (x_1 - x_2)} \quad (523)$$

$$(524)$$

Let's make the replacements in the scattering matrix.

$$i\langle k'; k | T | p'; p \rangle = \frac{(-i)^2 e_0 m_W^2 V_{ud}}{v\sqrt{2} \sin \theta_W} \times \quad (525)$$

$$\iint d^4 x_1 d^4 x_2 \underbrace{[\langle 0 | \epsilon_\mu^{s*}(k') e^{ik' \cdot x_1} \rangle}_{W^\dagger} \underbrace{\langle 0 | e^{ik \cdot x_1} \rangle}_{H} \underbrace{\int \frac{d^4 q}{(2\pi)^4} i \left[ \frac{-g^{\mu\rho} + \frac{q^\mu q^\rho}{m_W^2}}{q^2 - m_W^2 + i\varepsilon} \right] e^{-iq \cdot (x_2 - x_1)}}_{W\text{-propagator}} \quad (526)$$

$$\underbrace{e^{-ip' \cdot x_2} \bar{d}^{r_1}(p') | 0 \rangle}_{\bar{d}} \gamma_\rho \left( \frac{1 - \gamma_5}{2} \right) \underbrace{e^{-ip \cdot x_2} u^{r_2}(p) | 0 \rangle}_{u} \quad (527)$$

$$+ \frac{(-i)^2 e_0 m_W^2 V_{ud}}{v\sqrt{2} \sin \theta_W} \times \quad (528)$$

$$\iint d^4 x_1 d^4 x_2 \underbrace{[e^{-ip' \cdot x_1} \bar{d}^{r_1}(p') | 0 \rangle}_{\bar{d}} \gamma_\rho \underbrace{\int \frac{d^4 q}{(2\pi)^4} i \left[ \frac{-g^{\mu\rho} + \frac{q^\mu q^\rho}{m_W^2}}{q^2 - m_W^2 + i\varepsilon} \right] e^{-iq \cdot (x_1 - x_2)} \left( \frac{1 - \gamma_5}{2} \right)}_{W\text{-propagator}} \quad (529)$$

$$\underbrace{e^{-ip \cdot x_1} u^{r_2}(p) | 0 \rangle}_{u} \underbrace{\langle 0 | \epsilon_\mu^{s*}(k') e^{ik' \cdot x_2} \rangle}_{W^\dagger} \underbrace{\langle 0 | e^{ik \cdot x_2} \rangle}_{H} \quad (530)$$

Integrating  $x_1$  and  $x_2$  over the exponentials is the very definition—or one of many—of a 4-dim Dirac delta function.

$$i\langle k'; k | T | p'; p \rangle = \left[ \frac{i(-i)^2 e_0 m_W^2 V_{ud}}{v \sqrt{2} \sin \theta_W} \right] \int d^4 q \epsilon_\mu^{s*}(k') \left[ \frac{-g^{\mu\rho} + \frac{q^\mu q^\rho}{m_W^2}}{q^2 - m_W^2 + i\varepsilon} \right] \bar{d}^{r_1}(p') \quad (531)$$

$$\gamma_\rho \left( \frac{1 - \gamma_5}{2} \right) u^{r_2}(p) (2\pi)^4 \delta^4(-k' - k - q) \delta^4(p' + p + q) \quad (532)$$

$$+ \left[ \frac{i(-i)^2 e_0 m_W^2 V_{ud}}{v \sqrt{2} \sin \theta_W} \right] \int d^4 q \bar{d}^{r_1}(p') \gamma_\rho \left( \frac{1 - \gamma_5}{2} \right) u^{r_2}(p) \quad (533)$$

$$\left[ \frac{-g^{\mu\rho} + \frac{q^\mu q^\rho}{m_W^2}}{q^2 - m_W^2 + i\varepsilon} \right] \epsilon_\mu^{s*}(k') (2\pi)^4 \delta^4(-k' - k - q) \delta^4(p' + p + q) \quad (534)$$

$$i\langle k'; k | T | p'; p \rangle = \left[ \frac{i(-i)^2 e_0 m_W^2 V_{ud}}{v \sqrt{2} \sin \theta_W} \right] (2\pi)^4 \epsilon_\mu^{s*}(k') \left[ \frac{-g^{\mu\rho} + \frac{q^\mu q^\rho}{m_W^2}}{q^2 - m_W^2 + i\varepsilon} \right] \bar{d}^{r_1}(p') \gamma_\rho \quad (535)$$

$$\left( \frac{1 - \gamma_5}{2} \right) u^{r_2}(p) \delta^4(p' + p - k' - k) \quad (536)$$

$$+ \left[ \frac{i(-i)^2 e_0 m_W^2 V_{ud}}{v \sqrt{2} \sin \theta_W} \right] (2\pi)^4 \bar{d}^{r_1}(p') \gamma_\rho \left( \frac{1 - \gamma_5}{2} \right) u^{r_2}(p) \quad (537)$$

$$\left[ \frac{-g^{\mu\rho} + \frac{q^\mu q^\rho}{m_W^2}}{q^2 - m_W^2 + i\varepsilon} \right] \epsilon_\mu^{s*}(k') \delta^4(p' + p - k' - k) \quad (538)$$

Now that the integral over  $q$  has been carried out over the  $\delta$ -functions, it is understood that  $q = k' + k = p' + p$  explicitly now.

$$i\langle k'; k | T | p'; p \rangle = \left[ \frac{-2ie_0 m_W^2 V_{ud}}{v \sqrt{2} \sin \theta_W} \right] (2\pi)^4 \epsilon_\mu^{s*}(k') \left[ \frac{-g^{\mu\rho} + \frac{q^\mu q^\rho}{m_W^2}}{q^2 - m_W^2 + i\varepsilon} \right] \quad (539)$$

$$\bar{d}^{r_1}(p') \gamma_\rho \left( \frac{1 - \gamma_5}{2} \right) u^{r_2}(p) \delta^4(p' + p - k' - k) \quad (540)$$

Recall from Peskin and Schroeder (4.73)[11]

$$i\langle k'; k | T | p'; p \rangle = (2\pi)^4 \delta^4(p' + p - k' - k) \cdot i\mathcal{M}(p', p \rightarrow k', k) \quad (541)$$

Finally, the invariant amplitude for Higgs associated production with a  $W^+$ -boson is

$$i\mathcal{M} = \left[ \frac{-2ie_0 m_W^2 V_{ud}}{v \sqrt{2} \sin \theta_W} \right] \epsilon_\mu^{s*}(k') \left[ \frac{-g^{\mu\rho} + \frac{q^\mu q^\rho}{m_W^2}}{q^2 - m_W^2 + i\varepsilon} \right] \bar{d}^{r_1}(p') \gamma_\rho \left( \frac{1 - \gamma_5}{2} \right) u^{r_2}(p)$$

(542)

## A.12 $H \rightarrow WW$ Lagrangian Density To Invariant Amplitude

For a Higgs boson decay to two  $W$  bosons, the Lagrangian density comes from the Higgs sector of the standard model Lagrangian. The  $Z$  boson and photon terms can be excluded.

$$\mathcal{L} = \underbrace{\frac{1}{2} (\partial_\mu H) (\partial^\mu H) + \frac{1}{2} \mu^2 H^2 + \frac{g^2 v^2}{4} W_\mu^\dagger W^\mu + \frac{g^2 v}{2} W_\mu^\dagger W^\mu H}_{\text{Higgs Sector}} - \underbrace{\frac{1}{4} \sum_{i=1,2} (\partial_\mu W_{i\nu} - \partial_\nu W_{i\mu}) (\partial^\mu W_i^\nu - \partial^\nu W_i^\mu)}_{\text{W boson kinetic terms}}$$

To calculate the invariant amplitude for the decay, I want the interaction Lagrangian.

$$\mathcal{L} = \frac{g^2 v}{2} W_\mu^\dagger W^\mu H$$

From this I need the interaction Hamiltonian density.

$$\mathcal{H}_I = \sum_{\text{fields}} \pi(x) \dot{\Phi}(x) - \mathcal{L}_I(x)$$

where  $\Phi(x)$  is a position-space field and  $\pi(x)$  is its conjugate momentum field. However, in this case there are no time-derivatives of fields in the interaction Lagrangian density. So it is simply

$$\begin{aligned} \mathcal{H}_I(x) &= -\mathcal{L} \\ &= -\frac{g^2 v}{2} W_\mu^\dagger W^\mu H \end{aligned}$$

The scattering matrix for this interaction is

$$\langle k_1, k_2 | S | p \rangle = \langle k_1, k_2 | 1 | p \rangle + i \langle k_1, k_2 | T | p \rangle$$

where we recall that the scattering matrix is defined as the time-evolution operator as  $t \rightarrow \infty$ .

$$\langle k_1, k_2 | S | p \rangle = \lim_{t \rightarrow \infty} \langle k_1, k_2 | e^{iH(2t)} | p \rangle$$

The interaction component here is what I want to calculate. From (4.90) Peskin,

$$i\langle k_1, k_2 | T | p \rangle = \lim_{t \rightarrow \infty(1-i\varepsilon)} \langle k_1, k_2 | T \exp \left[ -i \int_{-t}^t dt' H_I(t') \right] | p \rangle$$

That exponential expands as (from (4.22) Peskin)

$$T \exp \left[ -i \int_{-t}^t dt' H_I(t') \right] = 1 + (-i) \int_{-t}^t dt_1 H_I(t_1) + \frac{(-i)^2}{2!} \int_{-t}^t \int_{-t}^t dt_1 dt_2 T [H_I(t_1) H_I(t_2)] + \dots$$

This scenario is just a tree-level decay—there are no loops to consider or propagators between two spacetime coordinates  $x_1$  and  $x_2$ . Hence, let's consider only the contribution from the 1st order term. The interaction part of the scattering matrix becomes

$$i\langle k_1, k_2 | T | p \rangle \cong \langle k_1, k_2 | (-i) \int_{-t}^t dt_1 H_I(x_1) | p \rangle$$

where  $H_I(x) = \int d^3x \mathcal{H}_I(x)$ , and in the Hamiltonian I replaced the variable  $t$  with the full spacetime variable  $x$  because all components now come into play.

$$\begin{aligned} i\langle k_1, k_2 | T | p \rangle &= (-i) \langle k_1, k_2 | \int_{-t}^t dt_1 \int d^3x \mathcal{H}_I(x) | p \rangle \\ &= -i \langle k_1, k_2 | \int d^4x \mathcal{H}_I(x) | p \rangle \\ &= -i \int d^4x \langle k_1, k_2 | \mathcal{H}_I(x) | p \rangle \\ &= -i \int d^4x \langle k_1, k_2 | \frac{-g^2 v}{2} W_\mu^\dagger W^\mu H | p \rangle \\ &= \frac{-ig^2 v}{2} \int d^4x \langle k_1, k_2 | W_\mu^\dagger W^\mu H | p \rangle \end{aligned}$$

Assume the fields are now contracted with their state vectors.

If we go to my contractions section:

$$\begin{aligned} \langle k | W_\mu(x) &= \langle 0 | \varepsilon_\mu^*(k, \lambda) e^{ik \cdot x} \\ H | p \rangle &= e^{-ip \cdot x} | 0 \rangle \end{aligned}$$

Using these

$$\begin{aligned}
i\langle k_1, k_2 | T | p \rangle &= \frac{ig^2 v}{2} \int d^4 x \epsilon_\mu^*(k_1, \lambda_1) e^{ik_1 \cdot x} \epsilon^{*\mu}(k_2, \lambda_2) e^{ik_2 \cdot x} e^{-ip \cdot x} \\
&= \frac{ig^2 v}{2} \int d^4 x \epsilon_\mu^*(k_1, \lambda_1) \epsilon^{*\mu}(k_2, \lambda_2) e^{i(k_1 + k_2 - p) \cdot x} \\
&= \frac{ig^2 v}{2} \epsilon_\mu^*(k_1, \lambda_1) \epsilon^{*\mu}(k_2, \lambda_2) \delta^4(k_1 + k_2 - p) (2\pi)^4
\end{aligned}$$

Recall from (4.73) Peskin

$$\begin{aligned}
i\langle k_1, k_2 | T | p \rangle &= (2\pi)^4 \delta^4(k_1 + k_2 - p) \cdot i\mathcal{M}(p \rightarrow k_1, k_2) \\
\Rightarrow i\mathcal{M} &= \frac{ig^2 v}{2} \epsilon_\mu^*(k_1, \lambda_1) \epsilon^{*\mu}(k_2, \lambda_2)
\end{aligned}$$

### A.13 $H \rightarrow WW$ Invariant Amplitude to Decay Rate ( $\Gamma$ )

The decay rate from (4.83) Peskin is

$$\Gamma = \frac{1}{2m_H} \left[ \frac{d^3 k_1}{2E_1(2\pi)^3} \frac{d^3 k_2}{2E_2(2\pi)^3} \right] \sum_{\lambda_1, \lambda_2} |\mathcal{M}|^2 (2\pi)^4 \delta^4(k_1 + k_2 - p)$$

So let's square the amplitude

$$\begin{aligned}
i\mathcal{M} &= igm_W \epsilon_\mu^*(k_1, \lambda_1) \epsilon^{*\mu}(k_2, \lambda_2) \\
|\mathcal{M}|^2 &= g^2 m_W^2 (\epsilon_\mu^*(k_1, \lambda_1) \epsilon_\nu(k_1, \lambda_1)) (\epsilon^{*\mu}(k_2, \lambda_2) \epsilon^\nu(k_2, \lambda_2))
\end{aligned}$$

Now deal with the spin sum

$$\begin{aligned}
\sum_{\lambda_1, \lambda_2} |\mathcal{M}|^2 &= g^2 m_W^2 \sum_{\lambda_1, \lambda_2} (\epsilon_\mu^*(k_1, \lambda_1) \epsilon_\nu(k_1, \lambda_1)) (\epsilon^{*\mu}(k_2, \lambda_2) \epsilon^\nu(k_2, \lambda_2)) \\
&= g^2 m_W^2 \left( -g_{\mu\nu} + \frac{k_{1\mu} k_{1\nu}}{m_W^2} \right) \left( -g^{\mu\nu} + \frac{k_2^\mu k_2^\nu}{m_W^2} \right) \\
&= g^2 m_W^2 \left( g_{\mu\nu} g^{\mu\nu} - g_{\mu\nu} \frac{k_2^\mu k_2^\nu}{m_W^2} - g^{\mu\nu} \frac{k_{1\mu} k_{1\nu}}{m_W^2} + \frac{k_{1\mu} k_{1\nu} k_2^\mu k_2^\nu}{m_W^2} \right) \\
&= g^2 m_W^2 \left( 4 - \frac{k_2^2}{m_W^2} - \frac{k_1^2}{m_W^2} + \frac{(k_1 \cdot k_2)^2}{m_W^4} \right)
\end{aligned}$$

Recall that in a reaction the 4-momentum squared is a relativistic invariant. Using this invariant, we may alternate among before and after the decay, and viewing from the

lab frame or CM frame (or any other frame). In this case, let's try before and after decay entirely in the CM frame. This means  $\vec{p} = 0$ , and for the  $W$  boson energy and momenta  $E_1 = E_2 = E$ ,  $\vec{k}_1 = -\vec{k}_2 \equiv \vec{k}$ .

$$\Rightarrow \frac{k^2}{m_W^2} = \frac{E^2 - |\vec{k}|^2}{m_W^2} = \frac{(m_W^2 + |\vec{k}|^2) - |\vec{k}|^2}{m_W^2} = 1$$

Also,

$$\begin{aligned} (m_H, 0)^2 &= (E_1 + E_2, \vec{k}_1 + \vec{k}_2 = 0)^2 \\ m_H^2 &= 4E_2^2 = 4(m_W^2 + |\vec{k}|^2) \\ m_H^2 &= 4m_W^2 + 4|\vec{k}|^2 \\ m_H^2 - 2m_W^2 &= 2(m_W^2 + 2|\vec{k}|^2) \\ \frac{m_H^2 - 2m_W^2}{2} &= k_1 \cdot k_2 \end{aligned}$$

where in the last line I used

$$\begin{aligned} k_1 \cdot k_2 &= (E_1, \vec{k}_1) \cdot (E_2, \vec{k}_2) \\ &= (E, \vec{k}) \cdot (E_2, -\vec{k}) \\ &= E^2 + |\vec{k}|^2 \\ &= (m_W^2 + |\vec{k}|^2) + |\vec{k}|^2 \\ &= m_W^2 + 2|\vec{k}|^2 \end{aligned}$$

Now we may put these results back into the spin-summed invariant amplitude.

$$\begin{aligned}
\sum_{\lambda_1, \lambda_2} |\mathcal{M}|^2 &= g^2 m_W^2 \left( 4 - 1 - 1 + \frac{(m_H^2 - 2m_W^2)^2}{4m_W^4} \right) \\
&= g^2 m_W^2 \left( 2 + \frac{m_H^2 - 4m_W^2 m_H^2 + 4m_W^4}{4m_W^4} \right) \\
&= g^2 m_W^2 \left( 2 + \frac{m_H^4}{4m_W^4} - \frac{m_H^2}{m_W^2} + 1 \right) \\
&= g^2 m_W^2 \left( \frac{3m_H^4}{4m_W^4} \cdot \frac{4m_W^4}{m_H^4} + \frac{m_H^4}{4m_W^4} - \frac{m_H^4}{4m_W^4} \cdot \frac{4m_W^4}{m_H^4} \cdot \frac{m_H^2}{m_W^2} \right) \\
&= g^2 m_W^2 \frac{m_H^4}{4m_W^4} \left( 1 + \frac{12m_W^4}{m_H^4} - \frac{4m_W^2}{m_H^2} \right) \\
&= \frac{g^2 m_H^4}{4m_W^4} \left( 1 - \frac{4m_W^2}{m_H^2} + \frac{12m_W^4}{m_H^4} \right)
\end{aligned}$$

Put this into the decay rate.

$$\begin{aligned}
d\Gamma &= \frac{1}{2m_H} \left[ \frac{d^3 k_1}{2E_1(2\pi)^3} \frac{d^3 k_2}{2E_2(2\pi)^3} \right] \frac{g^2 m_H^4}{4m_W^4} \left( 1 - \frac{4m_W^2}{m_H^2} + \frac{12m_W^4}{m_H^4} \right) (2\pi)^4 \delta^4(k_1 + k_2 - p) \\
\Gamma &= \frac{g^2 m_H^3}{32(2\pi)^2 m_W^2} \left( 1 - \frac{4m_W^2}{m_H^2} + \frac{12m_W^4}{m_H^4} \right) \int \frac{d^3 \vec{k}_1}{E_1} \frac{d^3 \vec{k}_2}{E_2} \delta(E_1 + E_2 - E_p) \delta^3(\vec{k}_1 + \vec{k}_2 - \vec{p})
\end{aligned}$$

In the CM frame,  $E_p = m_H$  and  $\vec{p} = 0$ .

$$\begin{aligned}
\Gamma &= \frac{g^2 m_H^3}{32(2\pi)^2 m_W^2} \left( 1 - \frac{4m_W^2}{m_H^2} + \frac{12m_W^4}{m_H^4} \right) \int \frac{d^3 \vec{k}_1}{E_1} \frac{d^3 \vec{k}_2}{E_2} \delta(E_1 + E_2 - m_H) \delta^3(\vec{k}_1 + \vec{k}_2) \\
\Gamma &= \frac{g^2 m_H^3}{32(2\pi)^2 m_W^2} \left( 1 - \frac{4m_W^2}{m_H^2} + \frac{12m_W^4}{m_H^4} \right) \int \frac{d^3 \vec{k}}{\sqrt{m_W^2 + |\vec{k}_1|^2}} \frac{d^3 \vec{k}}{\sqrt{m_W^2 + |\vec{k}_2|^2}} \delta(E_1 + E_2 - m_H) \delta^3(\vec{k}_1 + \vec{k}_2)
\end{aligned}$$

Perform the  $k_2$  integration. Because of  $\delta^3(\vec{k}_1 + \vec{k}_2)$ , this will just enforce  $\vec{k}_1 = -\vec{k}_2 \Rightarrow |\vec{k}_1|^2 = |\vec{k}_2|^2$ . Since we are dealing only with these momenta squared now, let's drop the index and just use  $|\vec{k}|$ .

$$\Gamma = \frac{g^2 m_H^3}{32(2\pi)^2 m_W^2} \left( 1 - \frac{4m_W^2}{m_H^2} + \frac{12m_W^4}{m_H^4} \right) \int \frac{d^3 \vec{k}}{m_W^2 + |\vec{k}|^2} \delta(E_1 + E_2 - m_H)$$

Express the remaining differential in spherical coordinates  $d^3\vec{k} = |\vec{k}|^2 d|\vec{k}| \sin \theta d\theta d\phi$ , where  $\int \sin \theta d\theta d\phi = 4\pi$ .

$$\Gamma = \frac{g^2 m_H^3}{32(2\pi)^2 m_W^2} \left(1 - \frac{4m_W^2}{m_H^2} + \frac{12m_W^4}{m_H^4}\right) \int \frac{|\vec{k}|^2 d|\vec{k}| \sin \theta d\theta d\phi}{m_W^2 + |\vec{k}|^2} \delta(E_1 + E_2 - m_H)$$

In the CM frame,  $E_1 = E_2 = \sqrt{m_W^2 + |\vec{k}|^2}$ .

$$\Gamma = \frac{g^2 m_H^3}{8(4\pi)m_W^2} \left(1 - \frac{4m_W^2}{m_H^2} + \frac{12m_W^4}{m_H^4}\right) \int d|\vec{k}| \frac{|\vec{k}|^2}{m_W^2 + |\vec{k}|^2} \delta\left(2\sqrt{m_W^2 + |\vec{k}|^2} - m_H\right)$$

We must take care here. The integral is over  $|\vec{k}|$  but the argument of the  $\delta$ -function has more than one zero, so there is an ambiguity of which value  $|\vec{k}|$  should take from the integration. Fortunately, it is possible to expand the  $\delta$ -function as follows:

$$\delta(f(x)) = \sum_j \frac{1}{f'(x_0^j)} \delta(x - x_0^j)$$

where  $j$  counts over the zeros of  $f(x)$  and  $f' = \frac{df}{dx}$ . Let  $f(k) = 2\sqrt{m_W^2 + |\vec{k}|^2} - m_H$  and find the zeros:

$$\begin{aligned} m_H &= 2\sqrt{m_W^2 + |\vec{k}|^2} \\ \frac{m_H^2}{4} &= m_W^2 + |\vec{k}|^2 \\ \frac{1}{4} (m_H^2 - 2m_W^2) &= k^2 \\ \pm \frac{1}{2} \sqrt{m_H^2 - 2m_W^2} &= k \end{aligned}$$

However, a negative momentum magnitude doesn't make sense so we only use the

positive one.

$$\begin{aligned}
f'(k) &= \frac{2k}{\sqrt{m_W^2 + k^2}} \\
f'(k_0) &= \frac{\sqrt{m_H^2 - 4m_W^2}}{\sqrt{m_W^2 + \frac{1}{4}m_H^2 - m_W^2}} \\
f'(k_0) &= \frac{\sqrt{m_H^2 - 4m_W^2}}{\frac{1}{2}m_H^2} \\
f'(k_0) &= \frac{2}{m_H} \sqrt{m_H^2 - 4m_W^2} \\
\Rightarrow \delta(f(k)) &= -\frac{m_H}{2\sqrt{m_H^2 - 4m_W^2}} \delta\left(|\vec{k}| - \frac{1}{2}\sqrt{m_H^2 - 4m_W^2}\right)
\end{aligned}$$

Put this into the decay rate.

$$\begin{aligned}
\Gamma &= \frac{g^2 m_H^3}{32\pi m_W^2} \left(1 - \frac{4m_W^2}{m_H^2} + \frac{12m_W^4}{m_H^4}\right) \int d|\vec{k}| \frac{|\vec{k}|^2}{m_W^2 + |\vec{k}|^2} \frac{m_H}{2\sqrt{m_H^2 - 4m_W^2}} \delta\left(|\vec{k}| - \frac{1}{2}\sqrt{m_H^2 - 4m_W^2}\right) \\
&= \frac{g^2 m_H^3}{32\pi m_W^2} \left(1 - \frac{4m_W^2}{m_H^2} + \frac{12m_W^4}{m_H^4}\right) \frac{\frac{1}{4}(m_H^2 - 4m_W^2)}{m_W^2 + \frac{1}{4}(m_H^2 - 4m_W^2)} \frac{m_H}{2\sqrt{m_H^2 - 4m_W^2}} \\
&= \frac{g^2 m_H^3}{32\pi m_W^2} \left(1 - \frac{4m_W^2}{m_H^2} + \frac{12m_W^4}{m_H^4}\right) \frac{\frac{1}{4}(m_H^2 - 4m_W^2)}{\frac{1}{4}m_H^2} \frac{m_H}{2\sqrt{m_H^2 - 4m_W^2}} \\
&= \frac{g^2 m_H^3}{32\pi m_W^2} \left(1 - \frac{4m_W^2}{m_H^2} + \frac{12m_W^4}{m_H^4}\right) \frac{\sqrt{m_H^2 - 4m_W^2}}{2m_H} \\
&= \frac{g^2 m_H^3}{64\pi m_W^2} \left(1 - \frac{4m_W^2}{m_H^2} + \frac{12m_W^4}{m_H^4}\right) \sqrt{1 - \frac{4m_W^2}{m_H^2}} \\
&= \boxed{\frac{G_F m_H^3}{8\sqrt{2}\pi} \left(1 - \frac{4m_W^2}{m_H^2} + \frac{12m_W^4}{m_H^4}\right) \sqrt{1 - \frac{4m_W^2}{m_H^2}}}
\end{aligned}$$

where  $G_F = \frac{\sqrt{2}g^2}{8m_W^2} \Rightarrow \frac{G_F}{\sqrt{2}} = \frac{g^2}{8m_W^2}$ .